The Synthesis and *In Vitro* Evaluation of siRNAs Modified at the Backbone with a Novel Triazole-Based Internucleotide Linkage and Abasic Alkyl-Chain Linkages of Varying Length

by

Tim Efthymiou

A dissertation submitted in partial fulfillment of the qualifications required for the degree of

Doctor of Philosophy

University of Ontario Institute of Technology
Faculty of Science
Applied Bioscience

April 2013

Abstract

For over a decade, the use of double-stranded short interfering RNAs (siRNAs) to silence the expression of genes associated with disease at the translational level has gained much attention. Using a highly conserved endogenous pathway within cells, siRNA technology displays a high degree of target specificity and potency. However, traits required for the successful design of siRNA-based therapeutics such as resistance to nuclease-mediated degradation, improved cell membrane permeability and reduced off-target toxicity, are compromised by the native structure of duplex RNA′s charged backbone. This study therefore focused on synthesizing novel and neutrally-charged triazole-linked nucleoside dimer analogs which were incorporated throughout siRNA duplexes using DMT-phosphoramidite chemistry, in order to attenuate the negative contributions of RNA′s native backbone. In order to further elucidate the mechanism of the RNA interference (RNAi) pathway, additional siRNAs were synthesized containing commercially available abasic alkyl spacers. Through the robust copper(I)-catalyzed Huisgen [3+2] cycloaddition, azide and alkyne nucleic acid monomers were joined through the heterocyclic linkage in nearly quantitative yields, producing the novel triazole-linked uracil-uracil (U_tU) and cytosine-uracil (C_tU) dimers. Results from cell-based assays indicate that triazole-modified siRNAs are capable of silencing the transiently-expressed reporter gene *firefly* luciferase and the endogenous gene glyceraldehyde-3-phosphate dehydrogenase (GAPDH) in a dose-dependent manner. In addition, modifying the 3′-overhangs of siRNAs with the triazole backbone linkage, gave rise to increased nuclease resistance well beyond that of wild-type siRNA. Duplex RNAs containing abasic spacer linkages in the sense strand also maintained activity while targeting the luciferase reporter gene, indicating the capability to tune the efficacy of siRNA constructs by altering their thermodynamic profiles, in addition to providing evidence for an alternative RNAi mechanism. The studies describe herein, emphasize the compatibility of these novel backbone modifications with Watson-Crick interactions and with the RNAi pathway.

Acknowledgments

I would like to begin by giving my warmest and most sincere appreciation to my supervisor and Principal Investigator, Dr. Jean-Paul Desaulniers, for guiding me through this immensely life-altering experience with the utmost level of professionalism, enthusiasm, courtesy and compassion. In addition to providing me with the necessary funding and lab space, Dr. Desaulniers′ innate brilliance and stead-fast patience along with his constant reassurances and his unequivocal belief in my capabilities, served as a constant inspiration throughout my studies. I will always look upon this experience as a pleasure and an honor to have worked for such a friendly and helpful mentor.

I would like to thank my committee members, starting with Dr. Sean Forrester who served as a constant reminder that I must always maintain a balance between biology and chemistry in an interdisciplinary field. Dr. Forrester′s feedback and support was very insightful, which helped shape the direction of my biological study. I was truly blessed to have Dr. Bradley Easton on my committee, who always managed to put things into a new perspective due to his expertise as a chemist. His friendly demeanor and honest critique was extremely helpful in addressing any issues with my thermodynamic and synthetic studies. My warmest gratitude should also extend to Dr. Tony Yan from Brock University, who served as my external examiner. As a nucleic acid chemist with extensive experience in the field, I have been extremely fortunate to have Dr. Yan overlooking my progress throughout the years. Dr. Yan′s suggestions and critique were instrumental in quickly distinguishing my strengths from my weaknesses earlier on in my studies, making me strive to improve myself and to maintain a firm understanding of the scientific literature. Lastly, I would like to thank Dr. Yuri Bolshan for agreeing to serve as my University examiner. Dr. Bolshan′s guidance and unequivocal knowledge in synthetic organic chemistry has been sharpening both my practical and theoretical knowledge of synthetic mechanisms and reinforcing the basics in the field.

There are many others to whom I must extend my thanks for their kind support, friendly hospitality, and for the use of their extremely useful instrumentation. I would like to begin by thanking Dr. Holly Jones-Taggart for allowing me to use her lab space, her instrumentation, and for graciously donating some of her MCF-7 cells. I definitely

wouldn′t have made it very far in my studies if it wasn′t for her generosity with her lab equipment, her materials and cells, and for the help I received from her accommodating students. I would like to thank Robert Thompson for allowing me to use his workbench in Dr. Jones-Taggart′s lab on a regular basis and for his insight on how to properly work with MCF-7 cells. I would like to give a special thanks to Dr. Jones-Taggart′s previous student, Jessica Lyons, who essentially taught me everything I know about cell culturing.

For allowing me to perform the bulk of my cell-based assays in her lab and for the use of her wonderful spectroluminometer, I would like to give my deepest gratitude to Dr. Julia Green-Johnson. In addition to her unwavering generosity, Dr. Green-Johnson′s uplifting cheerfulness always made my day a little brighter while in her presence. I also give a warm thanks to Dr. Ayush Kumar for allowing me the bench-space to perform my bacterial work, along with granting me unlimited access to his qPCR instrument. Dr. Kumar went out of his way to help me interpret my qPCR results and for that, I am extremely grateful. I would also like to thank Dr. Kumar′s PhD candidate, Dinesh Fernando, for walking me through the complexities of qPCR and the necessary instrumentation.

Characterizing my compounds of interest would have been quite difficult had I not been given the assistance I needed from our trustworthy group of lab technicians here at UOIT. I would like to begin by thanking Michael Allison for training me to perform my own Mass Spectrometry experiments and for maintaining the instrument throughout the years. I would like to give a special thanks to Genevieve Barnes who assisted me with numerous NMR characterizations and who in addition, was my true friend, my colleague, and my security blanket during those trying and somewhat stressful undergraduate chemistry labs. I can not thank Dr. Darcy Burns from U of T enough for helping me acquire my initial set of NMRs and for being such a jovial character with a wealth of knowledge where NMR spectrometry was concerned.

My research could not have been possible without the help of the volunteers, work-study students, undergraduate thesis students, and MSc candidates who have joined Dr. Desaulniers′ group since the beginning. Whether I received direct assistance from these students to drive my project forward, or just enjoyed their polite and friendly

conversation, they all helped sustain a pleasant work environment. I would like to give special thanks to Ms. Wei Gong who received her MSc in December of 2012. Wei provided me with much needed assistance while putting together the most recent manuscript which was accepted for publication in October of 2012. There were many times when Wei became the target for a lot of my ridiculous outbursts over the last two years so I thank her for putting up with me.

Naturally, I can not forget to thank my parents and my sister for always pushing me to do better, and for ensuring a constant flow of unflinching support and home-cooked meals which at times, were desperately needed.

Lastly, I would like to thank my wife, Leila, who is the best thing that′s ever happened to me and who has always been a source of encouragement for the past twelve years of my life. With her unwavering support, her patience, and her easy-going nature, my studies remained a much easier and more fulfilling endeavour to undertake.

Statement of Contributions

Both the design and execution of each experiment performed throughout my studies were supervised by Dr. Jean-Paul Desaulniers. All experiments performed for Manuscript I (Chapter II) were carried out by myself, with the exception of the UV-monitored thermal denaturation studies carried out by Dr. Christopher Wilds of Concordia University. For Manuscript II (Chapter III), both Brandon Peel and Vanthi Huynh helped with the cell-based transfections and dual-luciferase reporter assays, while Jaymie Oentoro performed the nuclease stability assays. Concerning Manuscript III (Chapter IV), Vanthi Huynh and Brandon Peel assisted with the cell-based luciferase assays. The introductions, the results and discussion sections for all three manuscripts were written by me and by Dr. Desaulniers. This thesis was written entirely by the author.

Statements of Originality

To the best of the author′s knowledge, all materials presented within this thesis were considered novel contributions to the scientific community upon submission for peer review and subsequent publication.

Manuscript I: Efthymiou, T. C.; Desaulniers, J.-P. Synthesis and Properties of Oligonucleotides that Contain a Triazole-Linked Nucleic Acid Dimer, *J. Heterocycl. Chem*. **2011**, *48*, 533-539.

This manuscript describes the step-wise synthesis of a novel triazole-linked uracil-uracil (U_tU) nucleoside analog dimer, utilizing the copper (I)-catalyzed variant of the Huisgen [3+2] "click" cycloaddition. The results from this study indicate this unique triazole-based internucleoside linkage to be compatible with Watson-Crick base pair interactions, while slightly lowering the thermostabilities of synthetic DNA duplexes when terminally positioned. These results provided grounds to apply this novel backbone modification within synthetic RNA molecules designed for gene-silencing purposes.

Manuscript II: Efthymiou, T. C., Huynh, V., Oentoro, J., Peel, B., Desaulniers, J.-P. Efficient synthesis and cell-based silencing activity of siRNAs that contain triazole backbone linkages, *Bioorg. Med. Chem. Lett*. **2012**, *22*, 1722-1726.

This manuscript describes the step-wise synthesis of a unique triazole-linked cytosine-uracil (C_tU) nucleoside analog dimer using the "click" cycloaddition, and the site-specific incorporation of this dimer and the previously-reported U_tU dimer, throughout synthetic short-interfering RNA (siRNA) molecules. This study illustrates the successful targeting and down-regulation of messenger RNA expression *in vitro*, performed by these triazole-modified siRNAs. To our knowledge, this was the first study which detailed the functional activity of synthetic siRNAs containing this unique triazole backbone modification.

Manuscript III: Efthymiou, T. C.; Peel, B.; Huynh, V.; Desaulniers, J.-P. Evaluation of siRNAs that contain internal variable-length spacer linkages, *Bioorg. Med.Chem. Lett*. **2012**, *22*, 5590-5594.

This manuscript describes the use of a simple and effective method of controlling siRNA activity through the chemical introduction of abasic alkyl-chain linkages of variable length. This study demonstrates how the deliberate introduction of destabilizing abasic modifications throughout duplex siRNAs can produce functional gene-silencing constructs through manipulation of their thermodynamic profiles. In addition, this study provides further evidence supporting the existence of an alternative endogenous RNA interference (RNAi) mechanism within cells.

Table of Contents

Appendix I – Chapter II

Appendix II – Chapter III

Appendix IV – Detailed Experimental Procedures

List of Figures

Chapter I

Chapter II

Chapter III

Chapter IV

Appendix I

Appendix II

Appendix III

List of Tables

Chapter II

Chapter III

Chapter IV

Appendix I

Appendix II

Appendix III

List of Abbreviations

2′-F	2′-deoxy-2′-fluoro-ribonucleic acid
2′-FANA	2′-deoxy-2′-fluoro-*β*-D-arabinonucleic acid
2′-*O*-Me	2′-*O*-methyl
2′-*O*-MOE	2′-*O*-methoxyethyl
2′-O-TBS	2′-*O*-*tert*-butyldimethylsilyl
ACE	bis(acetoxyethoxy)orthoformate
Ago2	Argonaute 2
AS	Antisense
ASO	Antisense oligonucleotide
BP	Boranophosphate
CD	Circular dichroism
$CDCl_3$	Deuterated chloroform
C. elegans	*Caenorhabditis elegans*
Clp1	Cleavage and Polyadenylation Factor 1
CPG	Controlled Pore Glass
C_tU	Cytosine-Triazole-Uracil nucleoside analog dimer
CuAAC	Cu(I)-Assisted Azide-Alkyne Cycloaddition
DCC	Dicyclohexylcarbodiimide
DCM	Dichloromethane
DCU	Dicyclohexyl urea
dF	Difluorotoluene
DIPEA	Diisopropylethylamine
DMAP	Dimethylaminopyridine
DMEM	Dulbecco′s modified eagle medium
DMF	Dimethylformamide

DMSO	Dimethylsulfoxide
DMT	Dimethoxytrityl
DNA	Deoxyribonucleic acid
DOD	bis(trimethylsiloxy)cyclododecyloxysilyl ether
dsDNA	Double-stranded DNA
dsRNA	Double-stranded RNA
EDC	Ethyl dimethylaminopropyl carbodiimide
EDTA	Ethylenediaminetetraacetic acid
EMAM	Ethanolic Methylamine/Aqueous Methylamine
ESI MS	Electrospray ionization mass spectrometry
qRT-PCR	Quantitative real-time polymerase chain reaction
Q-TOF	Quantitative time-of-flight
EtOAc	Ethyl acetate
EtOH	Ethanol
FBS	Fetal bovine serum
FDA	Food and Drug Administration
GAPDH	Glyceraldehyde-3-phosphate dehydrogenase
HBTU	*O*-Benzotriazole-*N*,*N*,*N*′,*N*′-tetramethyl-uronium-hexafluorophosphate
HCl	Hydrochloric acid
HF	Hydrofluoric acid
HOBt	1-Hydroxybenzotriazole
HPLC	High-performance liquid chromatography
HRMS	High-resolution mass spectrometry
IDT	Integrated DNA Technologies
KCl	Potassium chloride
LNA	Locked nucleic acid
MALDI-TOF	Matrix-assisted laser desorption/ionization time-of-flight

MeOH	Methanol
MHz	Megahertz
mRNA	Messenger RNA
NMR	Nuclear magnetic resonance
PAGE	Polyacrylamide gel electrophoresis
PAZ	Piwi Argonaute Zwille
PIWI	P-Element Induced Wimpy
PNA	Peptide nucleic acid
PS	Phosphorothioate
RDE-4	RNAi Defective-4
RISC	RNA-induced silencing complex
RLC	RISC loading complex
RNA	Ribonucleic acid
RNAi	RNA interference
RT	Reverse transcription
SDOM	Standard deviation of the mean
siRNA	Short-interfering RNA
TANA	Thioacetamido nucleic acid
TAR	*Trans*-activation response
TBAF	Tetrabutylammonium fluoride
TBSCl	*Tert*-butyldimethylsilyl chloride
TEA	Triethylamine
TLC	Thin layer chromatography
THF	Tetrahydrofuran
T_m	Melting temperature
TOMCl	Triisopropylsilyloxymethyl chloride
TRBP	TAR RNA binding protein

U_tU	Uracil-Triazole-Uracil nucleoside analog dimer
UV	Ultraviolet

Chapter I – Literature Review

1.0 Nucleic Acid Therapeutics

There are a myriad of diseases with roots linked to uncontrollable gene expression, gene mutations, and viral infections.[1] Diseases which are related to deviant expression of endogenous genes such as cancer and Alzheimer′s disease,[2, 3] or the mis-expression of genes introduced by viruses are difficult to diagnose and treat with modern day therapeutics because of their lower tissue, oligonucleotide, or protein-target specificity. With a focus on existing therapies for the treatment of cancer, patients can undergo invasive surgery to remove the affected tissues. Although less invasive, radiation and chemotherapies are non-specific alternatives to surgery, which affect healthy cells along with the diseased cells.[4] It is well known that these existing therapies can produce harsh side effects and are often plagued with instances of disease recurrence.[4] In order to overcome these issues associated with current therapeutic strategies, the growing trend in molecular biology has been to effectively control the expression of problematic proteins involved with undesirable pathologies, either at the transcriptional,[5, 6] or translational level.[7] In addition, the ability to control the expression of genes is crucial towards increasing our understanding of gene function and to ultimately advance the development of gene-modulating therapeutics. Most therapeutics today are used to destabilize or deactivate over-expressed proteins or multi-protein complexes by binding to these proteins of interest, or to bind to those further upstream or downstream within the signalling pathway thus preventing proper signal transduction.[3] An alternative to these small-molecule drugs is the use of nucleic acid-based anti-gene agents, which have shown great capability and promise as prospective gene-silencing therapeutics, along with their continued use as indispensible tools used for functional genomics.[8] In addition to their potential anti-gene properties, nucleic acid polymers can be manipulated to form useful aptamers designed to disrupt protein function through binding-induced conformational changes[3, 9] and to perform as molecular probes.[10, 11]

1.1 Antisense Oligonucleotides

In 1978, it was demonstrated by Stephensen and Zamecnik that chemically synthesized oligonucleotides can effectively target and interrupt the translation of complementary RNA molecules once introduced in cells.[12] The study involved the introduction of antisense oligonucleotides (ASOs), which are exogenous single-stranded DNA or RNA-based oligonucleotides with sequences complimentary to their DNA or RNA targets.[6] These ASOs demonstrated effective targeting and repressed expression of viral RNA molecules belonging to *Rous sarcoma*.[12] Since then, chemically or enzymatically synthesized antisense oligonucleotides (ASOs) have been employed as very powerful tools used to control gene expression through post-transcriptional targeting of complimentary mRNA molecules, thus preventing their translation.[13] As a result of this discovery, it follows that a commercially available therapeutic known as Vitravene[14, 15] has incorporated ASO technology into their pharmacophore, with many others still undergoing clinical trials.[3, 14, 16] The discovery of effective small-molecule therapeutics is a difficult task due to their lack of specificity for their intended targets in the cell.[15] Alternatively, disrupting the expression of oncogenes with ASOs is showing great promise due to the potential of increased specificity from Watson-Crick hybridization.[17] Significant research has been performed on ASOs in order to increase their target specificity, binding affinity and resiliency within physiological environments.

Although the framework of ASO constructs generally employs the use of the deoxyribose moiety, RNA-based ASOs have also previously been employed and have displayed favourable transcript targeting.[18] The gene-silencing mode of action for typical DNA-based ASOs once inside the cell, begins with the single-stranded oligonucleotide construct annealing to its mRNA target producing a DNA/RNA hybrid.[3, 19] This hybrid duplex is either rendered as non-translatable due to blocking of the ribosome,[20] or it recruits a member of the RNAse III family referred to as RNAse H, which recognizes and binds to the hybrid duplex and cleaves the target mRNA transcript.[19, 21]

1.2 Short-Interfering RNA

Natural mechanisms exist within cells which guard organisms from disease arising from exogenous virulents, or from the unregulated expression of endogenous genes. Unlike the route through which ASOs downregulate gene expression, an endogenous and highly conserved mechanism known as RNA interference (RNAi) was discovered in 1998 by Fire and Mello while studying the model organism *C. elegans*.[22] In this study, researchers were comparing the RNA interference capabilities of antisense RNAs to dsRNAs, by targeting the abundant *unc-22* gene which expresses a non-essential muscle protein and noting the resultant phenotypes.[22] This was a continuation from earlier research showing evidence that reduced expression of the same *unc-22* transcript was obtained through the introduction of sense RNA, which in turn produced antisense RNA in the cell.[23] The RNAi pathway is a natural defense against invasive genetic information,[24] and is essential for eukaryotic cells to self-regulate the expression of endogenous genes. This regulation is performed using double-stranded RNA molecules known as short-interfering RNAs (siRNAs) which range from 19 to 21 base pairs in length, and contain distinct 2-nucleotide long 3′-overhangs at each end of the duplex. These siRNAs are then incorporated into a multi-eznyme complex known as the RNA-Induced Silencing Complex (RISC). The RISC complex selects one strand of the RNA duplex as the active antisense or "guide" strand while discarding the inactive sense or "passenger" strand and together, they target messenger RNAs based on Watson-Crick complementarity for subsequent degradation.[25]

Significant contributions towards the advancement of siRNA technology can be largely attributed to the research history and expansion of our knowledge of ASOs.[3] As a result, siRNAs have become the most commonly used tool for discovering protein function and elucidating transduction pathways due to their ability to promote the accurate targeting and facile cleavage of mRNAs.[8] Disruption of mRNA translation has been crucial in distinguishing between different protein subtypes, which was difficult to perform using traditional small-molecule drugs[26] and gene knockouts.[27]

1.2.1 The Known RNAi Mechanism in Human Cells

Under natural circumstances, siRNAs are produced through the act of cleaving longer double-stranded RNA (dsRNA) molecules which are exogenously introduced into cells. These long dsRNAs are recognized and cleaved into shorter duplex RNAs with 2-nucleotide 3′ sticky ends by an enzyme known as Dicer.[25] Dicer is part of a heterotrimer with the *trans*-activation response (TAR) RNA binding protein (TRBP) and an endonuclease known as Argonaute 2 (Ago2).[28] With a bound newly-formed siRNA, this complex is referred to as the RISC loading complex (RLC).[25, 29] The Dicer-TRBP portion of the RLC helps select the active guide strand from the passenger strand of the siRNA by assessing the duplex′s natural thermodynamic asymmetry. The guide strand selection process starts with the TRBP protein determining the least thermodynamically stable end of the duplex.[30] Once the least thermodynamically stable end of the siRNA and subsequently the guide strand is determined, Dicer-TRBP then transfers the duplex to Ago2.[29] Ago2 then proceeds to cleave the inactive passenger strand of the siRNA duplex. The cleavage site on this strand opposes nucleotide residues 10 and 11 from the 5′-end of the guide strand.[29, 31, 32] The passenger strand is subsequently discarded from the complex, leaving the active guide strand whose 5′-end formed the least thermodynamically stable portion of the siRNA duplex as determined by Dicer-TRPB of the RLC.[29] The remaining RISC-guide complex which is also referred to as active RISC, is responsible for targeting and binding to the mRNA transcripts containing sequences complementary to that of the antisense strand.[33] Once the guide-mRNA duplex is formed, Ago2 proceeds to cleave the transcript at the site of the phosphodiester linkage, once again opposite from antisense residues 10 and 11, counting from the 5′-end (Figure 1.1).[31, 33]

1.2.2 RISC in Other Organisms

Depending on the organism, there are different sets of proteins which comprise the RLC complex. In *Drosophila* for instance, the dsRNA binding protein in the RLC is R2D2; whereas in *C. elegans*, it is the RDE-4 protein.[25, 28] It is understood that regardless of the organism being studied, all dsRNA binding proteins are responsible for helping prepare siRNAs for Ago2 loading by sensing the RNA duplex′s thermodynamic asymmetry to determine which of the strands will become the active guide strand. In humans, although it is clear that TRBP is required for siRNAs to proceed with RNAi, it is not entirely clear as to the exact role of this particular dsRNA binding protein. Studies have shown that TRBP senses the asymmetry of siRNA duplexes by binding to the most thermodynamically stable end of the duplex. However, more characterization is required.[28, 30]

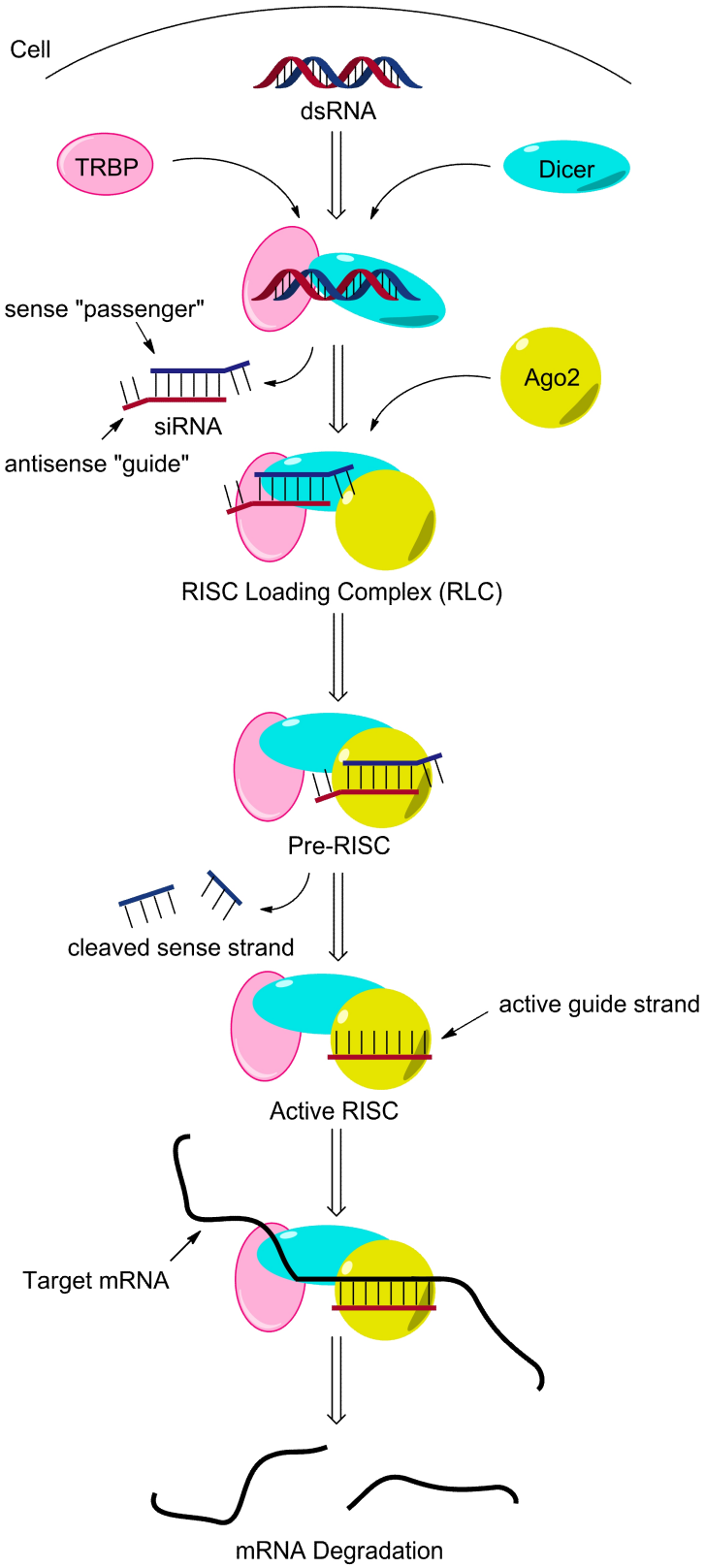

Figure 1.1 RISC-mediated RNA Interference pathway following the production of siRNAs.

1.2.3 Argonaute 2 Endonuclease

The Ago2 endonuclease is an essential component of the RNAi pathway, since it carries out the majority of the pathway′s catalytic activity. Of the four isoforms of Argonaute proteins found in humans, it was determined that RNAi activity could not be properly guided without Ago2 playing the key role of removing the inactive passenger strand from the siRNA duplex and degrading the target transcript after guide strand hybridization.[25, 31-36] There are conflicting views as to whether Ago2 is complexed with Dicer and TRBP whilst guiding the active guide strand towards its target, or that it dissociates from the heterotrimeric complex and performs RNAi on its own.[28] Prior to forming the pre-RISC complex which occurs once the siRNA is loaded into Ago2, the 5′-ends of the RNA duplex are phosphorylated by a kinase known as Clp1.[34, 37] It has been shown that 5′-phosphorylation of the guide strand is essential in order to properly associate with Ago2 and form the active RISC complex.[37]

The Ago2 endonuclease is made up of three main domains: The PIWI domain at the amino terminus; the centrally localized Mid section; and the PAZ domain at the carboxyl terminus.[31, 32, 34, 38] The PIWI domain is known as the section responsible for the enzyme′s catalytic activity and resembles the structure of the RNAse H endonuclease. The Mid domain has been shown to bind to the 5′-phosphorylated end of the antisense strand, while the PIWI domain binds to the strand′s 5′-region. While the PAZ domain is known to interact with the 3′-overhang of the antisense strand, there isn′t any noticeable interaction between the enzyme and the strand′s 3′-region.[32, 33] Having been elucidated, these Ago2-guide interactions can provide further assistance when chemically modifying designer oligonucleotides.

1.3 Problems with ASOs and siRNAs

The evolution of clinically approved antisense and siRNA-based therapeutics has been slow due to problems inherent with the native nucleic acid sugar-phosphate backbone.[8, 35, 39] These problems to be addressed include: 1) the susceptibility of the phosphodiester linkage to enzymatic cleavage; 2) its polyanionic charge density; and 3) off-target toxicity.[3, 7, 8] In DNA as well as RNA, the phosphodiester linkage is easily hydrolyzed

and susceptible to cleavage by endo- and exo-nucleases in the blood serum thus limiting their half-life under physiological conditions.[35, 40] The multiple anionic nature of the phosphate backbone in both DNA and RNA reduces their cell membrane permeability, affecting their delivery to target cells.[7, 8, 41, 42] This excessive charge density on the native backbone also makes it more difficult for ASOs or siRNAs to interact with serum transport proteins such as albumin,[8] in addition to making them more susceptible to enzyme-assisted hydrolysis as a result of heavy hydration.[8, 35] Particular to RNA, there is also the problem of having the 2′-OH functionality on the ribose moiety which can attack the adjacent phosphate group, thus truncating the construct by cyclizing into a stable five-membered heterocycle.[43, 44] Another problem which is commonly displayed when targeting transcripts for degradation using ASOs or siRNAs is the issue of off-target toxicity[45-47] and activation of the host′s immune system.[48, 49] Focusing primarily on siRNAs, there is evidence that the RISC-guide complex can incorrectly target non-homologous anti-parallel sequences thus knocking down the wrong transcript. This is thought to occur when Watson-Crick base pairing occurs between the off-target transcript and the guide strand′s ′seed′ region, referring to nucleotide residues 2 to 8 from the 5′-end, forming the guide-target hybrid despite the presence of base-pair mismatches elsewhere in the duplex.[8, 35] In light of this behaviour, chemical modification of the residues within the seed region on the guide strand of siRNAs, has proven to reduce off-target toxicity in cells.[8, 35] In order to address these drawbacks, chemical modification of native oligonucleotide structures is essential for the development of clinically feasible anti-gene agents which are: 1) less susceptible to enzymatic cleavage by endo/exonucleases thus increasing their bioavailability; 2) display increased cell membrane permeability through minimizing the poly-anionic nature of the backbone; and 3) have increased specificity for target mRNA. While mitigating these known issues through chemical modification, a fine balance must be maintained between the chemical enhancements and the pharmacological utility of the modified compounds.

1.4 Chemical Modification of Nucleic Acids

1.4.1 Chemical Synthesis of Oligonucleotides

Other than being responsible for the propagation of genetic information, it was later determined that oligonucleotides could serve other unique purposes. The production of synthetic genes could lead to novel proteins used for medical or industrial application,[50] or nucleotide derivatives can serve as antitumor and antiviral agents.[51-53] Another component of oligonucleotide-based technology was the additional functionality which could be extracted from these derivatives through the chemical modification of their native structures. In order to implement these modifications more effectively in a site-specific manner, the development of an alternative strategy to chemically synthesize DNA and RNA molecules became a desirable goal. The original and familiar technology involving the use of enzymatic means to grow polynucleotide chains had its drawbacks such as poor nucleobase insertion accuracy, and the inability to control the specificity of introducing unnatural bases or nucleosides within the growing construct.[54] After several attempts to optimize synthetic strategies for both DNA and RNA,[50, 55] it was determined that synthesis performed on a solid-support was the simplest and most efficient technology,[50, 54] and has remained the primary strategy through which oligonucleotides are synthesized today.

Synthesis of both DNA and RNA molecules on a controlled-pore glass (CPG) solid support is typically performed using DMT-phophoramidite chemistry,[54, 56] where nucleotide building blocks containing specific 5′ and 3′ protecting groups are joined together through a step-wise process. This optimized and fully-automated form of synthetic chemistry can be utilized to effectively yield any oligonucleotide sequence with high efficiency. In addition, this method allows the incorporation of virtually any designer molecule into the growing sequence, provided it contains all of the necessary protecting groups in order to form the native phosphodiester internucleotide linkage.

Unlike the natural 5′ to 3′ direction of DNA and RNA synthesis within biological systems, solid-support synthesis of oligonucleotides typically occurs in the opposite direction (3′ to 5′) with very few alternative methodologies.[44] Unless the goal is to insert a modified nucleoside analog at the 3′-end of the designer sequence, the solid support itself will contain the first of the known four DNA or five RNA bases. The initial step in solid-support DMT-phosphoramidite chemistry involves the removal of the acid-labile dimethoxytrityl group which protects the 5′-alcohol of the nucleoside on the support using trichloroacetic acid. Having exposed the 5′-OH of the nucleoside on the support, it is now prepared to couple with the 3′-phosphoramidite group of the incoming nucleobase (Figure 1.2).

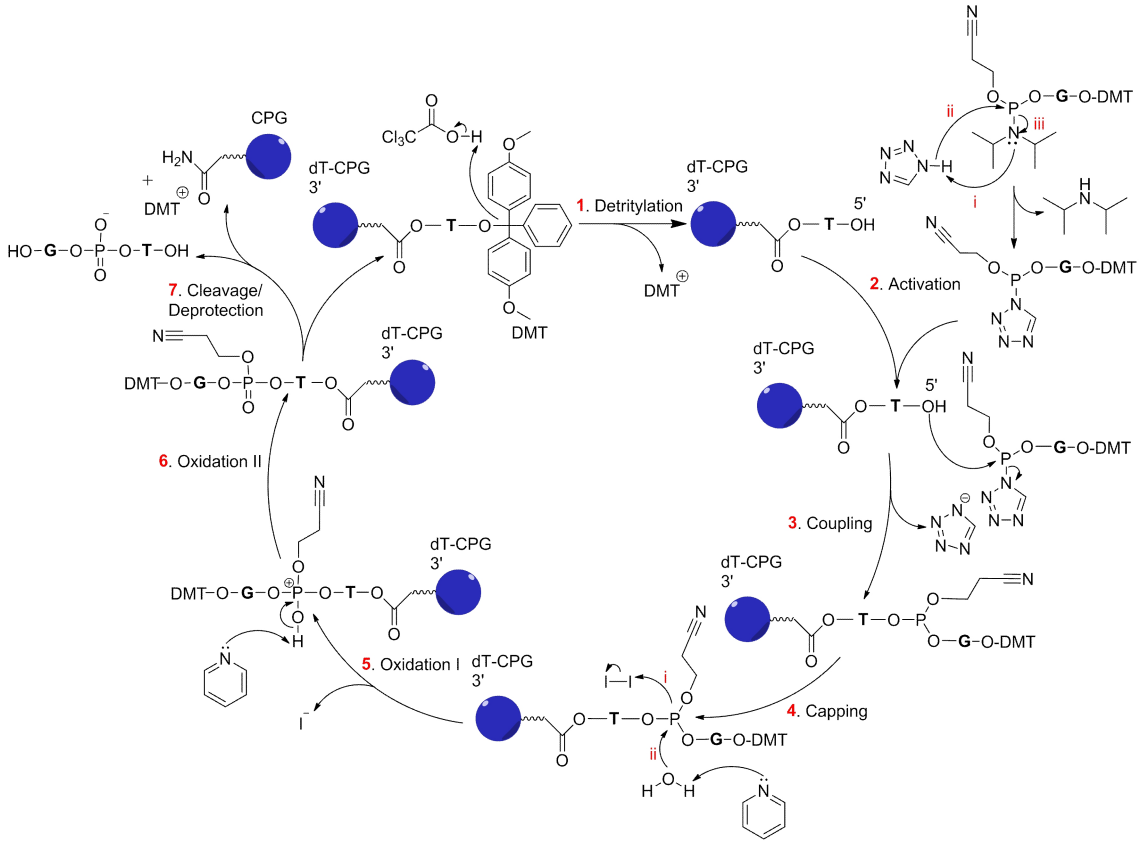

Figure 1.2 Step-Wise Automated Solid-Support Synthesis of Oligonucleotides Using DMT-phosphoramidite Chemistry.

The second synthetic step involves activating the incoming 3′-phosphoramidite group with 1*H*-tetrazole. This occurs through 1*H*-tetrazole's extremely rapid protonation of the

tertiary amine, followed by an attack of the phosphorus center by tetrazole′s anion and subsequent displacement of diisopropylamine. Being a much better leaving group, the use of tetrazole to activate the phosphoramidite and form the more reactive tetrazolide intermediate,[57] greatly facilitates the attack on the phosphorus center by the exposed 5′-OH on the solid support (Figure 1.2).

The next step involves coupling the new base to the solid support. As previously mentioned, this occurs when the exposed 5′-OH on the support attacks the incoming phosphorus center, thus displacing the tetrazole anion which deprotonates the 5′-oxygen. This has been referred to as the cyanoethyl-protected phosphite intermediate (Figure 1.2).[50, 55] Alternatives to using 1H-tetrazole as activators such as 5-ethylthio- or 5-benzylthio-1H-tetrazole[58] are widely being used in order to reduce coupling times and to enhance coupling efficiency due to their increased acidity and nucleophilicity.

The following is a precautionary measure which involves utilizing an acetic anhydride solution to effectively cap any remaining 5′-OH groups which did not successfully react with the incoming residue. The protected alcohol is then prevented from reacting with any successive bases which would introduce anomalies in the desired oligonucleotide sequence (Figure 1.2).

The synthesis continues with oxidation of the phosphite in order to form the cyanoethyl-protected phosphotriester intermediate; the precursor to the desired phosphodiester linkage. By adding I_2 as a solution in pyridine and water, iodine acts a Lewis acid creating an electrophilic center after forming an unstable P-I bond. Water then attacks the P^+ center displacing iodide (I^-) and is fully deprotonated by pyridine giving us the aforementioned phosphotriester intermediate (Figure 1.2).

This particular juncture in the step-wise synthetic procedure immediately following the final oxidation step presents the opportunity to either continue elongating the oligonucleotide sequence through repetition of the six-step cycle, or to remove the support from the automated synthesizer once the desired sequence is complete. The solid support is then treated with NH_4OH in order to deprotect all nucleobase exocyclic amines and to eliminate the β-cyanoethyl protecting group giving us the native phosphodiester

linkage, all while simultaneously cleaving the oligonucleotide from the solid support (Figure 1.2). After synthesizing RNA oligonucleotides, there is the necessity for an additional deprotection step of RNA′s 2′-hydroxyl group which is performed following base deprotection and cleavage from the solid support.[59]

The entire automated process for chemically synthesizing DNA molecules using the DMT-phosphoramidite method just described, is also compatible with the synthesis of RNA molecules. The most commonly used building blocks for they synthesis of RNA oligonucleotides are 5′-*O*-DMT-2′-*O*-*tert*-butyldimethylsilyl (2′-*O*-TBS) protected phosphoramidites. However, through constant exposure to basic conditions during each step of oligonucleotide synthesis, the 2′-*O*-TBS protecting group on RNA amidites has been known to migrate to the 3′ position on the ribose sugar. This 2′ to 3′-*O*-TBS migration would ultimately lead to the unfavourable production of 2′ – 5′ phosphodiester linkages for each subsequent base addition.[44] It is for this reason that alternative RNA phosphoramidites containing 2′ protecting groups that are resilient to 2′ – 3′ migration are often used such as 2′-*O*-triisopropylsilyloxymethyl (2′-*O*-TOM) protected phosphoramidites.[60] Both the 2′-*O*-TBS and TOM silyl ethers are fluoride ion-labile and are removed following the concerted base deprotection and solid-support cleavage step.

Advancements in the automated synthesis of RNA oligonucleotides have yielded methodologies that can produce RNA molecules with comparable efficiency, speed, and purity to DNA molecules. An alternative to DMT-phosphoramidite chemistry for RNA synthesis was devised in 1998 known as bis(acetoxyethoxy)orthoformate (ACE) chemistry.[61] The use of ACE chemistry for RNA synthesis can not only mitigate the issue of 2′ – 3′ migration which 2′-*O*-TBS protected RNA oligonucleotides can undergo, but it eliminates the growing oligonucleotide′s exposure to harsh acidic conditions due to the repetitive 5′ detritylation step. Increased exposure to acidic conditions during DNA and RNA synthesis can ultimately lead to depurination, which describes the hydrolytic cleavage of the purine-ribose glycosidic linkage.[62] ACE chemistry involves the use of 3′-phosphoramidites which are 5′-silyl ether and 2′-orthoester protected. The unique 2′-*O*-bis(2-acetoxyethoxy)methyl (ACE) protecting group is used with a fluoride ion-labile 5′-*O*-silyl protecting group such as 5′-*O*-bis(trimethylsiloxy)cyclododecyloxysilyl ether

(DOD). The synthetic scheme is similar to DMT-phosphoramidite chemistry in that RNA oligonucleotides are synthesized in the 3′ to 5′ direction. However, instead of the acidic conditions use to detritylate the 5′ end prior to activation and 3′ – 5′ coupling in DMT chemistry, a source of fluoride ions is required to deprotect the 5′-silyl ether. The finished RNA oligonucleotide is exposed to mild acidic conditions, only following the base deprotection/support cleavage step in order to remove the acid-labile 2′-*O*-ACE group.[61]

1.4.2 Common Chemical Modifications of the Ribose Sugar

There are three main sites within an oligonucleotide where chemical modifications have been studied: the ribose sugar, the nitrogenous base and the phosphodiester backbone linkage. With respect to RNAs, modifications to the ribose moiety have been heavily researched. A widely used sugar modification involves methylating the 2′-OH group (2′-*O*-Me), which has shown to increase siRNA stability and potency depending on where the modification is performed within the construct, by blocking the free 2′-OH′s nucleophilicity and preventing sequence truncation as mentioned earlier (Figure 1.3). For example, a report by Collingwood and colleagues (2008) demonstrated that the preferred structure of siRNA molecules due their observed potency when compared to unmodified siRNA included an alternating pattern of 2′-*O*-Me sugar modifications in either the antisense or sense strand. This alternating pattern was shown to provide good siRNA stability while retaining potency, when targeting two different types of human genes *in vitro*.[40] Another sugar modification which has the capability of recruiting RNAse H for RNA degradation when incorporated into ASOs and can act as a suitable ligand for polymerases, is the 2′-deoxy-2′-fluoroarabinonucleic acid (2′-FANA) nucleoside analog (Figure 1.3).[63, 64] Although typically used as a DNA mimic in ASO-based applications, reports have demonstrated that siRNAs containing sense strands which are moderately or entirely made up of 2′-FANA residues retain their potency, are more resilient to cleavage by nucleases and are less prone to stimulating innate immune responses.[65] Another sugar modification which has produced RNA analogs with high binding affinity is the locked nucleic acid (LNA) modification, which involves the linkage between the 2′-OH and the 4′ sugar carbon through a methylene group (Figure 1.3). This covalent linkage, as well as the aforementioned 2′-*O*-Me modification, induces a locked C_3′-endo pucker

conformation of the ribose which enhances RNA′s natural A-form helical structure.[13, 66-69] When added to the 5′ end of the sense strand in an siRNA molecule, the LNA modification was shown to improve the guide strand′s incorporation into the RISC complex through biasing the duplex′s thermostability, thus reducing any non-specific targeting by the sense strand and increasing the overall silencing efficiency.[70] Other 2′-sugar modifications such as 2′-*O*-methoxyethyl (2′-*O*-MOE) and 2′-flouro RNA (2′-F-RNA) positioned throughout the siRNA construct in either the sense or antisense strands (Figure 1.3) have also shown to produce stable molecules less prone to enzyme digestion and displaying a reduction in off-target toxicity.[63, 64, 68] Most of the sugar modifications, particularly the 2′ modifications allow the siRNA molecule to retain its native Watson-Crick base-pairing characteristics while increasing its stability within biological environments. Although sugar modifications such as 2′ alkylation have shown potential,

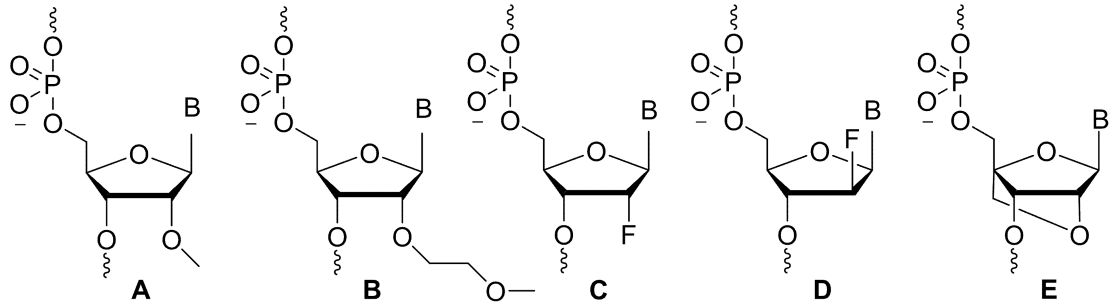

Figure 1.3 Common modifications to the 2′-OH of the furanose sugar: (**A**) 2′-*O*-methyl (2′-*O*-Me); (**B**) 2′-*O*-methoxyethyl (2′-*O*-MOE); (**C**) 2′-fluoro (2′-F); (**D**) 2′-deoxy-2′-fluoroarabinonucleic acid (2′-FANA) and ; (**E**) 2′,4′-locked nucleic acid (LNA)

there is still the possibility that enzymatic cleavage of the polyanionic RNA backbone can occur, which is likely a main factor in delaying the use of these modifications in commercial therapeutics.

1.4.3 Common Chemical Modifications of the Nitrogenous Bases

Modification of the known nucleobases is typically achieved by conjugating new functionalities to specific sites on both the purine and pyrimidine heterocycles, or by substituting the nucleobases with unnatural groups. Nucleobases are the most frequently modified portions of nucleic acids due to the presence of easily modifiable sites, shorter

synthetic routes for their modification, and the functional versatility of the derivatized products.[71, 72] In the form of nucleotide phosphoramidite building blocks typically used to chemically synthesize DNA and RNA oligonucleotides through an automated process,[55, 73] nucleobase analogues can be site-specifically incorporated throughout the oligomer. Similarly, nucleotide sugar or backbone modifications can be incorporated into synthetic oligonucleotides using this process. However, unlike certain modified sugars or phosphates, all modified nucleobases have the advantage of unrestricted positioning throughout growing polynucleotides.[74]

1.4.3.1 Bioconjugation of Nitrogenous Bases

Synthetically conjugating select functionalities or large molecules to specific sites on either purine, or pyrimidine nucleobase heterocycles, can significantly alter the thermodynamic properties, conformational arrangements and delivery capabilities of the resultant modified oligonucleotides. The most common accessible sites for chemical alteration on the purine heterocycles include, but are not limited to the 7-aza or deaza and the N^9-positions of both adenine and guanine, the 6-*N* exocyclic amine of guanine and the 2-*N* exocyclic amine of adenine. Regarding the pyrimidine heterocycles, positions C5, the 4-*N* exocyclic amine of cytosine and the N^1-positions are most notable for chemical modification.[75]

1.4.3.2 Nucleobase Substitution

Finding suitable substitutions for nucleobases which are compatible within DNA and RNA strands and duplexes is another prominent area of research. The discovery of 2,4-difluorotoluene (dF) (Figure 1.4), an analog which can replace thymidine in DNA and RNA oligomers,[76, 77] eventually lead to trials involving its incorporation in siRNA duplexes as a replacement for uracil. Work done by Xia and associates showed that siRNA guide strands containing single dF substitutions in the 5′ region displayed decreased non-specific targeting, increased RNA stacking abilities due its non-polar nature and conjugated system, and increased the strand′s affinity for binding to the RISC complex.[78] Despite these promising results, it was also shown that dF substitutions in the center of the guide strand were detrimental to the overall stability of the siRNA construct,

and placement anywhere else along the duplex lowered the overall melting temperature due to dF′s inability to hydrogen bond with its compliment.[78]

Following the discovery of nucleobase analogs such as dF, growing interest within the scientific community focused on the potential of such prospective modifications. Since it was determined that Watson-Crick interactions are not solely responsible for the hybridization of DNA and RNA strands,[79] the development of nucleobase analogs and substitutions focused on using highly conjugated substituents, capable of stacking with near and opposing neighbours.[80] Some examples of alternative base substitutions include pyrene and benzene residues which can behave as universal bases with enhanced stacking capabilities due to their complete aromaticity and have provided extensive probing capabilities to modified oligonucleotides (Figure 1.4).[77]

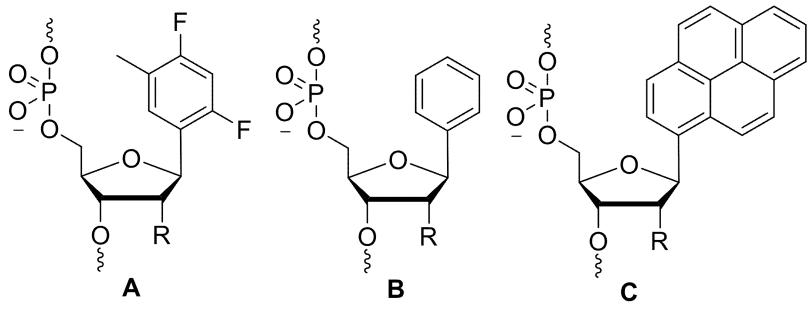

Figure 1.4 Non-hydrogen bonding substitutions for existing nucleobases with enhanced stacking and fluorescent capabilities: (**A**) 2,4-difluorotoluene (dF); (**B**) C1′-benzene; (**C**) C1′-pyrene. C2′-R refers to ribose or deoxyribose sugar.

1.4.4 Typical Modifications of the Sugar-Phosphate Backbone

While most studies concentrate on chemically modifying the sugar and nucleobase moieties within nucleic acids, fewer studies have focused on altering the native backbone due to the complexity and multi-step fashion of the proposed synthetic strategies and the reactivity of certain alterations to the automated process of synthesizing designer oligonucleotides.[81] However, some modifications to the backbone have proven to be quite effective and have led to the synthesis of novel DNA/RNA-based oligomers as well as polypeptides. One of the more popular modifications involves the substitution of a non-bridging oxygen atom with a sulphur atom producing a phosphorothioate (PS) linkage,[3, 8] which have been shown to stabilize siRNA molecules by inhibiting endonuclease cleavage and increase their circulation half-life by enhancing their binding

affinity for serum transport proteins (Figure 1.5).[3] A 21 base-pair ASO entirely comprised of PS linkages known as Vitravene, was the first ASO to be FDA approved as an antiviral agent for the treatment of cytomegaloviral infection of the eye in immunocompromised patients.[14] Despite these promising results, it has been found that siRNA duplexes containing PS modifications near the center of the sense strand or across the Ago2 cleavage site are non-functional,[8] and extensive PS modification can give rise to cytotoxic effects.[3, 8] One example that attempts to resolve this problem of cytotoxicity as an alternative to PS involves the introduction of a borane ($^{-}BH_3$) moiety in the phosphodiester linkage (Figure 1.5).[35, 82] Shaw and coworkers have found that this modification has been shown to increase siRNA potency when compared to the PS modification.[82] Furthermore, the boranophosphate (BP) modified siRNA molecule does not induce significant cytotoxicity in mammalian cells and can be readily incorporated into DNA and RNA oligomers by DNA or RNA polymerase with high binding specificity.[82]

PS and BP backbone modifications were chosen so as to provide added stability to oligonucleotide scaffolds, without compromising the ability to synthesize DNA or RNA molecules through polymerase activity.[82, 83] It is important to note that although both the PS and BP backbone modifications maintain natural synthesis of DNA or RNA oligomers,[82, 83] the problem inherent in the BP backbone modification in particular, is that all native unmodified nucleotides are replaced with those that are BP-modified.[82] This drawback concerning BP modification is important to address because there is much evidence to support the optimization of ASOs or siRNAs through selective modification in specified regions, thus improving resistance and functionality of the resultant molecules.[70, 82, 84] Another concern is that by introducing an additional functionality attached to the phosphate group, adds another chiral center to the oligonucleotide. The consideration of stereochemistry during the design and synthesis of modified oligomers is an important factor when trying to determine duplex thermostability, as well as target affinity.[85-87] Despite the aforementioned backbone modifications, they are not fully resistant to degradation and still retain the anionic nature of the siRNA complex, which remains the main culprit leading to decreased cell membrane permeability and hydrolysis. Expanding our repertoire of oligonucleotide backbone modifications, increases the

chance of discovering a unique and favourable nucleic acid modification profile with globalized applications. Unnatural modifications involved in replacing the phosphodiester, or the entire sugar-phosphate linkage could advance our pursuit in the discovery of this unique profile, which would propagate the development of ASOs and siRNA duplexes with effective gene-silencing capabilities *in vivo*, while still maintaining structural and functional integrity.

1.4.4.1 Unnatural Oligonucleotide Backbone Modifications

During the discovery of novel backbone modifications involving the replacement of native nucleotide structures, there is one modification that has shown considerable promise for some time and has been implicated in the formation of novel peptides and DNA oligomers. This has been achieved through the replacement of the sugar-phosphate backbone with repeating *N*-(2-aminoethyl) glycine units, where the nucleobases are attached to the chain via a methylene amide, forming what are known as peptide nucleic acids (PNAs) (Figure 1.5).[5, 83, 85, 88-94] Synthesized in 1991 by Nielsen and colleagues,[94] PNA is a DNA mimic which follows standard Watson-Crick base pairing and maintains a six-atom distance between successive bases in a strand, similar to wild-type strands of DNA and RNA. PNAs can form hybrid duplexes with DNA or RNA and also triplexes with all three constituents with remarkable binding affinities, even found to be notably higher than in natural DNA/RNA homo and heteroplexes.[83, 92, 95] PNAs are uncharged achiral molecules that are resistant to enzymatic cleavage and pass through cell membranes much more readily than their polyanionic counterparts.[83, 91, 92, 95] These properties inherited by PNAs are attributed to the amide linkages between successive nucleobases, which are neutral and therefore much more stable than the anionic phosphate linkages in native DNA/RNA molecules.

Aside from blocking gene expression at the translational level, ASOs have also been employed to invade double-stranded genomic DNA (dsDNA) and bind to their compliments, which is of interest to researchers who wish to discover the means of controlling gene expression at the transcriptional level. Development of synthetic oligonucleotides which are capable of dsDNA invasion with rapidity and efficiency was progressing slowly prior to the discovery of PNA.[5] PNA may be the simple yet effective

solution to the problem of dsDNA invasion because of its remarkable ability to sense and anneal to its complimentary sequence with very high affinity, and is a testament to the possibilities inherited through the chemical manipulation of oligonucleotides.

In addition to PNA as a novel backbone replacement modification, a number of studies have proven the rather non-discriminating nature of the RNAi pathway towards adopting and utilizing backbone homologues of this nature. Several backbone replacements have also shown compatibility within ASO constructs. Although few in number, some successful examples of backbone-modified siRNA constructs include: 1) a study by Iwase and associates showing that siRNAs containing a 3′- overhang amide-bond linkage displayed promising results;[96] and 2) a study by Zhang and associates involving a heterocyclic morpholino structure replacing the sugar.[97] This indicates that non-ionic backbone modifications are compatible with siRNA duplex formation and function. Examples of other novel backbone modifications incorporated into ASOs with comparable attributes to their native counterparts include: 1) double-constrained thymine dimers with 2′-4′ ethylene ribose bridges, joined by a cyclic phosphotriester internucleotide linkage (1,3,2-dioxaphosphorinane);[66] 2) benzene rings in place of the ribose sugar;[11] and 3) the N3′-P5′ phosphoramidate linkage.[98]

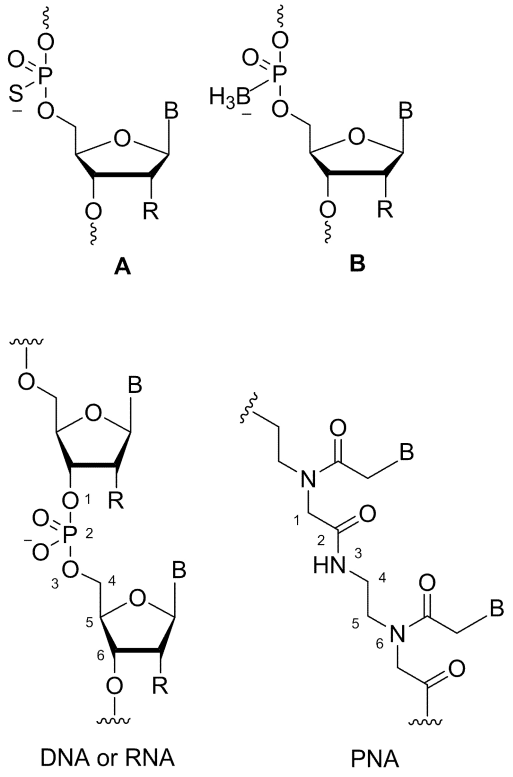

Figure 1.5 Structures of common phosphate backbone modifications: (**A**) phosphorothioate (PS), and (**B**) boranophosphate (-BH_3); and a comparison of the native DNA/RNA backbone with the unique peptide nucleic acid (PNA) scaffold. R-group denotes ribose or deoxyribose sugar.

The evidence supporting the compatibility of novel and diverse backbone modifications such as the successful PNA scaffold with antisense or RNAi applications, suggests the

likely discovery of new and effective backbone modification strategies in order to enhance the structural integrity, thermodynamic properties, cell membrane permeability and enzymatic resistance of both DNA and RNA-based oligonucleotides.

1.5 Click Chemistry

Since its discovery by Meldal and Sharpless in 2001,[99] the Cu(I)-catalyzed adaptation of Huisgen's 1,3-dipolar [3 + 2] azide-alkyne (CuAAC) cycloaddition has not only earned the title of "click" reaction, but has nearly become synonomous with the term due its speed, versatility, simplicity and its broad application.[100-103] This particular click cycloaddition has had a considerable impact on chemical transformations leading to the production of new materials[104, 105] and libraries of molecules with applications in biological systems.[101] The CuAAC reaction is an ideal bioorthogonal transformation because it can be performed under various environmental conditions, is high-yielding and expedient, the azide and alkyne moieties are physiologically inert,[106] and the regio- and stereospecificity of the triazole product is tightly controlled.[99] The CuAAC reaction gives rise to only the 1,4-disubstituted 1,2,3-triazole isomer, and in some cases eliminates the need for further purification of the final product.[99, 101, 103]

1.5.1 Modifying Nucleic Acids with Click Chemistry

Although there are many examples of chemical transformations being used to modify nucleic acid residues, click chemistry is becoming ubiquitous in its ability to modify the three main areas of nucleic acids with relative ease. According to the literature, most click-mediated modifications are performed on the nitrogenous bases by introducing novel base analogues,[107-110] attaching fluorophores or isotopic elements for molecular imaging,[71, 111-113] forming inter-strand linkages between oligonucleotides,[114-116] and the bioconjugation of molecules used for the assisted delivery of nucleic acid-based therapies.[117] Click chemistry has also given researchers the opportunity to target the backbone using a fairly simple synthetic procedure, with the goal of negating the effects imposed on nucleic acid derivatives through the problematic sugar-phosphate linkage. Knowing that the polyanionic structure of the native phosphodiester linkage is one of the main problems faced by oligonucleotides trying to emerge on the market as therapeutic

agents,[3, 35] click chemistry can introduce a neutrally-charged and physiologically stable heterocycle at this site. Another desirable property associated with the 1,2,3-triazole is its ability to form hydrogen bonds through N^2 and N^3 of the heterocycle,[101] which could allow triazole-linked polymers to interact with biological molecules such as blood-serum proteins, thus increasing their circulatory half-lives and biodistribution in living systems.

The use of triazoles in biological systems has gained popularity, due to their chemically inert nature within natural systems.[101, 105, 118] Triazoles have been used for many years as

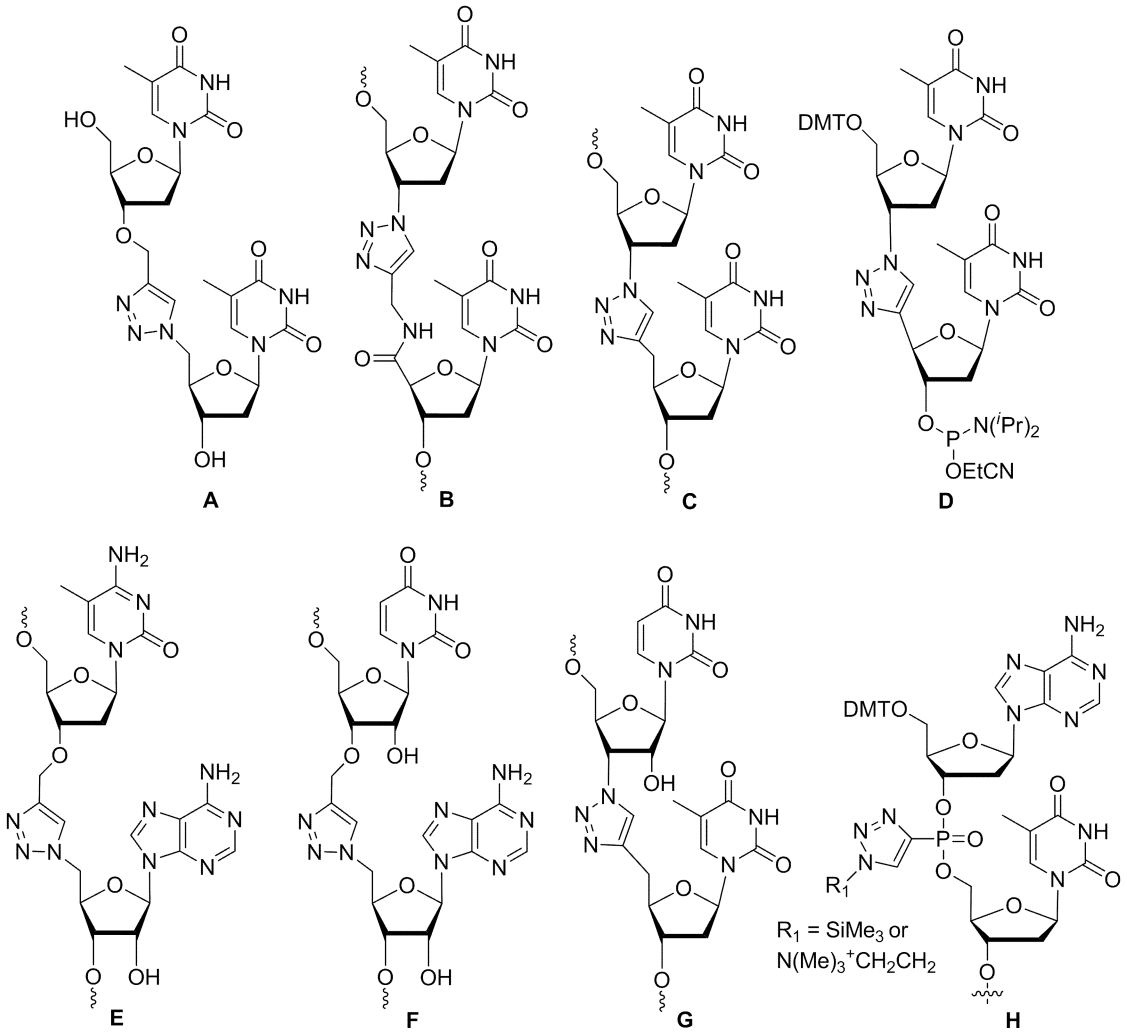

Figure 1.6 Examples of novel and unnatural non-phosphate triazole-linked nucleoside dimer analogues and a triazole-modified phosphate linkage, all introduced through the Cu(I) catalyzed "click" cycloaddition. Triazole-linked dimers **A**-**D** and **H** have found use in oligodeoxyribonucleotides, whereas **E**-**G** have formed both RNA and RNA:DNA chimeric oligonucleotides.

the basis for several varieties of antiviral and antifungal pharmaceuticals.[87] A widely studied antiviral pharmaceutical known as Virazole, is a nucleoside analogue with a substituent 1,2,4-triazole isoform tethered to the 1′ position of the furanose ring.[52, 119-121] Although there are other examples of oligonucleotides which tether nucleobases or nucleobase analogues to the sugar through a triazole linkage,[122, 123] or that link iterative bases through novel triazole-based internucleotide linkages (Figure 1.6),[81, 124-130] there is a need for expanding the use of triazole linkages within an siRNA context.

1.6 Modifying Nucleic Acids with Non-Phosphate Alkyl-Chain Linkages

Besides modifications to the existing backbone or the synthesis and implementation of novel sugar-phosphate replacement scaffolds, another avenue of backbone modifications which lacks sufficient investigation involves altering the physical distance between adjoined nucleotides. Given that the typical distance separating iterative bases in native oligonucleotides is in the form of a repetitive six atom linkage along the sugar-phosphate backbone: O3′, P, O5′, C5′, C4′, and C3′ (Figure 1.5), studies have associated alterations to this distance with potentially favourable changes to the physical and functional characteristics of modified oligomers.[131-133]

1.6.1 Physical Characteristics of Alkyl Chain-Modified Duplex Oligonucleotides

Many studies have investigated the target affinity and conformation of oligonucleotides which have been modified with nucleoside dimers, joined through non-phosphate alkyl linkers which increase the native inter-nucleobase distance by one atom. Influenced by PNA and its high affinity for both RNA and DNA target sequences, some studies adopted the use of alternative amide-based linkages. One such study by Kochetkova et al. synthesized a thymine-thymine dinucleoside linked through an amide and aminomethyl-based linker.[133] Through UV-monitored thermal denaturation experiments, the thermal stabilities of DNA duplexes steadily decreased as the number of modified dimers increased. A similar study observed the same phenomenon in dsDNA molecules when modified with one or more thioacetamido nucleic acid (TANA) linkages. In addition, TANA-modified DNA duplexes were noticeably transitioning from their natural B-form helical conformation, to the more RNA-like A-form conformation.[134] A contrasting study

characterized the RNA-binding affinities of DNA strands modified with several different amide-based linkages.[131] A general trend was observed, favouring the RNA binding capabilities of these amide-modified DNA strands, despite the presence of these seven atom inter-nucleobase linkages.

1.6.2 Functional Characteristics of Alkyl Chain-Modified siRNAs

Although the aforementioned studies were helpful in outlining the compatibility of alkyl chain linkages within DNA:DNA and DNA:RNA hybrid duplexes, few studies have shown the functional characteristics of DNA or RNA molecules containing these modifications. Using an amino-based linkage which shortens the native inter-nucleobase distance by two atoms, Sobczak et al. discovered that siRNA duplexes, modified at their 3′-overhangs with amino-linked thymine-thymine dimers were still capable of silencing their endogenous gene transcript with a potency comparable to wild-type, and greater than the activity of an siRNA known to target the same transcript.[135] Even more intriguing was the discovery made in 2009 by Ueno et al, whereby siRNAs containing variable-length alkyl-chain bulges which were centrally located between residues in the sense strand, were as efficacious at silencing the target reporter gene as the wild-type construct.[11] Of greater interest, was the discovery that an siRNA containing an abasic site on its sense strand upon inserting an alkyl-chain linkage, was still capable of silencing its target with a potency comparable to the siRNA with all of its nitrogenous bases, modified with an alkyl bulge of similar length.[11] These observations not only demonstrate the feasibility of introducing non-phosphate alkyl chain internucleotide linkages, but support the production of functional abasic oligonucleotides containing spacers of variable length to be used as ligands for the RNAi pathway.

1.7 Passenger Strand Cleavage and RNAi Activity

Given the world-wide utility of siRNAs for various biological purposes, the literature shows that remarkably little is known about the exact stepwise mechanism through which the process of RNAi is conducted. Some studies have attempted to elucidate this mechanism, with a particular focus on the steps involved while forming the active RISC-guide complex following the cleavage and removal of the passenger strand.[31, 36, 136] As

mentioned earlier, the endonuclease Ago2 is responsible for cleaving the passenger strand at the phosphate linkage, opposite residues 10 and 11 counting from the 5′ end of the guide strand, prior to its removal from the duplex. However, some studies have shown retention of the silencing activity elicited by siRNAs with sense strands containing chemical modifications surrounding, or directly within the Ago2 cleavage site.[29, 137] This phenomenon suggests the possibility of an alternative RNAi pathway, devoid of any physical sense strand cleavage event. By modifying the passenger strand with non-cleavable functionalities, the existence of this alternative pathway can be proven with more validity.

1.8 Research Objectives

The ability to silence the expression of any gene at the translational level, has proven its ubiquitous utility in the discovery of gene function and can eventually become a powerful therapeutic tool used to control genetic disease. The endogenous RNAi process provides us with an avenue through which synthetic siRNAs can enforce the down-regulation of gene expression with high accuracy and efficacy at low concentrations. Studies have proven that chemical modification of siRNAs is required to overcome their limitations such as poor cell membrane permeability, susceptibility to nuclease-mediated degradation and off-target toxicity. These drawbacks within both DNA and RNA molecules result from the negatively charged phosphodiester linkage which can be enzymatically hydrolyzed and can suffer an intramolecular attack from the 2′-OH group in ribonucleic acids.

The primary focus of this study involved chemically modifying the sugar-phosphate backbone of both DNA and RNA oligonucleotides. Novel PNA-based nucleoside dimer analogs containing a neutrally charged triazole-based internucleotide linkage introduced through “click” chemistry, were site-specifically introduced throughout synthetic oligonucleotides. These triazole-linked nucleoside dimer analogs should be compatible within duplex DNA and RNA molecules and ultimately within siRNAs. This hypothesis was supported by the demonstrated use of the triazole heterocycle within the backbone of DNA molecules in the literature and the relative ease of its synthesis, along with the success of the popular DNA-mimic known as PNA which served as our scaffold. Based

on this hypothesis, the following are the tests that were performed involving our triazole-linked nucleoside dimer analogs: 1) to check the hybridization capabilities of these dimers within duplex DNA molecules and whether or not they increase or decrease the thermostability of these duplexes. Since they proved compatible and destabilizing within duplex DNAs; 2) both physical and functional characteristics of duplex siRNAs which contain these modifications throughout the sense strand, and within the 3′ overhangs of either strand were monitored. The physical characteristics of interest were siRNA duplex thermostability, helical conformation, and nuclease stability. The potency of our siRNAs was tested by targeting the transiently-expressed reporter gene *firefly* luciferase and the endogenous gene GAPDH using cell-based assays. Upon discovering that siRNAs modified with our neutral triazole-based internucleotide linkages were very capable of silencing gene expression, maintaining RNA′s helical conformation and proved to last longer in blood serum than native siRNAs, the effects of using simpler, neutrally-charged and destabilizing modifications positioned throughout siRNAs were explored. For the final phase of this study: 3) the physical and functional characteristics of *f*. luciferase-targeting siRNAs which were modified with abasic alkyl chain linkages of varying length were assessed. As was performed in the previous phase of this study, the thermostability and helical conformation of these spacer-modified siRNAs were monitored, and the potency of these siRNAs was tested within cell-based assays by targeting the *firefly* luciferase transcript.

References – Chapter I – Literature Review:

1. Cencic, R.; Robert, F.; Pelletier, J., Identifying small molecule inhibitors of eukaryotic translation initiation, in *Method. Enzymol.* **2007**, J. Lorsch, Editor. p. 269-302.

2. Chen, Y.; Bodles, A., Amyloid precursor protein modulates beta-catenin degradation. *J. Neuroinflamm.* **2007**, *4*.

3. Corey, D.R., Chemical modification: the key to clinical application of RNA interference? *J. Clin. Invest.* **2007**, *117*, 3615-3622.

4. Gore, L.; Degregori, J.; Porter, C.C., Targeting developmental pathways in children with cancer: what price success? *Lancet Oncol.* **2013**, *14*, e70-78.

5. Kaihatsu, K.; Janowski, B.A.; Corey, D.R., Recognition of chromosomal DNA by PNAs. *Chem. Biol.* **2004**, *11*, 749-758.

6. Crooke, S.T., Basic Principles of Antisense Technology, in *Antisense Drug Technology* **2009**, CRC Press.

7. Dassie, J.P.; Liu, X.-y.; Thomas, G.S.; Whitaker, R.M.; Thiel, K.W.; Stockdale, K.R.; Meyerholz, D.K.; McCaffrey, A.P.; McNamara, J.O.; Giangrande, P.H., Systemic administration of optimized aptamer-siRNA chimeras promotes regression of PSMA-expressing tumors. *Nat. Biotech.* **2009**, *27*, 839-846.

8. Watts, J.K.; Deleavey, G.F.; Damha, M.J., Chemically modified siRNA: tools and applications. *Drug Discov. Today.* **2008**, *13*, 842-855.

9. Keefe, A.D.; Pai, S.; Ellington, A., Aptamers as therapeutics. *Nat. Rev. Drug Discov.* **2010**, *9*, 537-550.

10. Musumeci, D.; Roviello, G.N.; Moccia, M.; Pedone, C.; Bucci, E.M.; Sapio, R.; Valente, M.; Fumero, S., Bent oligonucleotide duplexes as hmgb1 inhibitors: A comparative study. *Nucleosides Nucleotides Nucleic Acids.* **2007**, *26*, 1447-1450.

11. Ueno, Y.; Kawamura, A.; Takasu, K.; Komatsuzaki, S.; Kato, T.; Kuboe, S.; Kitamura, Y.; Kitabe, Y., Synthesis and properties of a novel molecular beacon containing a benzene-phosphate backbone at its stem moiety. *Org. Biomol. Chem.* **2009**, *7*, 2761-2769.

12. Stephenson, M.L.; Zamecnik, P.C., Inhibition of Rous sarcoma viral RNA translation by a specific oligodeoxyribonucleotide. *Proc. Natl. Acad. Sci. USA.* **1978**, *75*, 285-288.

13. Manoharan, M., Oligonucleotide Conjugates in Antisense Technology, in *Antisense Drug Technology* **2009**, CRC Press.

14. Mercola, D., Combined Antisense Therapy and Chemotherapy in Animal Models, in *Antisense Drug Technology* **2009**, CRC Press.

15. Grillone, L., The Development of Antisense Oligonucleotides as Antivirals, in *Antisense Drug Technology* **2009**, CRC Press.

16. Nyce, J., Respirable Antisense Oligonucleotides (RASONs), in *Antisense Drug Technology* **2009**, CRC Press.

17. Gewirtz, l., Nucleic Acid Therapeutics for the Treatment of Human Leukemia, in *Antisense Drug Technology* **2009**, CRC Press.

18. Tomizawa, J.I.; Itoh, T.; Selzer, G.; Som, T., Inhibition of ColE1 RNA primer formation by a plasmid-specified small RNA. *Proc. Natl. Acad. Sci. USA.* **1981**, *78*, 1421-1425.

19. Dan Cook, P., Medicinal Chemistry of Antisense Oligonucleotides, in *Antisense Drug Technology* **2009**, CRC Press.

20. Crooke, S.T., Basic Principles of Antisense Therapeutics, in *Antisense Research and Application* **1998**, Springer Berlin Heidelberg. p. 1-50.

21. Patureau, B.M.; Hudson, R.H.E.; Damha, M.J., Induction of RNase H activity by arabinose-peptide nucleic acid chimeras. *Bioconjugate Chem.* **2007**, *18*, 421-430.

22. Fire, A.; Xu, S.Q.; Montgomery, M.K.; Kostas, S.A.; Driver, S.E.; Mello, C.C., Potent and specific genetic interference by double-stranded RNA in *Caenorhabditis elegans*. *Nature.* **1998**, *391*, 806-811.

23. Fire, A.; Albertson, D.; Harrison, S.W.; Moerman, D.G., Production of antisense RNA leads to effective and specific inhibition of gene expression in *C. elegans* muscle. *Development.* **1991**, *113*, 503-514.

24. Ding, S.-W.; Voinnet, O., Antiviral immunity directed by small RNAs. *Cell.* **2007**, *130*, 413-426.

25. van den Berg, A.; Mols, J.; Han, J.H., RISC-target interaction: Cleavage and translational suppression. *Biochim. Biophys. Acta.* **2008**, *1779*, 668-677.

26. Peng Ho, S., Application of Antisense Oligonucleotides to the Study of CNS Protein Function, in *Antisense Drug Technology* **2009**, CRC Press.

27. Macris, M.; Glazer, e., Targeted Genome Modification via Triple Helix Formation, in *Antisense Drug Technology* **2009**, CRC Press.

28. Daniels, S.M.; Gatignol, A., The Multiple Functions of TRBP, at the Hub of Cell Responses to Viruses, Stress, and Cancer. *Microbiol. Mol. Biol. Rev.* **2012**, *76*, 652-666.

29. Matranga, C.; Tomari, Y.; Shin, C.; Bartel, D.P.; Zamore, P.D., Passenger-strand cleavage facilitates assembly of siRNA into Ago2-containing RNAi enzyme complexes. *Cell.* **2005**, *123*, 607-620.

30. Gredell, J.A.; Dittmer, M.J.; Wu, M.; Chan, C.; Walton, S.P., Recognition of siRNA Asymmetry by TAR RNA Binding Protein. *Biochemistry.* **2010**, *49*, 3148-3155.

31. Wang, B.; Li, S.; Qi, H.H.; Chowdhury, D.; Shi, Y.; Novina, C.D., Distinct passenger strand and mRNA cleavage activities of human Argonaute proteins. *Nat. Struct. Mol. Biol.* **2009**, *16*, 1259-U1276.

32. Wang, Y.L.; Sheng, G.; Juranek, S.; Tuschl, T.; Patel, D.J., Structure of the guide-strand-containing argonaute silencing complex. *Nature.* **2008**, *456*, 209-U234.

33. Lima, W.F.; Wu, H.; Nichols, J.G.; Sun, H.; Murray, H.M.; Crooke, S.T., Binding and Cleavage Specificities of Human Argonaute2. *J. Biol. Chem.* **2009**, *284*, 26017-26028.

34. Deleavey, G.F.; Damha, M.J., Designing Chemically Modified Oligonucleotides for Targeted Gene Silencing. *Chem. Biol.* **2012**, *19*, 937-954.

35. Bumcrot, D.; Manoharan, M.; Koteliansky, V.; Sah, D.W.Y., RNAi therapeutics: a potential new class of pharmaceutical drugs. *Nat. Chem. Biol.* **2006**, *2*, 711-719.

36. Leuschner, P.J.F.; Ameres, S.L.; Kueng, S.; Martinez, J., Cleavage of the siRNA passenger strand during RISC assembly in human cells. *Embo Rep.* **2006**, *7*, 314-320.

37. Kenski, D.M.; Cooper, A.J.; Li, J.J.; Willingham, A.T.; Haringsma, H.J.; Young, T.A.; Kuklin, N.A.; Jones, J.J.; Cancilla, M.T.; McMasters, D.R.; Mathur, M.; Sachs, A.B.; Flanagan, W.M., Analysis of acyclic nucleoside modifications in siRNAs finds sensitivity at position 1 that is restored by 5′-terminal phosphorylation both *in vitro* and *in vivo*. *Nucleic Acids Res.* **2010**, *38*, 660-671.

38. Schirle, N.T.; MacRae, I.J., The Crystal Structure of Human Argonaute2. *Science.* **2012**, *336*, 1037-1040.

39. Luo, P.; Leitzel, J.C.; Zhan, Z.-Y.J.; Lynn, D.G., Analysis of the Structure and Stability of a Backbone-Modified Oligonucleotide: Implications for Avoiding Product Inhibition in Catalytic Template-Directed Synthesis. *J. Am. Chem. Soc.* **1998**, *120*, 3019-3031.

40. Collingwood, M.A.; Rose, S.D.; Huang, L.Y.; Hillier, C.; Amarzguioui, M.; Wiiger, M.T.; Soifer, H.S.; Rossi, J.J.; Behlke, M.A., Chemical modification patterns compatible with high potency Dicer-substrate small interfering RNAs. *Oligonucleotides.* **2008**, *18*, 187-199.

41. Jeong, J.H.; Mok, H.; Oh, Y.-K.; Park, T.G., siRNA Conjugate Delivery Systems. *Bioconjugate Chem.* **2009**, *20*, 5-14.

42. Bramsen, J.B.; Laursen, M.B.; Nielsen, A.F.; Hansen, T.B.; Bus, C.; Langkjaer, N.; Babu, B.R.; Hojland, T.; Abramov, M.; Van Aerschot, A.; Odadzic, D.; Smicius, R.; Haas, J.; Andree, C.; Barman, J.; Wenska, M.; Srivastava, P.; Zhou, C.; Honcharenko, D.; Hess, S.; Mueller, E.; Bobkov, G.V.; Mikhailov, S.N.; Fava, E.; Meyer, T.F.; Chattopadhyaya, J.; Zerial, M.; Engels, J.W.; Herdewijn, P.; Wengel, J.; Kjems, J., A large-scale chemical modification screen identifies design rules to generate siRNAs with high activity, high stability and low toxicity. *Nucleic Acids Res.* **2009**, *37*, 2867-2881.

43. Lavergne, T.; Bertrand, J.R.; Vasseur, J.J.; Debart, F., A Base-Labile Group for 2 ′-OH Protection of Ribonucleosides: A Major Challenge for RNA Synthesis. *Chem.-Eur. J.* **2008**, *14*, 9135-9138.

44. Muller, S.; Wolf, J.; Ivanov, S.A., Current strategies for the synthesis of RNA. *Curr. Org. Synth.* **2004**, *1*, 293-307.

45. Levin, A.; Henry, S.; Monteith, D.; Templin, M., Toxicity of Antisense Oligonucleotides, in *Antisense Drug Technology* **2009**, CRC Press.

46. John, M.; Constien, R.; Akinc, A.; Goldberg, M.; Moon, Y.A.; Spranger, M.; Hadwiger, P.; Soutschek, J.; Vornlocher, H.P.; Manoharan, M.; Stoffel, M.; Langer, R.; Anderson, D.G.; Horton, J.D.; Koteliansky, V.; Bumcrot, D., Effective RNAi-mediated gene silencing without interruption of the endogenous microRNA pathway. *Nature.* **2007**, *449*, 745-U712.

47. Khaliq, S.; Khaliq, S.A.; Zahur, M.; Ijaz, B.; Jahan, S.; Ansar, M.; Riazuddin, S.; Hassan, S., RNAi as a new therapeutic strategy against HCV. *Biotechnol. Adv.* **2010**, *28*, 27-34.

48. Jackson, A.L.; Linsley, P.S., Recognizing and avoiding siRNA off-target effects for target identification and therapeutic application. *Nat. Rev. Drug Discov.* **2010**, *9*, 57-67.

49. Robbins, M.; Judge, A.; MacLachlan, I., siRNA and Innate Immunity. *Oligonucleotides.* **2009**, *19*, 89-101.

50. Alvaradourbina, G.; Sathe, G.M.; Liu, W.C.; Gillen, M.F.; Duck, P.D.; Bender, R.; Ogilvie, K.K., Automated Synthesis of Gene Fragments. *Science.* **1981**, *214*, 270-274.

51. Lin, J.; Roy, V.; Wang, L.; You, L.; Agrofoglio, L.A.; Deville-Bonne, D.; McBrayer, T.R.; Coats, S.J.; Schinazi, R.F.; Eriksson, S., 3 ′-(1,2,3-Triazol-1-yl)-3 ′-deoxythymidine analogs as substrates for human and Ureaplasma parvum thymidine kinase for structure-activity investigations. *Bioorg. Med. Chem.* **2010**, *18*, 3261-3269.

52. Streeter, D.G.; Witkowsk.Jt; Khare, G.P.; Sidwell, R.W.; Bauer, R.J.; Robins, R.K.; Simon, L.N., Mechanism of Action of 1-*b*-D-Ribofuranosyl-1,2,4-Triazole-

3-Carboxamide (Virazole), A New Broad-Spectrum Antiviral Agent. *Proc. Natl. Acad. Sci. USA.* **1973**, *70*, 1174-1178.

53. Baraniak, D.; Kacprzak, K.; Celewicz, L., Synthesis of 3 ′-azido-3 ′-deoxythymidine (AZT)-Cinchona alkaloid conjugates via click chemistry: Toward novel fluorescent markers and cytostatic agents. *Bioorg. Med. Chem. Lett.* **2011**, *21*, 723-726.

54. Scaringe, S.A.; Francklyn, C.; Usman, N., Chemical Synthesis of Biologically Active Oligoribonucleotides using *b*-Cyanoethyl Protected Ribonucleoside Phosphoramidites. *Nucleic Acids Res.* **1990**, *18*, 5433-5442.

55. Ohtsuka, E.; Ikehara, M.; Soll, D., Recent developments in the chemical synthesis of polynucleotides. *Nucleic Acids Res.* **1982**, *10*, 6553-6570.

56. Caruthers, M.H., Chemical Synthesis of DNA and DNA Analogs. *Accounts Chem. Res.* **1991**, *24*, 278-284.

57. Dahl, B.H.; Nielsen, J.; Dahl, O., Mechanistic studies on the phosphoramidite coupling reaction in oligonucleotide synthesis 1. Evidence for nucleophilic catalysis by tetrazole and rate variations with the phosphorus substituents. *Nucleic Acids Res.* **1987**, *15*, 1729-1743.

58. Wu, X.; Pitsch, S., Synthesis and pairing properties of oligoribonucleotide analogues containing a metal-binding site attached to b-D-allofuranosyl cytosine. *Nucleic Acids Res.* **1998**, *26*, 4315-4323.

59. Ellington, A.; Pollard, J.D., Jr., Synthesis and purification of oligonucleotides. *Current protocols in molecular biology / edited by Frederick M. Ausubel ... [et al.]*. **2001**, *Chapter 2*, Unit2.11-Unit12.11.

60. Pitsch, S.; Weiss, Patrick A.; Jenny, L.; Stutz, A.; Wu, X., Reliable Chemical Synthesis of Oligoribonucleotides (RNA) with 2′-*O*-[(Triisopropylsilyl)oxy]methyl(2′-*O*-tom)-Protected Phosphoramidites. *Helv. Chim. Acta.* **2001**, *84*, 3773-3795.

61. Scaringe, S.A., Advanced 5′-Silyl-2′-Orthoester Approach to RNA Oligonucleotide Synthesis, in *Method. Enzymol.* **2000**. p. 3-18.

62. Tripathi, S.; Misra, K.; Sanghvi, Y.S., One-ot synthesis of TBMPS (*bis* (*tert*-butyl)-1 pyrenylmethyl-silyl) chloride as a novel fluorescent silicon-based protecting group for protection of 5 ′-OH nucleosides and its use as purification handle in oligonucleotide synthesis. *Nucleosides Nucleotides Nucleic Acids.* **2005**, *24*, 1345-1351.

63. Li, F.; Sarkhel, S.; Wilds, C.J.; Wawrzak, Z.; Prakash, T.P.; Manoharan, M.; Egli, M., 2 ′-fluoroarabino- and arabinonucleic acid show different conformations, resulting in deviating RNA affinities and processing of their heteroduplexes with RNA by RNase H. *Biochemistry.* **2006**, *45*, 4141-4152.

64. Watts, J.K.; Damha, M.J., 2′F-Arabinonucleic acids (2′F-ANA) - History, properties, and new frontiers. *Can. J. Chemistry.* **2008**, *86*, 641-656.

65. Deleavey, G.F.; Watts, J.K.; Alain, T.; Robert, F.; Kalota, A.; Aishwarya, V.; Pelletier, J.; Gewirtz, A.M.; Sonenberg, N.; Damha, M.J., Synergistic effects between analogs of DNA and RNA improve the potency of siRNA-mediated gene silencing. *Nucleic Acids Res.* **2010**, *38*, 4547-4557.

66. Zhou, C.; Plashkevych, O.; Chattopadhyaya, J., Double Sugar and Phosphate Backbone-Constrained Nucleotides : Synthesis, Structure, Stability, and Their Incorporation into Oligodeoxynucleotides. *J. Org. Chem.* **2009**, *74*, 3248-3265.

67. Wengel, J., LNA (Locked Nucleic Acid), in *Antisense Drug Technology* **2009**, CRC Press.

68. Dean, N.; Butler, M.; Monia, B.; Manoharan, M., Pharmacology of 2′-O-(2-Methoxy)ethyl- Modified Antisense Oligonucleotides, in *Antisense Drug Technology* **2009**, CRC Press.

69. Obika, S.; Rahman, S.M.A.; Song, B.; Onoda, M.; Koizumi, M.; Morita, K.; Imanishi, T., Synthesis and properties of 3 ′-amino-2 ′,4 ′-BNA, a bridged nucleic acid with a N3 ′-> P5 ′ phosphoramidate linkage. *Bioorg. Med. Chem.* **2008**, *16*, 9230-9237.

70. Cho, I.S.; Kim, J.; Lim, D.H.; Ahn, H.C.; Kim, H.; Lee, K.B.; Lee, Y.S., Improved serum stability and biophysical properties of siRNAs following chemical modifications. *Biotechnol. Lett.* **2008**, *30*, 1901-1908.

71. Dodd, D.W.; Swanick, K.N.; Price, J.T.; Brazeau, A.L.; Ferguson, M.J.; Jones, N.D.; Hudson, R.H.E., Blue fluorescent deoxycytidine analogues: convergent synthesis, solid-state and electronic structure, and solvatochromism. *Org. Biomol. Chem.* **2010**, *8*, 663-666.

72. Peacock, H.; Maydanovych, O.; Beal, P.A., N-2-Modified 2-aminopurine ribonucleosides as minor-groove-modulating adenosine replacements in duplex RNA. *Org. Lett.* **2010**, *12*, 1044-1047.

73. Caruthers, M.H.; Barone, A.D.; Beaucage, S.L.; Dodds, D.R.; Fisher, E.F.; McBride, L.J.; Matteucci, M.; Stabinsky, Z.; Tang, J.Y., Chemical Synthesis of Deoxyoligonucleotides by the Phosphoramidite Method. *Method. Enzymol.* **1987**, *154*, 287-313.

74. Wilson, J.N.; Kool, E.T., Fluorescent DNA base replacements: reporters and sensors for biological systems. *Org. Biomol. Chem.* **2006**, *4*, 4265-4274.

75. Efthymiou, T.; Gong, W.; Desaulniers, J.-P., Chemical Architecture and Applications of Nucleic Acid Derivatives Containing 1,2,3-Triazole Functionalities Synthesized via Click Chemistry. *Molecules.* **2012**, *17*, 12665-12703.

76. Kim, T.W.; Kool, E.T., A series of nonpolar thymidine analogues of increasing size: DNA base pairing and stacking properties. *J. Org. Chem.* **2005**, *70*, 2048-2053.

77. Kool, E.T., Replacing the nucleohases in DNA with designer molecules. *Accounts Chem. Res.* **2002**, *35*, 936-943.

78. Xia, J.; Noronha, A.; Toudjarska, I.; Li, F.; Akinc, A.; Braich, R.; Frank-Kamenetsky, M.; Rajeev, K.G.; Egli, M.; Manoharan, M., Gene Silencing Activity of siRNAs with a Ribo-difluorotoluyl Nucleotide. *ACS Chem. Biol.* **2006**, *1*, 176-183.

79. Schweitzer, B.A.; Kool, E.T., Aromatic Nonpolar Nucleosides as Hydrophobic Isosteres of Pyrimidine and Purine Nucleosides. *J. Org. Chem.* **1994**, *59*, 7238-7242.

80. Kocalka, P.; Andersen, N.K.; Jensen, F.; Nielsen, P., Synthesis of 5-(1,2,3-triazol-4-yl)-2′deoxyuridines by a click chemistry approach: Stacking of triazoles in the major groove gives increased nucleic acid duplex stability. *ChemBioChem.* **2007**, *8*, 2106-2116.

81. Krishna, H.; Caruthers, M.H., Alkynyl Phosphonate DNA: A Versatile "Click"able Backbone for DNA-Based Biological Applications. *J. Am. Chem. Soc.* **2012**, *134*, 11618-11631.

82. Hall, A.H.S.; Wan, J.; Spesock, A.; Sergueeva, Z.; Shaw, B.R.; Alexander, K.A., High potency silencing by single-stranded boranophosphate siRNA. *Nucleic Acids Res.* **2006**, *34*, 2773-2781.

83. Bialy, L.; Diaz-Mochon, J.J.; Specker, E.; Keinicke, L.; Bradley, M., Dde-protected PNA monomers, orthogonal to Fmoc, for the synthesis of PNA-peptide conjugates. *Tetrahedron.* **2005**, *61*, 8295-8305.

84. Bajor, Z.; Sagi, G.; Tegyey, Z.; Kraicsovits, F., PNA-DNA chimeras containing 5-alkynyl-pyrimidine PNA units. Synthesis, binding properties, and enzymatic stability. *Nucleosides Nucleotides Nucleic Acids.* **2003**, *22*, 1963-1983.

85. Tedeschi, T.; Corradini, R.; Marchelli, R.; Pushl, A.; Nielsen, P.E., Racemization of chiral PNAs during solid-phase synthesis: effect of the coupling conditions on enantiomeric purity. *Tetrahedron-Asymmetr.* **2002**, *13*, 1629-1636.

86. Lusvarghi, S.; Murphy, C.T.; Roy, S.; Tanious, F.A.; Sacui, I.; Wilson, W.D.; Ly, D.H.; Armitage, B.A., Loop and Backbone Modifications of Peptide Nucleic Acid Improve G-Quadruplex Binding Selectivity. *J. Am. Chem. Soc.* **2009**, *131*, 18415-18424.

87. Modzelewska-Banachiewicz, B.; Michalec, B.; Kaminska, T.; Mazur, L.; Koziol, A.E.; Banachiewicz, J.; Ucherek, M.; Kandefer-Szerszen, M., Synthesis and

biological activity of (Z) and (E) isomers of 3-(3,4-diaryl-1,2,4-triazole-5-yl)prop-2-enoic acid. *Monatsh Chem.* **2009**, *140*, 439-444.

88. Howarth, N.M.; Lindsell, W.E.; Murray, E.; Preston, P.N., Lipophilic peptide nucleic acids containing a 1,3-diyne function: synthesis, characterization and production of derived polydiacetylene liposomes. *Tetrahedron.* **2005**, *61*, 8875-8887.

89. Qu, G.R.; Zhang, Z.G.; Guo, H.M.; Geng, M.W.; Xia, R., Microwave-promoted facile and efficient preparation of N-(alkoxycarbonylmethyl) nucleobases - Building blocks for peptide nucleic acids. *Molecules.* **2007**, *12*, 543-551.

90. Thomson, S.A.; Josey, J.A.; Cadilla, R.; Gaul, M.D.; Hassman, C.F.; Luzzio, M.J.; Pipe, A.J.; Reed, K.L.; Ricca, D.J.; Wiethe, R.W.; Noble, S.A., Fmoc mediated synthesis of peptide nucleic acids. *Tetrahedron.* **1995**, *51*, 6179-6194.

91. Wojciechowski, F.; Hudson, R.H.E., A Convenient Route to *N*-[2-(Fmoc)aminoethyl]glycine Esters and PNA Oligomerization Using a Bis-*N*-Boc Nucleobase Protecting Group Strategy. *J. Org. Chem.* **2008**, *73*, 3807-3816.

92. Wu, Y.; Xu, J.C.; Liu, J.; Jin, Y.X., Synthesis of N-Boc and N-Fmoc dipeptoids with nucleobase residues as peptoid nucleic acid monomers. *Tetrahedron.* **2001**, *57*, 3373-3381.

93. Dueholm, K.L.; Egholm, M.; Behrens, C.; Christensen, L.; Hansen, H.F.; Vulpius, T.; Petersen, K.H.; Berg, R.H.; Nielsen, P.E.; Buchardt, O., Synthesis of Peptide Nucleic-Acid Monomers Containing the 4 Natural Nucleobases - Thymine, Cytosine, Adenine, and Guanine and Their Oligomerization. *J. Org. Chem.* **1994**, *59*, 5767-5773.

94. Nielsen, P.E.; Egholm, M.; Berg, R.H.; Buchardt, O., Sequence-Selective Recognition of DNA by Strand Displacement with a Thymine-Substituted Polyamide. *Science.* **1991**, *254*, 1497-1500.

95. Breipohl, G.; Knolle, J.; Langner, D.; Omalley, G.; Uhlmann, E., Synthesis of polyamide nucleic acids (PNAs) using a novel Fmoc/Mmt protecting-group combination. *Bioorg. Med. Chem. Lett.* **1996**, *6*, 665-670.

96. Iwase, R.; Toyama, T.; Nishimori, K., Solid-phase synthesis of modified RNAs containing amide-linked oligoribonucleosides at their 3 ′-end and their application to siRNA. *Nucleosides Nucleotides Nucleic Acids.* **2007**, *26*, 1451-1454.

97. Zhang, N.; Tan, C.; Cai, P.; Zhang, P.; Zhao, Y.; Jiang, Y., RNA interference in mammalian cells by siRNAs modified with morpholino nucleoside analogues. *Bioorg. Med. Chem. Lett.* **2009**, *17*, 2441-2446.

98. Gryaznov, S.; Chen, J.-K., Oligodeoxyribonucleotide N3′ -> P5′ phosphoramidates: Synthesis and hybridization properties. *J. Am. Chem. Soc.* **1994**, *116*, 3143-3144.

99. Kolb, H.C.; Finn, M.G.; Sharpless, K.B., Click Chemistry: Diverse Chemical Function from a Few Good Reactions. *Angew. Chem. Int. Ed.* **2001**, *40*, 2004-2021.

100. Amblard, F.; Cho, J.H.; Schinazi, R.F., Cu(I)-Catalyzed Huisgen Azide-Alkyne 1,3-Dipolar Cycloaddition Reaction in Nucleoside, Nucleotide, and Oligonucleotide Chemistry. *Chem. Rev.* **2009**, *109*, 4207-4220.

101. Kolb, H.C.; Sharpless, K.B., The growing impact of click chemistry on drug discovery. *Drug Discov. Today.* **2003**, *8*, 1128-1137.

102. Meldal, M.; Tornoe, C.W., Cu-Catalyzed Azide-Alkyne Cycloaddition. *Chem. Rev.* **2008**, *108*, 2952-3015.

103. Rostovtsev, V.V.; Green, L.G.; Fokin, V.V.; Sharpless, K.B., A stepwise Huisgen cycloaddition process: Copper(I)-catalyzed regioselective "ligation" of azides and terminal alkynes. *Angew. Chem. Int. Edit.* **2002**, *41*, 2596-2599.

104. de Miguel, G.; Wielopolski, M.; Schuster, D.I.; Fazio, M.A.; Lee, O.P.; Haley, C.K.; Ortiz, A.L.; Echegoyen, L.; Clark, T.; Guldi, D.M., Triazole Bridges as Versatile Linkers in Electron Donor-Acceptor Conjugates. *J. Am. Chem. Soc.* **2011**, *133*, 13036-13054.

105. van Dijk, M.; Nollet, M.L.; Weijers, P.; Dechesne, A.C.; van Nostrum, C.F.; Hennink, W.E.; Rijkers, D.T.S.; Liskamp, R.M.J., Synthesis and Characterization of Biodegradable Peptide-Based Polymers Prepared by Microwave-Assisted Click Chemistry. *Biomacromolecules.* **2008**, *9*, 2834-2843.

106. El-Sagheer, A.H.; Brown, T., Click chemistry with DNA. *Chem. Soc. Rev.* **2010**, *39*, 1388-1405.

107. Saito, Y.; Escuret, V.; Durantel, D.; Zoulim, F.; Schinazi, R.F.; Agrofoglio, L.A., Synthesis of 1,2,3-triazolo-carbanucleoside analogues of ribavirin targeting an HCV in replicon. *Bioorg. Med. Chem.* **2003**, *11*, 3633-3639.

108. El Akri, K.; Bougrin, K.; Balzarini, J.; Faraj, A.; Benhida, R., Efficient synthesis and *in vitro* cytostatic activity of 4-substituted triazolyl-nucleosides. *Bioorg. Med. Chem. Lett.* **2007**, *17*, 6656-6659.

109. Ming, X.; Seela, F., A Nucleobase-Discriminating Pyrrolo-dC Click Adduct Designed for DNA Fluorescence Mismatch Sensing. *Chem.-Eur. J.* **2012**, *18*, 9590-9600.

110. Xiong, Z.; Qiu, X.-L.; Huang, Y.; Qing, F.-L., Regioselective synthesis of 5-trifluoromethyl-1,2,3-triazole nucleoside analogues via TBS-directed 1,3-dipolar cycloaddition reaction. *J. Fluorine Chem.* **2011**, *132*, 166-174.

111. Gramlich, P.M.E.; Warncke, S.; Gierlich, J.; Carell, T., Click-click-click: Single to triple modification of DNA. *Angew. Chem. Int. Edit.* **2008**, *47*, 3442-3444.

112. Ostergaard, M.E.; Guenther, D.C.; Kumar, P.; Baral, B.; Deobald, L.; Paszczynski, A.J.; Sharma, P.K.; Hrdlicka, P.J., Pyrene-functionalized triazole-linked 2 ′-deoxyuridines-probes for discrimination of single nucleotide polymorphisms (SNPs). *Chem. Comm.* **2010**, *46*, 4929-4931.

113. Seela, F.; Ingale, S.A., "Double Click" Reaction on 7-Deazaguanine DNA: Synthesis and Excimer Fluorescence of Nucleosides and Oligonucleotides with Branched Side Chains Decorated with Proximal Pyrenes. *J. Org. Chem.* **2010**, *75*, 284-295.

114. Xiong, H.; Seela, F., Cross-Linked DNA: Site-Selective "Click" Ligation in Duplexes with Bis-Azides and Stability Changes Caused by Internal Cross-Links. *Bioconjugate Chem.* **2012**, *23*, 1230-1243.

115. El-Sagheer, A.H., Very stable end-sealed double stranded DNA by click chemistry. *Nucleosides Nucleotides Nucleic Acids.* **2009**, *28*, 315-323.

116. Jacobsen, M.F.; Ravnsbaek, J.B.; Gothelf, K.V., Small molecule induced control in duplex and triplex DNA-directed chemical reactions. *Org. Biomol. Chem.* **2010**, *8*, 50-52.

117. Seela, F.; Xiong, H.; Budow, S., Synthesis and ′double click′ density functionalization of 8-aza-7-deazaguanine DNA bearing branched side chains with terminal triple bonds. *Tetrahedron.* **2010**, *66*, 3930-3943.

118. Liu, Y.Q.; Zhang, L.H.; Wan, J.P.; Li, Y.S.; Xu, Y.H.; Pan, Y.J., Design and synthesis of cyclo[-Arg-Gly-Asp-Psi(triazole)-Gly-Xaa-] peptide analogues by click chemistry. *Tetrahedron.* **2008**, *64*, 10728-10734.

119. Huffman, J.H.; Sidwell, R.W.; Khare, G.P.; Witkowsk.Jt; Allen, L.B.; Robins, R.K., In Vitro Effect of 1-*b*-D-Ribofuranosyl-1,2,4-Triazole-3-Carboxamide (Virazole, ICN 1229) on Deoxyribonucleic Acid and Ribonucleic Acid Viruses. *Antimicrob. Agents Ch.* **1973**, *3*, 235-241.

120. Witkowski, J.T.; Robins, R.K.; Khare, G.P.; Sidwell, R.W., Synthesis and antiviral activity of 1,2,4-triazole-3-thiocarboxamide and 1,2,4-triazole-3-carboxamidine ribonucleosides. *J. Med. Chem.* **1973**, *16*, 935-937.

121. Witkowski, J.T.; Robins, R.K.; Sidwell, R.W.; Simon, L.N., Design, synthesis, and broad spectrum antiviral activity of 1-*b*-D-ribofuranosyl-1,2,4-triazole-3-carboxamide and related nucleosides. *J. Med. Chem.* **1972**, *15*, 1150-1154.

122. Chittepu, P.; Sirivolu, V.R.; Seela, F., Nucleosides and oligonucleotides containing 1,2,3-triazole residues with nucleobase tethers: Synthesis via the azide-alkyne ′click′ reaction. *Bioorg. Med. Chem.* **2008**, *16*, 8427-8439.

123. Nakahara, M.; Kuboyama, T.; Izawa, A.; Hari, Y.; Imanishi, T.; Obika, S., Synthesis and base-pairing properties of C-nucleotides having 1-substituted 1H-1,2,3-triazoles. *Bioorg. Med. Chem. Lett.* **2009**, *19*, 3316-3319.

124. El-Sagheer, A.H.; Brown, T., Synthesis and Polymerase Chain Reaction Amplification of DNA Strands Containing an Unnatural Triazole Linkage. *J. Am. Chem. Soc.* **2009**, *131*, 3958-3964.

125. Fujino, T.; Yamazaki, N.; Isobe, H., Convergent synthesis of oligomers of triazole-linked DNA analogue (TLDNA) in solution phase. *Tetrahedron Lett.* **2009**, *50*, 4101-4103.

126. Lucas, R.; Neto, V.; Hadj Bouazza, A.; Zerrouki, R.; Granet, R.; Krausz, P.; Champavier, Y., Microwave-assisted synthesis of a triazole-linked 3′-5′ dithymidine using click chemistry. *Tetrahedron Lett.* **2008**, *49*, 1004-1007.

127. Chandrasekhar, S.; Srihari, P.; Nagesh, C.; Kiranmai, N.; Nagesh, N.; Idris, M.M., Synthesis of Readily Accessible Triazole-Linked Dimer Deoxynucleoside Phosphoramidite for Solid-Phase Oligonucleotide Synthesis. *Synthesis-Stuttgart.* **2010**, 3710-3714.

128. El-Sagheer, A.H.; Brown, T., New strategy for the synthesis of chemically modified RNA constructs exemplified by hairpin and hammerhead ribozymes. *Proc. Natl. Acad. Sci. USA.* **2010**, *107*, 15329-15334.

129. Mutisya, D.; Selvam, C.; Kennedy, S.D.; Rozners, E., Synthesis and properties of triazole-linked RNA. *Bioorg. Med. Chem. Lett.* **2011**, *21*, 3420-3422.

130. Fujino, T.; Endo, K.; Yamazaki, N.; Isobe, H., Synthesis of Triazole-linked Analogues of RNA ((TL)RNA). *Chem. Lett.* **2012**, *41*, 403-405.

131. Pallan, P.S.; von Matt, P.; Wilds, C.J.; Altmann, K.-H.; Egli, M., RNA-binding affinities and crystal structure of oligonucleotides containing five-atom amide-based backbone structures. *Biochemistry.* **2006**, *45*, 8048-8057.

132. Ueno, Y.; Yoshikawa, K.; Kitamura, Y.; Kitade, Y., Effect of incorporation of alkyl linkers into siRNAs on RNA interference. *Bioorg. Med. Chem. Lett.* **2009**, *19*, 875-877.

133. Kochetkova, S.V.; Kolganova, N.A.; Timofeev, E.N.; Florent′ev, V.L., Oligonucleotide analogues containing the internucleotide linker C3 ′-NH-CO-CH_2-N(CH_3)-C5 ′. *Russian J. Bioorg. Chem.* **2008**, *34*, 453-459.

134. Kaur, H.; Arora, A.; Gogoi, K.; Solanke, P.; Gunjal, A.D.; Kumar, V.A.; Maiti, S., Effects for the Incorporation of Five-atom Thioacetamido Nucleic Acid (TANA) Backbone on Hybridization Thermodynamics and Kinetics of DNA Duplexes. *J. Phys. Chem. B.* **2009**, *113*, 2944-2951.

135. Sobczak, M.; Kubiak, K.; Janicka, M.; Sierant, M.; Mikolajczyk, B.; Nawrot, B., Synthesis, physico-chemical and biological properties of DNA and RNA oligonucleotides containing short alkylamino internucleotide bond. *Collect. Czech. Chem. Commun.* **2011**, *76*, 1471-1486.

136. Bramsen, J.B.; Laursen, M.B.; Damgaard, C.K.; Lena, S.W.; Babu, B.R.; Wengel, J.; Kjems, J., Improved silencing properties using small internally segmented interfering RNAs. *Nucleic Acids Res.* **2007**, *35*, 5886-5897.

137. Addepalli, H.; Meena; Peng, C.G.; Wang, G.; Fan, Y.; Charisse, K.; Jayaprakash, K.N.; Rajeev, K.G.; Pandey, R.K.; Lavine, G.; Zhang, L.; Jahn-Hofmann, K.; Hadwiger, P.; Manoharan, M.; Maier, M.A., Modulation of thermal stability can enhance the potency of siRNA. *Nucleic Acids Res.* **2010**, *38*, 7320-7331.

Chapter II – Manuscript I

Synthesis and Properties of Oligonucleotides that Contain a Triazole-Linked Nucleic Acid Dimer

Tim C. Efthymiou and Jean-Paul Desaulniers*

Published in:

Journal of Heterocyclic Chemistry **2011**, *48*, 533-539.

DOI: 10.1002/jhet.532

2.0 Abstract

New chemically modified oligonucleotides at the site of the backbone are needed to improve the properties of oligonucleotides. A practical synthesis for a triazole-linked nucleoside dimer based on a PNA-like structure has been developed. This involves synthesizing two uracil-based monomers that contain either an azide or an alkyne functionality, followed by copper-catalyzed 1,3-dipolar cycloaddition. This dimer was incorporated within an oligonucleotide via phosphoramidite chemistry and UV-monitored thermal denaturation data illustrates slight destabilization relative to its target complementary sequence. This chemically modified dimer will allow for a future investigation of its properties within DNA and RNA-based applications.

2.1 Introduction

Oligonucleotides have found tremendous use as biological tools and as agents with therapeutic promise. One promising example involves RNA interference (RNAi), and exploiting this pathway has become a major tool in elucidating gene function [1]. Furthermore, utilization of the RNAi pathway by administering short interfering RNAs (siRNAs) to cells [2] has offered therapeutic hope in combating diseased cells with aberrant gene expression profiles [3]. Despite awareness of this potential, improvements in enzymatic stability, biodistribution, cell-membrane permeability, and reducing off-target effects are still needed [4, 5]. One way to potentially overcome these limitations involves altering the stability and specificity profile of the siRNA through chemical modification.

Within the areas of siRNA, the most common type of chemical modification involves alterations within the ribose moiety. Extensive studies involving 2′-*O*-Me, fluorinated sugars and locked nucleic acids (LNA) have shown favorable siRNA knockdown results depending on its position and sequence context [6–9]. Studies involving chemical modification of the backbone within the field of siRNA are less prevalent than sugar modifications. Some key examples include the negatively charged backbone modification involving a phosphorothioate [10] and boranophosphates [11]. Backbone-altering modifications such as a morpholino analogue [12] and neutral amide bonds at 3′ overhangs of siRNA duplexes, have shown favorable results when utilized for gene-knockdown studies [13, 14]. Therefore, it is possible that the RNAi pathway will adopt less conventional backbone modifications at specific positions of the oligonucleotide. Given that siRNA duplexes exhibit thermodynamic asymmetry, being able to potentially destabilize the 5′ end of the guide strand with novel backbone modifications may offer favorable properties. Outside of the RNAi field, modified backbone constructs could have many other potential applications such as in antisense technology, artificial aptamer design or template driven enzymatic reactions. To explore this prospective, we are interested in pursuing alternative backbone modifications such as nonionic hydrophobic backbone mimics.

Within the field of backbone modified oligonucleotides, one of the most successful examples involves peptide nucleic acid (PNA) [15] and this has shown remarkable stability and specificity to its complementary targets [16, 17]. PNA synthesis occurs by the successful amide-bond formation between an acid and an amine with high-yields. Therefore, we envisioned that a scaffold based on a triazole functional group would serve as a potentially good candidate (Fig. 2.7). To date, a number of different triazole-based backbone modifications have been reported [18–20] from the one presented herein.

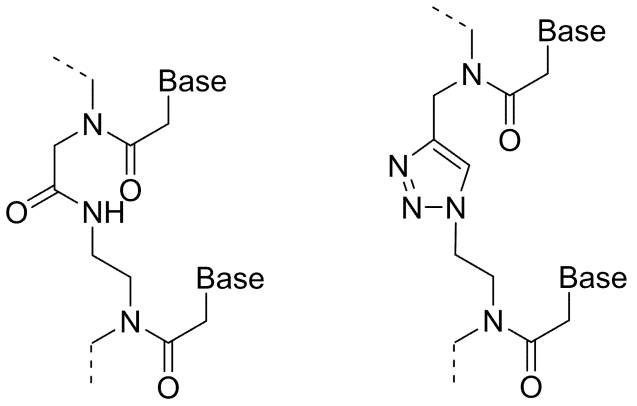

Figure 2.7 Chemical differences between peptide nucleic acid (left) and triazole-linke nucleic acid (right).

The repetitive backbone unit in most analogues, including PNA, contains six atoms. Although the six-atom spacer unit dominates by choice for a large number of chemically modified nucleic acids, analogues with shorter (five atom linker) [21–23] and longer backbones (seven atom linker) [24, 25] have shown varying degrees of specificity to its target, depending on its sequence context and type of backbone. This suggests that site-specific incorporation of unnatural nucleoside backbones of different atom lengths can produce functioning oligonucleotides, capable of binding to their complement strand with varying specificity and stability. As such, chemically modifying oligonucleotides could offer an alternative way to fine-tune their functional effects.

We hypothesized that a copper (I)-catalyzed Huisgen [3 + 2] cycloaddition [26] based on a PNA-type structure would generate an alternative scaffold for bridging adjacent nucleotides together. We report the synthesis of a modified 1,4-triazole-linked uracil dimer through a distance of seven atoms and report its compatibility with hybridization to a complement sequence when appended at the 5′ or 3′ end of a DNA oligonucleotide.

2.2 Materials and Methods

2.2.1 General Synthetic Methods

Unless otherwise noted, all starting materials were obtained from commercial sources and were used without any additional purification. Anhydrous CH_2Cl_2, THF, and DMF were purchased from Sigma-Aldrich and degassed by stirring under a dry N_2 atmosphere. Purification by flash chromatography was carried out with Silicycle Siliaflash 60 (230–400 mesh) according to the procedure of Still et al. [27] ^{1}H NMR spectra were recorded in DMSO-d_6 or $CDCl_3$ at 400 or 500 MHz and ^{13}C NMR spectra were recorded at 100 or 125 MHz. High-Resolution MS (HRMS) was recorded on a Micromass AutoSpec Ultima Magnetic sector mass spectrometer.

2.2.2 Synthesis and Characterization of Organic Compounds

2.2.2.1 Synthesis of 2-(tert-Butyldimethylsilyloxy)ethanamine – Compound (1)

To a solution of ethanolamine (9.6 mL, 159 mmol) in 100 mL of CH_2Cl_2 was dissolved imidazole (10.8 g, 159 mmol) and this solution was cooled in an ice-water bath. To this solution was added *tert*-butyldimethylsilyl chloride (24 g, 159 mmol) and the reaction mixture was stirred overnight at rt. Sat. $NaHCO_3$ was added and the resulting mixture was partitioned. The organic fractions were concentrated *in vacuo* to afford the title compound as a clear light yellow oil (26.8 g, 96%). [28]

2.2.2.2 Synthesis of *N*-(2-(*tert*-Butyldimethylsilyloxy)ethyl)prop-2-yn-1-amine – Compound (2)

To a solution of **1** (10 g, 57 mmol) in 100 mL of CH_2Cl_2 was added diisopropylethylamine (3.7 g, 28.5 mmol), and this solution was cooled in an ice-water bath. To this solution was added 3-bromoprop-1-yne (3.4 g, 28.5 mmol) dropwise over 30 min. This reaction mixture was stirred at rt. until TLC analysis indicated the complete consumption of starting material (3 h). Sat. $NaHCO_3$ was added and the reaction mixture was partitioned. The organic fraction was concentrated *in vacuo*, to afford an oil which was purified by silica gel chromatography eluting with a gradient of hexanes/EtOAc (7:3 to 3:7) to afford the title compound as a clear yellow oil (2.9 g, 71%); ^{1}H NMR (500

MHz, $CDCl_3$) δ 0.07 (s, 6H), 0.90 (s, 9H), 1.67 (br s, 1H), 2.21 (s, 1H), 2.80 (t, 2H, *J* = 5.5 Hz), 3.46 (s, 2H), 3.75 (t, 2H, *J* = 5.1 Hz); ^{13}C NMR (100 MHz, CDCl3) δ -5.36, 25.89, 29.66, 38.18, 50.52, 62.32, 71.21, 82.15; ESI-HRMS (ES^+) *m/z* calcd for $C_{11}H_{23}NOSi$: 213.1549, found 214.1626 $[M + H]^+$. Anal. Calcd. For $C_{11}H_{23}NOSi$: C, 61.91; H, 10.86. Found: C, 61.56; H, 10.49.

2.2.2.3 Synthesis of *N*-(2-(*tert*-Butyldimethylsilyloxy)ethyl)-uracil-1-yl-*N*-(prop-2-yn-1-yl)acetamide – Compound (3)

To a solution of uracil-1-yl acetic acid (2.4 g, 14 mmol) in 240 mL of DMF was added diisopropylethylamine (1.8 g, 14 mmol) and this solution was cooled in an ice-water bath. The acid was activated with the addition of *O*-Benzotriazole-*N*,*N*,*N*′,*N*′-tetramethyl-uronium-hexafluorophosphate (5.3 g, 14 mmol) to the stirring solution over the course of 5 min, followed by the dropwise addition of **2** (2 g, 9.4 mmol) over 15 min. The reaction mixture was stirred for 24 h at ambient temperature and then extracted with EtOAc and the organic layer was washed with H_2O and brine (x3). The organic layer was collected and concentrated *in vacuo* to afford the crude product. This crude product was purified by flash chromatography with a gradient of hexanes/EtOAc (7:3) to 100% EtOAc to elute the title compound as a white solid (1.5 g, 44%). Compound **3** is a pair of rotamers; the signals to the major (ma.) and minor (mi.) rotamers are designated; ^{1}H NMR (500 MHz, $CDCl_3$) δ 0.04 (s, 2H, mi.), 0.08 (s, 4H, ma.), 0.88 (s, 3H, mi.), 0.89 (s, 6H, ma.), 2.25 (br s, 0.66H, ma.), 2.41 (br s, 0.33H, mi.), 3.58 (t, 0.6H, *J* = 5.3 Hz, mi.), 3.65 (t, 1.4H, *J* = 5.2 Hz, ma.), 3.76 (t, 0.6H, *J* = 5.3 Hz, mi.), 3.85 (t, 1.4H, *J* = 5.0 Hz, ma.), 4.27 (2s, 2H), 4.68 (m, 2H), 5.71–5.74 (m, 1H), 7.13 (d, 0.66H, *J* = 7.9 Hz, ma.), 7.17 (d, 0.33H, *J* = 7.9 Hz, mi.), 9.43 (br s, 0.66H, ma.), 9.48 (br s, 0.33H, mi.); ^{13}C NMR (125 MHz, $CDCl_3$) δ -5.61, -5.55, -5.41, -5.36, -3.72, -3.53, 17.94, 18.11, 18.28, 25.54, 25.69, 25.75, 25.81, 25.89, 25.96, 35.16, 38.67, 48.03, 48.06, 48.78, 49.55, 60.58, 61.67, 72.72, 73.59, 77.93, 78.13, 102.13, 102.24, 145.02, 145.09, 150.90, 150.93, 163.58, 166.30, 166.66; ESI-HRMS (ES^+) *m/z* calcd for $C_{17}H_{27}N_3O_4Si$: 365.1771, found 366.1845 $[M + H]^+$. Anal. Calcd. for $C_{17}H_{27}N_3O_4Si$: C, 55.86; H, 7.45; N, 11.50. Found: C, 55.67; H, 7.80; N, 11.89.

2.2.2.4 Synthesis of 2-Azidoethanamine – Compound (**4**)

To a solution of NaN_3 (23.8 g, 366 mmol) in 200 mL of water was added 2-bromoethylamine hydrobromide (25 g, 122 mmol) and this solution was heated to 75 °C. The reaction mixture was stirred for 24 h and was then cooled in an ice-water bath. To the cooled solution was added NaOH (28.5 g, 712.5 mmol) and the reaction mixture was stirred until the NaOH was fully dissolved. To this aqueous solution was added Et_2O (x3). The ether fractions were collected, dried over Na_2SO_4 and evaporated *in vacuo* to afford the title compound as a clear oil (6.7 g, 64%). The ^1H proton and ^{13}C NMR shifts were confirmed with the report by Mayer and Maier. [29]

2.2.2.5 Synthesis of Ethyl 2-(2-azidoethylamino)acetate – Compound (5)

To a solution of **4** (5 g, 58.1 mmol) in 100 mL of DMF was added triethylamine (5.9 g, 58.1 mmol). Ethyl 2-bromoacetate (5.8 g, 34.9 mmol) was then added dropwise over 15 min to the stirring solution and the reaction was stirred for 4 h at room temperature. The solution was then extracted with EtOAc, washed with H_2O (three times) and the EtOAc fractions were collected and dried over Na_2SO_4. This solution was evaporated under reduced pressure to yield a crude orange oil. The oil was loaded directly onto a silica column for purification by gradient eluting with hexanes/EtOAc (5:5) to 100% EtOAc to afford the title compound as a clear light yellow oil (5.0 g, 83%); ^1H NMR (400 MHz, $CDCl_3$) δ 1.25 (t, 3H, J = 7.1 Hz), 1.98 (br s, 1H), 2.80 (t, 2H, J = 5.7 Hz), 3.39 (t, 2H, J = 5.9 Hz), 3.40 (s, 2H), 4.17 (q, 2H, J = 7.4 Hz); ^{13}C NMR (100 MHz, $CDCl_3$) δ 14.09, 48.01, 50.50, 51.33, 60.74, 172.07; ESI-HRMS (ES^+) *m/z* calcd for $C_6H_{12}N_4O_2$: 172.0960, found 173.1034 $[M + H]^+$. Anal. Calcd. for $C_6H_{12}N_4O_2$: C, 41.85; H, 7.02; N, 32.54. Found: C, 41.65; H, 6.82; N, 32.12.

2.2.2.6 Synthesis of Ethyl 2-(*N*-(2-azidoethyl)-uracil-1-yl-acetamido)acetate – Compound (**6**)

To a solution of uracil-1-yl acetic acid (1.1 g, 6.4 mmol) in 100 mL of anhydrous DMF under N_2 was added dicyclohexylcarbodiimide (1.3 g, 6.4 mmol) and 1*N*-hydroxybenzotriazole (1.0, 6.4 mmol). This solution was stirred for 15 min on an ice-water bath, followed by 1 h of stirring at ambient temperature. To this solution was

added compound **5** (1 g, 5.8 mmol) dropwise over 10 min, and the reaction mixture was stirred for 24 h after which the DCU precipitate was collected by filtration. The filtrate was dried down *in vacuo*, dissolved in EtOAc, and washed with water and brine (x3). The EtOAc solutions were concentrated *in vacuo*. The resulting crude product was dissolved in a minimal amount of CH_2Cl_2 and purified by flash chromatography with a gradient of hexanes/EtOAc (5:5) to 100% EtOAc to elute the title compound as a white solid (1.2 g, 62%). Compound **6** is comprised of a pair of rotamers, each displaying signals of equal intensity; ^{1}H NMR (500 MHz, $CDCl_3$) δ 1.28 (t, 1.5H, *J* = 7.1 Hz), 1.33 (t, 1.5H, *J* = 7.1 Hz), 3.55 (s, 2H), 3.59 (t, 1H, *J* = 5.6 Hz), 3.66 (t, 1H, *J* = 5.4 Hz), 4.12 (s, 1H), 4.21 (q, 1H, *J* = 7.1 Hz), 4.26 (s, 1H), 4.28 (q, 1H, *J* = 7.1 Hz), 4.49 (s, 1H), 4.72 (s, 1H), 5.74 (d, 0.5H, *J* = 6.0 Hz), 5.75 (d, 0.5H, *J* = 5.6 Hz), 7.20 (d, 0.5H, *J* = 2.0 Hz), 7.21 (d, 0.5H, *J* = 2.0 Hz), 9.08 (br s, 1H); ^{13}C NMR (125 MHz, $CDCl_3$) δ 14.11, 47.75, 47.82, 48.05, 48.31, 48.86, 49.84, 49.92, 50.95, 61.67, 62.31, 102.30, 102.38, 145.02, 145.14, 150.90, 150.92, 163.44, 167.16, 167.46, 168.64, 169.03; ESI-HRMS (ES^+) *m/z* calcd for $C_{12}H_{16}N_6O_5$: 324.1182, found 325.1262 $[M + H]^+$. Anal. Calcd. For $C_{12}H_{16}N_6O_5$: C, 44.44; H, 4.97; N, 25.91. Found: C, 44.40; H, 5.10; N, 25.41.

2.2.2.7 Synthesis of Ethyl 2-(*N*-(2-(4-((*N*-(2-(*tert*-butyldimethylsilyloxy)ethyl)-uracil-1-yl-acetamido)methyl)-1*H*-1,2,3-triazol-1-yl)ethyl)-Uracil-1-yl-acetamido)acetate – Compound (7)

To a solution of compounds **3** (677 mg, 1.9 mmol) and **6** (600 mg, 1.9 mmol) dissolved in 18 mL of THF/*t*-BuOH/H_2O (1:1:1) was added sodium ascorbate (733 mg, 3.7 mmol) followed by Cu(II)SO_4 (231 mg, 925 μmol). This reaction mixture was stirred for 24 h at room temperature and then extracted with CH_2Cl_2. The organic layer was washed with H_2O (three times) to wash off the excess copper. The precipitate in the organic layer was collected by filtration and washed with cold H_2O to afford the crude product. This crude product was redissolved in minimal CH_2Cl_2/MeOH for 1 h and purified by flash column chromatography eluting with 5% (10% NH_4OH in MeOH) in CH_2Cl_2 to afford the title compound as a white solid (1.3 g, 98%). Compound **7** is a mixture of rotamers with varying signal intensities. ^{1}H NMR (400 MHz, DMSO-d_6) δ 0.03 (s, 2H), 0.05 (m, 4H), 0.85, 0.86 (2s, 9H), 1.18 (t, 1.5H, *J* = 7.2 Hz), 1.23 (t, 1.5H, *J* = 7.0 Hz), 3.48–3.50 (m, 1H), 3.63–3.91 (m, 4H), 4.01–4.03 (m, 1H), 4.08 (q, 1.2H, *J* = 7.3 Hz), 4.16 (q, 0.8H, *J* =

7.3 Hz), 4.24, 4.29 (2s, 1H), 4.44–4.77 (m, 9H), 5.56 (d, 2H, *J* = 7.8 Hz), 7.31–7.47 (m, 2H), 7.89, 8.05, 8.13, 8.24 (4s, 1H), 11.29 (br m, 2H); ^{13}C NMR (100 MHz, DMSO-d_6) δ -5.45, -5.39, 13.99, 14.04, 17.89, 18.04, 25.82, 25.90, 41.05, 47.31, 47.58, 47.91, 48.00, 60.18, 60.65, 60.83, 61.25, 100.57, 100.79, 123.70, 124.04, 124.12, 124.61, 143.18, 143.34, 143.41, 143.56, 146.12, 146.19, 146.29, 146.50, 146.54, 150.92, 150.98, 151.04, 151.07, 151.11, 163.76, 163.80, 163.81, 163.85, 163.88, 166.74, 166.82, 166.88, 166.90, 167.43, 167.97, 168.03, 168.85, 169.15; ESI-HRMS (ES^+) *m/z* calcd for $C_{29}H_{43}N_9O_9Si$: 689.2953, found 690.3030 $[M + H]^+$. Anal. Calcd. for $C_{29}H_{43}N_9O_9Si$: C, 50.50; H, 6.28. Found: C, 50.47; H, 6.24.

2.2.2.8 Synthesis of *N*-(2-(*tert*-Butyldimethylsilyloxy)ethyl)-uracil-1-yl-*N*-((1-(2-(uracil-1-yl-*N*-(2-hydroxyethyl)acetamido)ethyl)-1*H*-1,2,3-triazol-4-yl)methyl)acetamide – Compound (**8**)

To a solution of compound **7** (300 mg, 435 µmol) suspended in 12 mL of dry THF, drops of MeOH were added until the compound was dissolved. To this solution was then added $LiBH_4$ (544 µL, 1.09 mmol) and the reaction mixture was refluxed until TLC analysis indicated the complete consumption of starting material (1.5 h). This reaction mixture was quenched with MeOH and dried down *in vacuo* to afford the crude product. The crude product was then redissolved in minimal CH_2Cl_2/MeOH and purified by flash column chromatography eluting with a gradient of 10% NH_4OH in MeOH (5 to 15%) in CH_2Cl_2 to afford the title compound as a white crystalline solid (213 mg, 76%). Compound **8** is a mixture of rotamers with varying signal intensities; ^{1}H NMR (500 MHz, DMSO-d_6) δ 0.03 (s, 2H), 0.05 (s, 4H), 0.85, 0.87 (2s, 9H), 3.16–3.27 (m, 2H), 3.43–3.54 (m, 4H), 3.63–3.74 (m, 3H), 3.80–3.87 (m, 2H), 4.36–4.38 (m, 1H), 4.46 (t, 1.2H, *J* = 6.3 Hz), 4.51 (t, 0.8H, *J* = 6.3 Hz), 4.56–4.81 (m, 6H), 4.94–5.00 (m, 1H), 5.54–5.58 (m, 2H), 7.35–7.47 (m, 2H), 7.87, 8.04, 8.13, 8.23 (4s, 1H), 11.30 (br s, 2H); ^{13}C NMR (DMSO-d_6) δ -5.44, -5.37, 17.91, 18.05, 25.83, 25.92, 30.74, 41.04, 46.24, 46.55, 46.71, 46.92, 48.29, 48.32, 48.51, 49.07, 49.26, 58.49, 58.81, 58.85, 60.21, 60.85, 100.57, 100.63, 123.76, 124.11, 124.55, 143.23, 143.39, 143.43, 143.58, 146.48, 146.52, 146.58, 151.04, 151.08, 151.11, 163.84, 163.87, 166.69, 166.74, 166.81, 167.43, 167.54; ESI-HRMS (ES^+) *m/z* calcd for $C_{27}H_{41}N_9O_8Si$: 647.2847, found 648.2918 $[M + H]^+$.

Anal. Calcd. for $C_{27}H_{41}N_9O_8Si$: C, 50.06; H, 6.38; N, 19.46. Found: C, 50.23; H, 6.84; N, 19.36.

2.2.2.9 Synthesis of *N*-(2-(bis(4-methoxyphenyl)(phenyl)methoxy)ethyl)-2-(Uracil-1-yl)-*N*-(2-(4-((2-(Uracil-1-yl)-*N*-(2-((2,3,3-trimethylbutan-2-yl)oxy)ethyl)acetamido)methyl)-1*H*-1,2,3-triazol-1-yl)ethyl)acetamide – Compound (9)

To a solution of compound **8** (1.06 g, 1.64 mmol) dissolved in 10 mL of dry pyridine under N_2, was added an excess of 4,4′-dimethoxytrityl chloride (1.66 g, 4.91 mmol) until TLC analysis revealed the consumption of starting material. This reaction mixture was stirred overnight at room temperature while under N_2, after which the entire mixture was extracted with CH_2Cl_2 and washed with H_2O (two times). The organic fractions were collected, dried over Na_2SO_4 and subsequently condensed *in vacuo* to afford the crude product. The crude was dissolved in minimal CH_2Cl_2/MeOH and purified by flash column chromatography eluting with a gradient of MeOH (5 to 15%) in CH_2Cl_2 to afford the title compound as a white solid (1.22 g, 79%). Compound **9** is a mixture of rotamers with varying signal intensities; ^{1}H NMR (400 MHz, $CDCl_3$) δ 0.03 (s, 2H), 0.06 (s, 4H), 0.86, 0.88 (2s, 9H), 2.87–2.94 (m, 1.5H), 3.03–3.08 (m, 0.5H), 3.20 (t, 1.5H, *J* = 4.7 Hz), 3.26 (t, 0.5H, *J* = 4.5 Hz), 3.29–3.31 (m, 0.2H), 3.36–3.43 (m, 0.3H), 3.46–3.55 (m, 2.5H), 3.60–3.67 (m, 2H), 3.72–3.75 (m, 0.75H), 3.76, 3.77 (2s, 7H), 3.80 (t, 1.25H, *J* = 4.9 Hz), 4.51 (t, 1.5H, *J* = 5.3 Hz), 4.55 (t, 0.5H, *J* = 5.3 Hz), 4.59 (s, 1H), 4.63–4.64 (m, 1H), 4.67 (s, 3H), 4.73 (d, 1H, *J* = 7.4 Hz), 5.51–5.55 (m, 1H), 5.62 (d, 0.1H, *J* = 1.6 Hz), 5.64 (d, 0.1H, *J* = 1.6 Hz), 5.64–5.68 (m, 0.8H), 6.57 (d, 0.1H, *J* = 7.8 Hz), 6.66 (d, 0.7H, *J* = 7.8 Hz), 6.80–6.84 (m, 4.3H), 7.06–7.09 (m, 0.8H), 7.17–7.36 (m, 7.2H), 7.71, 7.81, 7.88, 7.94 (4s, 1H), 10.11 (br s, 2H); ^{13}C NMR (100 MHz, $CDCl_3$) δ -5.44, -5.16, 18.13, 18.29, 25.61, 25.83, 25.90, 41.33, 44.08, 47.64, 47.74, 48.27, 48.50, 48.62, 48.87, 48.93, 49.09, 55.23, 60.41, 60.66, 60.79, 60.98, 87.24, 87.39, 102.02, 102.21, 102.25, 113.15, 113.25, 124.37, 125.24, 127.18, 127.24, 127.86, 127.98, 128.15, 129.91, 130.08, 135.03, 135.09, 135.70, 143.49, 143.76, 144.01, 144.05, 144.65, 145.00, 145.10, 145.15, 145.21, 145.54, 151.26, 151.32, 151.38, 151.46, 158.42, 158.67, 158.71, 163.91, 164.00, 164.08, 166.48, 167.25, 167.67. ESI-HRMS (ES^+) *m/z* calcd for $C_{48}H_{59}N_9O_{10}Si$: 949.4154, found 972.4035 $[M + Na]^+$. Anal. Calcd. for $C_{48}H_{59}N_9O_{10}Si$: C, 60.68; H, 6.26; N, 13.27. Found: C, 60.50; H, 6.28; N, 12.90.

2.2.2.10 Synthesis of *N*-(2-(bis(4-methoxyphenyl)(phenyl)methoxy)ethyl)-2-(Uracil-1-yl)-*N*-((1-(2-(2-(Uracil-1-yl)-*N*-(2-hydroxyethyl)acetamido)ethyl)-1*H*-1,2,3-triazol-4-yl)methyl)acetamide – Compound (10)

To a solution of compound **9** (1.12 g, 1.18 mmol) dissolved in 26 mL of dry THF was added TBAF (926 mg, 3.54 mmol). This reaction mixture was stirred for 12 h at room temperature and then extracted with CH_2Cl_2. The organic layer was washed with H_2O and brine (x2), at which point the combined organic fractions were dried over Na_2SO_4, and evaporated under reduced pressure. The crude was dissolved in minimal CH_2Cl_2/MeOH and purified by flash column chromatography, first eluting with 100% CH_2Cl_2 followed by a gradient of MeOH (5 to 15%) in CH_2Cl_2 to afford the title compound as a yellow solid (840 mg, 85%). Compound **10** is a mixture of rotamers with varying signal intensities; ^{1}H NMR (400 MHz, $CDCl_3$) δ 2.49 (br s, 1H), 2.98 (br s, 1H), 3.16–3.20 (br m, 2H), 3.27–3.31 (m, 3H), 3.45–3.57 (m, 4H), 3.68–3.81 (m, 8H), 4.45–4.80 (m, 8H), 5.50–5.53 (m, 0.8H), 5.56–5.60 (m, 1.2H), 6.63 (d, 0.15H, *J* = 8.2 Hz), 6.66 (d, 0.35H, *J* = 7.8 Hz), 6.78–6.83 (m, 4H), 7.17–7.31 (m, 8.5H), 7.69, 7.88, 7.90, 8.09 (4s, 1H), 10.20–10.42 (br m, 2H); ^{13}C NMR (100 MHz, $CDCl_3$) δ 22.13, 27.75, 29.14, 29.64, 42.18, 47.37, 48.29, 49.13, 50.35, 55.24, 59.15, 60.78, 68.46, 87.23, 87.32, 101.65, 101.91, 107.85, 113.16, 113.26, 124.97, 127.16, 127.99, 128.17, 129.92, 130.09, 135.15, 135.73, 143.56, 144.11, 144.28, 145.47, 146.36, 151.41, 151.47, 158.40, 158.64, 164.30, 164.39, 164.56, 167.63, 167.68; ESI-HRMS (ES^+) *m/z* calcd for $C_{42}H_{45}N_9O_{10}$: 835.3289, found 858.3217 $[M + Na]^+$. Anal. Calcd. for $C_{42}H_{45}N_9O_{10}$: C, 60.35; H, 5.43. Found: C, 60.72; H, 5.81.

2.2.2.11 Synthesis of 2-(*N*-(2-(4-((*N*-(2-(bis(4-methoxyphenyl)(phenyl)methoxy)ethyl)-2-(Uracil-1-yl)acetamido)methyl)-1*H*-1,2,3-triazol-1-yl)ethyl)-2-(Uracil-1-yl)acetamido)ethyl (2-cyanoethyl) diisopropylphosphoramidite – Compound (11)

To a solution of compound **10** (230 mg, 275 µmol) dissolved in 6 mL of dry CH_2Cl_2 under N_2, was added diisopropylethylamine (196 mg, 1.51 mmol) along with 4-dimethylaminopyridine (16.8 mg, 138 µmol). To this solution was added 2-cyanoethyl *N*,*N*-diisopropylchlorophosphoramidite (195 mg, 825 µmol), until TLC analysis revealed the maximum consumption of starting material. This mixture was then stirred for 6 h at room temperature under N_2 and dried *in vacuo* to afford the crude product. The crude was

dissolved in minimal 2% triethylamine in hexanes/acetone and purified by flash column chromatography eluting with a gradient of 2% triethylamine in acetone/hexanes (1:1 to 4:1) to afford the title compound as a white solid (180 mg, 63%). Compound **11** is a mixture of rotamers with varying signal intensities; ^{1}H NMR (400 MHz, $CDCl_3$) δ 1.14–1.19 (m, 12H), 2.62–2.66 (m, 3.25H), 2.92 (t, 1H, *J* = 3.9 Hz), 3.07 (t, 0.75H, *J* = 4.3 Hz), 3.21 (t, 1.25H, *J* = 4.7 Hz), 3.26 (t, 0.5H, *J* = 4.3 Hz), 3.29–3.37 (m, 0.25H), 3.54–3.61 (m, 5.5H), 3.70–3.77 (m, 2H), 3.78 (s, 6.25H), 3.81–3.90 (m, 2.25H), 4.52 (t, 1H, *J* = 5.3 Hz), 4.55 (t, 0.5H, *J* = 5.5 Hz), 4.61–4.65 (m, 2H), 4.70 (s, 2.5H), 4.74–4.77 (m, 1H), 5.52–5.55 (m, 1H), 5.66–5.70 (m, 1H), 6.56 (d, 0.33H, *J* = 7.8 Hz), 6.63 (d, 0.66H, *J* = 7.8 Hz), 6.81–6.84 (m, 4H), 7.17–7.31 (m, 12H), 7.70, 7.76, 7.89, 7.95 (4s, 1H); ^{13}C NMR (100 MHz, $CDCl_3$) δ 14.10, 14.84, 20.45, 20.52, 22.66, 23.34, 24.58, 24.62, 24.65, 24.69, 24.77, 29.24, 29.34, 29.66, 31.72, 31.89, 33.80, 34.43, 41.51, 43.02, 43.14, 45.82, 47.67, 47.80, 48.29, 48.60, 48.71, 48.93, 53.76, 55.26, 58.08, 58.30, 60.53, 60.70, 60.80, 69.48, 87.29, 87.42, 102.08, 102.20, 102.25, 113.27, 117.90, 118.12, 125.13, 127.24, 128.01, 128.20, 130.12, 135.05, 135.09, 143.39, 143.82, 144.05, 145.07, 145.46, 151.24, 151.34, 151.45, 158.71, 158.75, 163.63, 163.87, 163.91, 166.67, 167.41, 167.74; ESI-HRMS (ES^+) *m/z* calcd for $C_{51}H_{62}N_{11}O_{11}P$: 1035.4368, found 1058.4298 $[M + Na]^+$.

2.2.3 Procedure for the Chemical Synthesis of Oligonucleotides

All standard *β*-cyanoethyl DNA phosphoramidites, solid supports and reagents were purchased from Glen Research. All oligonucleotides were synthesized on an Applied Biosystems 394 DNA/RNA synthesizer using a 0.2 µM cycle with a 25 s coupling time for unmodified phosphoramidites. All phosphoramidites were dissolved in anhydrous acetonitrile to a 0.1 M concentration immediately prior to synthesis. Synthesis on solid phase was accomplished using 0.2 µM solid supports. Cleavage of the unmodified oligonucleotides from their solid supports was performed through exposure to 1.5 mL of 30% NH_4OH for 2 h at room temperature, followed by incubation in 30% NH_4OH at 55 ^{o}C overnight. All oligonucleotides were purified on a 20% denaturing polyacrylamide gel by utilizing the ″crush and soak″ method, followed by ethanol precipitation and desalting through Millipore 3000 MW cellulose centrifugal filters. The oligonucleotides were characterized by MALDI-TOF mass spectrometry (Waters Tofspec-2E) (Table 2.1).

2.2.3.1 Synthesis of 5′ and 3′ Triazole-Modified Oligonucleotides

Phosphoramidite **11** was attached to the 5′ end of the growing oligonucleotide being synthesized on the ABI 394 DNA/RNA synthesizer, with an increased coupling time of 600 s. To perform the 3′ modification, compound **11** was attached to a Universal III solid support (Glen Research) via the ABI 394 synthesizer with a 600 s coupling time. Cleavage from the Universal III solid support was performed through exposure to 1.5 mL of 2 M NH_3 in MeOH for 30 min at room temperature, followed by incubation in 30% NH_4OH at 55 °C for 8 h.

2.2.3.2 Oligonucleotide Sequences Used in the Study

Oligonucleotides synthesized using standard dT/dA supports: (i) 5′-AAG AGA GAG AAA AA–3′; (ii) 5′–TTT TTC TCT CTC TT–3′; and (iii) 5′–**UU**T TTC TCT CTC TT–3′. The **UU**–3′ modified sequence synthesized on the Universal III solid support: 5′–TTT TTC TCT CTC **UU**–3′. The sequence 5′-AAG AGA GAG AAA AA-3′ was purchased and purified from Integrated DNA Technologies.

2.3 Results

2.3.1 Synthesis of Uracil-Based Alkyne Monomer

Our strategy involves the synthesis of a uracil-based monomer possessing an alkyne functional group and a uracil-based monomer with an azide. For the synthesis of the uracil-based alkyne monomer, the first step involved *tert*-butyldimethylsilyl (TBS) protection of ethanolamine and this was conducted using TBSCl under standard basic conditions to afford **1** in 96% yield. Alkylation of **1** with propargyl bromide generated the alkyne **2** as a liquid in 71% yield. Utilizing peptide bond coupling conditions involving HBTU, the alkyne **2** was amide-bond coupled to uracil-1-yl acetic acid [30] to afford compound **3** as a white solid in 44% yield (Scheme 2.1).

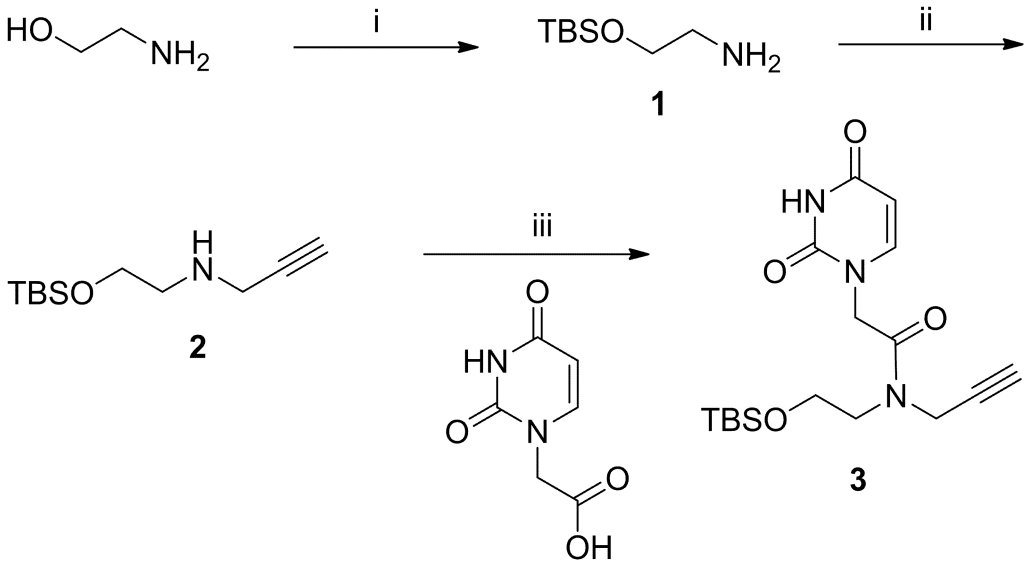

Scheme 2.1 Reagents and conditions: (i) 1 equiv imidazole, 1 equiv TBS-Cl, DCM, room temperature 96% yield of **1**; (ii) 0.5 equiv DIPEA, 0.5 equiv propargyl bromide, DCM, room temperature, 3 h, 71% yield of **2**; (iii) 1.5 equiv uracil-1-yl acetic acid, 1.5 equiv DIPEA, 1.5 equiv HBTU, DMF, 24 h, 44% yield of **3**.

2.3.2 Synthesis of Uracil-Based Azide Monomer

For the synthesis of the azide-based uracil monomer **6**, 2-azidoethylamine **4** was prepared by the addition of 2-bromoethylamine to an aqueous solution of sodium azide. Alkylation of **4** with a limiting amount of ethyl 2-bromoacetate afforded compound **5** as an off-colored liquid in 83% yield. This liquid **5** was amide-bond coupled with uracil-1-yl acetic acid using DCC/HOBt to afford the azide-based uracil monomer, compound **6** in 62% yield (Scheme 2.2).

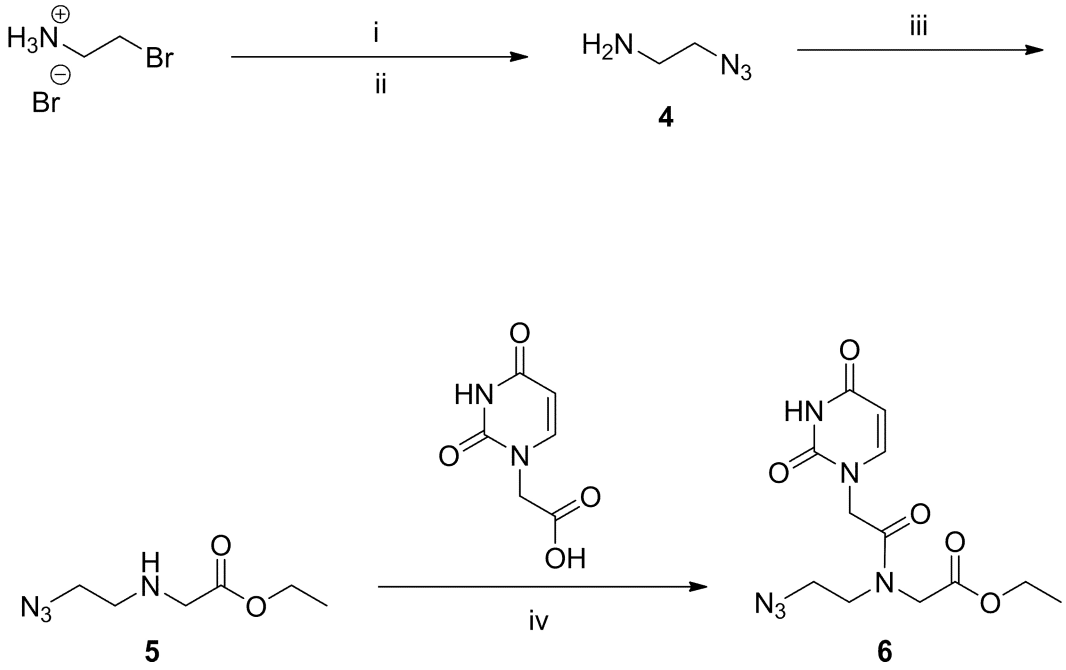

Scheme 2.2 Reagents and conditions: (i) 3 equiv NaN_3, H_2O, 75 °C, 24 h; (ii) 5.8 equiv NaOH, 0 °C, Et_2O, 64% yield of **4**; (iii) 1 equiv NEt_3, 0.6 equiv ethyl 2-bromoacetate, DMF, 4 h, 83% yield of **5**; (iv) 1.1 equiv uracil-1-yl acetic acid, 1.1 equiv DCC, 1.1 equiv HOBt, DMF, 24 h, 62% yield of **6**.

2.3.3 Synthesis of Triazole-Linked Uracil Nucleoside Dimer Phosphoramidite

With respect to the synthesis of the phosphoramidite, the first task was to cyclize both monomers together. Under copper (I) conditions, 1,4-triazole formation occurred with copper sulfate and sodium ascorbate to afford a white solid **7** in 98% yield. This newly formed dimer **7** was selectively reduced with 2.5 equivalents of $LiBH_4$ in a methanol/THF mixture to afford the alcohol **8** in 76% yield. Alcohol **8** was treated with

4,4′-dimethoxytrityl-chloride (DMT-Cl) to afford the compound **9** in 79% yield. The subsequent removal of the TBS group using TBAF provided the alcohol **10** in 85% yield. This was then followed by synthesis of phosphoramidite **11** by reacting alcohol **10** with 2-cyanoethyl *N*,*N*-diisopropylchlorophosphoramidite to afford a clear oil in 63% yield (Scheme 2.3). With this phosphoramidite **11**, its incorporation within a DNA oligonucleotide was accomplished by employing solid-phase oligonucleotide synthesis on a 394 ABI synthesizer.

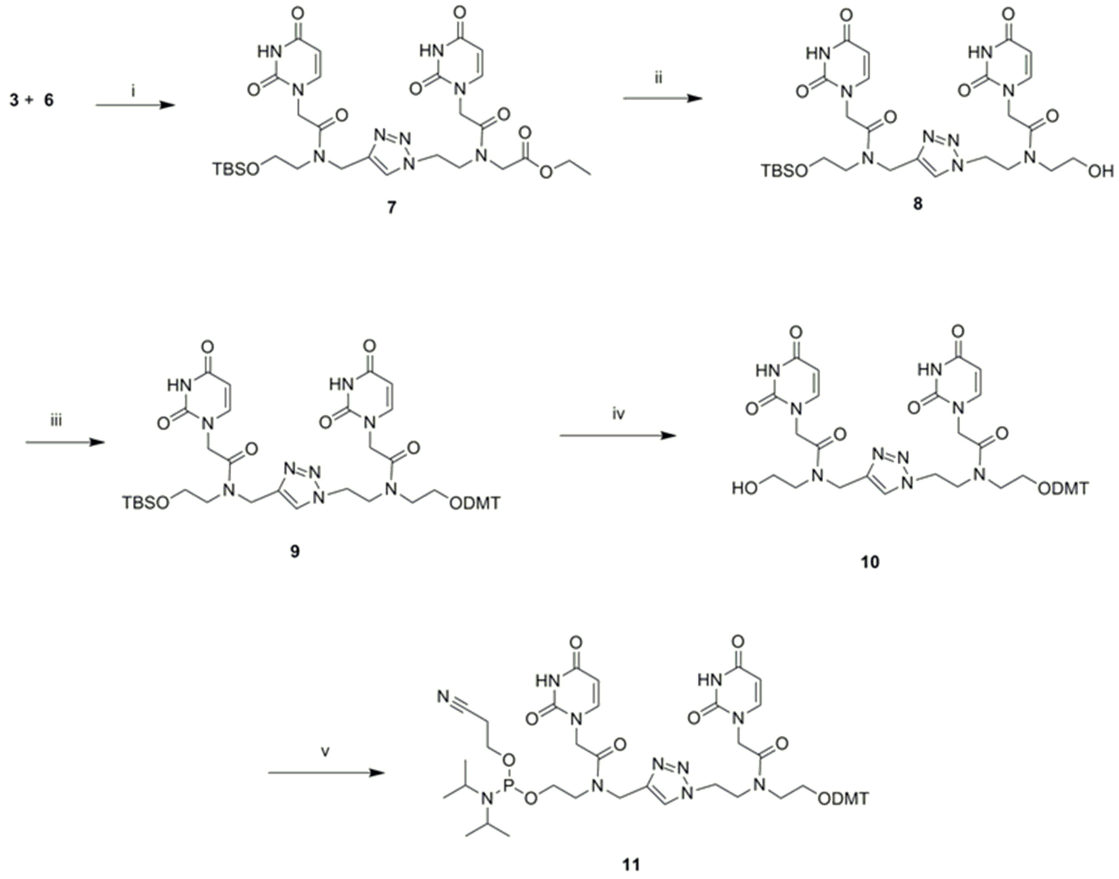

Scheme 2.3 Reagents and conditions: (i) 2 equiv sodium ascorbate, 0.5 equiv Cu(II)SO_4, THF/*t*-BuOH/H_2O (1:1:1), 24 h, 98% yield of **7**; (ii) 2.5 equiv $LiBH_4$, THF/MeOH (12:1), reflux 1.5 h, 76% yield of **8**; (iii) 3 equiv DMT-Cl, pyridine, 24 h, 79% yield of **9**; (iv) 3 eq TBAF, THF, 12 h, 85% yield of **10**; (v) 2 equiv 2-cyanoethyl *N*,*N*-diisopropylchlorophosphoramidite, 5.5 equiv DIPEA, 0.5 equiv DMAP, DCM, 8 h, 63% yield of **11**.

2.3.4 Melting Temperatures (T_m) Through UV-Monitored Thermal Denaturation

UV-melting denaturation studies indicate that moderate destabilization occurs with the UU-dimer on both the 5′ and 3′ position relative to the native strand (Table 2.1). A reduction in T_m of 4.5 °C and 2.8 °C is observed when native TT is replaced with the UU-dimer modification at the 5′ end and the 3′ end, respectively. However, this suggests a certain degree of compatibility as the T_m values for both modified oligonucleotides are higher when compared to corresponding 12-mer sequences lacking the heterocyclic pyrimidine dimer (**UU**) (Table 2.1). In comparison to other studies [31] and that of Kraicsovits and coworkers, a similar T_m drop was observed when compared to a PNA-DNA chimera that contained a PNA element at the terminal end [32].

Table 2.1 UV-melting denaturation studies.

Entry	Sequence	T_m (°C)	ΔT_m (°C)[a]
I	5′ TTTTTCTCTCTCTT 3′	40.9	0
II	5′ TTTTTCTCTCTC**UU** 3′	38.1	−2.8
III	5′ TTTTTCTCTCTC 3′	37.1	−3.8
IV	5′ **UU**TTTCTCTCTCTT 3′	36.4	−4.5
V	5′ TTTCTCTCTCTT 3′	35.3	−5.6

UV melting temperatures for duplexes to complement strand DNA (5′-AAG AGA GAG AAA AA-3′). The total strand concentration ranged from 2.4 to 3.0 µM in 90 mM NaCl, 10 mM sodium phosphate, and 1 mM EDTA at pH 7.0.
[a]For the ΔT_m values, the T_m of Entry I is the reference (T_m = 40.9 °C).

2.4 Discussion & Conclusion

In conclusion, a facile and practical synthesis of a new uracil-uracil dimer linked together through a triazole functionality has been developed and is readily synthesized from inexpensive starting material precursors. Our alkyne-uracil monomer **3** was synthesized in 44% yield and the azide-uracil monomer **6** was generated in 62% yield. Following heterocyclic cyclization, the phosphoramidite **11** was generated in four steps in 32% yield. Incorporation of the heterocyclic dimer at both the 5′ and 3′ ends of DNA oligonucleotides suggests a certain degree of compatibility when analyzed by UV-monitored thermal denaturation. The effects of this modification within different positions of other various oligonucleotides will be investigated. Notwithstanding, these oligonucleotides may have potential use when targeted at messenger RNA in diseased cells, or for other downstream applications.

Acknowledgments

We are grateful to UOIT and NSERC for funding. We thank Dr. Darcy Burns of Trent University for assistance with NMR spectroscopy and Dr. Christopher Wilds for his assistance with T_m measurements.

Supplementary Data

Refer to Appendix I for additional tables and all NMR spectra.

References and Notes – Chapter II – Manuscript I:

[1] Hannon, G. J. *Nature* **2002**, *418*, 244.

[2] Elbashir, S. M.; Harborth, J.; Lendeckel, W.; Yalcin, A.; Weber, K.; Tuschl, T. *Nature* **2001**, *411*, 494.

[3] Huang, C.; Li, M.; Chen, C. Y.; Yao, Q. Z. *Expert Opin. Ther. Targets* **2008**, *12*, 637.

[4] Corey, D. R. *Nat. Chem. Biol*. **2007**, *3*, 8.

[5] Watts, J. K.; Deleavey, G. F.; Damha, M. J *Drug Discov*. *Today* **2008**, *13*, 842.

[6] Braasch, D. A.; Jensen, S.; Liu, Y. H.; Kaur, K.; Arar, K.; White, M. A.; Corey, D. R. *Biochemistry* **2003**, *42*, 7967.

[7] Elmen, J.; Thonberg, H.; Ljungberg, K.; Frieden, M.; Westergaard, M.; Xu, Y. H.; Wahren, B.; Liang, Z. C.; Urum, H.; Koch, T.; Wahlestedt, C. *Nucleic Acids Res.* **2005**, *33*, 439.

[8] Watts, J. K.; Choubdar, N.; Sadalapure, K.; Robert, F.; Wahba, A. S.; Pelletier, J.; Pinto, B. M.; Damha, M. J. *Nucleic Acids Res*. **2007**, *35*, 1441.

[9] Allerson, C. R.; Sioufi, N.; Jarres, R.; Prakash, T. P.; Naik, N.; Berdeja, A.; Wanders, L.; Griffey, R. H.; Swayze, E. E.; Bhat, B. *J. Med. Chem.* **2005**, *48*, 901.

[10] Harborth, J.; Elbashir, S. M.; Vandenburgh, K.; Manninga, H.; Scaringe, S. A.; Weber, K.; Tuschl, T. *Antisense Nucleic Acid Drug Dev.* **2003**, *13*, 83.

[11] Hall, A. H. S.; Wan, J.; Spesock, A.; Sergueeva, Z.; Shaw, B. R.; Alexander, K. A. *Nucleic Acids Res*. **2006**, *34*, 2773.

[12] Zhang, N.; Tan, C.; Cai, P.; Zhang, P.; Zhao, Y.; Jiang, Y. *Bioorg. Med. Chem*. **2009**, *17*, 2441.

[13] Iwase, R.; Toyama, T.; Nishimori, K. *Nucleosides Nucleotides Nucleic Acids* **2007**, *26*, 1451.

[14] Potenza, N.; Moggio, L.; Milano, G.; Salvatore, V.; Di Blasio, B.; Russo, A.; Messere, A. *Int. J. Mol. Sci.* **2008**, *9*, 299.

[15] Dueholm, K. L.; Egholm, M.; Behrens, C.; Christensen, L.; Hansen, H. F.; Vulpius, T.; Petersen, K. H.; Berg, R. H.; Nielsen, P. E.; Buchardt, O. *J. Org. Chem.* **1994**, *59*, 5767.

[16] Corradini, R.; Sforza, S.; Tedeschi, T.; Totsingan, F.; Marchelli, R. *Curr. Top. Med. Chem.* **2007**, *7*, 681.

[17] Porcheddu, A.; Giacomelli, G. *Curr. Med. Chem.* **2005**, *12*, 2561.

[18] Isobe, H.; Fujino, T.; Yamazaki, N.; Guillot-Nieckowski, M.; Nakamura, E. *Org. Lett.* **2008**, *10*, 3729.

[19] El-Sagheer, A. H.; Brown, T. *J. Am. Chem. Soc.* **2009**, *131*, 3958.

[20] Fujino, T.; Yamazaki, N.; Isobe, H. *Tetrahedron Lett.* **2009**, *50*, 4101.

[21] Schoning, K. U.; Scholz, P.; Guntha, S.; Wu, X.; Krishnamurthy, R.; Eschenmoser, A. *Science* **2000**, *290*, 1347.

[22] Zhang, L. L.; Peritz, A.; Meggers, E. *J. Am. Chem. Soc.* **2005**, *127*, 4174.

[23] Pallan, P. S.; von Matt, P.; Wilds, C. J.; Altmann, K. H.; Egli, M. *Biochemistry* **2006**, *45*, 8048.

[24] DeMesmaeker, A.; Jouanno, C.; Wolf, R. M.; Wendeborn, S. *Bioorg. Med. Chem. Lett.* **1997**, *7*, 447.

[25] Denapoli, L.; Iadonisi, A.; Montesarchio, D.; Varra, M.; Piccialli, G. *Bioorg. Med. Chem. Lett*. **1995**, *5*, 1647.

[26] Rostovtsev, V. V.; Green, L. G.; Fokin, V. V.; Sharpless, K. B. *Angew. Chem. Int. Ed.* **2002**, *41*, 2596.

[27] Still, W. C.; Kahn, M.; Mitra, A. *J. Org. Chem.* **1978**, *43*, 2923.

[28] Thansandote, P.; Gouliaras, C.; Turcotte-Savard, M. O.; Lautens, M. *J. Org. Chem.* **2009**, *74*, 1791.

[29] Mayer, T.; Maier, M. E. *Eur. J. Org. Chem.* **2007**, 4711.

[30] Kryatova, O. P.; Connors, W. H.; Bleczinski, C. F.; Mokhir, A. A.; Richert, C. *Org. Lett.* **2001**, *3*, 987.

[31] Wenninger, D.; Seliger, H. Nucleosides Nucleotides **1997**, *16*, 977.

[32] Bajor, Z.; Sagi, G.; Tegyey, Z.; Kraicsovits, F. *Nucleosides Nucleotides Nucleic Acids* **2003**, *22*, 1963.

Connecting Statement I

Having clearly established the compatibility of the unnatural triazole-based linkage with Watson-Crick interactions in duplex DNA molecules, and having determined that it is a destabilizing modification from the Chapter I study, our results paved the way towards the use of this unnatural linkage within synthetic siRNA constructs. In the following study, we chemically incorporated both triazole-linked uracil-uracil and cytosine-uracil nucleoside dimer analogs throughout siRNAs using phosphoramidite chemistry. These siRNAs were designed to either target the exogenous *firefly* luciferase reporter gene or the endogenous glyceraldehyde-3-phosphoate dehydrogenase (GAPDH) gene. We characterized the resultant triazole-modified siRNAs using Circular Dichroism spectroscopy and UV-monitored thermal denaturation experiments, while ascertaining their efficacy through a dual-reporter luciferase assay and qRT-PCR.

Chapter III – Manuscript II

Efficient synthesis and cell-based silencing activity of siRNAs that contain triazole backbone linkages

Tim C. Efthymiou, Vanthi Huynh, Jaymie Oentoro, Brandon Peel, and Jean-Paul Desaulniers*

Published in:

Bioorganic & Medicinal Chemistry Letters **2012**, *22*, 1722-1726.

DOI:10.1016/j.bmcl.2011.12.104

3.0 Abstract

An efficient synthesis of siRNAs modified at the backbone with a triazole functionality is reported. Through the use of 4,4′-dimethoxytrityl (DMT) phosphoramidite chemistry, triazole backbone dimers were site-specifically incorporated throughout various siRNAs targeting both firefly luciferase and glyceraldehyde-3-phosphate dehydrogenase (GAPDH) gene transcripts as representatives of an exogenous and endogenous gene, respectively. Following the successful silencing of the firefly luciferase reporter gene, triazole-modified siRNAs were also found to be capable of silencing GAPDH in a dose-dependent manner. Backbone modifications approaching the 3′-end on the sense strand were tolerated without compromising siRNA potency. This study highlights the compatibility of triazole-modified siRNAs within the RNAi pathway, and the modification′s potential to impart favorable properties to siRNAs designed to target other endogenous genes.

3.1 Introduction

In 1998, Fire and Mello reported that short interfering RNAs (siRNAs) could be introduced into cells in *Caenorhabditis elegans* and block gene expression.[1] This process involves the incorporation of siRNAs into an RNA-induced silencing complex (RISC), which serves to select and deliver the guide strand to its target messenger RNA (mRNA) for selective gene silencing.[2] Since this discovery, there has been considerable interest in utilizing siRNAs as potential therapeutic agents in combating disease.[3] However, natural siRNAs are prone to degradation by nucleases and exhibit poor cell membrane permeability due to their polyanionic charge. There is wide interest in chemically modifying siRNAs in order to alleviate the aforementioned problems.

A vast number of studies have thoroughly explored the properties of chemically modified oligonucleotides that contain the unnatural architecture at the sugars[4] and bases.[5] However, relatively very little has been done with respect to modifying the internucleotide linkage of siRNAs with nonionic moieties. With respect to negatively charged backbone mimics, phosphorothioates (PS) have been shown to be accommodated within the RNAi pathway; however, ranges in potency are often observed and cytotoxicity is a concern.[6] Alternatively, functional data of siRNAs bearing boranophosphate linkages show RNAi compatibility and offer enhanced potency comparable to PS with reduced cytotoxicity.[7]

With respect to nonionic backbone modifications, two studies have shown that these can be accommodated within the 3′-overhangs of siRNAs. Iwase and co-workers have shown that an amide linkage enhances thermodynamic stability and resistance to nucleases.[8] Potenza and co-workers have also illustrated that an amide-bond at the 3′-end of siRNAs acts as a substrate for the RNAi pathway.[9]

The crystal structure of the RISC complex by Patel et al., complexed with a duplex oligonucleotide reveals that a number of key phosphodiester contacts are necessary for its interaction with the protein complex; however, many of these ionic contacts are not present on the sense strand of the oligonucleotide.[10] Therefore, we envisioned that by modifying the sense strand, we could synthesize novel siRNAs with uncharged

backbones within the duplex that could thus serve as appropriate substrates for the RNAi pathway without compromising their potency.

Utilizing the well-known Cu(I)-assisted Huisgen 1,3-dipolar cycloaddition,[11] the triazole moiety can be introduced as an uncharged oligonucleotide backbone modification with relative ease. Although a variety of triazole-modified oligonucleotide mimics have been reported, most constructs are DNA-based.[12] Reports of click-ligated RNAs include one from El-Sagheer and Brown,[13] who were successful in synthesizing functional hairpin ribozymes containing both cross- and intra-strand triazole linkages. Other reports of triazoles within RNAs include work from Das and co-workers,[14a] and most recently from Rozners and co-workers[14b] who demonstrated site-specific incorporation of a triazole-linked nucleoside dimer within RNAs.

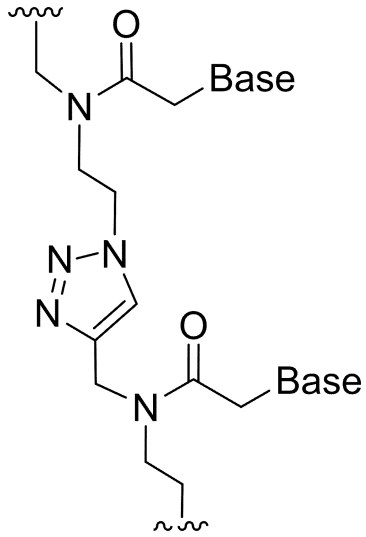

Figure 3.8 Triazole-Linked Nucleic Acid

In previous work, we have synthesized a triazole-linked nucleoside dimer phosphoramidite based on a PNA-like structure, and this modification displayed compatibility when hybridized to its complement.[15] Despite the numerous examples of distinct nucleoside backbone derivatives linked together through a triazole moiety, none of the derivatives have been reported as substrates within the RNAi pathway. Herein, we report the incorporation of triazole-linked nucleic acids based on a PNA-type scaffold (Fig. 3.8) within duplex siRNAs. The RNAs display effective gene silencing and thus exhibit a high degree of compatibility as RNAi substrates.

3.2 Materials and Methods

3.2.1 General Synthetic Methods

Unless otherwise noted, all starting materials were obtained from commercial sources and were used without any additional purification. Anhydrous CH_2Cl_2, THF and DMF were purchased from Sigma-Aldrich and degassed by stirring under a dry N_2 atmosphere.

Purification by flash column chromatography was carried out with Silicycle Siliaflash 60 (230-400 mesh) according to the procedure of Still, Kahn, and Mitra.[16] ^{1}H NMR, ^{13}C NMR, and ^{31}P NMR spectra were recorded at 400 or 500 MHz, 100 or 125 MHz, and 167 MHz, respectively, in either DMSO-d_6 or $CDCl_3$. ESI-MS spectra were recorded on a Waters Quattro Micro MS. Both HRMS and ESI Q-TOF spectra were recorded on an Agilent Q-TOF. Circular Dichroism (CD) spectroscopy and UV-monitored thermal denaturation were both performed on a Jasco J-815 CD equipped with temperature control.

3.2.2 Procedure for the Chemical Synthesis of Oligonucleotides

All standard *β*-cyanoethyl RNA phosphoramidites, reagents and solid supports were purchased from Chemgenes Corporation and Glen Research. Wild-type sequences were purchased and purified from Integrated DNA Technologies (IDT). All modified oligonucleotides were synthesized on an Applied Biosystems 394 DNA/RNA synthesizer using 0.2 μM or 1.0 μM cycles with 16 min coupling times for all modified and unmodified phosphoramidites. All commercial phosphoramidites were dissolved in anhydrous acetonitrile to a concentration of 0.1 M, while chemically synthesized triazole-modified phosphoramidites were dissolved to a concentration of 0.08 M. A lower concentration (0.08 M) of the triazole-linked amidite dimers was used because the compound was not fully soluble in acetonitrle at 0.1 M concentration. We observed an average coupling efficiency of >98% with the use of the triazole amidites as monitored by trityl cation absorbance. Sequences containing 3′ modifications were synthesized on 1.0 μM Universal III solid supports, while all other sequences were synthesized on 0.2 μM or 1.0 μM dT solid supports (Glen Research). Antisense sequences were chemically phosphorylated on the 5′ end using 2-[2-(4,4′-Dimethoxytrityloxy)ethylsulfonyl]ethyl-(2-cyanoethyl)-(N,N-diisopropyl)-phosphoramidite (Glen Research). Cleavage of oligonucleotides from their solid supports was performed through on-column exposure to 1.5 mL of EMAM (methylamine 40% wt. in H_2O and methylamine 33% wt. in ethanol, 1:1 (Sigma-Aldrich)) for 30 min at room temperature, followed by incubation in EMAM overnight to deprotect the bases. Crude oligonucleotides were precipitated in EtOH and desalted through Millipore Amicon Ultra 3000 MW cellulose centrifugal filters.

Oligonucleotides were excised from the 20% denatured gel and were gel purified, followed by desalting through centrifugal filters. Final oligonucleotide purity was visualized on a denaturing 20% polyacrylamide gel electrophoresis (PAGE) stained with ethidium bromide or by UV-shadowing. These RNAs were subjected to ESI Q-TOF to confirm their expected mass. Equimolar amounts of complimentary RNAs were annealed at 90 ^{o}C for 2 min in a binding buffer (75 mM KCl, 50 mM Tris-HCl, 3 mM $MgCl_2$, pH 8.3) and this solution was cooled slowly to room temperature to generate siRNAs.

3.2.3 Chemical and Structural Characterization of Oligonucleotides

3.2.3.1 Circular Dichroism Spectroscopy

Equimolar amounts of each RNA (2.4 nmol) were annealed to their compliment in 500 µL of a sodium phosphate buffer (90 mM NaCl, 10 mM Na_2HPO_4, 1 mM EDTA, pH 7) at 90 ^{o}C for 2 min and this solution was cooled slowly to rt. CD measurements of each duplex were recorded in quadruplicate from 200 to 310 nm at 20 ^{o}C in the sodium phosphate buffer, with a scanning rate of 10 nm/min and a 0.2 nm data pitch. The average of four accumulations was calculated using Jasco′s Spectra Manager version 2 software and adjusted against the baseline measurement of the buffer.

3.2.3.2 Melting Temperature (T_m) Determination Through UV-Monitored Thermal Denaturation

Melting temperatures (T_m) were measured in the sodium phosphate buffer at 260 nm with a temperature range of 10 to 95 ^{o}C. The temperature was increased at a rate of 0.5 ^{o}C/min while absorbance was measured at the end of each 0.5 ^{o}C increment. Absorbance readings were automatically adjusted against the baseline absorbance of the sodium phosphate buffer. After averaging the range of absorbance values obtained from three independent experiments for each siRNA, T_m′s were calculated using Meltwin version 3.5 software assuming the two-state model.[17]

3.2.3.3 High-Resolution Mass Spectrometry

Compounds **1** through **8** were analyzed through positive electrospray ionization using a mobile phase of acetonitrile/MeOH (95:5) with 0.1% formic acid. Being acid labile, the mobile phase for compound **8** was pure MeOH.

3.2.3.4 Quantitative Time-of-Flight Mass Spectrometry

All single-stranded RNAs were gradient eluted through a Zorbax Extend C18 HPLC column with a MeOH/H_20 (5:95) solution containing 200 mM hexafluoroisopropyl alcohol and 8.1 mM triethylamine, and finally with 70% MeOH. The eluted RNAs were subjected to ESI-MS (ES-), producing raw spectra of multiply-charged anions and through resolved isotope deconvolution, the molecular weights of the resultant neutral oligonucleotides were confirmed for all the RNAs (Table A6, Appx. II).

3.2.4 Methods for Culturing Eukaryotic Cells

HeLa cells were cultured in Dulbecco′s modified eagle′s medium (DMEM) containing 10% fetal bovine serum (FBS) (Perbio) and 1% Penicillin-Streptomycin (Sigma) at 37 ^oC with 5% CO_2. For passaging cells, a 1X solution of 0.25% Trypsin (SAFC Bioscience) as used to disperse the cells.

3.2.5 Time-Dependent Nuclease Stability Assays

Duplex siRNAs **wt**, **17**, **18** and **22** (12 μM) were incubated at 37 ^oC in 10 μL of a 13.5% solution of FBS for 0.5, 1, 1.5, 3 and 5 hours. In order to visualize duplex degradation as a function of time, samples were immediately resolved using 20% native PAGE after each incubation time. Gels were stained with a 3X solution of Gel Red nucleic acid stain (Biotium) for 30 min and visualized on a Fluorchem SP (Figure A51, Appx. II). These siRNAs were digested under similar identical conditions 5 and 12 hours, after which they were incubated at 95 ^oC to for 5 min to reduce or eliminate any residual nuclease activity and gradually cooled to room temperature. HeLa cells were transfected with 80 pM of each digested siRNA and efficiency was monitored using the protocol described below (Figure A52, Appx. II).

3.2.6 Gene-Silencing Capabilities of Triazole-Modified siRNAs

3.2.6.1 *Firefly* luciferase Dual-Reporter *In Vitro* Assay

Prior to transfection, HeLa cells were seeded on 12-well plates (Greiner Bio-One) at a density of 100,000 cells per well and incubated at 37 °C with 5% CO_2 in DMEM containing 10% FBS. After 24 hr, varying concentrations of anti-luciferase siRNAs **9** - **20** were co-transfected with both pGL3 (Promega) and pRLSV40 (York University) luciferase-expressing plasmids using Lipofectamine 2000 (Invitrogen) in Gibco′s Opti-Mem Reduced Serum Medium 1X (Invitrogen) according to the manufacturer′s protocol. After an additional 24 hr, cells were incubated in 1X passive lysis buffer (Promega) for 20 min at room temperature, and cell lysate was loaded onto white and opaque, 96-well plates (Costar). Using the Dual-luciferase Reporter Assay kit (Promega), observed luminescence was proportional to both *firefly* and *renilla* luciferase expression, recorded on a Synergy HT (Bio-Tek) plate luminometer. The ratio of *firefly*/*renilla* luminescence expressed as a percentage relates the reduction in *firefly* expression to siRNA efficacy when compared to untreated controls. Each value is the average of at least three independent experiments with the indicated error (SDOM).

3.2.6.2 Quantitative Real-Time Expression of Glyceraldehyde-3-Phosphate Dehydrogenase

On a 12-well plate, 65,000 HeLa cells were added to each well and incubated at 37 °C with 5% CO_2 in DMEM with 10% FBS. After 24 hr, cells were treated with 10 nM and 20 nM concentrations of anti-GAPDH siRNAs using Lipofectamine 2000 in 1X Opti-Mem according to the manufacturer′s protocol. Achieving a cellular concentration of approximately 260,000 cells/well after a total incubation time of 48 hr, cells were dispersed with trypsin and lysed for the reverse transcription (RT) of total RNA. RT was performed using the Cells-to-cDNA II kit (Applied Biosystems) following the manufacturer′s protocol. Amplification of GAPDH and 18S cDNA was accomplished on a CFX96 Real-Time reactor (BIO-RAD), using SsoFast EvaGreen Supermix (BIO-RAD) as the source of SYBR green and *Taq* Polymerase, along with 800 nM of GAPDH forward/reverse primers and 60 nM of 18S forward/reverse primers, all contained within 20 μL reaction volumes. The GAPDH forward and reverse primers were 5′- AGG GCT

GCT TTT AAC TCT GG -3′ and 5′- TTG ATT TTG GAG GGA TCT CG - 3′, respectively, yielding a 200-bp amplicon.[18] The 18S forward and reverse primers were 5′-CGG CTA CCA CAT CCA AGG AAG -3′ and 5′- CGC TCC CAA GAT CCA ACT AC -3′, respectively, yielding a 247-bp amplicon.[18] Non-reverse transcriptase controls were performed for each GAPDH and 18S sample, and a no-template control accompanied each set of GAPDH and 18S samples. The reactor protocol consisted of the following events: pre-heat to 95 °C for 60 sec; 40 cycles of denaturing at 95 °C for 5 sec and annealing/elongating at 47 °C for 20 sec. The protocol concluded with thermal denaturation analysis of the PCR products by raising the temperature from 65 to 95 °C at 0.5 °C/min and measuring the absorbance at 260 nm. GAPDH gene expression was normalized to 18S using the Comparative *Ct* method ($2^{(\Delta Ct_{18S}-\Delta Ct_{GAPDH})}$), while error was calculated as the overall coefficient of variance ($CV = \sqrt{CV_{18S}^2 + CV_{GAPDH}^2}$).

3.2.7 Synthesis and Characterization of Organic Compounds

3.2.7.1 Synthesis of 2-Azido-*N*-(2-(*tert*-butyldimethylsilyloxy)ethyl)ethanamine – Compound (1)

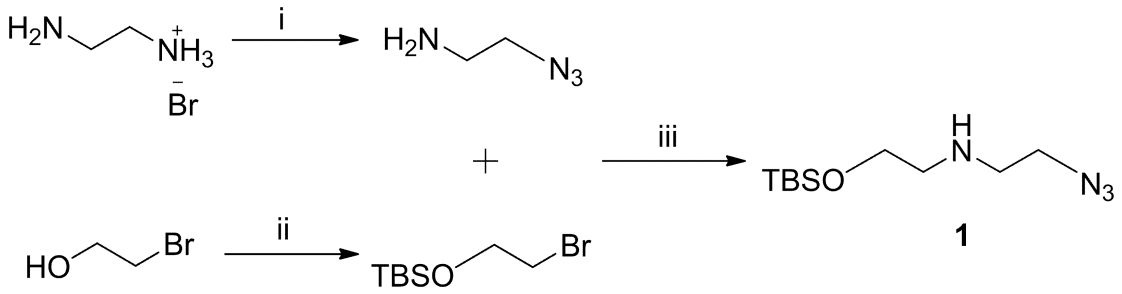

Scheme 3.4 Stepwise Synthesis of Compound **1**.

---

i. To a solution of NaN_3 (23.8 g, 366 mmol) in 200 mL of water was added 2-bromoethylamine hydrobromide (25 g, 122 mmol) and this solution was heated to 75 °C. The reaction mixture was stirred for 24 h and was then cooled in an ice-water bath. To the cooled solution was added NaOH (28.5 g, 712.5 mmol) and the reaction mixture was stirred until the NaOH was fully dissolved. To this aqueous solution was added Et_2O (x3). The ether fractions were collected, dried over Na_2SO_4 and evaporated *in vacuo* to

afford 2-azidoethanamine as a clear oil (6.7 g, 64%). The ^{1}H proton and ^{13}C NMR shifts were confirmed in the report by Mayer and Maier (Scheme 3.4).[19]

ii. To a solution of *tert*-butyldimethylsilyl chloride (TBS-Cl) (11.6 g, 77 mmol) in 25 mL of DMF was added imidazole (6.2 g, 91 mmol) followed by the dropwise addition of 2-bromoethanol (8.7 g, 70 mmol). The reaction mixture was stirred for 12 h at room temperature, extracted with EtOAc and washed with H_2O (x3). The combined organic fractions were dried over Na_2SO_4 and concentrated *in vacuo* to afford (2-bromoethoxy)(*tert*-butyl)dimethylsilane as a clear colourless oil (15.3 g, 92%) The ^{1}H proton and ^{13}C NMR shifts were confirmed in the report by Vader et al (Scheme 3.4).[20]

iii. The (2-bromoethoxy)(*tert*-butyl)dimethylsilane from step **ii** (5.8 g, 24.4 mmol) was added dropwise to a solution of 2-azidoethanamine from step **i** (2.1 g, 24.4 mmol) and diisopropylethylamine (6.7 g, 51.8 mmol) in 100 mL of dry DMF under N_2 while stirring in an ice bath. This reaction mixture was then stirred for an additional 48 h at room temperature. The solution was extracted with EtOAc and washed with H_2O and brine (x3). The EtOAc fractions were collected, dried over Na_2SO_4 and evaporated under reduced pressure to yield a crude orange oil. The oil was loaded directly onto a silica column by eluting with MeOH (2% to 10%) in CH_2Cl_2, to afford the title compound **1** as a clear yellow oil (2.3 g, 39%) (Scheme 3.4); ^{1}H NMR (400 MHz, $CDCl_3$) δ 0.07 (s, 6H), 0.91 (s, 9H), 1.67 (br s, 1H), 2.74 (t, 2H, J = 5.1 Hz), 2.83 (t, 2H, J = 5.5 Hz), 3.43 (t, 2H, J = 5.7 Hz), 3.72 (t, 2H, J = 5.3 Hz); ^{13}C NMR (100 MHz, $CDCl_3$) δ -5.4, 18.3, 25.9, 48.4, 51.4, 51.6, 62.3; ESI-HRMS (ES^+) *m/z* calcd for $[C_{10}H_{24}N_4OSi + H]+$: 245.1792, found 245.1797 $[M+H]^+$.

3.2.7.2 Synthesis of *N*-(1-(2-((2-Azidoethyl)(2-(*tert*-butyldimethylsilyloxy)ethyl)amino)-2-oxoethyl)-N^4-(benzoyl)cytosin-1-yl) – Compound (2)

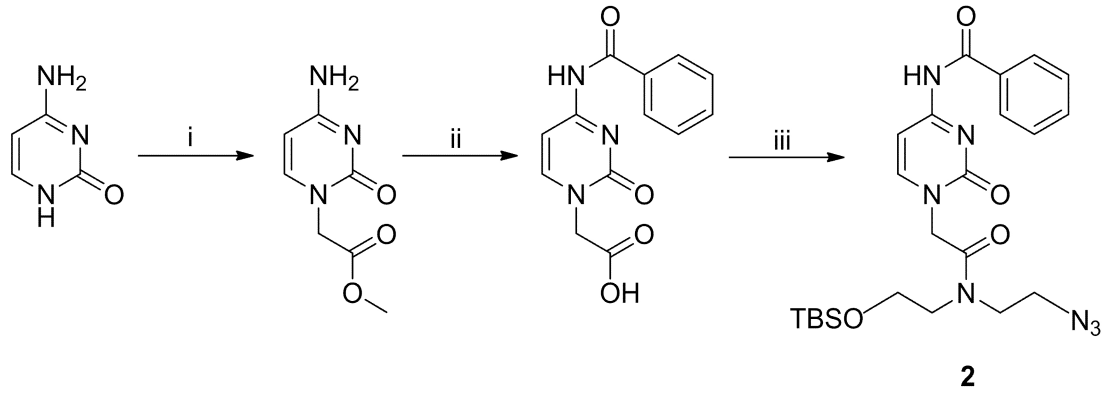

Scheme 3.5 Stepwise Synthesis of Compound **2**.

---

i. To a solution of cytosine (10 g, 90 mmol) in 400 mL of dry DMF was added NaH (2.2 g, 90 mmol) under N_2 in an ice-water bath. This solution was then stirred for 2 h at room temperature, followed by the dropwise addition of methyl bromoacetate (15.1 g, 99 mmol). The reaction was stirred for an additional 48 h at room temperature, after which the solvent was evaporated *in vacuo*. The crude remains were mixed with 200 mL of cold H_2O and stored at 4 ^oC to maximize precipitate formation. The suspension was filtered and washed with minimal amounts of cold H_2O and EtO_2 and recrystallized from MeOH/H_2O affording methyl cytosin-1-yl acetate as a light pink powder (9.9 g, 60%). ^1H proton and ^{13}C NMR shifts were confirmed in the report by Schwergold et al (Scheme 3.5).[21b]

ii. To a solution of methyl cytosin-1-yl acetate from step **i** (5.0 g, 27.3 mmol) in 50 mL of pyridine was added benzoylchloride (4.6 g, 32.8 mmol) and the reaction was stirred overnight at room temperature. The solvent was evaporated *in vacuo* and the crude remains were dissolved and stirred in 1M NaOH for 3 h. Using concentrated HCl, the pH of the solution was adjusted to 5.5 and any undesirable salts were removed through vacuum filtration. Upon further acidification to pH 2, the solution was filtered and the precipitate was washed with cold H_2O affording the N^4-benzoylprotected cytosin-1-yl

acetic acid building block as a light pink powder (4.1 g, 55%). ^{1}H proton and ^{13}C NMR shifts were confirmed in the report by Christensen et al (Scheme 3.5).[21a]

iii. To a round-bottom flask was added N^4-(benzoyl)cytosin-1-yl acetic acid from step **ii** (2.6 g, 9.5 mmol) in 100 mL of DMF and 5 mL of DMSO in order to further solubilise the starting material. After being placed in an ice bath, to this stirring solution was added compound **1** (2.3 g, 9.5 mmol) followed by activation of the acid for 30 min with 1-ethyl-3-(3-dimethylaminopropyl)carbodiimide hydrochloride (EDC-Cl) (3.7 g, 19.3 mmol). The reaction was then stirred overnight at room temperature and extracted with EtOAc and washed with H_2O and brine (x3). The combined organic fractions were dried over Na_2SO_4 and concentrated *in vacuo* yielding a crude oil. This oil was purified by flash column chromatography with a gradient of MeOH (1% to 5%) in CH_2Cl_2 to afford the title compound **2** as a white powder (2.5 g, 53%) (Scheme 3.5). Compound **2** is a mixture of slowly-exchanging rotamers; ^{1}H NMR (400 MHz, $CDCl_3$) δ 0.06 (s, 2H), 0.11 (s, 4H), 0.90 (s, 3H), 0.92 (s, 6H), 3.50-3.55 (m, 4H), 3.66 (t, 1H, J = 5.1), 3.71-3.74 (m, 1H), 3.79 (t, 0.5H, J = 5.3 Hz), 3.84 (t, 1.5H, J = 5.1 Hz), 4.83 (s, 0.5H), 4.85 (s, 1.5H), 7.53 (t, 3H, J = 7.62 Hz), 7.61-7.64 (m, 1.5H), 7.72 (d, 0.5H, J = 6.25 Hz), 7.90 (d, 2H, J = 7.03 Hz), 8.64 (br s, 1H); ^{13}C NMR (100 MHz, $CDCl_3$) δ -5.5, 11.6, 18.2, 18.3, 25.9, 46.2, 46.7, 48.3, 49.0, 49.6, 49.7, 49.9, 51.0, 61.1, 61.3, 96.7, 127.5, 129.0, 133.1, 149.9, 150.1, 155.5, 162.5, 162.6, 166.7, 167.3; ESI-HRMS (ES^+) *m/z* calcd for $[C_{23}H_{33}N_7O_4Si + H]^+$: 500.2436, found 500.2441 $[M+H]^+$.

3.2.7.3 Synthesis of *N*-(1-(2-((2-Azidoethyl)(2-(bis(4-methoxyphenyl)(phenyl)methoxy)ethyl)amino)-2-oxoethyl)-N^4-(benzoyl)cytosin-1-yl) – Compound (3)

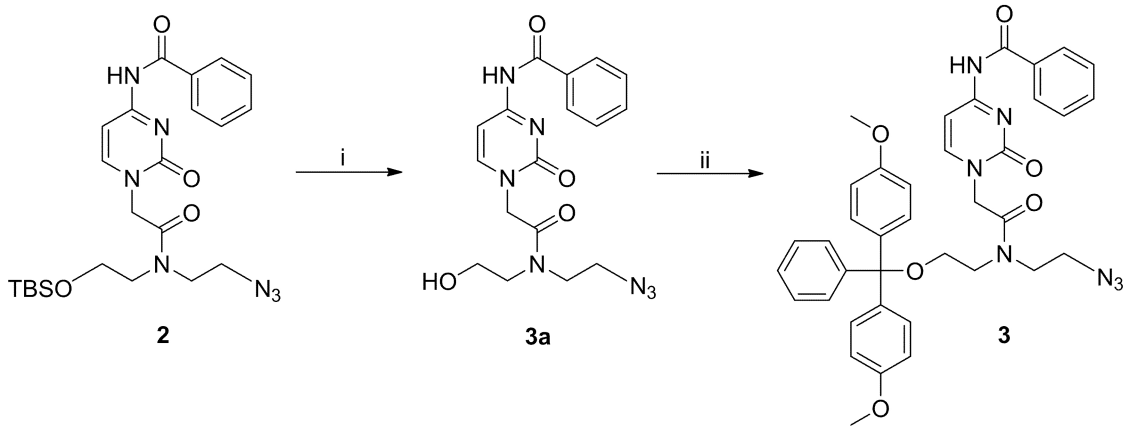

Scheme 3.6 Stepwise Synthesis of Compound **3**.

---

i. To a solution of compound **2** (2.5 g, 5.0 mmol) in 100 mL of CH_2Cl_2 was added an excess of 3HF/TEA (2.8 g, 17.5 mmol), and this reaction was stirred until TLC analysis indicated the complete conversion of starting material to the alcohol (4 h). The reaction was then quenched with MeOH, concentrated under reduced pressure and immediately subjected to silica column purification eluting with a gradient of MeOH (2% to 5%) in CH_2Cl_2. The combined fractions were concentrated and co-evaported with hexanes *in vacuo* affording compound **3a** as a white powder (1.7g, 91%) (Scheme 3.6). Compound **3a** is a mixture of slowly-exchanging rotamers; ^{1}H NMR (400 MHz, $CDCl_3$) δ 3.54 (s, 3H), 3.61-3.64 (m, 1.5H), 3.68 (d, 0.5H, *J* = 4.3 Hz), 3.70 (d, 1H, *J* = 4.7 Hz), 3.79-3.82 (m, 0.5H), 3.83-3.85 (m, 1.5H), 4.50 (br s, 1H), 4.83 (s, 0.5H), 4.94 (s, 1.5H), 7.47 (t, 2.5H, *J* = 7.6 Hz), 7.58 (t, 1.5H, *J* = 7.4 Hz), 7.70 (d, 0.5H, *J* = 2.3 Hz), 7.72 (d, 0.5H, *J* = 2.3 Hz), 7.90-7.94 (m, 2H), 9.16 (br s, 1H); ^{13}C NMR (100 MHz, $CDCl_3$) δ 46.6, 48.3, 49.0, 49.7, 50.0, 50.5, 50.9, 51.3, 59.9, 60.3, 97.1, 127.7, 127.8, 128.9, 132.9, 133.1, 150.3, 150.4, 156.2, 163.0, 163.2, 167.5, 167.7; ESI-HRMS (ES^+) *m/z* calcd for $[C_{17}H_{19}N_7O_4 + H]^+$: 386.1571, found 386.1582 $[M+H]^+$.

ii. To a solution of compound **3a** (1.7 g, 4.4 mmol) in 50 mL of dry pyridine under N_2 was added dimethoxytrityl chloride (DMT-Cl) (3.0 g, 8.8 mmol), and the reaction was stirred overnight at room temperature. The reaction was extracted with

EtOAc, washed with $NaHCO_3$ (x3) and dried over Na_2SO_4. The combined organic fractions were concentrated *in vacuo* and the crude remains were purified through flash column chromatography with a gradient of hexanes/EtOAc (7:3) to 100% EtOAc to elute the title compound **3** as a white solid (2.9 g, 99%) (Scheme 3.6). Compound **3** is a pair of rotamers; wherever possible, the signals to the major (ma.) and minor (mi.) rotamers are designated; ^{1}H NMR (400 MHz, $CDCl_3$) δ 3.35-3.41 (m, 2H), 3.46 (t, 3H, *J* = 5.3 Hz), 3.55 (t, 0.5H, *J* = 4.9 Hz), 3.67 (t, 2H, *J* = 4.5 Hz), 3.74 (t, 0.5H, *J* = 5.9 Hz), 3.82 (s, 1.5H, mi.), 3.83 (s, 4.5H, ma.), 4.83 (s, 0.5H, mi.), 4.92 (s, 1.5H, ma.), 6.85-6.90 (m, 4H), 7.24 (t, 0.5H, *J* = 7.0 Hz), 7.28-7.29 (m, 2.5H), 7.30 (s, 3.5H), 7.35 (t, 2H, *J* = 7.6 Hz), 7.39-7.42 (m, 2.5H), 7.54 (t, 2H, *J* = 7.6 Hz), 7.62-7.66 (m, 1H), 7.71 (d, 0.3H, *J* = 7.4 Hz, mi.), 7.93 (d, 1.7H, *J* = 7.4 Hz, ma.), 8.77 (br s, 1H); ^{13}C NMR (100 MHz, $CDCl_3$) δ 13.7, 19.1, 22.6, 30.6, 31.9, 46.2, 47.1, 47.7, 48.9, 49.0, 49.4, 49.6, 49.9, 55.2, 55.3, 61.1, 61.8, 64.3, 86.6, 87.3, 96.5, 113.2, 113.3, 126.8, 127.2, 127.5, 127.9, 128.0, 128.2, 129.0, 129.9, 130.1, 133.1, 135.2, 135.8, 144.2, 144.6, 149.8, 158.5, 158.7, 162.5, 166.6, 167.1; ESI-HRMS (ES^+) *m/z* calcd for $[C_{38}H_{37}N_7O_6 + H]^+$: 688.2878, found 688.2878 $[M+H]^+$.

3.2.7.4 Synthesis of *N*-(2-(*tert*-Butyldimethylsilyloxy)ethyl)prop-2-yn-1-amine – Compound (4)

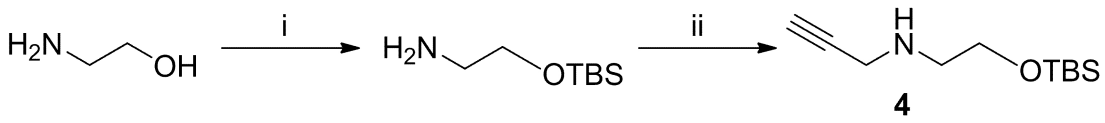

4

Scheme 3.7 Stepwise Synthesis of Compound **4**.

---

i. To a solution of ethanolamine (9.6 mL, 159 mmol) in 100 mL of CH_2Cl_2 was dissolved imidazole (10.8 g, 159 mmol) and this solution was cooled in an ice-water bath. To this solution was added *tert*-butyldimethylsilyl chloride (24 g, 159 mmol) and the reaction mixure was stirred overnight at rt. Sat. $NaHCO_3$ was added and the resulting mixture was partitioned. The organic fractions were dried over Na_2SO_4 and concentrated *in vacuo* to afford 2-(*tert*butyldimethylsilyloxy) ethanamine as a clear light yellow oil (26.8 g, 96%) (Scheme 3.7).[22]

ii. To a solution of 2-(*tert*-butyldimethylsilyloxy)ethanamine from step **i** (10 g, 57 mmol) in 100 mL of CH_2Cl_2 was added diisopropylethylamine (DIPEA) (3.7 g, 28.5 mmol), and this solution was cooled in an ice-water bath. To this solution was added 3-bromoprop-1-yne (3.4 g, 28.5 mmol) dropwise over 30 min. This reaction mixture was stirred at rt. until TLC analysis indicated the complete consumption of starting material (3 h). Sat. $NaHCO_3$ was added and the reaction mixture was partitioned. The organic fraction was dried over Na_2SO_4 and concentrated *in vacuo*, to afford an oil which was purified by silica gel chromatography eluting with a gradient of hexanes/EtOAc (7:3 to 3:7) to afford the title compound **4** as a clear yellow oil (2.9 g, 71%) (Scheme 3.7); ^{1}H NMR (500 MHz, $CDCl_3$) δ 0.07 (s, 6H), 0.90 (s, 9H), 1.67 (br s, 1H), 2.21 (s, 1H), 2.80 (t, 2H, *J* = 5.5 Hz), 3.46 (s, 2H), 3.75 (t, 2H, *J* = 5.1 Hz); ^{13}C NMR (125 MHz, $CDCl_3$) δ -5.4, -5.2, 18.3, 25.8, 26.0, 38.2, 50.5, 62.3, 71.2, 71.2, 82.2; ESI-HRMS (ES^+) *m/z* calcd for $[C_{11}H_{23}NOSi + H]^+$: 214.1622, found 214.1626 $[M + H]^+$.

3.2.7.5 Synthesis of *N*-(2-(*tert*-Butyldimethylsilyloxy)ethyl)-uracil-1-yl-*N*-(prop-2-ynyl)acetamide – Compound (5)

To a solution of uracil-1-yl acetic acid[23] (4.0 g, 23.5 mmol) in 100 mL of dry DMF was added compound **4** (4.5 g, 21.1 mmol), and this solution was cooled in an ice-water bath. Following the addition of EDC-Cl (9.0 g, 46.9 mmol) to the solution, the acid was activated for 30 min while stirring. The reaction mixture was then stirred for 12 h at room temperature, extracted with EtOAc and washed with H_2O and brine (x3). The combined organic fractions were dried over Na_2SO_4 and concentrated *in vacuo* to afford the crude product. This crude product was purified by flash column chromatography with a gradient of hexanes/EtOAc (7:3) to 100% EtOAc to elute the title compound **5** as a white solid (5.0 g, 65%). Compound **5** is a pair of rotamers; wherever possible, the signals to the major (ma.) and minor (mi.) rotamers are designated; ^{1}H NMR (500 MHz, $CDCl_3$) δ 0.04 (s, 2H, mi.), 0.08 (s, 4H, ma.), 0.88 (s, 3H, mi.), 0.89 (s, 6H, ma.), 2.25 (br s, 0.66H, ma.), 2.41 (br s, 0.33H, mi.), 3.58 (t, 0.6H, *J* = 5.3 Hz, mi.), 3.65 (t, 1.4H, *J* = 5.2 Hz, ma.), 3.76 (t, 0.6H, *J* = 5.3 Hz, mi.), 3.85 (t, 1.4H, *J* = 5.0 Hz, ma.), 4.27 (2s, 2H), 4.68 (m, 2H), 5.71-5.74 (m, 1H), 7.13 (d, 0.66H, *J* = 7.9 Hz, ma.), 7.17 (d, 0.33H, *J* = 7.9 Hz, mi.), 9.43 (br s, 0.66H, ma.), 9.48 (br s, 0.33H, mi.); ^{13}C NMR (125 MHz, $CDCl_3$) δ -5.6, -5.4, -3.7, -3.5, 17.9, 18.1, 18.3, 25.5, 25.7, 25.8, 25.9, 26.0, 35.2, 38.7, 48.0, 48.1, 48.8,

49.6, 60.6, 61.7, 72.7, 73.6, 77.9, 78.1, 102.1, 102.2, 145.0, 145.1, 150.9, 163.6, 166.3, 166.7; ESI-HRMS (ES^+) *m/z* calcd for $[C_{17}H_{27}N_3O_4Si + H]^+$: 366.1844, found 366.1845 $[M + H]^+$.

3.2.7.6 Synthesis of *N*-(1-(2-((2-(bis(4-Methoxyphenyl)(phenyl)methoxy)ethyl)(2-(4-((*N*-(2-((*tert*butyldimethylsilyl)oxy)ethyl)-2-(uracil-1-yl)acetamido)methyl)-1*H*-1,2,3-triazol-1-yl)ethyl)amino)-2-oxoethyl)-N^4-(benzoyl)cytosin-1-yl) – Compound (6)

To a solution of compound **3** (1.2 g, 1.7 mmol) and compound **5** (570 mg, 1.6 mmol) dissolved in 70 mL of THF/H_2O (3:2) was added sodium ascorbate (519 mg, 2.6 mmol) until fully dissolved. To this mixture was added $CuSO_4$ (220 mg, 880 pmol), and the reaction was stirred for 4 h at room temperature. The reaction was extracted with EtOAc, washed with H_2O (x3) and the combined organic fractions were dried over Na_2SO_4. The organic layer was concentrated under reduced pressure and the resultant crude product was purified by flash column chromatography eluting with a gradient of MeOH (2% to 5%) in CH_2Cl_2 to afford the title compound **6** as a white solid (1.6 g, 98%). Compound **6** is a mixture of slowly-exchanging rotamers; ^{1}H NMR (400 MHz, $CDCl_3$) δ 0.06 (s, 2H), 0.10 (s, 4H), 0.90 (s, 3H), 0.92 (s, 6H), 3.03 (m, 1.5H), 3.12 (m, 0.5H), 3.24-3.28 (m, 2.5H), 3.51-3.54 (m, 1H), 3.55-3.57 (m, 1.5H), 3.63-3.69 (m, 2H), 3.74-3.78 (m, 2H), 3.81 (s, 1.5H), 3.83 (s, 4.5H), 4.49-4.52 (m, 1.5H), 4.56-4.57 (m, 0.5H), 4.72 (br s, 1.5H), 4.74-4.78 (dd, 3.5H, *J* = 7.0 Hz), 4.84 (d, 0.5H, *J* = 5.1 Hz), 4.88 (s, 0.5H), 5.59-5.70 (m, 1H), 6.81-6.84 (m, 1H), 6.87 (d, 3H, *J* = 9.0 Hz), 7.23 (d, 3H, *J* = 2.3 Hz), 7.25 (s, 2H), 7.27-7.29 (m, 2H), 7.31 (s, 1.5H), 7.34 (d, 2.5H, *J* = 4.7 Hz), 7.38-7.42 (m, 0.5H), 7.52 (t, 2.5H, *J* = 7.6 Hz), 7.60-7.63 (m, 1H), 7.70-7.73 (m, 0.25H), 7.75 (s, 0.5H), 7.93-8.02 (m, 2H), 8.07 (d, 0.25H, *J* = 7.4 Hz), 9.66 (br s, 0.5H), 9.85 (br s, 0.5H); ^{13}C NMR (100 MHz, $CDCl_3$) δ -5.5, 18.1, 18.3, 25.8, 25.9, 41.8, 44.0, 47.6, 47.7, 47.9, 48.0, 48.4, 48.6, 48.7, 49.0, 49.1, 49.2, 50.9, 55.2, 60.7, 60.8, 87.3, 96.8, 101.6, 101.7, 113.1, 113.2, 124.7, 124.9, 127.2, 127.9, 128.0, 128.1, 128.7, 128.8, 129.9, 130.1, 132.9, 133.0, 135.1, 135.8, 143.4, 144.1, 144.2, 145.7, 146.0, 149.9, 151.1, 155.7, 158.4, 158.7, 163.3, 164.0, 164.1, 166.6, 167.4, 167.5, 167.7; ESI-HRMS (ES^+) *m/z* calcd for $[C_{55}H_{64}N_{10}O_{10}Si + H]^+$: 1053.4649, found 1053.4643 $[M+H]^+$; for $[C_{55}H_{64}N_{10}O_{10}Si + Na]^+$: 1075.4468, found 1075.4459 $[M+Na]^+$.

3.2.7.7 Synthesis of *N*-(1-(2-((2-(bis(4-methoxyphenyl)(phenyl)methoxy)ethyl)(2-(4-((2-(uracil-1-yl)-*N*-(2-hydroxyethyl)acetamido)methyl)-1*H*-1,2,3-triazol-1-yl)ethyl)amino)-2-oxoethyl)-N^4-(benzoyl)cytosin-1-yl) – Compound (7)

To a solution of compound **6** (1.3 g, 1.2 mmol) in 25 mL of THF was added TBAF (500 mg, 1.9 mmol), and this solution was stirred until TLC analysis displayed the complete conversion of starting material to the alcohol (2.5 h). After concentrating the reaction mixture *in vacuo*, the crude product was purified by flash column chromatography with a gradient of MeOH (2% to 15%) in CH_2Cl_2 eluting the title compound **7** as a white powder (1.1 g, 99%). Compound **7** is a mixture of slowly-exchanging rotamers; ^{1}H NMR (400 MHz, $CDCl_3$) δ 3.09 (br s, 1.5H), 3.15 (br s, 0.5H), 3.25-3.30 (m, 2H), 3.62 (d, 4H, *J* = 3.1 Hz), 3.73 (br s, 2H), 3.81 (s, 1.5H), 3.83 (s, 4.5H), 4.51 (d, 1.5H, *J* = 4.7 Hz), 4.59-4.61 (m, 0.5H), 4.67-4.71 (m, 3.5H), 4.82 (br s, 1.5H), 4.87-4.89 (m, 2H), 5.61 (t, 1H, *J* = 7.0 Hz), 6.88 (d, 4H, 9.0 Hz), 7.24 (s, 3H), 7.26 (s, 2H), 7.28-7.32 (m, 3H), 7.35 (d, 3.5H, *J* = 4.7 Hz), 7.38, (br s, 0.5H), 7.50 (t, 2H, *J* = 7.6 Hz), 7.58-7.61 (m, 1.5H), 7.76 (s, 0.5H), 8.00 (d, 1.5H, *J* = 7.8 Hz), 8.04 (d, 0.5H, *J* = 10.9 Hz), 9.72-9.85 (m, 2H); ^{13}C NMR (100 MHz, $CDCl_3$) δ 20.1, 43.0, 43,8, 47.4, 48.0, 48.9, 49.2, 48.0, 51.2, 51.3, 55.3, 59.6, 60.7, 60.8, 87.3, 87.4, 97.3, 101.6, 113.2, 113.3, 124.9, 125.6, 127.2, 128.0, 128.1, 128.2, 128.8, 129.9, 130.1, 132.9, 133.1, 135.1, 135.7, 143.3, 144.1, 144.2, 144.5, 146.0, 146.2, 150.0, 151.1, 151.2, 156.2, 158.2, 158.5, 158.7, 163.6, 164.1, 164.2, 167.0, 167.6, 167.8; ESI-HRMS (ES^+) *m/z* calcd for $[C_{49}H_{50}N_{10}O_{10} + H]^+$: 939.3784, found 939.3776 $[M+H]^+$; for $[C_{49}H_{50}N_{10}O_{10} + Na]^+$: 961.3604, found 961.3591 $[M+Na]^+$.

3.2.7.8 Synthesis of 2-(*N*-((1-(2-(2-(N^4-(benzoyl)cytosin-1-yl)-*N*-(2-(bis(4-methoxyphenyl)(phenyl)methoxy)ethyl)acetamido)ethyl)-1*H*-1,2,3-triazol-4-yl)methyl)-2-(uracil-1-yl)acetamido)ethyl (2-cyanoethyl) diisopropylphosphoramidite – Compound (8)

To a solution of compound **7** (300 mg, 320 μmol) in 10 mL of dry CH_2Cl_2 under N_2, was added DIPEA (227 mg, 1.8 mmol) and 4-dimethylaminopyridine (20 mg, 160 μmol) while stirring. To this mixture was added 2-cyanoethyl diisopropylphosphoramidochloridite (227 mg, 960 μmol), and the consumption of starting material was monitored by TLC (3 h). After concentrating this reaction *in vacuo*, the crude product was loaded directly on to a silica column for purification with a gradient of 2% triethylamine in acetone/hexanes (1:1 to 3:1) to afford the title compound

8 as a white powder (266 mg, 73%). Compound **8** is a mixture of slowly-exchanging rotamers. The two phosphorus signals in the ^{31}P NMR spectrum are due to the diasteromeric nature of the ^{31}P atom for the respective phosphoramidite **8**; ^{1}H NMR (400 MHz, $CDCl_3$) δ 1.15-1.20 (m, 13H), 1.26 (s, 3H), 2.63-2.68 (m, 3H), 3.02 (br s, 1H), 3.13-3.18 (m, 1H), 3.21 (t, 1H, *J* = 4.3 Hz), 3.24-3.28 (m, 1H), 3.55-3.67 (m, 6H), 3.75-3.79 (m, 2.5H), 3.80 (s, 1.5H), 3.81 (s, 4.5H), 3.82-3.90 (m, 1.5H), 4.51 (t, 1.5H, *J* = 4.5 Hz), 4.55 (t, 0.5H, *J* = 4.7 Hz), 4.70 (s, 2H), 4.75 (d, 2.5H, *J* = 4.3 Hz), 4.79 (d, 0.5H, *J* = 3.1 Hz), 4.88 (s, 1H), 5.66-5.69 (m, 1H), 6.85 (d, 4H, *J* = 9.0 Hz), 7.21 (d, 2H, *J* = 2.3 Hz), 7.23 (m, 2H), 7.28-7.29 (m, 0.5H), 7.32 (d, 3.5H, *J* = 3.9 Hz), 7.37-7.40 (m, 1H), 7.52 (t, 2.5H, *J* = 7.6 Hz), 7.60-7.63 (m, 1H), 7.79 (s, 0.5H), 7.95-8.01 (m, 2H); ^{13}C NMR (100 MHz, $CDCl_3$) δ 20.3, 20.4, 24.5, 24.6, 24.7, 26.6, 29.2, 29.6, 31.7, 31.8, 41.7, 42.9, 43.0, 43.1, 43.5, 46.0, 47.1, 47.5, 47.8, 48.0, 48.5, 48.8, 49.0, 51.0, 53.8, 55.2, 58.1, 58.2, 58.4, 60.6, 60.8, 60.9, 69.4, 87.2, 87.3, 96.8, 101.6, 106.5, 113.1, 113.2, 117.9, 118.1, 123.6, 124.7, 124.9, 127.2, 127.8, 127.9, 128.0, 128.1, 128.6, 128.8, 129.9, 130.1, 132.9, 133.0, 135.1, 143.3, 144.1, 144.2, 146.1, 149.9, 151.1, 155.7, 158.4, 158.7, 163.3, 164.0, 164.2, 166.8, 167.5, 167.6; ^{31}P NMR (167 MHz, $CDCl_3$) δ 149.02 and 149.56; ESI-HRMS (ES^+) *m/z* calcd for $[C_{58}H_{67}N_{12}O_{11}P + Na]^+$: 1161.4682, found 1161.4672 $[M+Na]^+$.

3.3 Results

3.3.1 Synthesis of DMT-Protected Cytosine Azide Monomer

In this paper, we expanded the scope of siRNA sequences and modified them with a cytosine-triazole-uracil (C_tU) dimer in addition to the uracil-triazole-uracil (U_tU) dimer previously synthesized. Synthesis of the C_tU dimer phosphoramidite commenced through the generation of 2-azidoethanamine from bromoethylamine combined with sodium azide. This compound was alkylated with 2-bromoethoxy-*tert*-butyldimethylsilane[20] in 39% yield to afford azide linker **1**. Utilizing EDC as a coupling reagent, this compound was amide-bond coupled to N^4-benzoylcytosin-1-yl acetic acid[21] to generate monomer **2** in 62% yield. TBS-deprotection of **2** with 3HF-TEA afforded a monoalcohol, which was then protected with a 4,4′-dimethoxytrityl group (DMT) to produce compound **3** in 90% yield (Scheme 3.8).

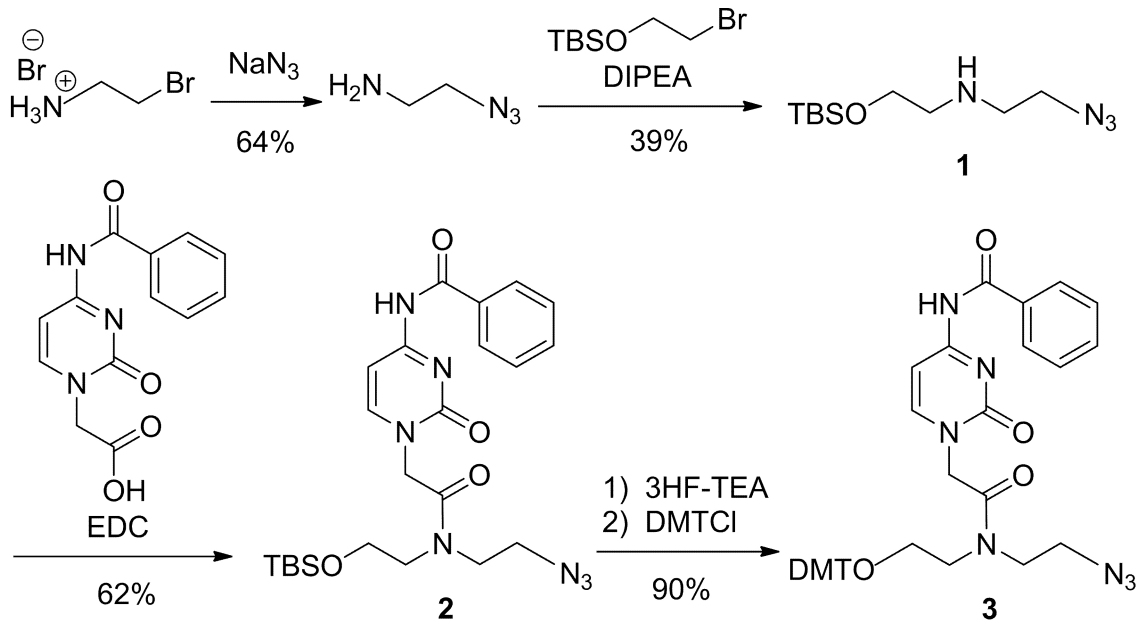

Scheme 3.8 Synthesis of azide intermediate.

3.3.2 Synthesis of Uracil Alkyne Monomer

In order to generate an appropriate alkyne monomer, alkyne linker **4** was synthesized in 71% yield by treating TBS-protected ethanolamine with limiting equivalents of propargyl bromide. This linker was amide-bond coupled to uracil-1-yl acetic acid[24] using EDC as the coupling reagent to produce monomer **5** in 52% yield (Scheme 3.9).

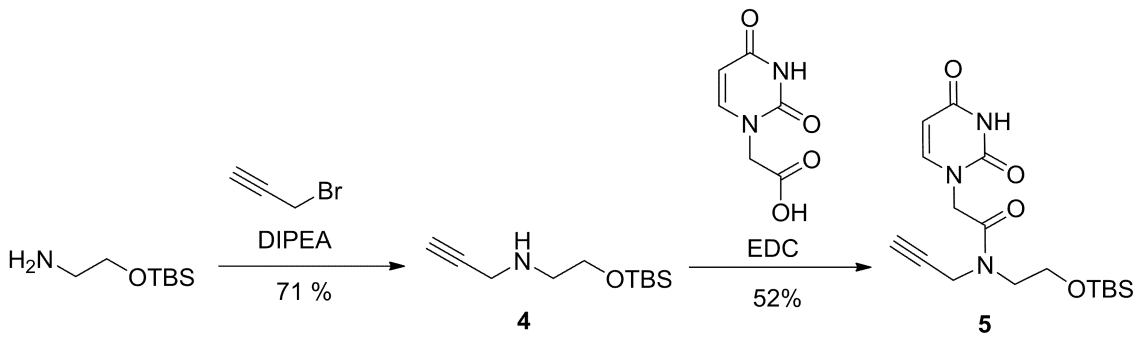

Scheme 3.9 Synthesis of alkyne intermediate.

3.3.3 Synthesis of Triazole-Linked C_tU Phosphoramidite

With both azide (**3**) and alkyne (**5**) monomers available, 1,4-triazole formation catalyzed with $CuSO_4$ and sodium ascorbate in a THF/H_2O solution afforded compound **6** in 98% yield. TBAF deprotection of the silyl protective group on compound 6 afforded compound **7** in 99% yield. Finally, compound **7** was treated with a phosphitylating reagent to afford the phosphoramidite **8** in 73% yield (Scheme 3.10). Both the C_tU and U_tU phosphoramidites were used to synthesize a variety of triazole-modified siRNAs.

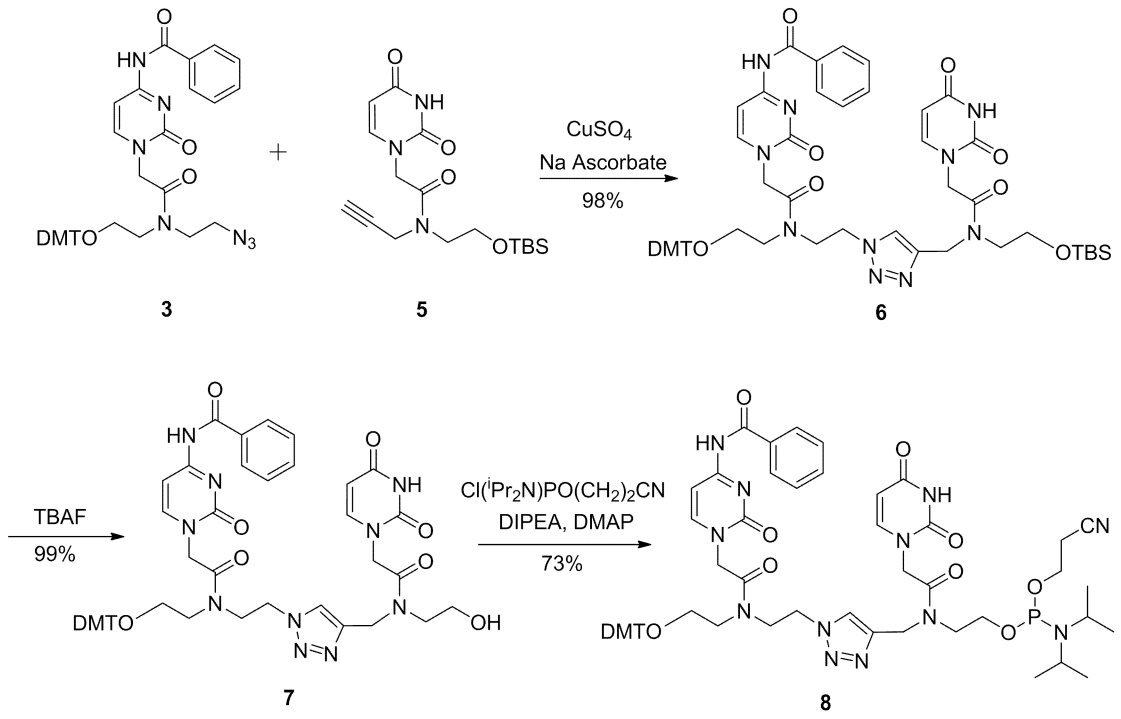

Scheme 3.10 Synthesis of C_tU phosphoramidite.

3.3.4 Helical Conformation and T_m's of Triazole-Modified siRNAs

Various siRNAs were synthesized, bearing one to three triazole backbone modifications through the use of an ABI DNA/RNA synthesizer. These siRNAs were designed to target *firefly* luciferase mRNA expressed within HeLa cells, in order to gauge their functionality within cells-based systems (Table 3.2).

To first examine the effects of our RNAs, we investigated the effect of circularly polarized light on our siRNA duplexes to determine whether our chemically modified duplexes were still able to retain A-type helical structure. Figure A50 (Appx. II) illustrates that the siRNAs retain the characteristic A-form helix; however, a loss of helicity for double-stranded RNAs that contain the internal triazole backbone modification is observed.

Table 3.2 Sequences of anti-luciferase siRNAs and T_m's

RNA	siRNA duplex	[a]T_m (°C)	ΔT_m (°C)
wt	5′- CUUACGCUGAGUACUUCGAtt -3′ 3′- ttGAAUGCGACUCAUGAAGCU -5′	71.4	--
9	5′- C$_t$UUACGCUGAGUACUUCGAtt -3′ 3′- ttGAAUGCGACUCAUGAAGCU -5′	71.1	-0.3
10	5′- C$_t$UUACGCUGAGUACUUCGAtt -3′ 3′- U$_t$UGAAUGCGACUCAUGAAGCU -5′	69.3	-2.1
11	5′- C$_t$UUACGCUGAGUAC$_t$UUCGAtt -3′ 3′- ttGAAUGCGACUCAUGAAGCU -5′	51.1	-20.3
12	5′- CU$_t$UACGCUGAGUACUUCGAtt -3′ 3′- ttGAAUGCGACUCAUGAAGCU -5′	67.9	-3.5
13	5′- CUUACGC$_t$UGAGUACUUCGAtt - 3′ 3′ - ttGAAUGCGACUCAUGAAGCU - 5′	58.4	-13.0
14	5′- CUUACGCUGAGUAC$_t$UUCGAtt - 3′ 3′ - ttGAAUGCGACUCAUGAAGCU - 5′	59.6	-11.4
15	5′- CUUACGCUGAGUAC$_t$UUCGAtt - 3′ 3′ - U$_t$UGAAUGCGACUCAUGAAGCU - 5′	63.9	-7.5
16	5′- CUUACGCUGAGUACU$_t$UCGAtt - 3′ 3′ - ttGAAUGCGACUCAUGAAGCU - 5′	62.9	-8.5
17	5′- CUUACGCUGAGUACUUCGAU$_t$U -3′ 3′ - ttGAAUGCGACUCAUGAAGCU - 5′	72.1	+0.7
18	5′- CUUACGCUGAGUACUUCGAU$_t$U- 3′ 3′ - U$_t$UGAAUGCGACUCAUGAAGCU - 5′	72.5	+1.1
19	5′- CUUACGCUGAGUACU$_t$UCGAU$_t$U -3′ 3′ - ttGAAUGCGACUCAUGAAGCU - 5′	61.7	-9.7
20	5′- CUUACGCUGAGUACU$_t$UCGAU$_t$U -3′ 3′- U$_t$UGAAUGCGACUCAUGAAGCU - 5′	62.2	-9.2
21	5′- CU$_t$UACGCUGAGUACU$_t$UCGAU$_t$U -3′ 3′ - ttGAAUGCGACUCAUGAAGCU - 5′	57.3	-14.1
22	5′- CUUACGCUGAGUACUUCGAtt - 3′ 3′-U$_t$UGAAUGCGACUCAUGAAGCU - 5′	73.1	+1.7

[a]T_ms were measured in triplicate in a sodium phosphate buffer (90 mM NaCl, 10 mM Na_2HPO_4, 1 mM EDTA, pH 7) at 260 nm, from 10 to 95 ^{0}C. **U$_t$U** corresponds to the uracil-triazole-uracil modification; **C$_t$U** corresponds to the cytosine-triazole-uracil modification.

In addition to the listing of luciferase-targeting siRNAs, Table 3.2 highlights melting temperature (T_m) data indicating that the modification can have either a destabilizing or stabilizing contribution on the dsRNA depending on its location.

In general, as the modification approaches the 5′-end of the sense strand, its contribution is less destabilizing. For example, RNAs **9**, **10** and **12** show very little destabilization relative to wild-type. However, the closer the modifications lie towards the center of the duplex, the greater the destabilizing contribution of that modification to the duplex. For instance, siRNAs **13–16** exhibit changes in T_m of ca. -7.5 to -13 °C. The effect of a U$_t$U modification on a 3′-overhang increases the T_m of siRNAs **15**, **17**, **18**, **20** and **22**, relative to the corresponding siRNA with dTdT overhangs, thus suggesting an

element of stability. This stabilizing effect has been observed with other oligonucleotides that bear 3′-overhangs.[8,25] However, this trend is only observed when the modification is not in combination with any other triazole modifications within the same oligonucleotide strand (siRNAs **19** and **21** do not exhibit any increase in T_m). Finally, siRNA **21** contains three U_tU modifications within the sense strand. This siRNA bears a drop in T_m of -14.1 °C. SiRNA **11** contains two C_tU modifications, and exhibits a T_m drop of -20.3 °C relative to wild-type. Overall, our T_m data is consistent with other similar studies involving PNA–DNA chimeras[26] and triazole-linked RNAs.[14b]

3.3.5 Silencing Activity of Triazole-Modified siRNAs Targeting *firefly* luciferase

To examine the effects of our backbone-modified siRNAs on the RNA interference pathway, we performed cell-based assays within HeLa cells. The cells were co-transfected with the siRNA duplexes identified in Table 3.2 at varying concentrations, along with plasmids expressing the target *firefly* luciferase and a non-target *Renilla* luciferase for use as an internal control. Following transfection with the desired siRNA construct, cells were lysed after 24 h, at which point luciferase activity was monitored (Fig. 3.9). The wild-type native siRNA inhibited luciferase expression in a dose-dependent manner, while the modified siRNAs triggered varying levels of silencing activity.

For siRNAs **9**–**12**, a reduction in potency relative to wild-type is generally observed, especially when using lower concentrations of siRNA (Fig. 3.9). These RNAs are chemically modified in the area of the 5′-sense region and in general, display a decrease in T_m relative to wild-type siRNA (Table 3.2). In accordance with other reports which have identified that siRNAs exhibit thermodynamic asymmetry,[27] our observations support that destabilizing this area may lead to decreased potency. SiRNAs **13** and **14** contain a single C_tU modification within an internal site of the sense strand, causing a large decrease in duplex thermal stability compared to wild-type (Table 3.2). There is also a noticeable decrease in potency observed with these two siRNAs relative to wild-type (Fig. 3.9).

RNAs **10**, **15**, **18**, **20** and **22** contain U_tU modifications at the 3′-overhang of the antisense strand. When the activity of these siRNAs is compared to their analogous RNAs lacking

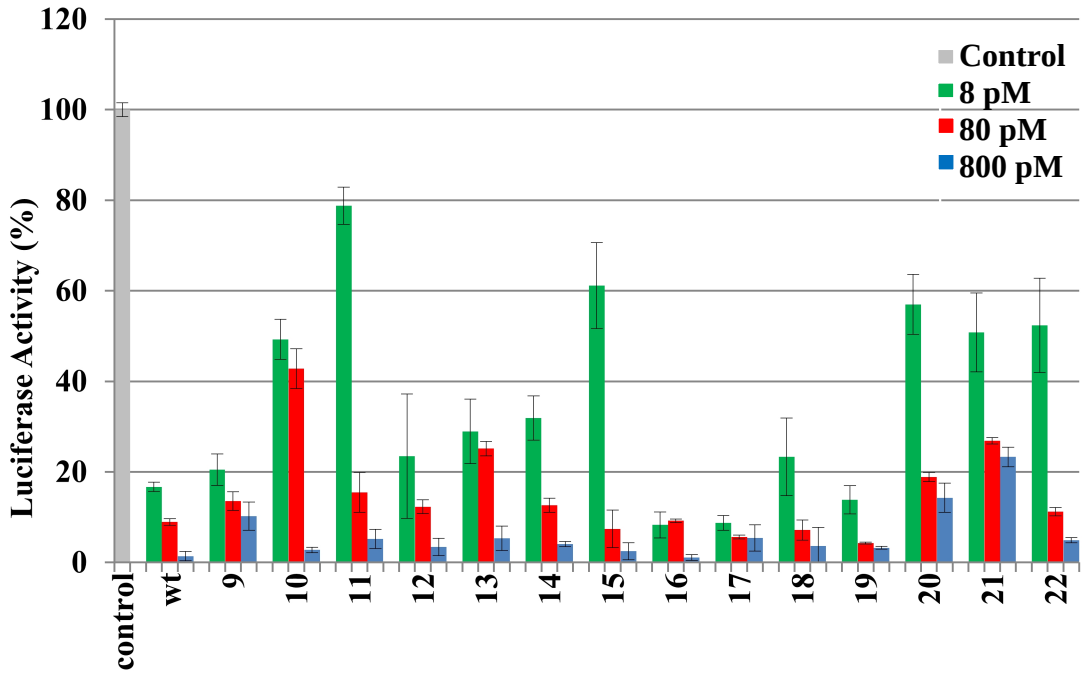

Figure 3.9 Reduction in *firefly* luciferase expression related to the potency of backbone-modified triazole-linked siRNAs using the Dual-luciferase reporter assay. The siRNAs were tested at 8, 80, and 800 pM, with *firefly* luciferase expression normalized to *Renilla* luciferase.

a 3′-U_tU modification in general, a reduction in activity is observed at lower concentrations. The effect of observing reduced activity of a large bulky 3′-modified overhang on the antisense has been previously observed.[28]

SiRNAs **16**, **17** and **19** contain U_tU modification at various positions near the 3′-end of the sense strand. Several of these siRNAs exhibit comparable or enhanced silencing when compared to wild-type siRNA. With respect to thermal stability, siRNAs **16** and **19** exhibit a drop in T_m. Destabilizing this area of the duplex along with the 3′-U_tU modification (siRNA **19**) may offer a favorable response by not only promoting favorable incorporation of the guide strand to form the active RISC-guide complex,[27a] but by increasing its resistance to nucleases.

3.3.6 Nuclease Stability of 3′-U_tU Modified siRNAs

To determine whether a 3′-U_tU modified overhang provides enhanced stability to nucleases, we performed time-dependent stability assays in serum. The analysis involving siRNAs **17**, **18** and **22** illustrated that these 3′-U_tU modified duplex siRNAs have reduced susceptibility to degradation by nucleases relative to wild-type native siRNA (Fig. A51, Appx. II).

3.3.7 Silencing Activity of siRNAs Containing Multiple Triazole-Based Linkages

Finally, siRNAs **11** and **21**, which contain multiple triazole modifications within their sense strands, exhibit low thermal stability and these siRNAs manage to effectively silence the target gene. This suggests that multiple triazoles within a duplex siRNA are compatible within the RNAi pathway, albeit at reduced silencing efficiency compared to wild-type.

3.3.8 RNAi Activity of Triazole-Modified siRNAs Targeting GAPDH

To determine whether this novel chemical modification would be amenable to endogenous targets, we synthesized and investigated the effect that our triazole backbone-modified siRNA would have on reducing the expression of glyceraldehyde-3-phosphate dehydrogenase (GAPDH). We synthesized three siRNAs bearing a U_tU triazole modification (siRNAs **24**–**26**). The siRNAs each contained a single U_tU modification placed either at positions **17**–**18**, **18**–**19**, or at the 3′-U_tU overhang of the sense strand (Table 3.3). The data from Figure 3.10 illustrates that our triazole-linked siRNAs show a dose-dependent downregulation of GAPDH at 10 and 20 nM comparable to wild-type (siRNA **23**). This result is significant because it highlights that our novel chemically modified siRNAs are capable of silencing relevant endogenous targets.

Table 3.3 Sequences of anti-GAPDH siRNAs

RNA	GAPDH siRNA duplex
23wt	5′ – GGUCAUCCAUGACAACUUUtt – 3′ 3′ – ttCCAGUAGGUACUGUUGAAA – 5′
24	5′ – GGUCAUCCAUGACAAC**U_tU**Utt – 3′ 3′ – ttCCAGUAGGUACUGUUGAAA – 5′
25	5′ – GGUCAUCCAUGACAACU**U_tU**tt – 3′ 3′ – ttCCAGUAGGUACUGUUGAAA – 5′
26	5′ – GGUCAUCCAUGACAACUUU**U_tU** – 3′ 3′ – ttCCAGUAGGUACUGUUGAAA – 5′

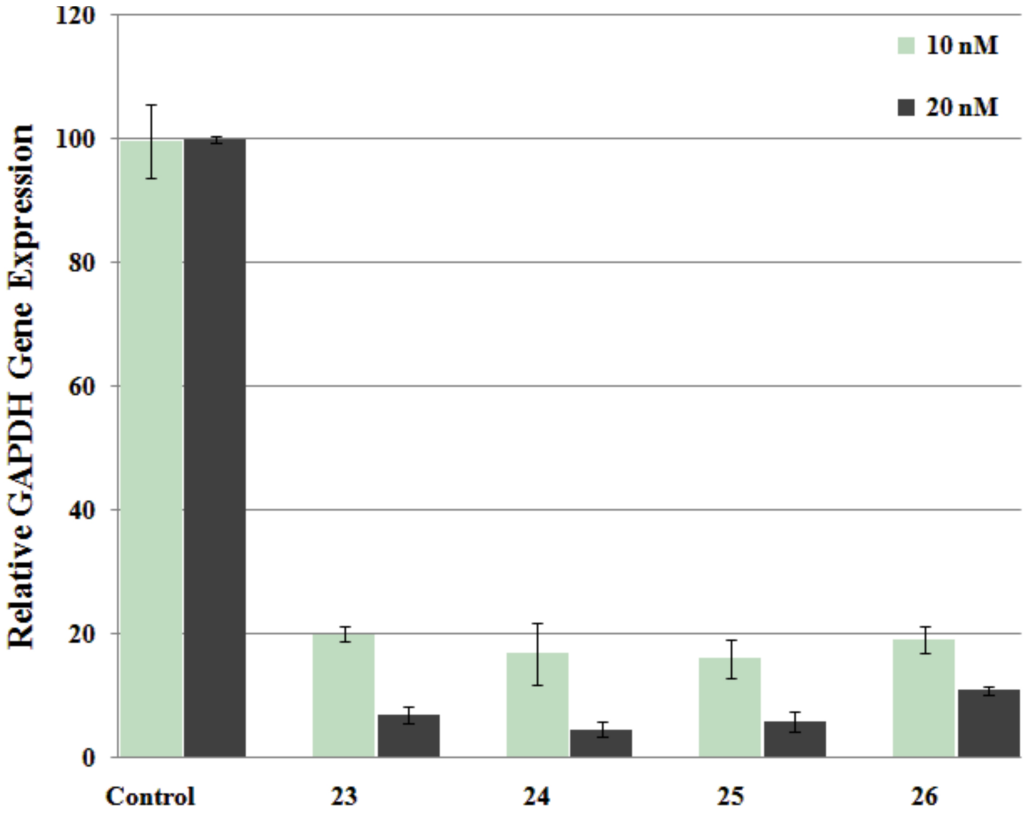

Figure 3.10 Analysis of GAPDH mRNA knockdown analyzed by real-time PCR following the treatment of HeLa cells with GAPDH siRNAs **23**–**26**. Levels of GAPDH expression were normalized to the internal reference gene 18S.

3.4 Discussion and Conclusion

In conclusion, we are reporting the practical synthesis of siRNAs bearing triazoles interspersed throughout the backbone via DMT-phosphoramidite chemistry. Monomers **3** and **5** were readily synthesized through standard amide-bond coupling conditions. Via click chemistry, the final triazole-linked C_tU dimer phosphoramidite **8** was synthesized with an overall yield of 33% from monomers **3** and **5**. All RNA duplexes are substrates for the RNAi pathway. Therefore, a triazole in place of a phosphodiester backbone shows compatibility within siRNA duplexes and suggests that other novel backbone modifications may also act as proper substrates. To the best of our knowledge, there are no other reports of non-ionic hydrophobic backbone mimics that silence gene expression when positioned within the internal Watson–Crick double-stranded region of siRNAs.

Acknowledgements

We acknowledge the National Sciences and Engineering Research Council and the Canada Foundation for Innovation for funding.

Supplementary Data

Supplementary data associated with this article can be found, in the online version, at doi:10.1016/j.bmcl.2011.12.104.

The Materials and Methods section of this chapter contains all relevant experimental details outlined in the Supplementary Data. Refer to Appendix II for all spectra and additional figures & tables.

References and Notes – Chapter III – Manuscript II:

1. Fire, A.; Xu, S. Q.; Montgomery, M. K.; Kostas, S. A.; Driver, S. E.; Mello, C. C. *Nature* **1998**, *391*, 806.

2. (a) Hammond, S. M.; Bernstein, E.; Beach, D.; Hannon, G. J. *Nature* **2000**, *404*, 293; (b) Nykänen, A.; Haley, B.; Zamore, P. D. *Cell* **2001**, *107*, 309.

3. (a) Manoharan, M. *Biochim. Biophys. Acta* **1999**, *1489*, 117; (b) Corey, D. R. *J. Clin. Invest.* **2007**, *117*, 3615; (c) Watts, J. K.; Deleavey, G. F.; Damha, M. J. *Drug Discovery Today* **2008**, *13*, 842.

4. (a) Dowler, T.; Bergeron, D.; Tedeschi, A.-L.; Paquet, L.; Ferrari, N.; Damha, M. J. *Nucleic Acids Res*. **2006**, *34*, 1669; (b) Braasch, D. A.; Jensen, S.; Liu, Y.; Kaur, K.; Arar, K.; White, M. A.; Corey, D. R. *Biochemistry* **2003**, *42*, 7967; (c) Saneyoshi, H.; Seio, K.; Sekine, M. *J. Org. Chem*. **2005**, *70*, 10453; (d) Chiu, Y. L.; Rana, T. M. *RNA* **2003**, *9*, 1034; (e) Elmén, J.; Thornberg, H.; Ljungberg, K.; Frieden, M.; Westergaard, M.; Xu, Y.; Wahren, B.; Liang, Z.; Ørum, H.; Koch, T.; Wahlestedt, C. *Nucleic Acids Res*. **2005**, *33*, 439; (f) Ueno, Y.; Hirai, M.; Yoshikawa, K.; Kitamura, Y.; Hirata, Y.; Kiuchi, K.; Kitade, Y. *Tetrahedron* **2008**, *64*, 11328; (g) Manoharan, M.; Akinc, A.; Pandey, R. K.; Qin, J.; Hadwiger, P.; John, M.; Mills, K.; Charisse, K.; Maier, M. A.; Nechev, L.; Greene, E. M.; Pallan, P. S.; Rozners, E.; Rajeev, K. G.; Egli, M. *Angew. Chem. Int. Ed*. **2011**, *50*, 2284; (h) Zhang, N.; Tan, C.; Cai, P.; Zhang, P.; Zhao, Y.; Jiang, Y. *Bioorg. Med. Chem*. **2009**, *17*, 2441.

5. (a) Somoza, A.; Silverman, A. P.; Miller, R. M.; Chelliserrykattil, J.; Kool, E. T. *Chemistry* **2008**, *14*, 7978; (b) Xia, J.; Noronha, A.; Toudjarska, I.; Li, F.; Akinc, A.; Braich, R.; Frank-Kamenetsky, M.; Rajeev, K. G.; Egli, M.; Manoharan, M. *ACS Chem. Biol*. **2006**, *1*, 176.

6. Amarzguioui, M.; Holen, T.; Babaie, E.; Prydz, H. *Nucleic Acids Res*. **2003**, *31*, 589. 7. Hall, A. H. S.; Wan, J.; Shaughnessy, E. E.; Shaw, B. R.; Alexander, K. A. *Nucleic Acids Res*. **2004**, *32*, 5991.

8. Iwase, R.; Toyama, T.; Nishimori, K. *Nucleosides Nucleotides Nucleic Acids* **2007**, *26*, 1451.

9. Potenza, N.; Moggio, L.; Milano, G.; Salvatore, V.; Di Blasio, B.; Russo, A.; Messere, A. *Int. J. Mol. Sci*. **2008**, *9*, 299.

10. Wang, Y.; Juranek, S.; Li, H.; Sheng, G.; Tuschl, T.; Patel, D. J. *Nature* **2008**, *456*, 921.

11. Rostovtsev, V. V.; Green, L. G.; Fokin, V. V.; Sharpless, K. B. *Angew. Chem. Int. Ed*. **2002**, *41*, 2596.

12. (a) Isobe, H.; Fujino, T.; Yamazaki, N.; Guillot-Nieckowski, M.; Nakamura, E. *Org. Lett.* **2008**, *10*, 3729; (b) Lucas, R.; Neto, V.; Bouazza, A. H.; Zerrouki, R.;

Granet, R.; Krausz, P.; Champavier, Y. *Tetrahedron Lett*. **2008**, *49*, 1004; (c) Fujino, T.; Yamazaki, N.; Isobe, H. *Tetrahedron Lett*. **2009**, *50*, 4101; (d) Chittepu, P.; Sirivolu, V. R.; Seela, F. *Bioorg. Med. Chem*. **2008**, *16*, 8427; (e) Chandrasekhar, S.; Srihari, P.; Nagesh, C.; Kiranmai, N.; Nagesh, N.; Idris, M. M. *Synthesis* **2010**, *21*, 3710; (f) El-Sagheer, A. H.; Brown, T. *J. Am. Chem. Soc*. **2009**, *131*, 3958; (g) Chouikhi, D.; Barluenga, S.; Winssinger, N. *Chem. Commun.* **2010**, *46*, 5476; (h) Varizhuk, A.; Chizhov, A.; Florentiev, V. *Bioorg. Chem*. **2011**, *39*, 127.

13. El-Sagheer, A. H.; Brown, T. *Proc. Natl. Acad. Sci. U.S.A.* **2010**, *107*, 15329.

14. (a) Parades, E.; Das, S. R. *Chembiochem* **2011**, *12*, 125; (b) Mutisya, D.; Selvam, C.; Kennedy, S. D.; Rozners, E. *Bioorg. Med. Chem. Lett*. **2011**, *21*, 3420.

15. Efthymiou, T. C.; Desaulniers, J.-P. *J. Heterocycl. Chem*. **2011**, *48*, 533.

16. Still, W. C.; Kahn, M.; Mitra, A. *J. Org. Chem.* **1978**, *43*, 2923.

17. McDowell, J. A.; Turner, D. H. *Biochemistry* **1996**, *35*, 14077.

18. Toriello, N. M.; Douglas, E. S.; Thaitrong, N.; Hsiao, S. C.; Francis, M. B.; Bertozzi, C. R.; Mathies, R. A. *PNAS* **2008**, *105*, 20173.

19. Mayer, T.; Maier, M.E. European *J. Org. Chem.* **2007**, *28*, 4711.

20. Vader, J.; Sengers, H.; de Groot, A. *Tetrahedron* **1989**, *45*, 2131.

21. (a) Christensen, L.; Hansen, H. F.; Koch, T.; Nielsen, P. E. *Nucleic Acids Res*. **1998**, *26*, 2735; (b) Schwergold, C.; Depecker, G.; Di Giorgio, C.; Patino, N.; Jossinet, F.; Ehresmann, B.; Terreux, R.; Cabrol-Bass, D.; Condom, R. *Tetrahedron* **2002**, *58*, 5675.

22. Thansandote, P.; Gouliaras, T.; Turcotte-Savard, M.-O.; Lautens, M. *J. Org. Chem.* **2009**, *74*, 1791.

23. Kryatova, O. P.; Connors, W. H.; Bleczinski, C. F.; Mokhir, A. A.; Richert, C. *Org. Lett.* **2001**, *3*, 987.

24. Liu, X. J.; Chen, R. Y.; Weng, L. H.; Leng, X. B. *Heteroatom Chem*. **2000**, *11*, 422.

25. Petersheim, M.; Turner, D. H. *Biochemistry* **1983**, *22*, 256.

26. Bajor, Z.; Sági, G.; Tegyey, Z.; Kraicsovits, F. *Nucleosides Nucleotides Nucleic Acids* **2003**, *22*, 1963.

27. (a) Schwarz, D. S.; Hutvágner, G.; Du, T.; Xu, Z.; Aronin, N.; Zamore, P. D. *Cell* **2003**, *115*, 199; (b) Addepalli, H.; Meena; Peng, C. G.; Wang, G.; Fan, Y.; Charisse, K.; Jayaprakash, K. N.; Rajeev, K. G.; Pandey, R. K.; Lavine, G.; Zhang, L.; Jahn-Hofmann, K.; Hadwiger, P.; Manoharan, M.; Maier, M. A. *Nucleic Acids Res*. **2010**, *38*, 7320.

28. Somoza, A.; Terrazas, M.; Eritja, R. *Chem. Commun*. **2010**, *46*, 4270.

Connecting Statement II

After confirming the results obtained from other studies by illustrating that siRNA activity can be modulated through enhancing the thermodynamic asymmetry of the duplex, we were inspired to further explore the promiscuity of RNAi machinery for other unnatural and destabilized duplex ligands. Our previous study illustrated a trend between thermodynamic asymmetry and siRNA activity as the position of the slightly-destabilizing triazole backbone linkage on the passenger strand approached the 5′ end of the preferred guide strand. These positive results inspired us to explore how the use of other unnatural and destabilizing modifications could alter the thermodynamic profiles, and ultimately the activity of siRNAs when positioned throughout the complex. We also wished to confirm suspicions made by other research groups who speculated on the existence of an alternative RNAi mechanism which does not require actual Ago2-mediated cleavage of the passenger strand in order to load the active guide strand into RISC. To explore these phenomena, the following study involved the chemical introduction of abasic positions along the passenger strands of siRNAs, using alkyl chain linkages of varying length and slightly different constitution. Several spacer-modified siRNAs were all designed to target the *firefly* luciferase reporter gene whithin HeLa cells, and their thermostabilities were characterized using UV-monitored thermal denaturation.

Chapter IV – Manuscript III

Evaluation of siRNAs that contain internal variable-length spacer linkages

Tim C. Efthymiou, Brandon Peel, Vanthi Huynh,
and Jean-Paul Desaulniers*

Published in:

Bioorganic & Medicinal Chemistry Letters **2012**, *22*, 5590-5594.

DOI: 10.1016/j.bmcl.2012.07.006

4.0 Abstract

The most widely accepted mechanism of RNAi-silencing involves the RNA-induced silencing complex (RISC) liberating the active antisense strand from the sense strand of an siRNA duplex to form an active RISC-antisense complex. This involves cleaving the sense strand between positions 9 and 10 from the 5′ end of the strand prior to dissociation. Destabilizing modifications near the center of the duplex in some cases can enhance the efficacy of the resultant construct and may trigger an alternative mechanism through which the sense strand is removed. By introducing alkyl spacers of varying lengths near or within the sense strand′s cleavage site, this study illustrates that siRNAs, in most cases, retained potent RNAi silencing activity. Our results highlight that by substituting the scissile phosphodiester linkage on the sense strand with non-cleavable alkyl chains provides a novel and alternative method to destabilize the central region of siRNAs.

4.1 Introduction

RNA interference (RNAi) is an endogenous gene silencing pathway.[1] The process involves the cleavage of double-stranded RNA into short-interfering RNAs (siRNAs).[2] The siRNAs are comprised of two strands, a sense and an antisense (AS) strand. The antisense strand recognizes the target messenger RNA through Watson-Crick base-pair specificity following sense strand removal. For activation, siRNAs serve as substrates for the RNA-induced silencing complex (RISC) and this complex directs the antisense RNA strand to the template mRNA strand.[3,4]

There has been considerable interest in utilizing siRNAs as biomolecular scaffolds to target genes of interest that may be associated with disease.[5] However, their impact has been delayed due to problems associated with permeability, stability and off-target effects.[6,7] In order to overcome these limitations, there is attention directed at utilizing chemical modifications to overcome some of the inherent problems associated with the native structure of RNA.[8–11]

Over the last number of years, there have been numerous studies aimed at evaluating the mechanism of the RNAi pathway, and elucidating the method through which RISC removes the sense strand.[12–15] This process is important because ultimately the antisense strand must target the desired mRNA. Several studies have confirmed that the catalytic portion of Argonaute 2 (Ago2) cleaves the sense strand between positions 9 and 10, starting from the 5′-end of the strand.[14–16] This cleavage is thought to promote the dissociation of the sense strand from the antisense strand to help initiate an active RISC-antisense RNA complex.

However, there have been a number of studies that suggest that RISC-mediated cleavage of the sense strand is not an essential feature that governs activity.[13,14,17] For example, Zamore and coworkers demonstrated that the substitution of the scissile phosphodiester on the sense strand with a phosphorothioate linkage significantly reduced cleavage by Ago2, yet RNAi activity was retained.[13] This study suggested that an alternative mechanism for sense strand dissociation was possible for RNAi activity. Other studies have illustrated that a pre-cleaved (nicked siRNA) at the sense strand′s Ago2 cleavage

site resulted in efficient RNAi activity, which indicates that an actual cleavage event per se is not an essential requirement to illicit a potent RNAi response.[14,18,19] Furthermore, Manoharan and coworkers demonstrated that a 2′-*O*-methyl or phosphorothioate modification at the Ago2 cleavage site of the sense strand with destabilizing chemical modifications were well tolerated within functional siRNAs.[17] Among those already mentioned, there are many other examples of chemical modifications performed on, or near the sense strand′s cleavage site that are well tolerated by RISC.[20–24]

One of the features that is believed to help promote a bypass mechanism involves destabilization of the central region of a siRNA. Many of the methods to achieve destabilization include the incorporation of chemically modified bases, mismatches and/or abasic sites.[14,24–26] Many of the reported modifications require multiple steps to synthesize and expertise in nucleoside phosphoramidite chemistry. The goal of this study is to retain siRNA efficacy through duplex destabilization using various alkyl linkers as simple alternatives to mismatches or other chemically modified derivatives. Alkyl linker phosphoramidites such as those used in this study are commercially available and thus their preparation does not rely on in-house multi-step phosphoramidite syntheses.

Based on the aforementioned reports and the well-established principle of thermodynamic asymmetry exhibited within siRNAs,[27–29] a variety of different length alkyl spacer chains was chosen for this study to replace typical destabilizing modifications.

4.2 Materials and Methods

4.2.1 General Methods

Unless otherwise noted, all starting materials were obtained from commercial sources and were used without any additional purification. ESI Q-TOF spectra were recorded on an Agilent QTOF. UV-monitored thermal denaturation was performed on a Jasco J-815 Spectropolarimeter equipped with temperature control.

4.2.2 Chemical Synthesis of Oligonucleotides

All standard *β*-cyanoethyl 2′-*O*-TBS protected RNA phosphoramidites along with spacer phosphoramidites, reagents, and solid supports were purchased from Chemgenes Corporation and Glen Research. Sequences such as the wild-type sense and 5′-phosphorylated antisense strands, those with segmented strands, and those containing hexaethyloxy-glycol (E17) modifications were purchased and purified from Integrated DNA Technologies (IDT). All spacer-modified oligonucleotides were synthesized on an Applied Biosystems 394 DNA/RNA synthesizer using 1.0 μM cycles with 16 min coupling times for all spacer and standard phosphoramidites. All phosphoramidites were dissolved in anhydrous acetonitrile to a concentration of 0.1 M. Spacer-modified sequences were synthesized on 1.0 μM dT solid supports (Glen Research). Cleavage of oligonucleotides from their solid supports was performed through on-column exposure to 1.5 mL of EMAM (methylamine 40% wt. in H_2O and methylamine 33% wt. in ethanol, 1:1 (Sigma-Aldrich)) for 30 min at room temperature, followed by incubation in EMAM overnight to deprotect the bases. After drying down the EMAM, the samples were resuspended in a solution of DMSO:3HF/TEA (100μL:125μL) and incubated at 65 ^{o}C for 2.5 hr in order to remove the 2′-*O*-TBS groups. Oligonucleotide purity was visualized on a denaturing 20% polyacrylamide gel electrophoresis (PAGE) stained with ethidium bromide. Crude oligonucleotides were precipitated in EtOH and desalted through Millipore Amicon Ultra 3000 MW cellulose centrifugal filters. Oligonucleotides were excised from the 20% denatured gel and were gel purified, followed by desalting through centrifugal filters. Equimolar amounts of complimentary RNAs were annealed at 90 ^{o}C for 2 min in a binding buffer (75 mM KCl, 50 mM Tris-HCl, 3 mM $MgCl_2$, pH 8.3) and this solution was cooled slowly to room temperature to generate siRNAs.

4.2.3 Chemical and Structural Characterization of Oligonucleotides

4.2.3.1 Melting Temperature (T_m) Determination Through UV-Monitored Thermal Denaturation

Equimolar amounts of each RNA strand (2.4 nmol) were annealed to their compliment in 400 µL of a sodium phosphate buffer (90 mM NaCl, 10 mM Na_2HPO_4, 1 mM EDTA, pH 7) at 90 °C for 2 min and this solution was cooled slowly to room temperature. Melting temperatures (T_m) were measured in the sodium phosphate buffer at 260 nm with a temperature range of 10 to 95 °C. The temperature was increased at a rate of 0.5 °C/min while absorbance was measured at the end of each 0.5 °C increment. Absorbance readings were automatically adjusted against the baseline absorbance of the sodium phosphate buffer. After averaging the range of absorbance values obtained from three independent experiments for each siRNA, T_m's were calculated using Meltwin version 3.5 software assuming the two-state model.[30]

4.2.3.2 Electrospray Ionization Quantitative Time-of-Flight Mass Spectrometry

All single-stranded RNAs were gradient eluted through a Zorbax Extend C18 HPLC column with a MeOH/H_20 (5:95) solution containing 200 mM hexafluoroisopropyl alcohol and 8.1 mM triethylamine, and finally with 70% MeOH. The eluted RNAs were subjected to ESI-MS (ES^-), producing raw spectra of multiply-charged anions and through resolved isotope deconvolution, the molecular weights of the resultant neutral oligonucleotides were confirmed for all the RNAs.

4.2.4 Methods for Culturing Eukaryotic Cells

HeLa cells were cultured in Dulbecco′s modified eagle′s medium (DMEM) containing 10% fetal bovine serum (FBS) (Perbio) and 1% Penicillin-Streptomycin (Sigma) at 37 °C with 5% CO_2. For passaging cells, a 1X solution of 0.25% Trypsin (SAFC Bioscience) was used to disperse the cells.

4.2.5 *Firefly* luciferase Dual-Reporter *In Vitro* Assay

Prior to transfection, HeLa cells were seeded on 12-well plates (Greiner Bio-One) at a density of 100,000 cells per well and incubated at 37 ^{o}C with 5% CO_2 in DMEM containing 10% FBS. After 24 hr, varying concentrations (20 pM, 80 pM, 160 pM, 400 pM) of all anti-luciferase siRNAs were co-transfected with both pGL3 (Promega) and pRLSV40 (York University) luciferase-expressing plasmids using Lipofectamine 2000 (Invitrogen) in Gibco′s Opti-Mem Reduced Serum Medium 1X (Invitrogen) according to the manufacturer′s protocol. After an additional 24 hr, cells were incubated in 1X passive lysis buffer (Promega) for 20 min at room temperature, and cell lysate was loaded onto white and opaque, 96-well plates (Costar). Using the Dual-luciferase Reporter Assay kit (Promega), observed luminescence was proportional to both *firefly* and *renilla* luciferase expression, recorded on a Synergy HT (Bio-Tek) plate luminometer. The ratio of *firefly*/*renilla* luminescence expressed as a percentage relates the reduction in *firefly* expression to siRNA efficacy when compared to untreated controls. Each value is the average of at least three independent experiments with the indicated error (SDOM).

4.3 Results

4.3.1 Variable-Length Abasic Alkyl Chain Linkages

The C3 spacer places three carbons between the oxygens of the phosphodiester linkages, which is exactly the same number of carbons between native RNA. The C4 and C5 spacer naturally have one or two additional carbons, respectively. These were chosen as it had been shown previously that alkyl bulges with increased carbon length can be used for siRNA constructs.[31] Each introduction of these alkyl spacer modifications was designed to replace the distance of a single nucleoside.

The E8 and C9 spacers contain eight or nine atoms between phosphodiester functionalities, respectively. The intention of these spacer derivatives is to span across two nucleotides with each introduction in RNA. Native RNA contains nine atoms between alternating phosphodiesters. Finally, the E17 spacer contains 17 atoms and is a mimic designed to span across three bases. Figure 4.11 illustrates the structural differences amongst the different alkyl spacer linkers used.

4.3.2 Spacer-Modified *firefly* luciferase-Targeting siRNAs

Various siRNAs were synthesized or purchased commercially that contained a combination of the linkers identified in Figure 4.11. The siRNAs generated target *firefly* luciferase mRNA transcribed from the plasmid pGL3 and expressed within mammalian cells (Table 4.4). The siRNAs were tested in a dose-dependent manner and their silencing data is illustrated in Figure 4.12.

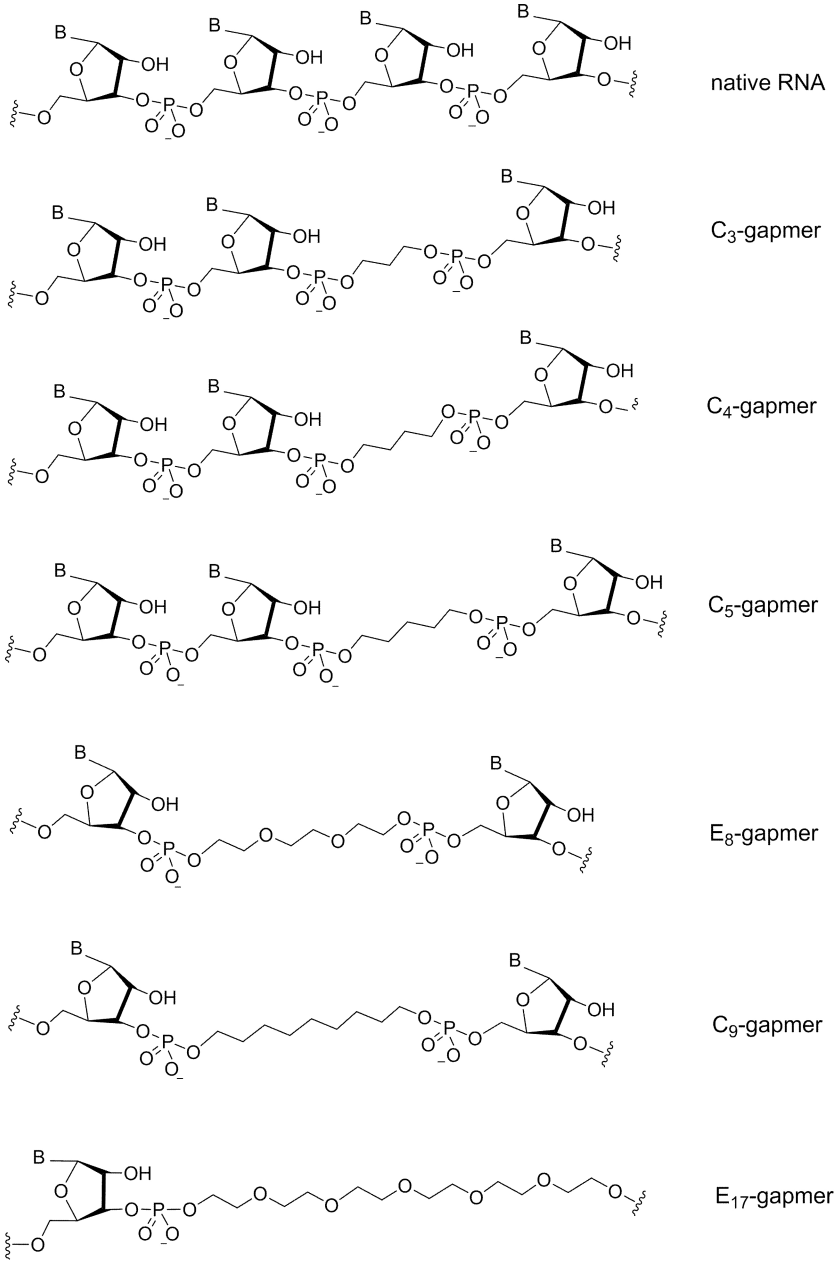

Figure 4.11 Structure of various alkyl spacer linkers used within siRNAs.

Table 4.4 Sequences of anti-luciferase siRNAs and T_m's[32]

RNA	siRNA duplex	T_m (°C)	ΔT_m (°C)
wt	5′- CUUACGCUGAGUACUUCGAtt -3′ 3′- ttGAAUGCGACUCAUGAAGCU -5′	71.4	--
1	5′- CUUC_4CGCUGAGUACUUCGAtt -3′ 3′- ttGAAUGCGACUCAUGAAGCU -5′	--	--
2	5′- CUUACGC_4UGAGUACUUCGAtt -3′ 3′- ttGAAUGCGACUCAUGAAGCU -5′	55.0	-16.4
3	5′- CUUC_4CGC_4UGAGUACUUCGAtt -3′ 3′- ttGAAUGCGACUCAUGAAGCU -5′	55.3	-16.1
4	5′- CUUACGCUGAGUC_4CUUCGAtt -3′ 3′- ttGAAUGCGACUCAUGAAGCU -5′	56.8	-14.6
5	5′- CUUACGCUGAGUACUC_4CGAtt -3′ 3′- ttGAAUGCGACUCAUGAAGCU -5′	--	--
6	5′- CUUACGCUGAGUC_3CUC_3CGAtt -3′ 3′- ttGAAUGCGACUCAUGAAGCU -5′	53.5	-17.9
7	5′- CUUACGCUGAGUC_4CUC_4CGAtt -3′ 3′- ttGAAUGCGACUCAUGAAGCU -5′	56.7	-14.7
8	5′- CUUACGCUGAGUC_5CUC_5CGAtt -3′ 3′- ttGAAUGCGACUCAUGAAGCU -5′	50.9	-20.5
9	5′- CUUACGCUC_3AGUACUUCGAtt -3′ 3′- ttGAAUGCGACUCAUGAAGCU -5′	52.3	-19.1
10	5′- CUUACGCUC_4AGUACUUCGAtt -3′ 3′- ttGAAUGCGACUCAUGAAGCU -5′	50.8	-20.6
11	5′- CUUACGCUC_5AGUACUUCGAtt -3′ 3′- ttGAAUGCGACUCAUGAAGCU -5′	50.6	-20.8
12	5′- CUUACGCUGC_3GUACUUCGAtt -3′ 3′- ttGAAUGCGACUCAUGAAGCU -5′	55.3	-16.1
13	5′- CUUACGCUGC_4GUACUUCGAtt -3′ 3′- ttGAAUGCGACUCAUGAAGCU -5′	52.4	-19.0
14	5′- CUUACGCUGC_5GUACUUCGAtt -3′ 3′- ttGAAUGCGACUCAUGAAGCU -5′	53.6	-17.8
15	5′- CUUACGCUC_3C_3GUACUUCGAtt -3′ 3′- ttGAAUGCGACUCAUGAAGCU -5′	49.7	-21.7
16	5′- CUUACGCUC_4C_4GUACUUCGAtt -3′ 3′- ttGAAUGCGACUCAUGAAGCU -5′	51.8	-19.6
17	5′- CUUACGCUC_5C_5GUACUUCGAtt -3′ 3′- ttGAAUGCGACUCAUGAAGCU -5′	50.5	-20.9
18	5′- CUUACGCUGAC_4UACUUCGAtt -3′ 3′- ttGAAUGCGACUCAUGAAGCU -5′	51.6	-19.8
19	5′- CUUACGCUC_4AC_4UACUUCGAtt -3′ 3′- ttGAAUGCGACUCAUGAAGCU -5′	48.8	-22.6
20	5′- CUUACGCUGC_4C_4UACUUCGAtt -3′ 3′- ttGAAUGCGACUCAUGAAGCU -5′	50.9	-20.5
21	5′- CUUACGC-E_8-AGUACUUCGAtt -3′ 3′- ttGAAUGCGACUCAUGAAGCU -5′	54.7	-16.7
22	5′- CUUACGCU-E_8-GUACUUCGAtt -3′ 3′- ttGAAUGCGACUCAUGAAGCU -5′	52.2	-19.2
23	5′- CUUACGCUG-E_8-UACUUCGAtt -3′ 3′- ttGAAUGCGACUCAUGAAGCU -5′	50.0	-21.4
24	5′- CUUACGC-C_9-AGUACUUCGAtt -3′ 3′- ttGAAUGCGACUCAUGAAGCU -5′	50.4	-21.0
25	5′- CUUACGCU-C_9-GUACUUCGAtt -3′ 3′- ttGAAUGCGACUCAUGAAGCU -5′	51.3	-20.1
26	5′- CUUACGCUG-C_9-UACUUCGAtt -3′ 3′- ttGAAUGCGACUCAUGAAGCU -5′	49.3	-22.1
27	5′- CUUACGC-E_{17}-GUACUUCGAtt -3′ 3′- ttGAAUGCGACUCAUGAAGCU -5′	54.4	-17.0
28	5′- CUUACGCU-E_{17}-UACUUCGAtt -3′ 3′- ttGAAUGCGACUCAUGAAGCU -5′	50.9	-20.5

4.3.3 Silencing Activity and T_m′s of siRNAs with Spacer Linkages in Distal Regions

Table 4.4 also highlights the melting temperature (T_m) for the various siRNAs. Not surprisingly, all linkers display a degree of destabilization. With respect to destabilization close to the 5′-end of the sense strand (siRNA **1**), a loss of activity relative to wild-type is observed. Activity is comparable to the parent siRNA as the duplex is destabilized closer to its center (siRNA **2**). In contrast, single modifications close to the 3′-end of the sense strand exhibit potency comparable to wild-type siRNA (siRNAs **4** and **5**). This observation is consistent with trends observed with the asymmetry rule of siRNAs.[28] However, if two alkyl chain linkages are placed at both position 4 and 7 (siRNA **3**) or at **13** and **16** (siRNAs 6–8) of the sense strand, this results in siRNAs exhibiting reduced gene silencing properties, likely due to the large destabilization occurring at those positions (Fig. 4.12**A**).

4.3.4 Effects of Spacer Linkages Within the Passenger Strand Ago2 Cleavage Site

We next turned our attention to multiple spacer modifications within the internal region of the siRNA, while continuing to focus on the Ago2 cleavage site (Fig. 4.12**B**). With respect to spanning two spacers across the 9–10 region of the sense strand of the siRNA, the C3-double spacer (siRNA **15**) was quite effective at all concentrations tested. In addition, as the number of atoms increased, a slight reduction in potency was observed, especially with a two atom increase in linker length (siRNA **17**) and at lower concentrations. Nevertheless, the gene-silencing capabilities of siRNAs bearing two spacers at these positions were relatively unhindered at higher concentrations. We investigated the effect of a double spacer linkage spanning positions 10–11 of the sense strand (siRNA **20**), and we observed that it was also quite effective at silencing, albeit at reduced efficacy to wild-type siRNA. With the addition of yet another spacer siRNA containing two C4 linkages across positions 9 and 11 of the sense strand (siRNA **19**), the collective data suggests that siRNAs containing multiple and destabilizing spacer units within the central region act as suitable substrates for the RNAi machinery.

4.3.5 Double and Triple-Abasic Spacers Spanning the Passenger Strand Ago2 Cleavage Site

Following these results, we focused our attention on non-cleavable linkers spanning across two (E8 and C9) to three (E17) nucleosides within the sense strand (Fig. 4.12**C**). We were surprised to find that even though these large linkers were presumably bypassing the sense strand cleavage mechanism, siRNA efficacy was not severely compromised as expected. It is noteworthy to observe that the duplex containing the E8 spacer across positions 9 and 10 (siRNA **22**) was capable of silencing luciferase with efficiency comparable to wild-type siRNA, despite containing the non-cleavable linkage. The siRNA with the C9 spacer spanning positions 9 and 10 (siRNA **25**) also demonstrated an active silencing profile, although not as potent as its E8 counterpart. It was generally found that E8 linker-modified siRNAs (siRNAs **21**–**23**) were slightly more effective at silencing than C9-modified siRNAs (siRNAs **24**–**26**). SiRNAs modified with non-cleavable E17 linkages (siRNAs **27** and **28**), spanning positions 8–10 or 9–11 did not silence as efficiently as the other spacers. This indicates that function was severely compromised by the extended linkage (covering the distance of three nucleobases).

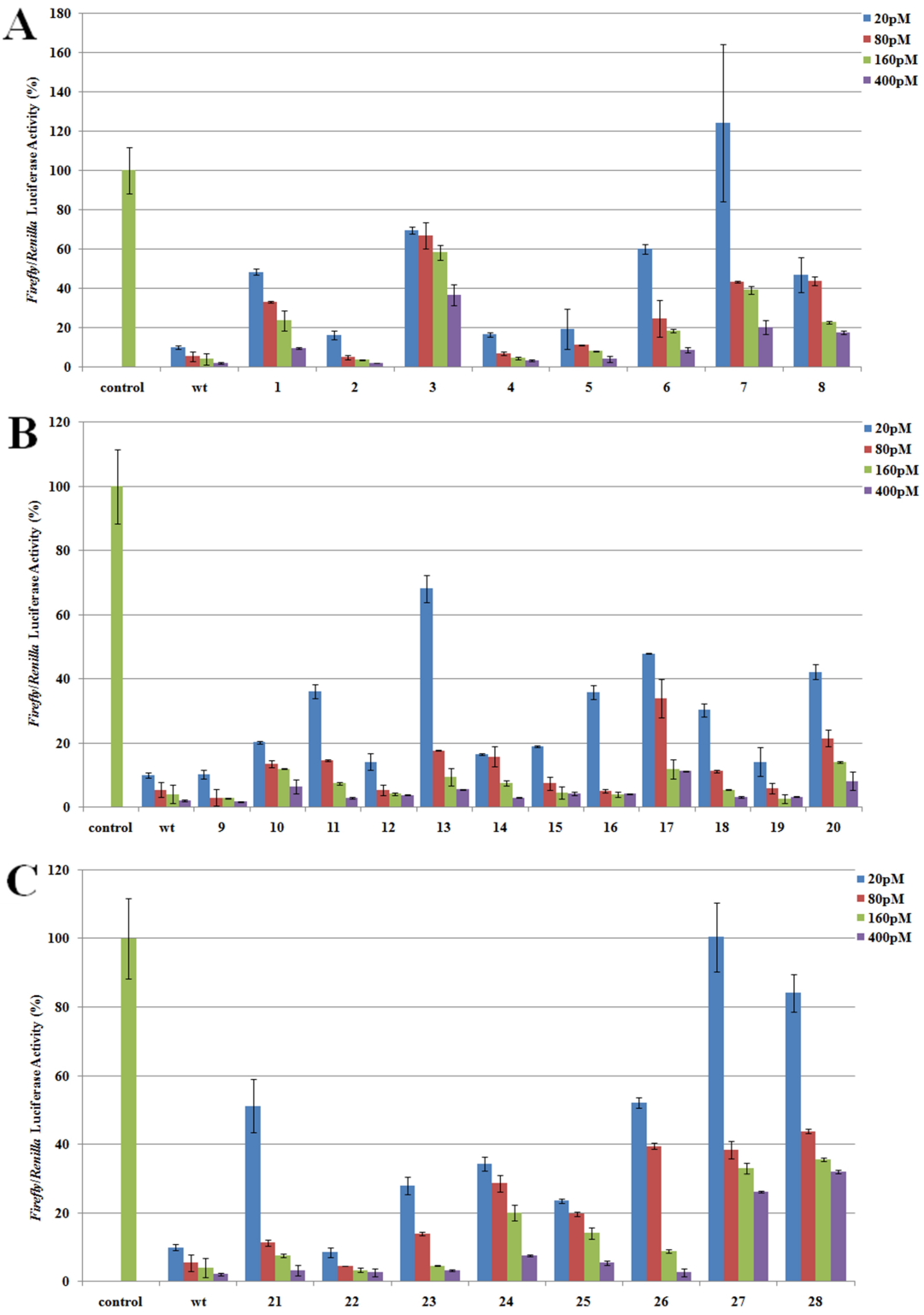

Figure 4.12 Reduction of luciferase activity as a function of siRNA activity using the Dual-luciferase reporter assay. Alkyl chain-modified siRNAs were tested in HeLa cells at 20, 80, 160 and 400 pM, with *firefly* luciferase expression normalized to *Renilla* luciferase. (A) siRNAs with alkyl spacers near the terminal ends of the sense strand. (B) Centrally-modified siRNAs, each containing one or two single (C3, C4 or C5) spacers. (C) Centrally-modified siRNAs, containing a double (E8 or C9) or a triple (E17) spacer.

4.4 Discussion and Conclusion

We are presenting a novel method to destabilize the central region through the use of simple alkyl linkers that are able to span within the central region of siRNAs. Many of the linkers used within siRNAs are capable of gene silencing as efficiently as wild-type

siRNA. Our data suggests that non-cleavable long linkers, up to nine atoms in length that span the equivalent of two nucleobases at and near the Ago2 cleavage site are effective substrates for the RNAi machinery. As this linker is increased to seventeen atoms, thus replacing three nucleobases, we observe a drop in efficacy. To confirm that the alkyl linker is essential for activity, we tested some ′true space′ (TS) siRNAs containing segmented sense strands annealed to unmodified antisense strands (Table A7, Appx. III). The segments varied in length in order that they reveal spaces in the sense strand with missing residues near and across the Ago2 cleavage site. These TS siRNAs were not capable of effective gene silencing signifying the importance of an actual linkage between residues that are separated by at least one space on the same strand. See Fig. A53 and Table A7 for details (Appx. III).

In conclusion, this study presents a simple means to destabilize the central region of siRNAs through the use of alkyl linkers. Alkyl linkers are attractive substituents due to their commercial availability and their robust compatibility with standard DMT-phosphoramidite chemistry and related protocols.[31,33] In addition, the longer neutrally-charged linkers such as E8, C9 and E17 assist in reducing the overall polyanionic charge of the siRNA. The ability to use a non-cleavable alkyl linker within the central region of an siRNA opens the future possibility of further chemically modifying it with desired functionality that can assist with some of the problems associated with siRNAs such as delivery, stability, and off-targeting. For example, designing a linker with positively-charged nitrogens at physiological pH may assist with cell membrane permeability. Future studies include delineating new structure–function relationships of novel functionalized spacer moieties within siRNAs.

Acknowledgements

We acknowledge the National Sciences and Engineering Research Council and the Canada Foundation for Innovation for funding.

Supplementary Data

Supplementary data associated with this article can be found, in the online version, at http://dx.doi.org/10.1016/j.bmcl.2012.07.006. These data include MOL files and InChiKeys of the most important compounds described in this article.

The Materials and Methods section of this chapter contains all relevant experimental details outlined in the Supplementary Data. Refer to Appendix III for additional figures and tables.

References and Notes – Chapter IV – Manuscript III:

1. Fire, A.; Xu, S. Q.; Montgomery, M. K.; Kostas, S. A.; Driver, S. E.; Mello, C. C. *Nature* **1998**, *391*, 806.

2. Knight, S. W.; Bass, B. L. Science 2001, 293, 2269.

3. Elbashir, S. M.; Harborth, J.; Lendeckel, W.; Yalcin, A.; Weber, K.; Tuschl, T. *Nature* **2001**, *411*, 494.

4. Bumcrot, D.; Manoharan, M.; Koteliansky, V.; Sah, D. W. Y. *Nat. Chem. Biol*. **2006**, *2*, 711.

5. Tuschl, T. *Nature Biotechnol*. **2002**, *20*, 446.

6. Watts, J. K.; Deleavey, G. F.; Damha, M. J. *Drug Discov. Today* **2008**, *13*, 842.

7. Snove, O.; Rossi, J. J. *ACS Chem. Biol*. **2006**, *1*, 274.

8. Peacock, H.; Kannan, A.; Beal, P. A.; Burrows, C. J. *J. Org. Chem*. **2011**, *76*, 7295.

9. Phelps, K.; Morris, A.; Beal, P. A. *ACS Chem. Biol*. **2012**, *7*, 100.

10. Chernolovskaya, E. L.; Zenkova, M. A. *Curr. Opin. Mol. Ther*. **2010**, *12*, 158.

11. Efthymiou, T. C.; Huynh, V.; Oentoro, J.; Peel, B.; Desaulniers, J.-P. *Bioorg. Med. Chem. Lett*. **2012**, *3*, 1722.

12. Elbashir, S. M.; Martinez, J.; Patkaniowska, A.; Lendeckel, W.; Tuschl, T. *EMBO J*. **2001**, *20*, 6877.

13. Matranga, C.; Tomari, Y.; Shin, C.; Bartel, D. P.; Zamore, P. D. *Cell* **2005**, *123*, 607.

14. Leuschner, P. J. F.; Ameres, S. L.; Kueng, S.; Martinez, J. *EMBO Rep*. **2006**, *7*, 314.

15. Rand, T. A.; Petersen, S.; Du, F. H.; Wang, X. D. *Cell* **2005**, *123*, 621.

16. Wang, Y. L.; Juranek, S.; Li, H. T.; Sheng, G.; Wardle, G. S.; Tuschl, T.; Patel, D. J. *Nature* **2009**, *461*, 754.

17. Addepalli, H.; Meena; Peng, C. G.; Wang, G.; Fan, Y. P.; Charisse, K.; Jayaprakash, K. N.; Rajeev, K. G.; Pandey, R. K.; Lavine, G.; Zhang, L. G.; Jahn-Hofmann, K.; Hadwiger, P.; Manoharan, M.; Maier, M. A. *Nucleic Acids Res*. **2010**, *38*, 7320.

18. Bramsen, J. B.; Laursen, M. B.; Damgaard, C. K.; Lena, S. W.; Babu, B. R.; Wengel, J.; Kjems, J. *Nucleic Acids Res*. **2007**, *35*, 5886.

19. Lu, X. Z.; Yang, G. D.; Zhang, J.; Fu, H. Y.; Jin, L. A.; Wei, M. Y.; Wang, L.; Lu, Z. F. *Appl. Microbiol. Biotechnol*. **2011**, *90*, 583.

20. Braasch, D. A.; Jensen, S.; Liu, Y. H.; Kaur, K.; Arar, K.; White, M. A.; Corey, D. R. *Biochemistry* **2003**, *42*, 7967.

21. Kraynack, B. A.; Baker, B. F. *RNA* **2006**, *12*, 163.

22. Deleavey, G. F.; Watts, J. K.; Alain, T.; Robert, F.; Kalota, A.; Aishwarya, V.; Pelletier, J.; Gewirtz, A. M.; Sonenberg, N.; Damha, M. J. *Nucleic Acids Res*. **2010**, *38*, 4547.

23. Fauster, K.; Hartl, M.; Santner, T.; Aigner, M.; Kreutz, C.; Bister, K.; Ennifar, E.; Micura, R. *ACS Chem. Biol*. **2012**, *7*, 581.

24. Petrova, N. S.; Meschaninova, M. I.; Venyaminova, A. G.; Zenkova, M. A.; Vlassov, V. V.; Chernolovskaya, E. L. *FEBS Lett*. **2011**, *585*, 2352.

25. Somoza, A. S. A. P.; Miller, R. M.; Chelliserrykattil, J.; Kool, E. T. *Chemistry* **2008**, *14*, 7978.

26. Hernandez, A. R.; Peterson, L. W.; Kool, E. T. *ACS Chem. Biol*. **2012**.

27. Aronin, N. *Gene Ther*. **2006**, *13*, 509.

28. Schwarz, D. S.; Hutvagner, G.; Du, T.; Xu, Z. S.; Aronin, N.; Zamore, P. D. *Cell* **2003**, *115*, 199.

29. Khvorova, A.; Reynolds, A.; Jayasena, S. D. *Cell* **2003**, *115*, 209.

30. McDowell, J. A.; Turner, D. H. *Biochemistry* **1996**, *35*, 14077.

31. Ueno, Y.; Yoshikawa, K.; Kitamura, Y.; Kitade, Y. *Bioorg. Med. Chem. Lett*. **2009**, *19*, 875.

32. T_m s were measured in triplicate in a sodium phosphate buffer (90 mM NaCl, 10 mM Na_2HPO_4, 1 mM EDTA, pH 7) at 260 nm, at a rate of 0.5 ^{0}C/min from 10 ^{0}C to 95 ^{0}C.

33. Caruthers, M. H. *Science* **1985**, *230*, 281.

Chapter V – General Discussion

The prospect of nucleic acid-based technology becoming a viable alternative to existing therapies is becoming more realistic as scientists continue to unveil methods of reducing their negative side effects and improve the delivery methods required to effectively administer them to affected tissues. With the ability to manipulate both a highly variable genetic sequence and the native structures of nucleic acids through chemical modification, a variety of nucleic acid derivatives have demonstrated great utility as protein ligands,[1] and as transcript-targeting agents,[2, 3] in addition to several other applications.

Many diseases are the result of the uncontrolled expression of certain genes such as growth-promoting factors and proto-oncogenes in cancer cells,[4] and exogenous genes from invasive virulents.[5, 6] In light of this knowledge, the rate at which the scientific community discovers endogenous genes which could lead to problematic protein products is steadily increasing. Therefore, the use of oligonucleotides to target and to effectively silence the expression of these genes at the translational level with extremely high accuracy and potency is a palatable prospect when comparing with the long and difficult processes of small-molecule drug discovery or re-purposing. As with any new therapy, the goal while implementing nucleic acid-based drugs is to increase their efficacy while minimizing toxicity to the recipient host. To strike this delicate balance, chemical modification of nucleic acids is required with a particular focus on the polyanionic and nuclease-cleavable phosphodiester backbone.

Very little studies have performed extensive backbone modifications which replace the existing native structures with unnatural moieties, rather than modifying the original structures. Even fewer studies have focused on these replacement modifications for the purpose of developing effective siRNA molecules. One such study replaced the ribose sugar with a morpholino moiety,[7] while another study replaced the 3′-overhangs with a PNA analog dimer.[8] Confirming the results found in these studies, siRNAs modified with the novel triazole-based internucleotide linkage proposed and synthesized with the

likeness of a PNA scaffold, showed greater resilience to degradation by nucleases while maintaining their potency. Greater nuclease stability was achieved with siRNAs containing the U_tU triazole-linked dimer as their 3′-overhangs and potency was maintained when modification to the sense strand destabilized the region nearest the 5′ end of the guide strand. In addition, results from this study matched most findings which notice a considerable reduction in siRNA potency upon direct modification of the antisense strand. Taken together, these findings illustrate the possibility of drastically improving siRNA technology by mitigating some of its side effects through heavy chemical modification and replacement of the native sugar-phosphate backbone.

Besides studies focusing on the development of clinically approved siRNA-based therapies, there is widespread use of the technology as a tool for molecular biologists to characterize specific gene targets by down-regulating their expression and recording the response.[9, 10] Companies such as Ambion – Life Technologies™, Dharmacon – Thermo Scientific and Sigma-Aldrich can not only design specific siRNA sequences for any desired target, but have also produced several pre-designed siRNA constructs which guarantee potent knockdown efficiency of popular gene transcripts. However, as previously outlined, native siRNAs are susceptible to hydrolytic cleavage which could ultimately limit their activity to short intervals, requiring frequent applications for sustained activity. Therefore, unique modifications to the native RNA backbone can not only benefit the design of potential siRNA-based pharmacophores, but can produce desirable constructs for their use in functional genomics due to their added nuclease-resistance as evidenced by the unique triazole linkage described.

Although there are a number of triazole-modified nucleic acid derivatives with several different uses ranging from materials and microarray development to molecular probes and antifungal agents, there are few examples of active siRNAs modified at the backbone with these heterocycles.[11] In addition to their other favorable properties, these neutrally-charged backbone modifications could add the potential for siRNAs to penetrate cellular membranes unassisted or with minimal assistance from transfection reagents. Increased membrane permeability and unassisted cellular delivery are favorable attributes for siRNAs, given that there are undesirable side-effects and inefficiencies associated with

current transfection methods[9] and since safe and efficient siRNA delivery remains the most prominent issue faced by the technology. This unique triazole linkage can also offer a conjugation site for small molecules which could add tissue-directing capabilities to modified oligonucleotides. By functionalizing various monomers with alkynes which have been protected with tissue-targeting small molecules, the "click" cycloaddition has been shown to produce 1,4,5-trisubstituted variants of the 1,2,3-triazole moiety.[12] The added steric bulk afforded by the additional small molecule tethered to the alkyne could help direct the molecule′s conjugation site on the final heterocycle. For instance, if the steric bulk of the monomer substituent attached to one end of the alkyne functionality is less than that of the small molecule attached on the opposing end, the result from the "click" cycladdition could favor the expected 1,4-triazole linkage between the azide-alkyne monomers, with the small molecule tethered to the triazole′s C5 position. The reverse could occur if the steric bulk of the small molecule would exceed the monomer portion of the alkyne. Future studies can focus on utilizing this form of control over the "click" cycladdition, by assessing the function of siRNA constructs containing small-molecule conjugates ranging from fluorescent substituents to tissue-directing ligands. Attaching compounds with fluorescent properties to the triazole heterocycle could provide insight into the intracellular fate of these siRNAs, along with their cell-trafficking capabilities visualized through live-cell imaging. There is also the added benefit of internalizing small molecules along the synthesized oligonucleotide backbone wherever the triazole-linked nucleoside dimer analogs have been positioned. In addition, the prospect of functionalizing the 5′-terminus is possible once the alcohol portion of the alkyne monomer is phosphitylated and the monomer is coupled to the growing oligomer, thus terminating the sequence with an alkyne functionality in preparation for the post-synthetic "click" attachment of various azide-tethered molecules.

The siRNAs which were modified with the novel triazole backbone linkage proposed in this study were not only successful at silencing the expression of a transiently-expressed reporter gene, but displayed potent activity when targeting an endogenous target transcript as well. Based on these findings, another continuation of this study could focus on targeting relevant genes which are implicated in perpetuating certain diseases. Currently, there are studies using phosphorothioate antisense oligonucleotides to target

relevant genes such as the anti-apoptosis gene Bcl-2[13] or the transcription factor c-myc,[14] both of which are overexpressed within cancer cells. Additional work can use the triazole-modified siRNAs produced in this study, to target similar genes within cancer cells. With enough time and effort, these studies could ultimately lead to the *in vivo* implementation of these unique derivatives, in addition to other modified siRNAs with therapeutic potential.

When triazole-linked analog dimers were placed near the center of siRNAs, duplex thermostability was significantly reduced along with silencing potency. Contrary to these findings and those obtained in similar studies involving centrally-modified siRNAs, a report by Maier and colleagues from Alnylam Pharmaceuticals observed an increase in efficacy resulting from centrally-destabilized duplex siRNAs containing mismatches or abasic sites.[15] In this study, they also re-confirmed the theoretical mechanism involving sense strand removal without the natural phosphodiester linkage at the putative Ago2 cleavage site. After replacing the two residues of the scissile site on the sense strand with 2′-*O*-Me protected nucleoside analogs or binding them through a phosphorothioate linkage, Maier and colleagues did not notice any reduction in potency from the parent siRNA. Although this study mirrored an earlier report which tested the same modifications on a nearly identical siRNA sequence,[16] its findings opposed those obtained by the earlier report and from others with similar discoveries.[17] The following study involving the use of abasic variable-length alkyl chain spacers succeeded in producing similar results to those obtained by Maier and colleagues.

With single spacer modifications either approaching the central portion or the 3′ end of the sense strand, modified siRNAs were destabilized while silencing activity was maintained. These results are in accordance with the enhancement of duplex thermodynamic asymmetry[18, 19] provided that the spacer is similar in length to a wild-type nucleoside and that the sense strand contains a single spacer. In addition, siRNAs containing abasic spacers in the G9 position and across the Ago2 cleavage site showed silencing activity comparable to wild type, provided that their lengths were either similar or shorter than native lengths. These results not only corroborate the findings by Maier and colleagues,[15] but give further credence to an alternative mechanism of sense strand

removal. Additionally, future studies can explore the use of abasic modifications containing alternate functionalities which could assist with siRNA delivery, stability and overall silencing capability.

Given that all spacer-modified siRNAs retained their function when targeting the *firefly* luciferase reporter gene, the prospect of functionalizing these spacers with tissue-directing or fluorescent molecules forms the basis of a desirable study. Commercially available alkyl chain phosphoramidites of varying length and with alternative functional groups within the chain, can offer points of conjugation for small molecules of interest. Using the automated process of DMT-phosphoramidite chemistry, these newly-functionalized spacers can be placed anywhere internally throughout designer siRNAs, and may add favorable properties in addition to duplex compatibility considering that internally-modified siRNAs were amenable to these destabilizing linkages.

An extension of this study involving these simple spacer linkages could be to prove definitively that these linkages which lack a phosphate moiety to be targeted for cleavage by Ago2, are indeed considered as non-cleavable linkages. The range of melting temperatures obtained for siRNAs modified at the Ago2 cleavage site within the sense strand (48.8 ^{o}C to 55.3 ^{o}C) suggest that although profoundly destabilized, these siRNAs retained their duplex format under physiological temperatures. Therefore, it is assumed with great confidence that any silencing activity observed by these particular siRNAs is the result of an alternative form of sense-strand removal, devoid of an actual cleavage event. To prove with definite certainty that the sense strand does indeed remain intact, at least from Ago2-mediated degradation, a future study can employ the use of fluorescence resonance energy transfer (FRET) imaging *in situ*.[20] FRET visualization involves the use of two communicating dyes placed on opposing ends of a long molecule; in this case the sense strand of an siRNA. When tethered to one another through an non-cleaved sense strand, these dyes can freely communicate with each other through a chain reaction involving the excitation of one dye, which then emits a wavelength spectrum which excites the distant second dye, thus producing a signal which can be visualized through fluorescence microscopy. This interaction between the two dyes on opposing ends of the sense strand would be disrupted once sense strand cleavage occurs. Since FRET

technology has previously gauged the integrity of siRNAs within cell-based systems,[21] it could find utility towards furthering our understanding of this alternative sense strand removal mechanism, in addition to assessing the fates of other modified siRNAs prepared in this study.

Ultimately, the RNA backbone modifications performed within this study provide several avenues, some of which are relatively simple using commercial sources through which to beneficially alter the thermodynamic profiles of siRNAs. Both triazole and spacer-modified siRNAs have proven their utility within cell-based assays and they further illustrate the extensive promiscuity of RNAi machinery for a variety of synthetic ligands.

References and Notes – Chapter V – General Discussion:

1. Keefe, A.D.; Pai, S.; Ellington, A., Aptamers as therapeutics. *Nat. Rev. Drug Discov.* **2010**, *9*, 537-550.

2. Dassie, J.P.; Liu, X.-y.; Thomas, G.S.; Whitaker, R.M.; Thiel, K.W.; Stockdale, K.R.; Meyerholz, D.K.; McCaffrey, A.P.; McNamara, J.O.; Giangrande, P.H., Systemic administration of optimized aptamer-siRNA chimeras promotes regression of PSMA-expressing tumors. *Nat. Biotech.* **2009**, *27*, 839-846.

3. Graff, J.R.; Konicek, B.W.; Vincent, T.M.; Lynch, R.L.; Monteith, D.; Weir, S.N.; Schwier, P.; Capen, A.; Goode, R.L.; Dowless, M.S.; Chen, Y.; Zhang, H.; Sissons, S.; Cox, K.; McNulty, A.M.; Parsons, S.H.; Wang, T.; Sams, L.; Geeganage, S.; Douglass, L.E.; Neubauer, B.L.; Dean, N.M.; Blanchard, K.; Shou, J.; Stancato, L.F.; Carter, J.H.; Marcusson, E.G., Therapeutic suppression of translation initiation factor eIF4E expression reduces tumor growth without toxicity. *J. Clin. Invest.* **2007**, *117*, 2638-2648.

4. Chen, X.; Kopecky, D.J.; Mihalic, J.; Jeffries, S.; Min, X.; Heath, J.; Deignan, J.; Lai, S.; Fu, Z.; Guimaraes, C.; Shen, S.; Li, S.; Johnstone, S.; Thibault, S.; Xu, H.; Cardozo, M.; Shen, W.; Walker, N.; Kayser, F.; Wang, Z., Structure-Guided Design, Synthesis, and Evaluation of Guanine-Derived Inhibitors of the eIF4E mRNA-Cap Interaction. *J. Med. Chem.* **2012**, *55*, 3837-3851.

5. Ding, S.-W.; Voinnet, O., Antiviral immunity directed by small RNAs. *Cell.* **2007**, *130*, 413-426.

6. Khaliq, S.; Khaliq, S.A.; Zahur, M.; Ijaz, B.; Jahan, S.; Ansar, M.; Riazuddin, S.; Hassan, S., RNAi as a new therapeutic strategy against HCV. *Biotechnol. Adv.* **2010**, *28*, 27-34.

7. Zhang, N.; Tan, C.; Cai, P.; Zhang, P.; Zhao, Y.; Jiang, Y., RNA interference in mammalian cells by siRNAs modified with morpholino nucleoside analogues. *Bioorg. Med. Chem. Lett.* **2009**, *17*, 2441-2446.

8. Iwase, R.; Toyama, T.; Nishimori, K., Solid-phase synthesis of modified RNAs containing amide-linked oligoribonucleosides at their 3 ′-end and their application to siRNA. *Nucleosides Nucleotides Nucleic Acids.* **2007**, *26*, 1451-1454.

9. Moore, C.B.; Guthrie, E.H.; Huang, M.T.-H.; Taxman, D.J., Short Hairpin RNA (shRNA): Design, Delivery, and Assessment of Gene Knockdown. *Method. Mol. Biol.* **2010**, *629*, 141-158.

10. Watts, J.K.; Deleavey, G.F.; Damha, M.J., Chemically modified siRNA: tools and applications. *Drug Discov. Today.* **2008**, *13*, 842-855.

11. Efthymiou, T.; Gong, W.; Desaulniers, J.-P., Chemical Architecture and Applications of Nucleic Acid Derivatives Containing 1,2,3-Triazole

Functionalities Synthesized via Click Chemistry. *Molecules.* **2012**, *17*, 12665-12703.

12. Xiong, Z.; Qiu, X.-L.; Huang, Y.; Qing, F.-L., Regioselective synthesis of 5-trifluoromethyl-1,2,3-triazole nucleoside analogues via TBS-directed 1,3-dipolar cycloaddition reaction. *J. Fluorine Chem.* **2011**, *132*, 166-174.

13. Spugnini, E.P.; Biroccio, A.; De Mori, R.; Scarsella, M.; D′Angelo, C.; Baldi, A.; Leonetti, C., Electroporation increases antitumoral efficacy of the bcl-2 antisense G3139 and chemotherapy in a human melanoma xenograft. *Journal of Translational Medicine.* **2011**, *9*, 10.

14. Leonetti, C.; Biroccio, A.; Benassi, B.; Stringaro, A.; Stoppacciaro, A.; Semple, S.C.; Zupi, G., Encapsulation of c-myc antisense oligodeoxynucleotides in lipid particles improves antitumoral efficacy *in vivo* in a human melanoma line. *Cancer Gene Ther.* **2001**, *8*, 459-468.

15. Addepalli, H.; Meena; Peng, C.G.; Wang, G.; Fan, Y.; Charisse, K.; Jayaprakash, K.N.; Rajeev, K.G.; Pandey, R.K.; Lavine, G.; Zhang, L.; Jahn-Hofmann, K.; Hadwiger, P.; Manoharan, M.; Maier, M.A., Modulation of thermal stability can enhance the potency of siRNA. *Nucleic Acids Res.* **2010**, *38*, 7320-7331.

16. Leuschner, P.J.F.; Ameres, S.L.; Kueng, S.; Martinez, J., Cleavage of the siRNA passenger strand during RISC assembly in human cells. *Embo Rep.* **2006**, *7*, 314-320.

17. Matranga, C.; Tomari, Y.; Shin, C.; Bartel, D.P.; Zamore, P.D., Passenger-strand cleavage facilitates assembly of siRNA into Ago2-containing RNAi enzyme complexes. *Cell.* **2005**, *123*, 607-620.

18. Khvorova, A.; Reynolds, A.; Jayasena, S.D., Functional siRNAs and rniRNAs exhibit strand bias. *Cell.* **2003**, *115*, 209-216.

19. Schwarz, D.S.; Hutvagner, G.; Du, T.; Xu, Z.S.; Aronin, N.; Zamore, P.D., Asymmetry in the assembly of the RNAi enzyme complex. *Cell.* **2003**, *115*, 199-208.

20. Wilson, J.N.; Kool, E.T., Fluorescent DNA base replacements: reporters and sensors for biological systems. *Org. Biomol. Chem.* **2006**, *4*, 4265-4274.

21. Jaerve, A.; Mueller, J.; Kim, I.I.H.; Rohr, K.; MacLean, C.; Fricker, G.; Massing, U.; Eberle, F.; Dalpke, A.; Fischer, R.; Trendelenburg, M.F.; Helm, M., Surveillance of siRNA integrity by FRET imaging. *Nucleic Acids Res.* **2007**, *35*.

Appendix I – Manuscript I

Synthesis and Properties of Oligonucleotides that Contain a Triazole-Linked Nucleic Acid Dimer

Tim C. Efthymiou and Jean-Paul Desaulniers*

Faculty of Science, University of Ontario Institute of Technology, Oshawa, Ontario, L1H 7K4, Canada
*E-mail: Jean-Paul.Desaulniers@uoit.ca

Received March 5, 2010
DOI 10.1002/jhet.532
Published online 8 February 2011 in Wiley Online Library (wileyonlinelibrary.com).

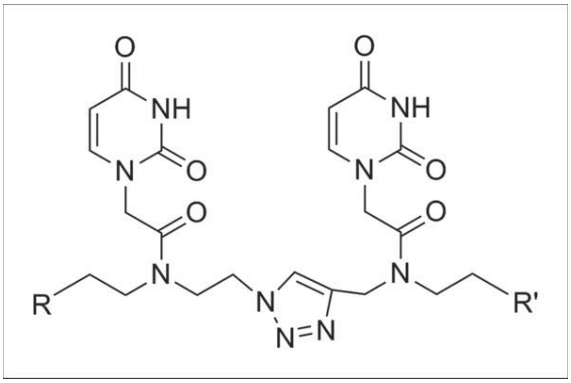

New chemically modified oligonucleotides at the site of the backbone are needed to improve the properties of oligonucleotides. A practical synthesis for a triazole-linked nucleoside dimer based on a PNA-like structure has been developed. This involves synthesizing two uracil-based monomers that contain either an azide or an alkyne functionality, followed by copper-catalyzed 1,3-dipolar cycloaddition. This dimer was incorporated within an oligonucleotide via phosphoramidite chemistry and UV-monitored thermal denaturation data illustrates slight destabilization relative to its target complementary sequence. This chemically modified dimer will allow for a future investigation of its properties within DNA and RNA-based applications.

J. Heterocyclic Chem., **48**, 533 (2011).

INTRODUCTION

Oligonucleotides have found tremendous use as biological tools and as agents with therapeutic promise. One promising example involves RNA interference (RNAi), and exploiting this pathway has become a major tool in elucidating gene function [1]. Furthermore, utilization of the RNAi pathway by administering short interfering RNAs (siRNAs) to cells [2] has offered therapeutic hope in combating diseased cells with aberrant gene expression profiles [3]. Despite awareness of this potential, improvements in enzymatic stability, biodistribution, cell-membrane permeability, and reducing off-target effects are still needed [4,5]. One way to potentially overcome these limitations involves altering the stability and specificity profile of the siRNA through chemical modification.

Within the areas of siRNA, the most common type of chemical modification involves alterations within the ribose moiety. Extensive studies involving 2′-*O*-Me, fluorinated sugars and locked nucleic acids (LNA) have shown favorable siRNA knockdown results depending on its position and sequence context [6–9]. Studies involving chemical modification of the backbone within the field of siRNA are less prevalent than sugar modifications. Some key examples include the negatively charged backbone modification involving a phosphorothioate [10] and boranophosphates [11]. Backbone-altering modifications such as a morpholino analogue [12] and neutral amide bonds at 3′ overhangs of siRNA duplexes, have shown favorable results when utilized for gene-knockdown studies [13,14]. Therefore, it is possible that the RNAi pathway will adopt less conventional backbone modifications at specific positions of the oligonucleotide. Given that siRNA duplexes exhibit thermodynamic asymmetry, being able to potentially destabilize the 5′ end of the guide strand with novel backbone modifications may offer favorable properties. Outside of the RNAi field, modified backbone constructs could have many other potential applications such as in antisense technology, artificial aptamer design or template driven enzymatic reactions. To explore this prospective, we are interested in pursuing alternative backbone modifications such as nonionic hydrophobic backbone mimics.

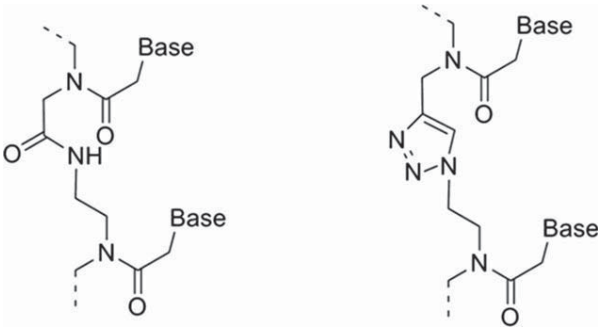

Figure 1. Chemical differences between peptide nucleic acid (left) and triazole-linked nucleic acid (right).

Within the field of backbone modified oligonucleotides, one of the most successful examples involves peptide nucleic acid (PNA) [15] and this has shown remarkable stability and specificity to its complementary targets [16,17]. PNA synthesis occurs by the successful amide-bond formation between an acid and an amine with high-yields. Therefore, we envisioned that a scaffold based on a triazole functional group would serve as a potentially good candidate (Fig. 1). To date, a number of different triazole-based backbone modifications have been reported [18–20] from the one presented herein.

RESULTS AND DISCUSSION

The repetitive backbone unit in most analogues, including PNA, contains six atoms. Although the six-atom spacer unit dominates by choice for a large number of chemically modified nucleic acids, analogues with shorter (five atom linker) [21–23] and longer backbones (seven atom linker) [24,25] have shown varying degrees of specificity to its target, depending on its sequence context and type of backbone. This suggests that site-specific incorporation of unnatural nucleoside backbones of different atom lengths can produce functioning oligonucleotides, capable of binding to their complement strand with varying specificity and stability. As such, chemically modifying oligonucleotides could offer an alternative way to fine-tune their functional effects.

We hypothesized that a copper (I)-catalyzed Huisgen [3 + 2] cycloaddition [26] based on a PNA-type structure would generate an alternative scaffold for bridging adjacent nucleotides together. We report the synthesis of a modified 1,4-triazole-linked uracil dimer through a distance of seven atoms and report its compatibility with hybridization to a complement sequence when appended at the 5′ or 3′ end of a DNA oligonucleotide.

Our strategy involves the synthesis of a uracil-based monomer possessing an alkyne functional group and a

Scheme 1. Reagents and conditions: (i) 1 equiv imidazole, 1 equiv TBS-Cl, DCM, room temperature 96% yield of **1**; (ii) 0.5 equiv DIPEA, 0.5 equiv propargyl bromide, DCM, room temperature, 3 h, 71% yield of **2**; (iii) 1.5 equiv uracil-1-yl acetic acid, 1.5 equiv DIPEA, 1.5 equiv HBTU, DMF, 24 h, 44% yield of **3**.

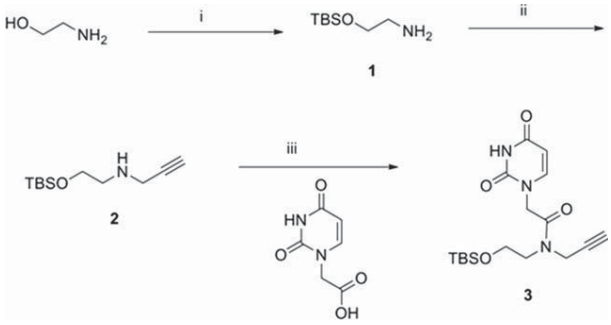

uracil-based monomer with an azide. For the synthesis of the uracil-based alkyne monomer, the first step involved *tert*-butyldimethylsilyl (TBS) protection of ethanolamine and this was conducted using TBSCl under standard basic conditions to afford **1** in 96% yield. Alkylation of **1** with propargyl bromide generated the alkyne **2** as a liquid in 71% yield. Utilizing peptide bond coupling conditions involving HBTU, the alkyne **2** was amide-bond coupled to uracil-1-yl acetic acid [27] to afford compound **3** as a white solid in 44% yield (Scheme 1).

For the synthesis of the azide-based uracil monomer **6**, 2-azidoethylamine **4** was prepared by the addition of 2-bromoethylamine to an aqueous solution of sodium azide. Alkylation of **4** with a limiting amount of ethyl 2-bromoacetate afforded compound **5** as an off-colored liquid in 83% yield. This liquid **5** was amide-bond coupled with uracil-1-yl acetic acid using DCC/HOBt to afford the azide-based uracil monomer, compound **6** in 62% yield (Scheme 2).

Scheme 2. Reagents and conditions: (i) 3 equiv NaN_3, H_2O, 75°C, 24 h; (ii) 5.8 equiv NaOH, 0°C, Et_2O, 64% yield of **4**; (iii) 1 equiv NEt_3, 0.6 equiv ethyl 2-bromoacetate, DMF, 4 h, 83% yield of **5**; (iv) 1.1 equiv uracil-1-yl acetic acid, 1.1 equiv DCC, 1.1 equiv HOBt, DMF, 24 h, 62% yield of **6**.

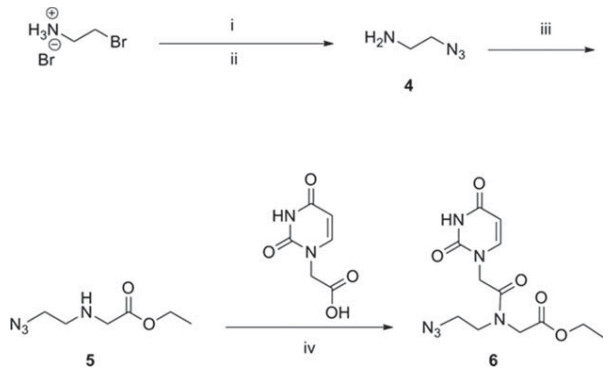

Scheme 3. Reagents and conditions: (i) 2 equiv sodium ascorbate, 0.5 equiv Cu(II)SO_4, THF/*t*-BuOH/H_2O (1:1:1), 24 h, 98% yield of **7**; (ii) 2.5 equiv $LiBH_4$, THF/MeOH (12:1), reflux 1.5 h, 76% yield of **8**; (iii) 3 equiv DMT-Cl, pyridine, 24 h, 79% yield of **9**; (iv) 3 eq TBAF, THF, 12 h, 85% yield of **10**; (v) 2 equiv 2-cyanoethyl *N,N*-diisopropylchlorophosphoramidite, 5.5 equiv DIPEA, 0.5 equiv DMAP, DCM, 8 h, 63% yield of **11**.

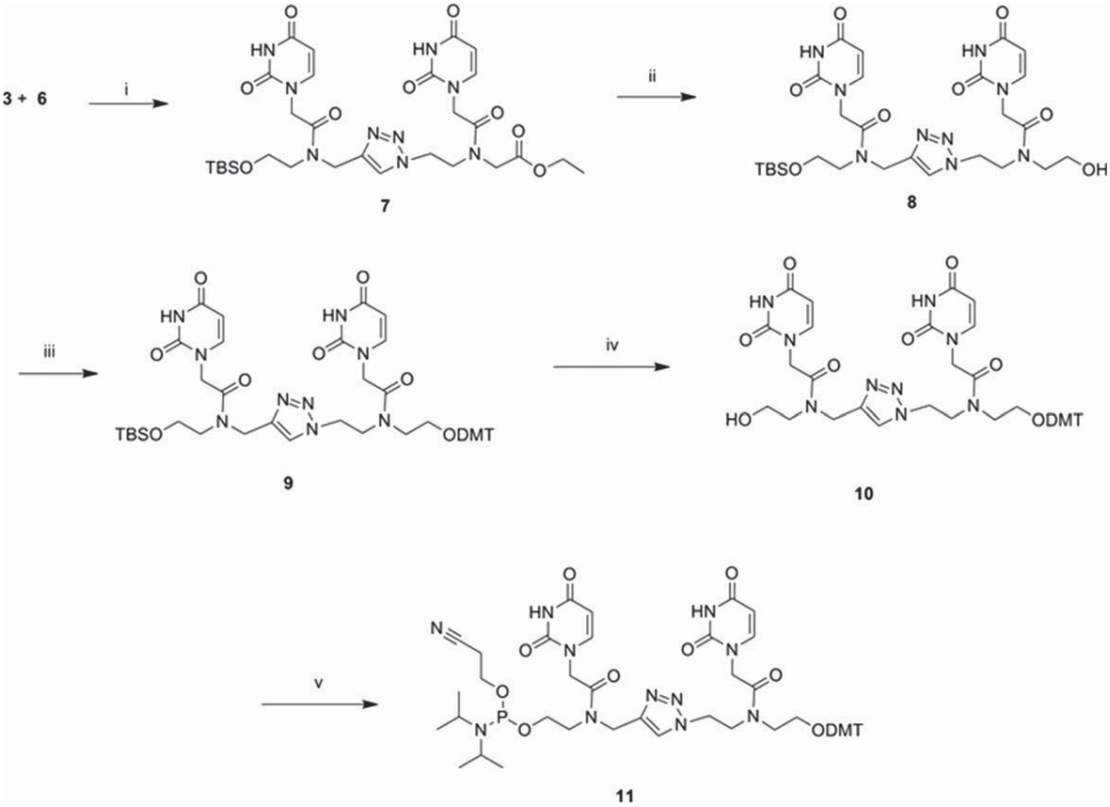

With respect to the synthesis of the phosphoramidite, the first task was to cyclize both monomers together. Under copper (I) conditions, 1,4-triazole formation occurred with copper sulfate and sodium ascorbate to afford a white solid **7** in 98% yield. This newly formed dimer **7** was selectively reduced with 2.5 equivalents of $LiBH_4$ in a methanol/THF mixture to afford the alcohol **8** in 76% yield. Alcohol **8** was treated with 4,4′-dimethoxytrityl-chloride (DMT-Cl) to afford the compound **9** in 79% yield. The subsequent removal of the TBS group using TBAF provided the alcohol **10** in 85% yield. This was then followed by synthesis of phosphoramidite **11** by reacting alcohol **10** with 2-cyanoethyl *N,N*-diisopropylchlorophosphoramidite to afford a clear oil in 63% yield (Scheme 3). With this phosphoramidite **11**, its incorporation within a DNA oligonucleotide was accomplished by employing solid-phase oligonucleotide synthesis on a 394 ABI synthesizer.

UV-melting denaturation studies indicate that moderate destabilization occurs with the UU-dimer on both the 5′ and 3′ position relative to the native strand (Table 1). A reduction in T_m of 4.5°C and 2.8°C is observed when native TT is replaced with the UU-dimer modification at the 5′ end and the 3′ end, respectively. However, this suggests a certain degree of compatibility as the T_m values for both modified oligonucleotides are higher when compared to corresponding 12-mer sequences lacking the heterocyclic pyrimidine dimer (**UU**) (Table 1). In comparison to other studies [28] and that of Kraicsovits and coworkers, a similar T_m drop was

Table 1

UV-melting denaturation studies.

Entry	Sequence	T_m (°C)	ΔT_m (°C)[a]
I	5′ TTTTTCTCTCTCTT 3′	40.9	0
II	5′ TTTTTCTCTCTC**UU** 3′	38.1	−2.8
III	5′ TTTTTCTCTCTC 3′	37.1	−3.8
IV	5′ **UU**TTTCTCTCTCTT 3′	36.4	−4.5
V	5′ TTTCTCTCTCTT 3′	35.3	−5.6

UV melting temperatures for duplexes to complement strand DNA (5′-AAG AGA GAG AAA AA-3′). The total strand concentration ranged from 2.4 to 3.0 μM in 90 mM NaCl, 10 mM sodium phosphate, and 1 mM EDTA at pH 7.0.

[a]For the ΔT_m values, the T_m of Entry I is the reference (T_m = 40.9 °C).

observed when compared to a PNA-DNA chimera that contained a PNA element at the terminal end [29].

CONCLUSIONS

In conclusion, a facile and practical synthesis of a new uracil-uracil dimer linked together through a triazole functionality has been developed and is readily synthesized from inexpensive starting material precursors. Our alkyne-uracil monomer **3** was synthesized in 44% yield and the azide-uracil monomer **6** was generated in 62% yield. Following heterocyclic cyclization, the phosphoramidite **11** was generated in four steps in 32% yield. Incorporation of the heterocyclic dimer at both the 5′ and 3′ ends of DNA oligonucleotides suggests a certain degree of compatibility when analyzed by UV-monitored thermal denaturation. The effects of this modification within different positions of other various oligonucleotides will be investigated. Notwithstanding, these oligonucleotides may have potential use when targeted at messenger RNA in diseased cells, or for other downstream applications.

EXPERIMENTAL

Unless otherwise noted, all starting materials were obtained from commercial sources and were used without any additional purification. Anhydrous CH_2Cl_2, THF, and DMF were purchased from Sigma-Aldrich and degassed by stirring under a dry N_2 atmosphere. Purification by flash chromatography was carried out with Silicycle Siliaflash 60 (230–400 mesh) according to the procedure of Still et al. [30] ^{1}H NMR spectra were recorded in DMSO-d_6 or $CDCl_3$ at 400 or 500 MHz and ^{13}C NMR spectra were recorded at 100 or 125 MHz. High-Resolution MS (HRMS) was recorded on a Micromass AutoSpec Ultima Magnetic sector mass spectrometer.

***2-(tert*-Butyldimethylsilyloxy)ethanamine (1).** To a solution of ethanolamine (9.6 mL, 159 mmol) in 100 mL of CH_2Cl_2 was dissolved imidazole (10.8 g, 159 mmol) and this solution was cooled in an ice-water bath. To this solution was added *tert*-butyldimethylsilyl chloride (24 g, 159 mmol) and the reaction mixture was stirred overnight at room temperature. Sat. $NaHCO_3$ was added and the resulting mixture was partitioned. The organic fractions were concentrated *in vacuo* to afford the title compound as a clear light yellow oil (26.8 g, 96%) [31].

***N*-(2-(*tert*-Butyldimethylsilyloxy)ethyl)prop-2-yn-1-amine (2).** To a solution of **1** (10 g, 57 mmol) in 100 mL of CH_2Cl_2 was added diisopropylethylamine (3.7 g, 28.5 mmol), and this solution was cooled in an ice-water bath. To this solution was added 3-bromoprop-1-yne (3.4 g, 28.5 mmol) dropwise over 30 min. This reaction mixture was stirred at room temperature until TLC analysis indicated the complete consumption of starting material (3 h). Sat. $NaHCO_3$ was added and the reaction mixture was partitioned. The organic fraction was concentrated *in vacuo*, to afford an oil which was purified by silica gel chromatography eluting with a gradient of hexanes/EtOAc (7:3 to 3:7) to afford the title compound as a clear yellow oil (2.9 g, 71%); ^{1}H NMR (500 MHz, $CDCl_3$) δ 0.07 (s, 6H), 0.90 (s, 9H), 1.67 (br s, 1H), 2.21 (s, 1H), 2.80 (t, 2H, J = 5.5 Hz), 3.46 (s, 2H), 3.75 (t, 2H, J = 5.1 Hz); ^{13}C NMR (100 MHz, $CDCl_3$) δ −5.36, 25.89, 29.66, 38.18, 50.52, 62.32, 71.21, 82.15; ESI-HRMS (ES^+) m/z calcd for $C_{11}H_{23}NOSi$: 213.1549, found 214.1626 $[M + H]^+$. Anal. Calcd. for $C_{11}H_{23}NOSi$: C, 61.91; H, 10.86. Found: C, 61.56; H, 10.49.

***N*-(2-(*tert*-Butyldimethylsilyloxy)ethyl)-uracil-1-yl-*N*-(prop-2-yn-1-yl)acetamide (3).** To a solution of uracil-1-yl acetic acid (2.4 g, 14 mmol) in 240 mL of DMF was added diisopropylethylamine (1.8 g, 14 mmol) and this solution was cooled in an ice-water bath. The acid was activated with the addition of *O*-benzotriazole-*N*,*N*,*N*′,*N*′-tetramethyl-uronium-hexafluorophosphate (5.3 g, 14 mmol) to the stirring solution over the course of 5 min, followed by the dropwise addition of **2** (2 g, 9.4 mmol) over 15 min. The reaction mixture was stirred for 24 h at ambient temperature and then extracted with EtOAc and the organic layer was washed with H_2O and brine (x3). The organic layer was collected and concentrated *in vacuo* to afford the crude product. This crude product was purified by flash chromatography with a gradient of hexanes/EtOAc (7:3) to 100% EtOAc to elute the title compound as a white solid (1.5 g, 44%). Compound **3** is a pair of rotamers; the signals to the major (ma.) and minor (mi.) rotamers are designated; ^{1}H NMR (500 MHz, $CDCl_3$) δ 0.04 (s, 2H, mi.), 0.08 (s, 4H, ma.), 0.88 (s, 3H, mi.), 0.89 (s, 6H, ma.), 2.25 (br s, 0.66H, ma.), 2.41 (br s, 0.33H, mi.), 3.58 (t, 0.6H, J = 5.3 Hz, mi.), 3.65 (t, 1.4H, J = 5.2 Hz, ma.), 3.76 (t, 0.6H, J = 5.3 Hz, mi.), 3.85 (t, 1.4H, J = 5.0 Hz, ma.), 4.27 (2s, 2H), 4.68 (m, 2H), 5.71–5.74 (m, 1H), 7.13 (d, 0.66H, J = 7.9 Hz, ma.), 7.17 (d, 0.33H, J = 7.9 Hz, mi.), 9.43 (br s, 0.66H, ma.), 9.48 (br s, 0.33H, mi.); ^{13}C NMR (125 MHz, $CDCl_3$) δ −5.61, −5.55, −5.41, −5.36, −3.72, −3.53, 17.94, 18.11, 18.28, 25.54, 25.69, 25.75, 25.81, 25.89, 25.96, 35.16, 38.67, 48.03, 48.06, 48.78, 49.55, 60.58, 61.67, 72.72, 73.59, 77.93, 78.13, 102.13, 102.24, 145.02, 145.09, 150.90, 150.93, 163.58, 166.30, 166.66; ESI-HRMS (ES^+) m/z calcd for $C_{17}H_{27}N_3O_4Si$: 365.1771, found 366.1845 $[M + H]^+$. Anal. Calcd. for $C_{17}H_{27}N_3O_4Si$: C, 55.86; H, 7.45; N, 11.50. Found: C, 55.67; H, 7.80; N, 11.89.

2-Azidoethanamine (4). To a solution of NaN_3 (23.8 g, 366 mmol) in 200 mL of water was added 2-bromoethylamine hydrobromide (25 g, 122 mmol) and this solution was heated to 75°C. The reaction mixture was stirred for 24 h and was then cooled in an ice-water bath. To the cooled solution was added NaOH (28.5 g, 712.5 mmol) and the reaction mixture was stirred until the NaOH was fully dissolved. To this aqueous solution was added Et_2O (x3). The ether fractions were collected, dried over Na_2SO_4, and evaporated *in vacuo* to afford the title compound as a clear oil (6.7 g, 64%). The ^{1}H proton and ^{13}C NMR shifts were confirmed with the report by Mayer and Maier [32].

Ethyl 2-(2-azidoethylamino)acetate (5). To a solution of **4** (5 g, 58.1 mmol) in 100 mL of DMF was added triethylamine (5.9 g, 58.1 mmol). Ethyl 2-bromoacetate (5.8 g, 34.9 mmol) was then added dropwise over 15 min to the stirring solution and the reaction was stirred for 4 h at room temperature. The solution was then extracted with EtOAc, washed with H_2O (three times) and the EtOAc fractions were collected and dried over Na_2SO_4. This solution was evaporated under reduced pressure to yield a crude orange oil. The oil was loaded directly onto a silica column for purification by gradient eluting with hexanes/EtOAc (5:5) to 100% EtOAc to afford the

title compound as a clear light yellow oil (5.0 g, 83%); ^{1}H NMR (400 MHz, $CDCl_3$) δ 1.25 (t, 3H, J = 7.1 Hz), 1.98 (br s, 1H), 2.80 (t, 2H, J = 5.7 Hz), 3.39 (t, 2H, J = 5.9 Hz), 3.40 (s, 2H), 4.17 (q, 2H, J = 7.4 Hz); ^{13}C NMR (100 MHz, $CDCl_3$) δ 14.09, 48.01, 50.50, 51.33, 60.74, 172.07; ESI-HRMS (ES^+) m/z calcd for $C_6H_{12}N_4O_2$: 172.0960, found 173.1034 $[M + H]^+$. Anal. Calcd. for $C_6H_{12}N_4O_2$: C, 41.85; H, 7.02; N, 32.54. Found: C, 41.65; H, 6.82; N, 32.12.

Ethyl 2-(*N*-(2-azidoethyl)-uracil-1-yl-acetamido)acetate (6). To a solution of uracil-1-yl acetic acid (1.1 g, 6.4 mmol) in 100 mL of anhydrous DMF under N_2 was added dicyclohexylcarbodiimide (1.3 g, 6.4 mmol) and 1*N*-hydroxybenzotriazole (1.0, 6.4 mmol). This solution was stirred for 15 min on an ice-water bath, followed by 1 h of stirring at ambient temperature. To this solution was added compound **5** (1 g, 5.8 mmol) dropwise over 10 min, and the reaction mixture was stirred for 24 h after which the DCU precipitate was collected by filtration. The filtrate was dried down *in vacuo*, dissolved in EtOAc, and washed with water and brine (x3). The EtOAc solutions were concentrated *in vacuo*. The resulting crude product was dissolved in a minimal amount of CH_2Cl_2 and purified by flash chromatography with a gradient of hexanes/EtOAc (5:5) to 100% EtOAc to elute the title compound as a white solid (1.2 g, 62%). Compound **6** is comprised of a pair of rotamers, each displaying signals of equal intensity; ^{1}H NMR (500 MHz, $CDCl_3$) δ 1.28 (t, 1.5H, J = 7.1 Hz), 1.33 (t, 1.5H, J = 7.1 Hz), 3.55 (s, 2H), 3.59 (t, 1H, J = 5.6 Hz), 3.66 (t, 1H, J = 5.4 Hz), 4.12 (s, 1H), 4.21 (q, 1H, J = 7.1 Hz), 4.26 (s, 1H), 4.28 (q, 1H, J = 7.1 Hz), 4.49 (s, 1H), 4.72 (s, 1H), 5.74 (d, 0.5H, J = 6.0 Hz), 5.75 (d, 0.5H, J = 5.6 Hz), 7.20 (d, 0.5H, J = 2.0 Hz), 7.21 (d, 0.5H, J = 2.0 Hz), 9.08 (br s, 1H); ^{13}C NMR (125 MHz, $CDCl_3$) δ 47.75, 47.82, 48.05, 48.31, 48.86, 49.84, 49.92, 50.95, 61.67, 62.31, 102.30, 102.38, 145.02, 145.14, 150.90, 150.92, 163.44, 167.16, 167.46, 168.64, 169.03; ESI-HRMS (ES^+) m/z calcd for $C_{12}H_{16}N_6O_5$: 324.1182, found 325.1262 $[M + H]^+$. Anal. Calcd. for $C_{12}H_{16}N_6O_5$: C, 44.44; H, 4.97; N, 25.91. Found: C, 44.40; H, 5.10; N, 25.41.

Ethyl 2-(*N*-(2-(4-((*N*-(2-(*tert*-Butyldimethylsilyloxy)ethyl)-uracil-1-yl-acetamido)methyl)-1*H*-1,2,3-triazol-1-yl)ethyl)-uracil-1-yl-acetamido)acetate (7). To a solution of compounds **3** (677 mg, 1.9 mmol) and **6** (600 mg, 1.9 mmol) dissolved in 18 mL of THF/*t*-BuOH/H_2O (1:1:1) was added sodium ascorbate (733 mg, 3.7 mmol) and Cu(II)SO_4 (231 mg, 925 μmol). This reaction mixture was stirred for 24 h at room temperature and then extracted with CH_2Cl_2. The organic layer was washed with H_2O (three times) to wash off the excess copper. The precipitate in the organic layer was collected by filtration and washed with cold H_2O to afford the crude product. This crude product was redissolved in minimal CH_2Cl_2/MeOH for 1 h and purified by flash column chromatography eluting with 5% (10% NH_4OH in MeOH) in CH_2Cl_2 to afford the title compound as a white solid (1.3 g, 98%). Compound **7** is a mixture of rotamers with varying signal intensities. ^{1}H NMR (400 MHz, DMSO-d_6) δ 0.03 (s, 2H), 0.05 (m, 4H), 0.85, 0.86 (2s, 9H), 1.18 (t, 1.5H, J = 7.2 Hz), 1.23 (t, 1.5H, J = 7.0 Hz), 3.48–3.50 (m, 1H), 3.63–3.91 (m, 4H), 4.01–4.03 (m, 1H), 4.08 (q, 1.2H, J = 7.3 Hz), 4.16 (q, 0.8H, J = 7.3 Hz), 4.24, 4.29 (2s, 1H), 4.44–4.77 (m, 9H), 5.56 (d, 2H, J = 7.8 Hz), 7.31–7.47 (m, 2H), 7.89, 8.05, 8.13, 8.24 (4s, 1H), 11.29 (br m, 2H); ^{13}C NMR (100 MHz, DMSO-d_6) δ −5.45, −5.39, 13.99, 14.04, 17.89, 18.04, 25.82, 25.90, 41.05, 47.31, 47.58, 47.91, 48.00, 60.18, 60.65, 60.83, 61.25, 100.57, 100.79, 123.70, 124.04, 124.12, 124.61, 143.18, 143.34, 143.41, 143.56, 146.12, 146.19, 146.29, 146.50, 146.54, 150.92, 150.98, 151.04, 151.07, 151.11, 163.76, 163.80, 163.81, 163.85, 163.88, 166.74, 166.82, 166.88, 166.90, 167.43, 167.97, 168.03, 168.85, 169.15; ESI-HRMS (ES^+) m/z calcd for $C_{29}H_{43}N_9O_9Si$: 689.2953, found 690.3030 $[M + H]^+$. Anal. Calcd. for $C_{29}H_{43}N_9O_9Si$: C, 50.50; H, 6.28. Found: C, 50.47; H, 6.24.

***N*-(2-(*tert*-Butyldimethylsilyloxy)ethyl)-uracil-1-yl-*N*-((1-(2-(uracil-1-yl-*N*-(2-hydroxyethyl)acetamido)ethyl)-1*H*-1,2,3-triazol-4-yl)methyl)acetamide (8).** To a solution of compound **7** (300 mg, 435 μmol) suspended in 12 mL of dry THF, drops of MeOH were added until the compound was dissolved. To this solution was then added $LiBH_4$ (544 μL, 1.09 mmol) and the reaction mixture was refluxed until TLC analysis indicated the complete consumption of starting material (1.5 h). This reaction mixture was quenched with MeOH and dried down *in vacuo* to afford the crude product. The crude product was then redissolved in minimal CH_2Cl_2/MeOH and purified by flash column chromatography eluting with a gradient of 10% NH_4OH in MeOH (5 to 15%) in CH_2Cl_2 to afford the title compound as a white crystalline solid (213 mg, 76%). Compound **8** is a mixture of rotamers with varying signal intensities; ^{1}H NMR (500 MHz, DMSO-d_6) δ 0.03 (s, 2H), 0.05 (s, 4H), 0.85, 0.87 (2s, 9H), 3.16–3.27 (m, 2H), 3.43–3.54 (m, 4H), 3.63–3.74 (m, 3H), 3.80–3.87 (m, 2H), 4.36–4.38 (m, 1H), 4.46 (t, 1.2H, J = 6.3 Hz), 4.51 (t, 0.8H, J = 6.3 Hz), 4.56–4.81 (m, 6H), 4.94–5.00 (m, 1H), 5.54–5.58 (m, 2H), 7.35–7.47 (m, 2H), 7.87, 8.04, 8.13, 8.23 (4s, 1H), 11.30 (br s, 2H); ^{13}C NMR (125 MHz, DMSO-d_6) δ −5.44, −5.37, 17.91, 18.05, 25.83, 25.92, 30.74, 41.04, 46.24, 46.55, 46.71, 46.92, 48.29, 48.32, 48.51, 49.07, 49.26, 58.49, 58.81, 58.85, 60.21, 60.85, 100.57, 100.63, 123.76, 124.11, 124.55, 143.23, 143.39, 143.43, 143.58, 146.48, 146.52, 146.58, 151.04, 151.08, 151.11, 163.84, 163.87, 166.69, 166.74, 166.81, 167.43, 167.54; ESI-HRMS (ES^+) m/z calcd for $C_{27}H_{41}N_9O_8Si$: 647.2847, found 648.2918 $[M + H]^+$. Anal. Calcd. for $C_{27}H_{41}N_9O_8Si$: C, 50.06; H, 6.38; N, 19.46. Found: C, 50.23; H, 6.84; N, 19.36.

***N*-(2-(Bis(4-methoxyphenyl)(phenyl)methoxy)ethyl)-2-(uracil-1-yl)-*N*-(2-(4-((2-(uracil-1-yl)-*N*-(2-((2,3,3-trimethylbutan-2-yl)oxy)ethyl)acetamido)methyl)-1*H*-1,2,3-triazol-1-yl)ethyl)acetamide (9).** To a solution of compound **8** (1.06 g, 1.64 mmol) dissolved in 10 mL of dry pyridine under N_2, was added an excess of 4,4′-dimethoxytrityl chloride (1.66 g, 4.91 mmol) until TLC analysis revealed the consumption of starting material. This reaction mixture was stirred overnight at room temperature. while under N_2, after which the entire mixture was extracted with CH_2Cl_2 and washed with H_2O (two times). The organic fractions were collected, dried over Na_2SO_4 and subsequently condensed *in vacuo* to afford the crude product. The crude was dissolved in minimal CH_2Cl_2/MeOH and purified by flash column chromatography eluting with a gradient of MeOH (5 to 15%) in CH_2Cl_2 to afford the title compound as a white solid (1.22 g, 79%). Compound **9** is a mixture of rotamers with varying signal intensities; ^{1}H NMR (400 MHz, $CDCl_3$) δ 0.03 (s, 2H), 0.06 (s, 4H), 0.86, 0.88 (2s, 9H), 2.87–2.94 (m, 1.5H), 3.03–3.08 (m, 0.5H), 3.20 (t, 1.5H, J = 4.7 Hz), 3.26 (t, 0.5H, J = 4.5 Hz), 3.29–3.31 (m, 0.2H), 3.36–3.43 (m, 0.3H), 3.46–3.55 (m, 2.5H), 3.60–3.67 (m, 2H), 3.72–3.75 (m, 0.75H), 3.76, 3.77 (2s, 7H), 3.80 (t, 1.25H, J = 4.9 Hz), 4.51 (t, 1.5H, J = 5.3 Hz), 4.55 (t, 0.5H, J = 5.3 Hz),

4.59 (s, 1H), 4.63–4.64 (m, 1H), 4.67 (s, 3H), 4.73 (d, 1H, J = 7.4 Hz), 5.51–5.55 (m, 1H), 5.62 (d, 0.1H, J = 1.6 Hz), 5.64 (d, 0.1H, J = 1.6 Hz), 5.64–5.68 (m, 0.8H), 6.57 (d, 0.1H, J = 7.8 Hz), 6.66 (d, 0.7H, J = 7.8 Hz), 6.80–6.84 (m, 4.3H), 7.06–7.09 (m, 0.8H), 7.17–7.36 (m, 7.2H), 7.71, 7.81, 7.88, 7.94 (4s, 1H), 10.11 (br s, 2H); ^{13}C NMR (100 MHz, $CDCl_3$) δ −5.44, −5.16, 18.13, 18.29, 25.61, 25.83, 25.90, 41.33, 44.08, 47.64, 47.74, 48.27, 48.50, 48.62, 48.87, 48.93, 49.09, 55.23, 60.41, 60.66, 60.79, 60.98, 87.24, 87.39, 102.02, 102.21, 102.25, 113.15, 113.25, 124.37, 125.24, 127.18, 127.24, 127.86, 127.98, 128.15, 129.91, 130.08, 135.03, 135.09, 135.70, 143.49, 143.76, 144.01, 144.05, 144.65, 145.00, 145.10, 145.15, 145.21, 145.54, 151.26, 151.32, 151.38, 151.46, 158.42, 158.67, 158.71, 163.91, 164.00, 164.08, 166.48, 167.25, 167.67. ESI-HRMS (ES^+) m/z calcd for $C_{48}H_{59}N_9O_{10}Si$ 949.4154, found 972.4035 $[M + Na]^+$. Anal. Calcd. for $C_{49}H_{59}N_9O_{10}Si$: C, 60.68; H, 6.26; N, 13.27. Found: C, 60.50; H, 6.28; N, 12.90.

***N*-(2-(Bis(4-methoxyphenyl)(phenyl)methoxy)ethyl)-2-(uracil-1-yl)-*N*-((1-(2-(2-(uracil-1-yl)-*N*-(2-hydroxyethyl)acetamido)ethyl)-1*H*-1,2,3-triazol-4-yl)methyl)acetamide (10).** To a solution of compound **9** (1.12 g, 1.18 mmol) dissolved in 26 mL of dry THF was added TBAF (926 mg, 3.54 mmol). This reaction mixture was stirred for 12 h at room temperature and then extracted with CH_2Cl_2. The organic layer was washed with H_2O and brine (×2), at which point the combined organic fractions were dried over Na_2SO_4, and evaporated under reduced pressure. The crude was dissolved in minimal CH_2Cl_2/MeOH and purified by flash column chromatography, first eluting with 100% CH_2Cl_2 followed by a gradient of MeOH (5 to 15%) in CH_2Cl_2 to afford the title compound as a yellow solid (840 mg, 85%). Compound **10** is a mixture of rotamers with varying signal intensities; ^{1}H NMR (400 MHz, $CDCl_3$) δ 2.49 (br s, 1H), 2.98 (br s, 1H), 3.16–3.20 (br m, 2H), 3.27–3.31 (m, 3H), 3.45–3.57 (m, 4H), 3.68–3.81 (m, 8H), 4.45–4.80 (m, 8H), 5.50–5.53 (m, 0.8H), 5.56–5.60 (m, 1.2H), 6.63 (d, 0.15H, J = 8.2 Hz), 6.66 (d, 0.35H, J = 7.8 Hz), 6.78–6.83 (m, 4H), 7.17–7.31 (m, 8.5H), 7.69, 7.88, 7.90, 8.09 (4s, 1H), 10.20–10.42 (br m, 2H); ^{13}C NMR (100 MHz, $CDCl_3$) δ 22.13, 27.75, 29.14, 29.64, 42.18, 47.37, 48.29, 49.13, 50.35, 55.24, 59.15, 60.78, 68.46, 87.23, 87.32, 101.65, 101.91, 107.85, 113.16, 113.26, 124.97, 127.16, 127.99, 128.17, 129.92, 130.09, 135.15, 135.73, 143.56, 144.11, 144.28, 145.47, 146.36, 151.41, 151.47, 158.40, 158.64, 164.30, 164.39, 164.56, 167.63, 167.68; ESI-HRMS (ES^+) m/z calcd for $C_{42}H_{45}N_9O_{10}$: 835.3289, found 858.3217 $[M + Na]^+$. Anal. Calcd. for $C_{42}H_{45}N_9O_{10}$: C, 60.35; H, 5.43. Found: C, 60.72; H, 5.81.

2-(*N*-(2-(4-((*N*-(2-(Bis(4-methoxyphenyl)(phenyl)methoxy)ethyl)-2-(uracil-1-yl)acetamido)methyl)-1*H*-1,2,3-triazol-1-yl)ethyl)-2-(uracil-1-yl)acetamido)ethyl (2-cyanoethyl) diisopropylphosphoramidite (11). To a solution of compound **10** (230 mg, 275 μmol) dissolved in 6 mL of dry CH_2Cl_2 under N_2, was added diisopropylethylamine (196 mg, 1.51 mmol) along with 4-dimethylaminopyridine (16.8 mg, 138 μmol). To this solution was added 2-cyanoethyl *N*,*N*-diisopropylchlorophosphoramidite (195 mg, 825 μmol), until TLC analysis revealed the maximum consumption of starting material. This mixture was then stirred for 6 h at room temperature under N_2 and dried *in vacuo* to afford the crude product. The crude was dissolved in minimal 2% triethylamine in hexanes/acetone and purified by flash column chromatography eluting with a gradient of 2% triethylamine in acetone/hexanes (1:1 to 4:1) to afford the title compound as a white solid (180 mg, 63%). Compound **11** is a mixture of rotamers with varying signal intensities; ^{1}H NMR (400 MHz, $CDCl_3$) δ 1.14–1.19 (m, 12H), 2.62–2.66 (m, 3.25H), 2.92 (t, 1H, J = 3.9 Hz), 3.07 (t, 0.75H, J = 4.3 Hz), 3.21 (t, 1.25H, J = 4.7 Hz), 3.26 (t, 0.5H, J = 4.3 Hz), 3.29–3.37 (m, 0.25H), 3.54–3.61 (m, 5.5H), 3.70–3.77 (m, 2H), 3.78 (s, 6.25H), 3.81–3.90 (m, 2.25H), 4.52 (t, 1H, J = 5.3 Hz), 4.55 (t, 0.5H, J = 5.5 Hz), 4.61–4.65 (m, 2H), 4.70 (s, 2.5H), 4.74–4.77 (m, 1H), 5.52–5.55 (m, 1H), 5.66–5.70 (m, 1H), 6.56 (d, 0.33H, J = 7.8 Hz), 6.63 (d, 0.66H, J = 7.8 Hz), 6.81–6.84 (m, 4H), 7.17–7.31 (m, 12H), 7.70, 7.76, 7.89, 7.95 (4s, 1H); ^{13}C NMR (100 MHz, $CDCl_3$) δ 14.10, 14.84, 20.45, 20.52, 22.66, 23.34, 24.58, 24.62, 24.65, 24.69, 24.77, 29.24, 29.34, 29.66, 31.72, 31.89, 33.80, 34.43, 41.51, 43.02, 43.14, 45.82, 47.67, 47.80, 48.29, 48.60, 48.71, 48.93, 53.76, 55.26, 58.08, 58.30, 60.53, 60.70, 60.80, 69.48, 87.29, 87.42, 102.08, 102.20, 102.25, 113.27, 117.90, 118.12, 125.13, 127.24, 128.01, 128.20, 130.12, 135.05, 135.09, 143.39, 143.82, 144.05, 145.07, 145.46, 151.24, 151.34, 151.45, 158.71, 158.75, 163.63, 163.87, 163.91, 166.67, 167.41, 167.74; ESI-HRMS (ES^+) m/z calcd for $C_{51}H_{62}N_{11}O_{11}P$: 1035.4368, found 1058.4298 $[M + Na]^+$.

Table 2

The oligonucleotides characterized by MALDI-TOF mass spectrometry.

Sequence	Calcd mass (g/mol)	Observed mass (g/mol)	Observed molecular ion
5′ TTTTTCTCTCT**CUU** 3′	4123	4122	$[M - H]^-$
5′ TTTTTCTCTCT $\overline{3'}$	3529	3530	$[M + H]^-$
5′ **UU**TTTCTCTCTTT 3′	4123	4164	$[M - H + K]^-$
5′ $\overline{\text{TTT}}$CTCTCTCTT 3′	3529	3530	$[M + H]^-$

Observed masses obtained from MALDI-TOF Mass Spectrometry. Polyacrylamide gel-purified samples were desalted using Millipore Zip-Tip C18-column micropipette tips to a final concentration of 5 μM. 5 μL of matrix solution (3-hydroxypicolinic acid at 25 mg/mL, dissolved in 50/50 acetonitrile/water with 5 mg/mL ammonium citrate) was added to each sample vial.

Oligonucleotide synthesis. All standard β-cyanoethyl DNA phosphoramidites, solid supports and reagents were purchased from Glen Research. All oligonucleotides were synthesized on an Applied Biosystems 394 DNA/RNA synthesizer using a 0.2 μM cycle with a 25 s coupling time for unmodified phosphoramidites. All phosphoramidites were dissolved in anhydrous acetonitrile to a 0.1M concentration immediately prior to synthesis. Synthesis on solid phase was accomplished using 0.2 μM solid supports. Cleavage of the unmodified oligonucleotides from their solid supports was performed through exposure to 1.5 mL of 30% NH_4OH for 2 h at room temperature, followed by incubation in 30% NH_4OH at 55°C overnight. All oligonucleotides were purified on a 20% denaturing polyacrylamide gel by utilizing the ''crush and soak'' method, followed by ethanol precipitation and desalting through Millipore 3000 MW cellulose centrifugal filters. The oligonucleotides were characterized by MALDI-TOF mass spectrometry (Waters Tofspec-2E) (Table 2).

Synthesis of 5′ TTTTTCTCTCTCUU 3′ and 5′ UUTTTCTCTCTCTT 3′. Phosphoramidite **11** was attached to the 5′ end of the growing oligonucleotide being synthesized on the ABI 394 DNA/RNA synthesizer, with an increased coupling time of 600 s. To perform the 3′ modification, compound **11** was attached to a Universal III solid support (Glen Research) via the ABI 394 synthesizer with a 600 s coupling time. Cleavage from the Universal III solid support was performed through exposure to 1.5 mL of 2M NH_3 in MeOH for 30 min at room temperature, followed by incubation in 30% NH_4OH at 55°C for 8 h.

Synthesized sequences. Oligonucleotides synthesized using standard dT/dA supports: (i) 5′-AAG AGA GAG AAA AA–3′; (ii) 5′–TTT TTC TCT CTC TT–3′; and (iii) 5′–**UU**T TTC TCT CTC TT–3′. The **UU**–3′ modified sequence synthesized on the Universal III solid support: 5′–TTT TTC TCT CTC **UU**–3′. The sequence 5′-AAG AGA GAG AAA AA-3′ was purchased and purified from Integrated DNA Technologies.

Acknowledgments. We are grateful to UOIT and NSERC for funding. We thank Dr. Darcy Burns of Trent University for assistance with NMR spectroscopy and Dr. Christopher Wilds for his assistance with T_m measurements.

REFERENCES AND NOTES

[1] Hannon, G. J. Nature 2002, 418, 244.

[2] Elbashir, S. M.; Harborth, J.; Lendeckel, W.; Yalcin, A.; Weber, K.; Tuschl, T. Nature 2001, 411, 494.

[3] Huang, C.; Li, M.; Chen, C. Y.; Yao, Q. Z. Expert Opin Ther Targets 2008, 12, 637.

[4] Corey, D. R. Nat Chem Biol 2007, 3, 8.

[5] Watts, J. K.; Deleavey, G. F.; Damha, M. J Drug Discov Today 2008, 13, 842.

[6] Braasch, D. A.; Jensen, S.; Liu, Y. H.; Kaur, K.; Arar, K.; White, M. A.; Corey, D. R. Biochemistry 2003, 42, 7967.

[7] Elmen, J.; Thonberg, H.; Ljungberg, K.; Frieden, M.; Westergaard, M.; Xu, Y. H.; Wahren, B.; Liang, Z. C.; Urum, H.; Koch, T.; Wahlestedt, C. Nucleic Acids Res 2005, 33, 439.

[8] Watts, J. K.; Choubdar, N.; Sadalapure, K.; Robert, F.; Wahba, A. S.; Pelletier, J.; Pinto, B. M.; Damha, M. J. Nucleic Acids Res 2007, 35, 1441.

[9] Allerson, C. R.; Sioufi, N.; Jarres, R.; Prakash, T. P.; Naik, N.; Berdeja, A.; Wanders, L.; Griffey, R. H.; Swayze, E. E.; Bhat, B. J Med Chem 2005, 48, 901.

[10] Harborth, J.; Elbashir, S. M.; Vandenburgh, K.; Manninga, H.; Scaringe, S. A.; Weber, K.; Tuschl, T. Antisense Nucleic Acid Drug Dev 2003, 13, 83.

[11] Hall, A. H. S.; Wan, J.; Spesock, A.; Sergueeva, Z.; Shaw, B. R.; Alexander, K. A. Nucleic Acids Res 2006, 34, 2773.

[12] Zhang, N.; Tan, C.; Cai, P.; Zhang, P.; Zhao, Y.; Jiang, Y. Bioorg Med Chem 2009, 17, 2441.

[13] Iwase, R.; Toyama, T.; Nishimori, K. Nucleosides Nucleotides Nucleic Acids 2007, 26, 1451.

[14] Potenza, N.; Moggio, L.; Milano, G.; Salvatore, V.; Di Blasio, B.; Russo, A.; Messere, A. Int J Mol Sci 2008, 9, 299.

[15] Dueholm, K. L.; Egholm, M.; Behrens, C.; Christensen, L.; Hansen, H. F.; Vulpius, T.; Petersen, K. H.; Berg, R. H.; Nielsen, P. E.; Buchardt, O. J Org Chem 1994, 59, 5767.

[16] Corradini, R.; Sforza, S.; Tedeschi, T.; Totsingan, F.; Marchelli, R. Curr Top Med Chem 2007, 7, 681.

[17] Porcheddu, A.; Giacomelli, G. Curr Med Chem 2005, 12, 2561.

[18] Isobe, H.; Fujino, T.; Yamazaki, N.; Guillot-Nieckowski, M.; Nakamura, E. Org Lett 2008, 10, 3729.

[19] Ei-Sagheer, A. H.; Brown, T. J Am Chem Soc 2009, 131, 3958.

[20] Fujino, T.; Yamazaki, N.; Isobe, H. Tetrahedron Lett 2009, 50, 4101.

[21] Schoning, K. U.; Scholz, P.; Guntha, S.; Wu, X.; Krishnamurthy, R.; Eschenmoser, A. Science 2000, 290, 1347.

[22] Zhang, L. L.; Peritz, A.; Meggers, E. J Am Chem Soc 2005, 127, 4174.

[23] Pallan, P. S.; von Matt, P.; Wilds, C. J.; Altmann, K. H.; Egli, M. Biochemistry 2006, 45, 8048.

[24] DeMesmaeker, A.; Jouanno, C.; Wolf, R. M.; Wendeborn, S. Bioorg Med Chem Lett 1997, 7, 447.

[25] Denapoli, L.; Iadonisi, A.; Montesarchio, D.; Varra, M.; Piccialli, G. Bioorg Med Chem Lett 1995, 5, 1647.

[26] Rostovtsev, V. V.; Green, L. G.; Fokin, V. V.; Sharpless, K. B. Angew Chem Int Ed 2002, 41, 2596.

[27] Kryatova, O. P.; Connors, W. H.; Bleczinski, C. F.; Mokhir, A. A.; Richert, C. Org Lett 2001, 3, 987.

[28] Wenninger, D.; Seliger, H. Nucleosides Nucleotides 1997, 16, 977.

[29] Bajor, Z.; Sagi, G.; Tegyey, Z.; Kraicsovits, F. Nucleosides Nucleotides Nucleic Acids 19632003, 22.

[30] Still, W. C.; Kahn, M.; Mitra, A. J Org Chem 1978, 43, 2923.

[31] Thansandote, P.; Gouliaras, C.; Turcotte-Savard, M. O.; Lautens, M. J Org Chem 2009, 74, 1791.

[32] Mayer, T.; Maier, M. E. Eur J Org Chem 2007, 4711.

5.0 Supplementary Information – Chapter II – Manuscript I

5.1 Tables

Table A5. The Oligonucleotides characterized by MALDI-TOF mass spectrometry.

Sequence	Calcd mass (g/mol)	Observed mass (g/mol)	Observed molecular ion
5′ TTTTTCTCTCTC**UU** 3′	4123	4122	$[M - H]^-$
5′ TTTTTCTCTCTC 3′	3529	3530	$[M + H]^-$
5′ **UU**TTTCTCTCTCTT 3′	4123	4164	$[M - H + K]^-$
5′ TTTCTCTCTCTT 3′	3529	3530	$[M + H]^-$

5.2 NMR Spectra

5.2.1 Proton NMR Spectrum of Compound 2

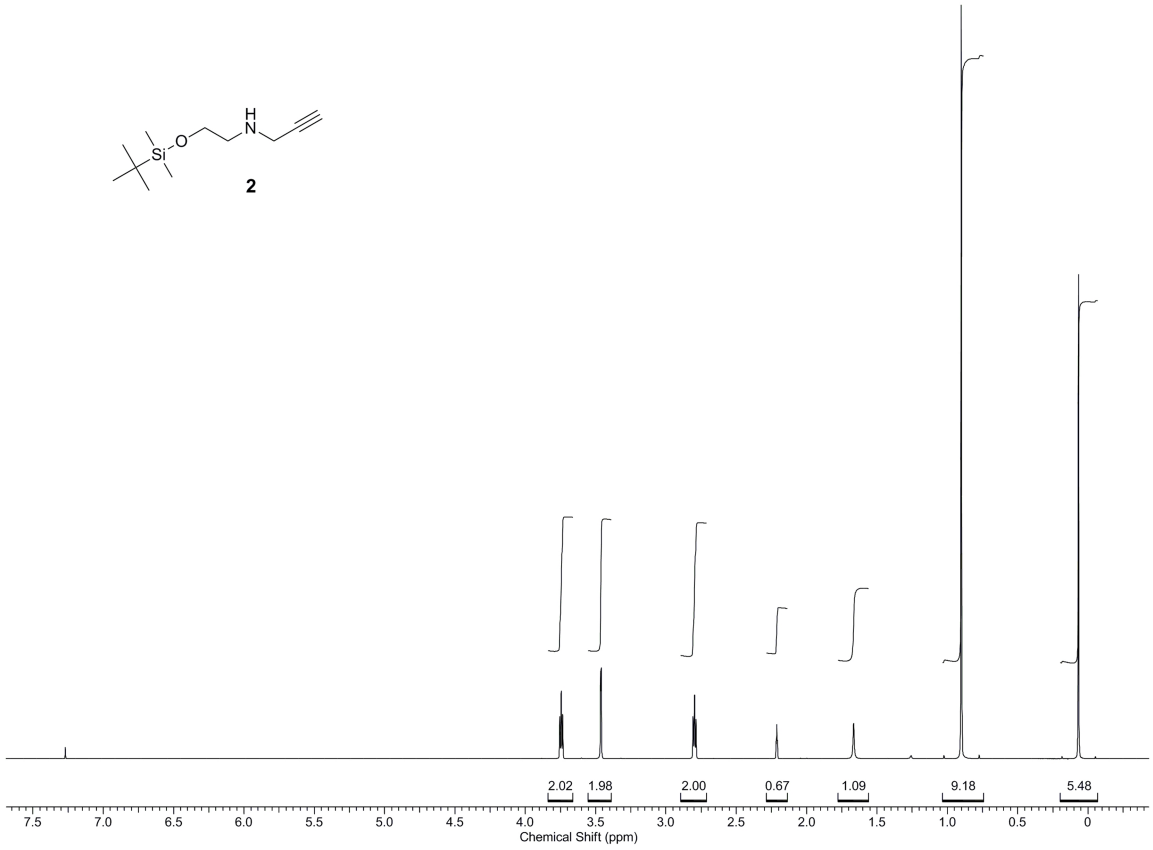

Figure A13. ^{1}H – NMR Spectrum of Compound **2** observed in $CDCl_3$ at 500 MHz.

5.2.2 Carbon NMR Spectrum of Compound 2

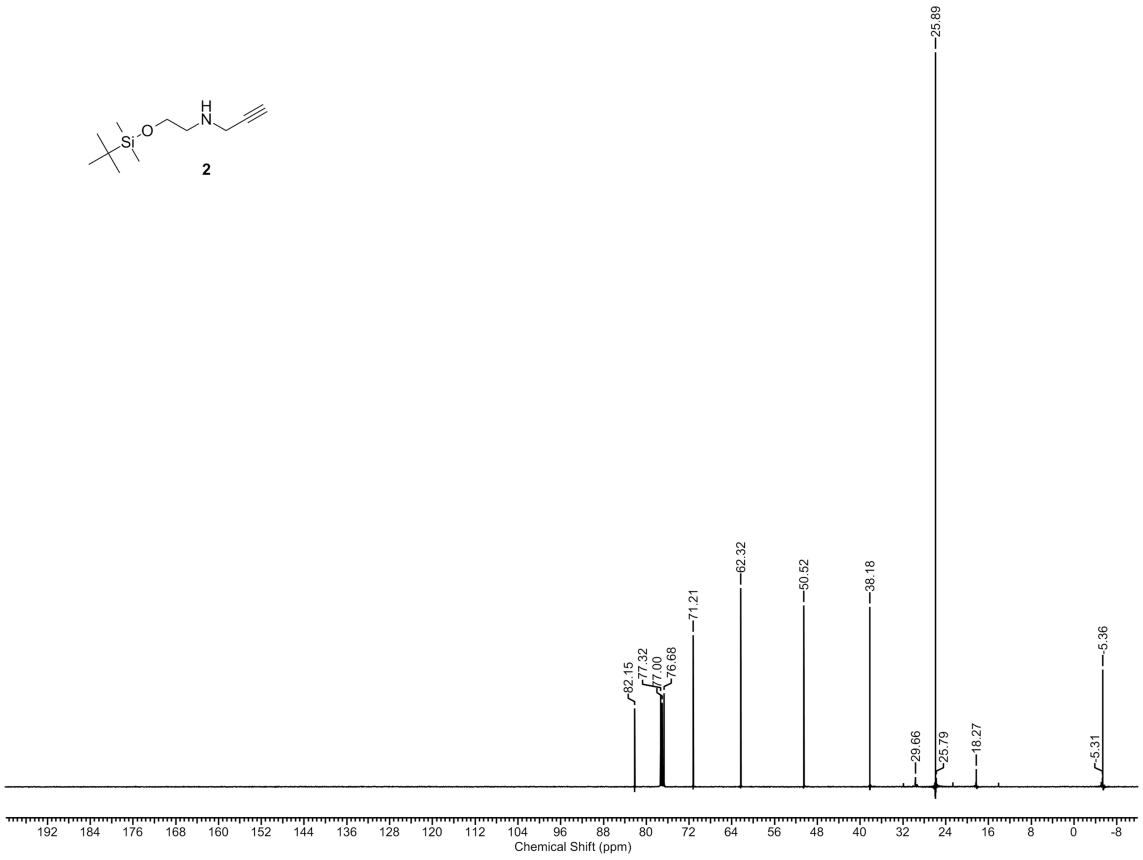

Figure A14. ^{13}C – NMR Spectrum of Compound **2** observed in $CDCl_3$ at 100 MHz.

5.2.3 Proton NMR Spectrum of Compound 3

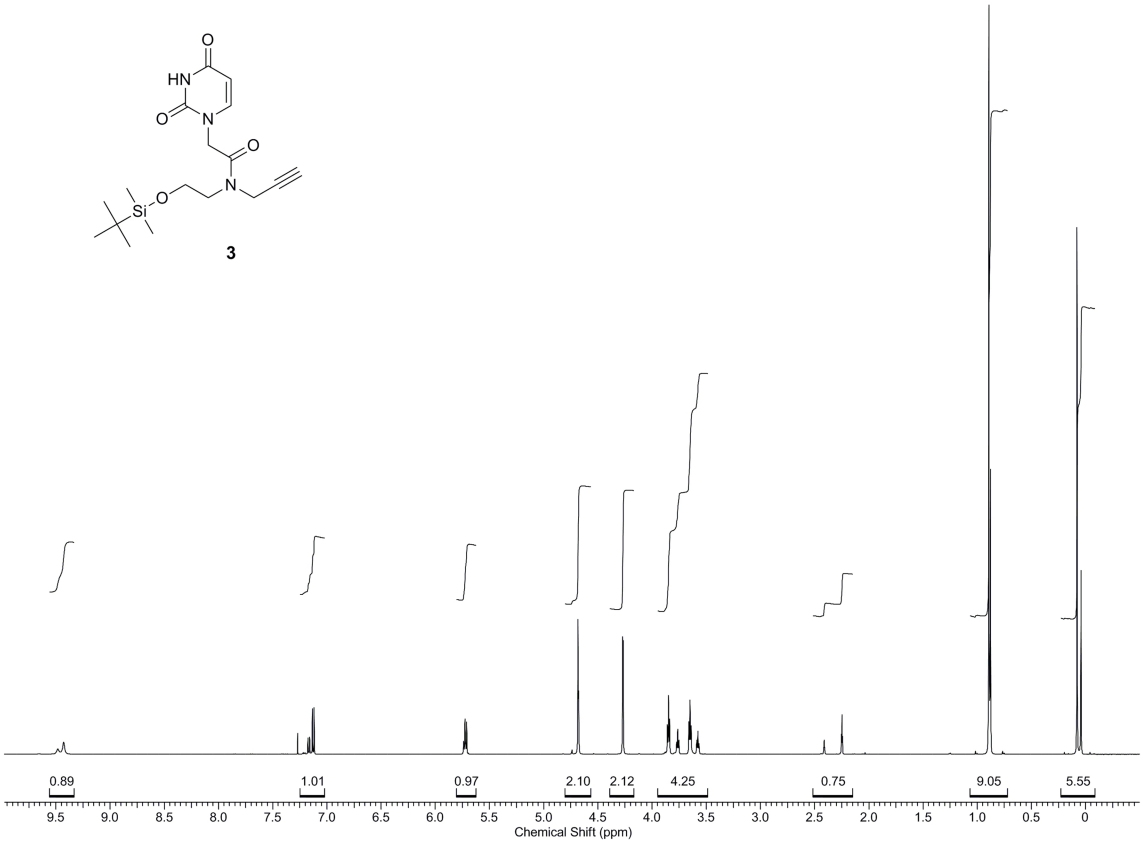

Figure A15. ^{1}H – NMR Spectrum of Compound **3** observed in $CDCl_3$ at 500 MHz.

5.2.4 Carbon NMR Spectrum of Compound 3

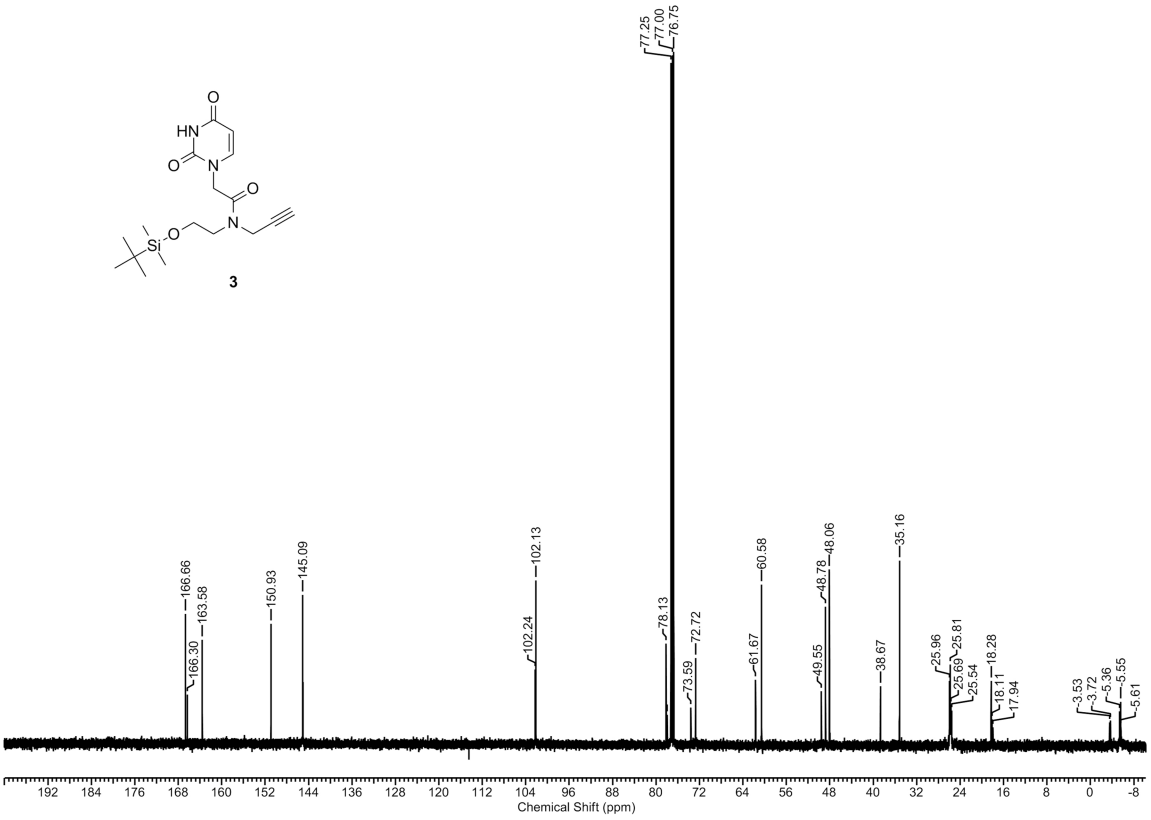

Figure A16. ^{13}C – NMR Spectrum of Compound **3** observed in $CDCl_3$ at 125 MHz.

5.2.5 Proton NMR Spectrum of Compound 5

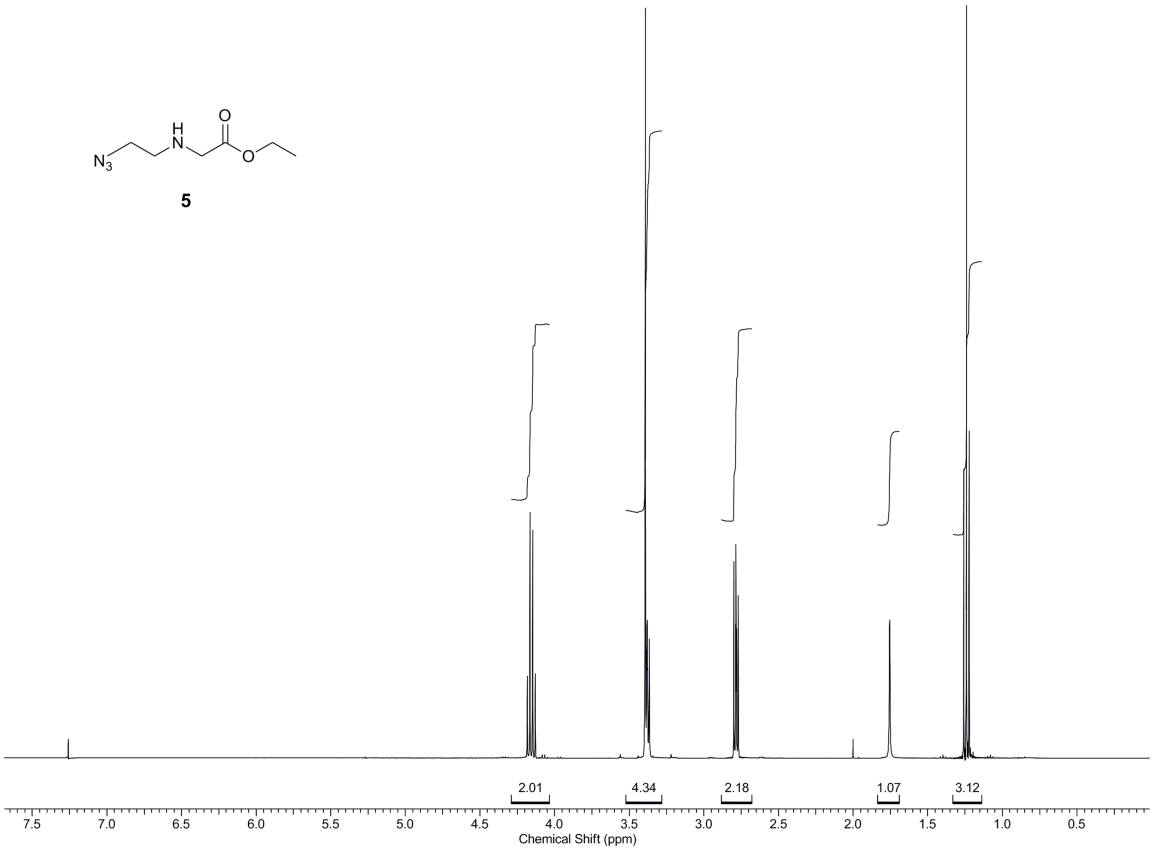

Figure A17. ^{1}H – NMR Spectrum of Compound **5** observed in $CDCl_3$ at 400 MHz.

5.2.6 Carbon NMR Spectrum of Compound 5

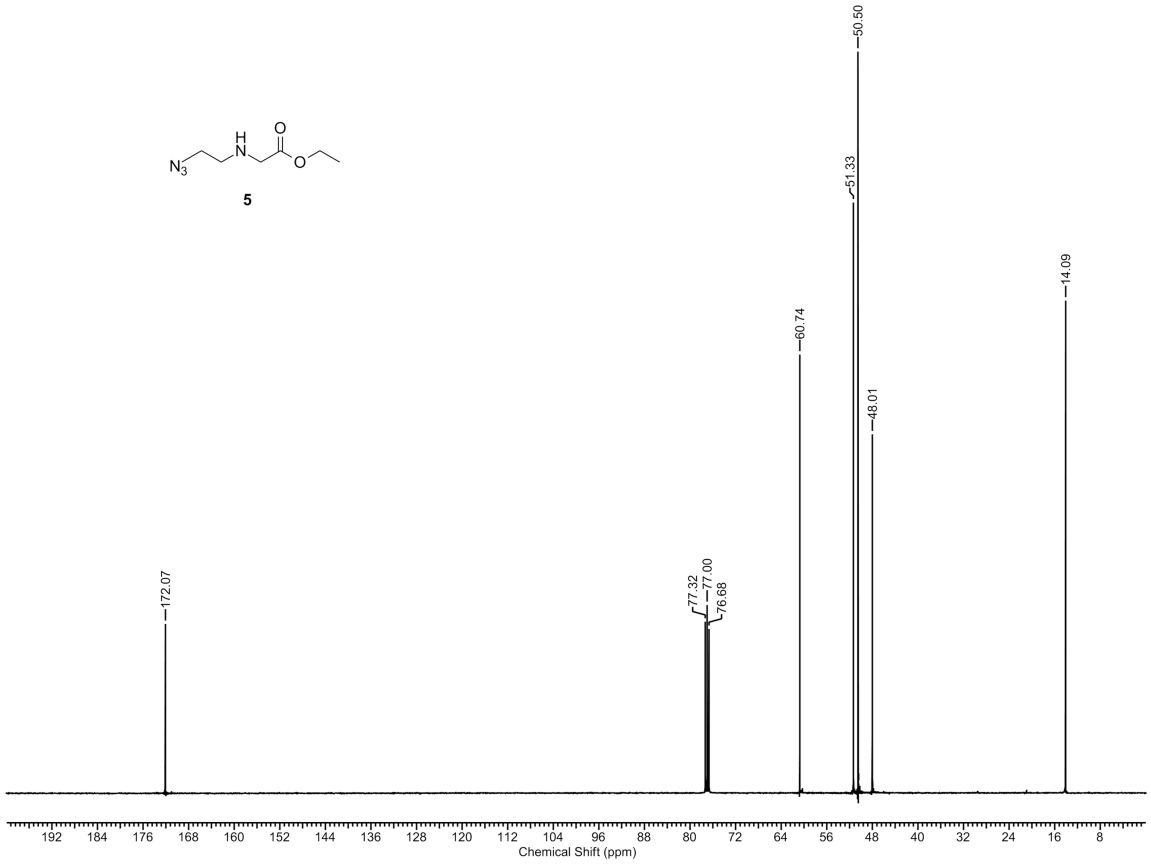

Figure A18. ^{13}C – NMR Spectrum of Compound **5** observed in $CDCl_3$ at 100 MHz.

5.2.7 Proton NMR Spectrum of Compound 6

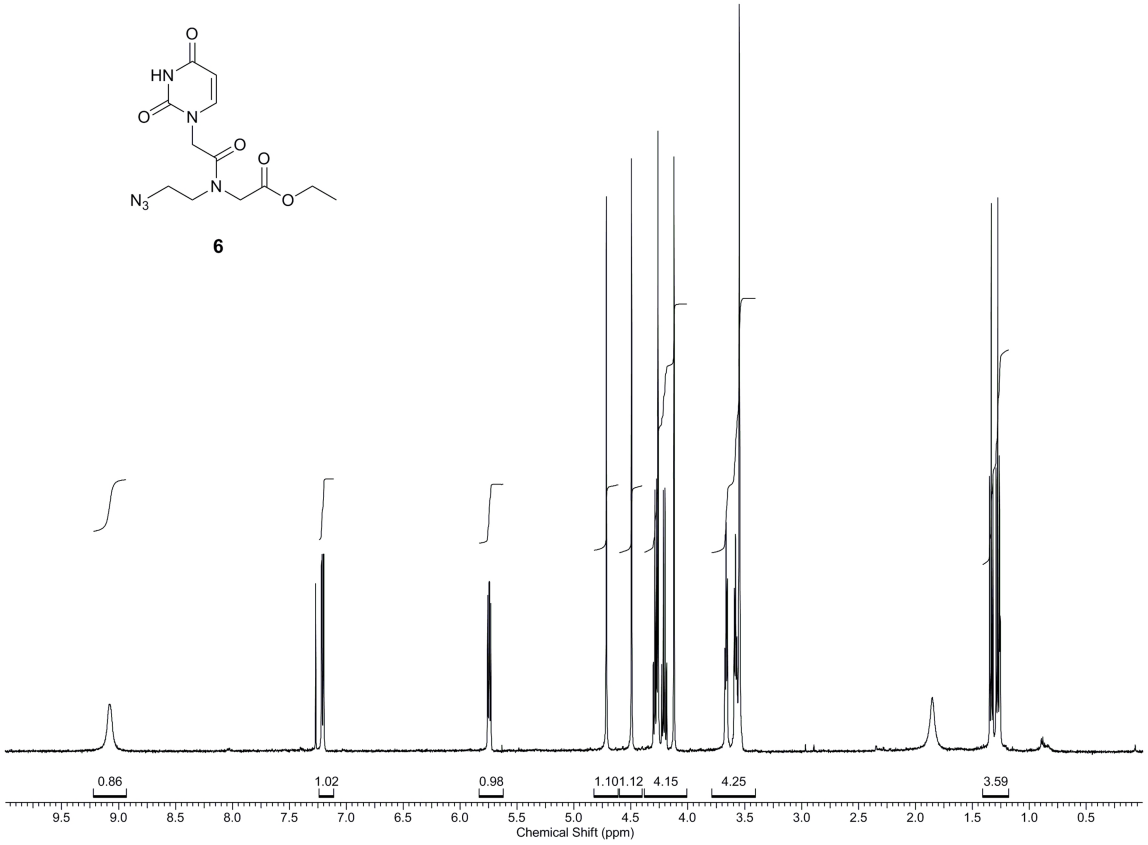

Figure A19. ^{1}H – NMR Spectrum of Compound **6** observed in $CDCl_3$ at 500 MHz.

5.2.8 Carbon NMR Spectrum of Compound 6

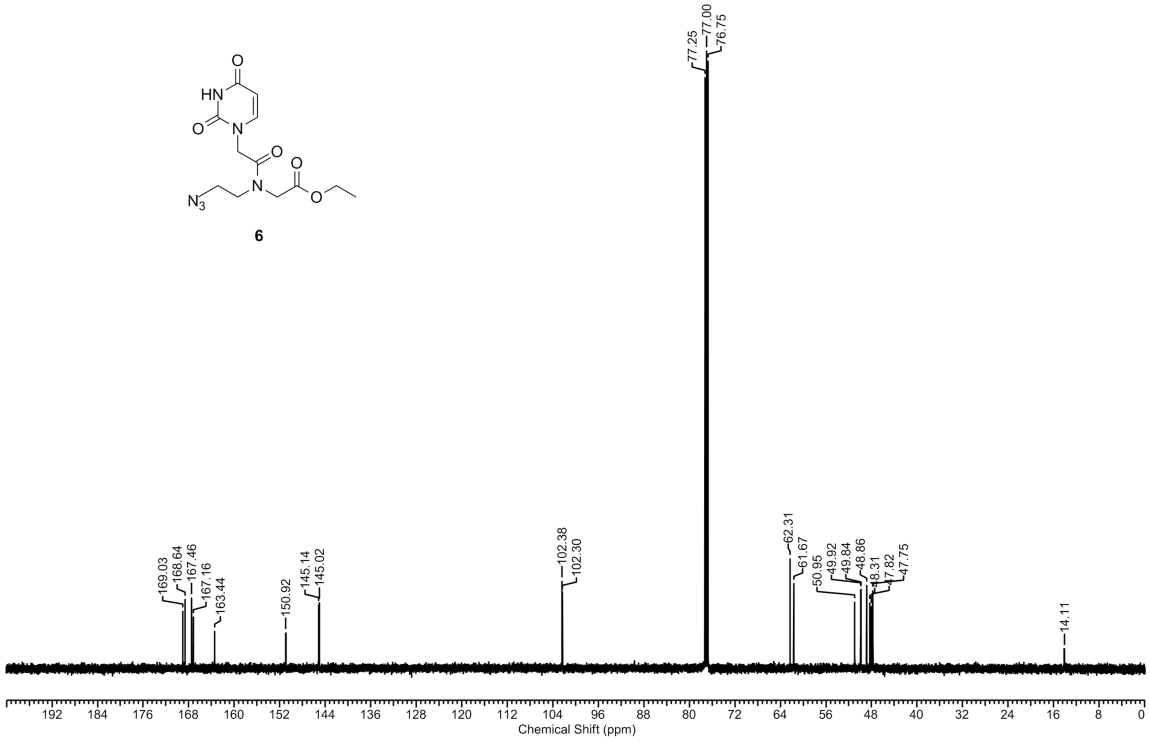

Figure A20. ^{13}C – NMR Spectrum of Compound **6** observed in $CDCl_3$ at 125 MHz.

5.2.9 Proton NMR Spectrum of Compound 7

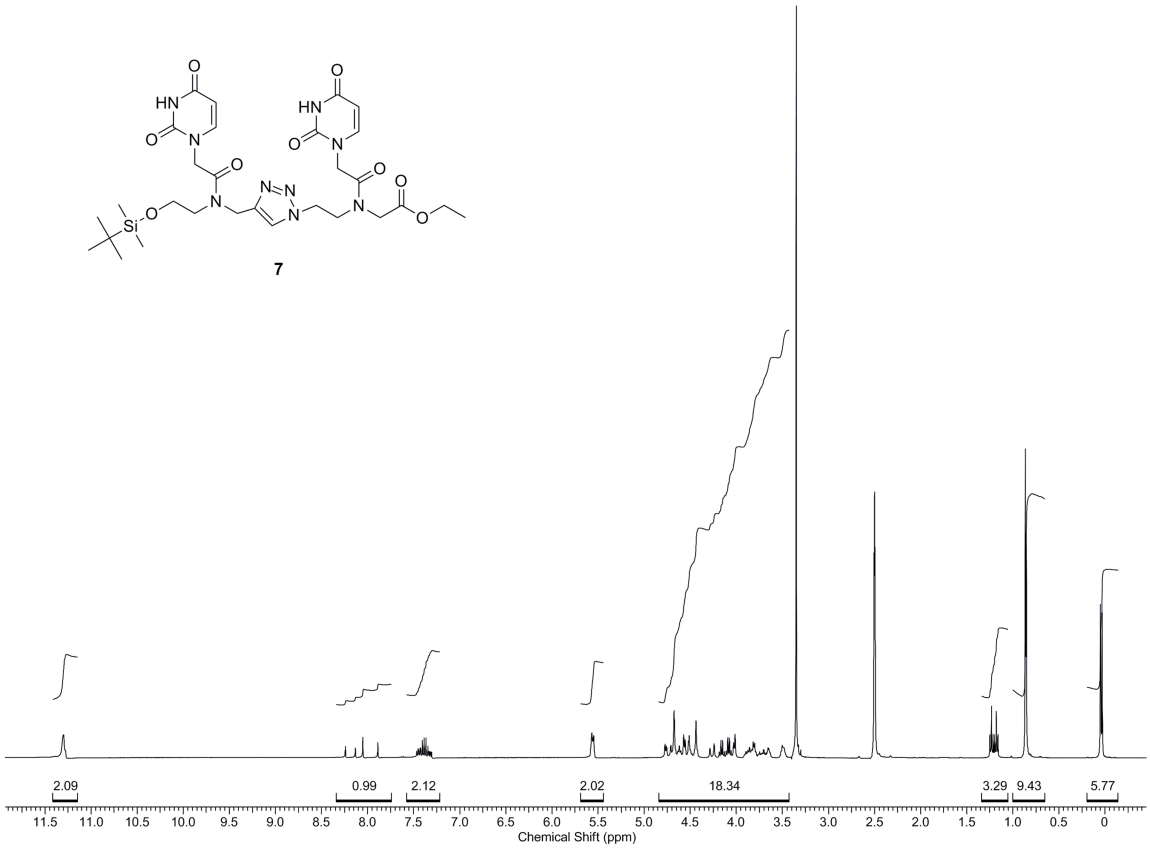

Figure A21. ^{1}H – NMR Spectrum of Compound **7** observed in DMSO-d_6 at 400 MHz.

5.2.10 Carbon NMR Spectrum of Compound 7

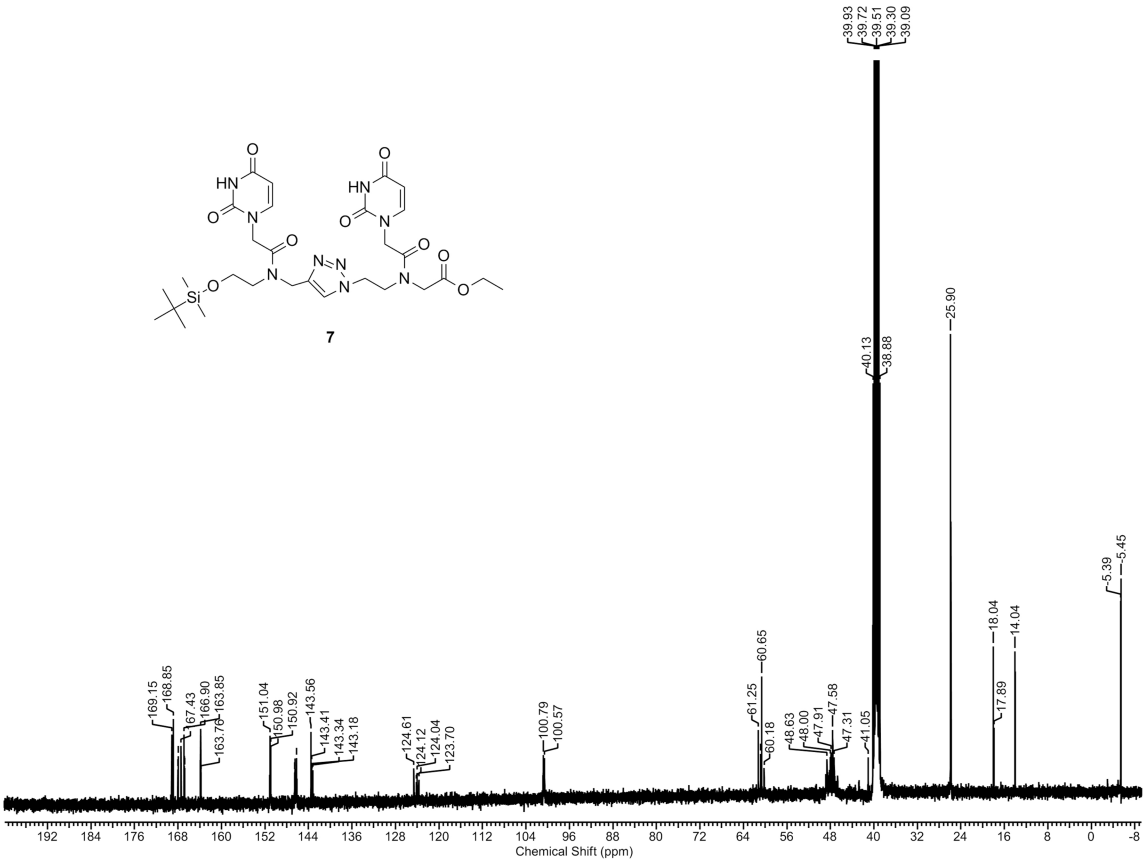

Figure A22. ^{13}C – NMR Spectrum of Compound **7** observed in DMSO-d_6 at 100 MHz.

5.2.11 Proton NMR Spectrum of Compound 8

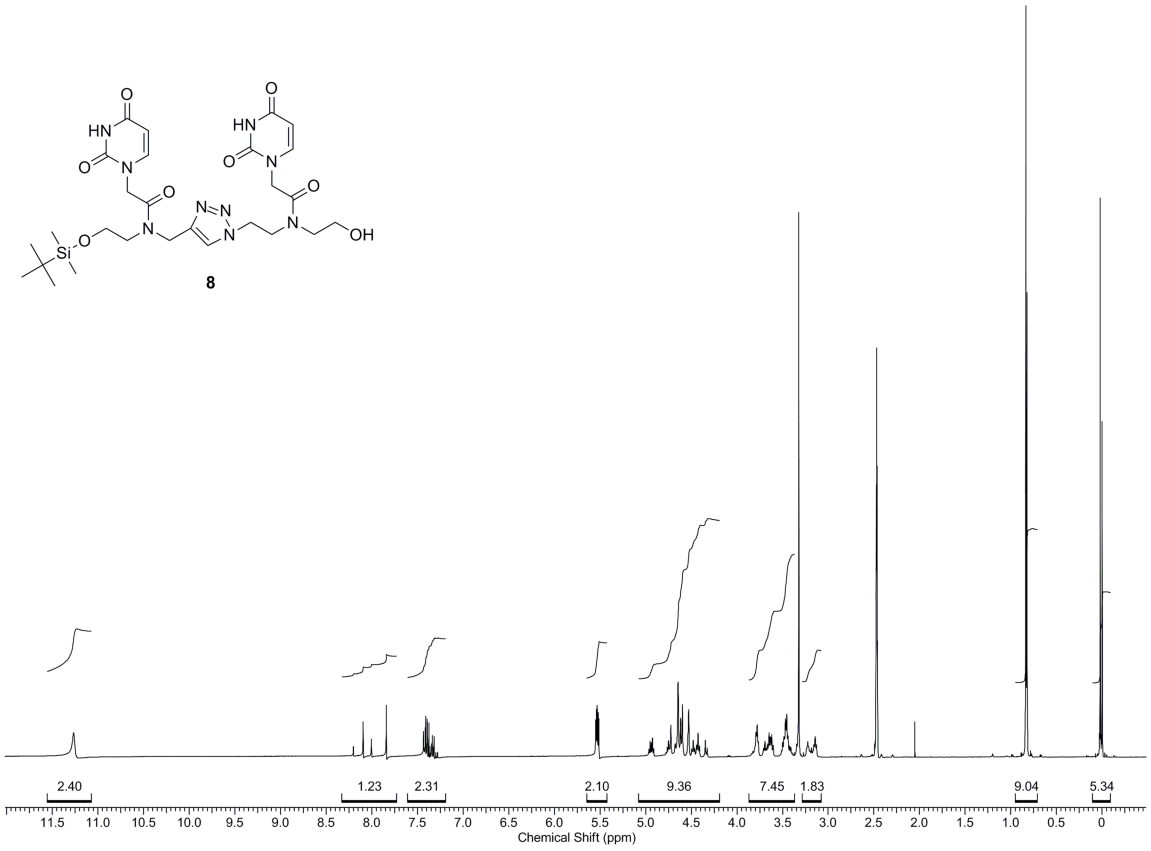

Figure A23. ^{1}H – NMR Spectrum of Compound **8** observed in DMSO-d_6 at 500 MHz.

5.2.12 Carbon NMR Spectrum of Compound 8

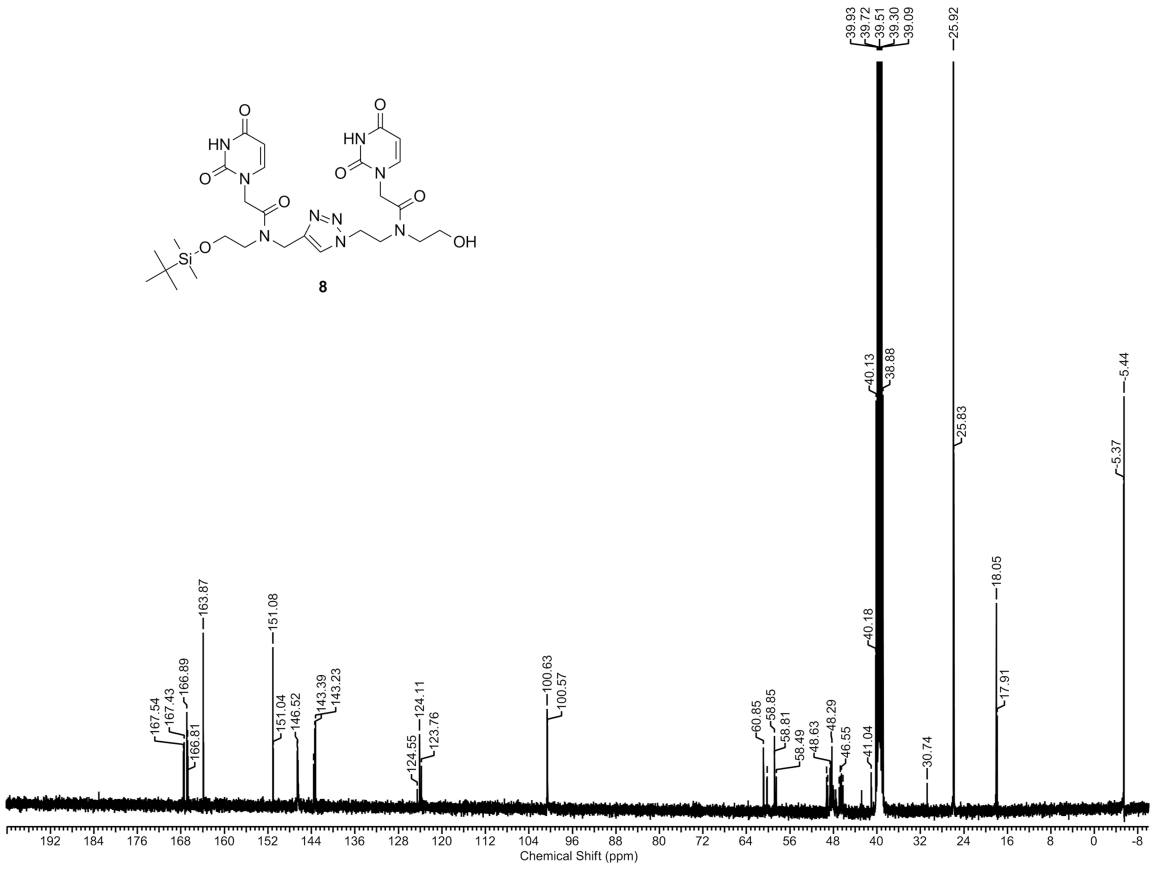

Figure A24. ^{13}C – NMR Spectrum of Compound **8** observed in DMSO-d_6 at 125 MHz.

5.2.13 Proton NMR Spectrum of Compound 9

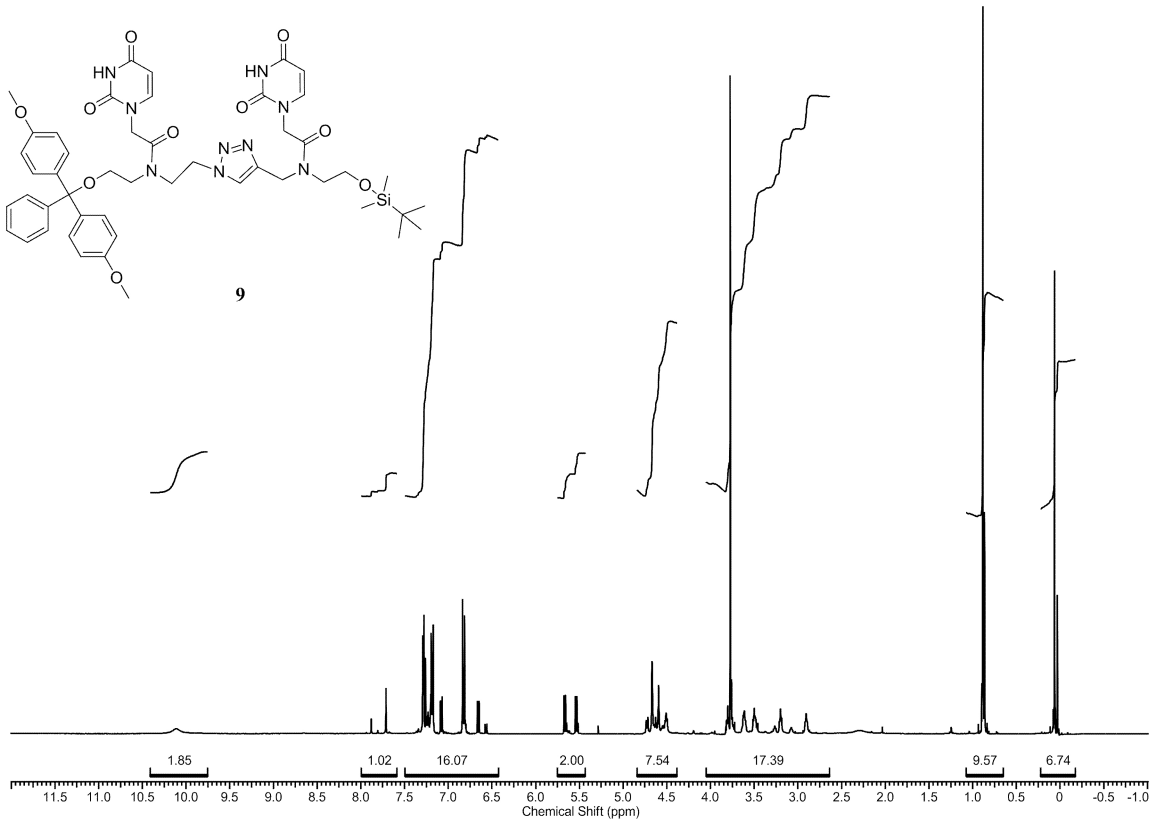

Figure A25. ^{1}H – NMR Spectrum of Compound **9** observed in $CDCl_3$ at 400 MHz.

5.2.14 Carbon NMR Spectrum of Compound 9

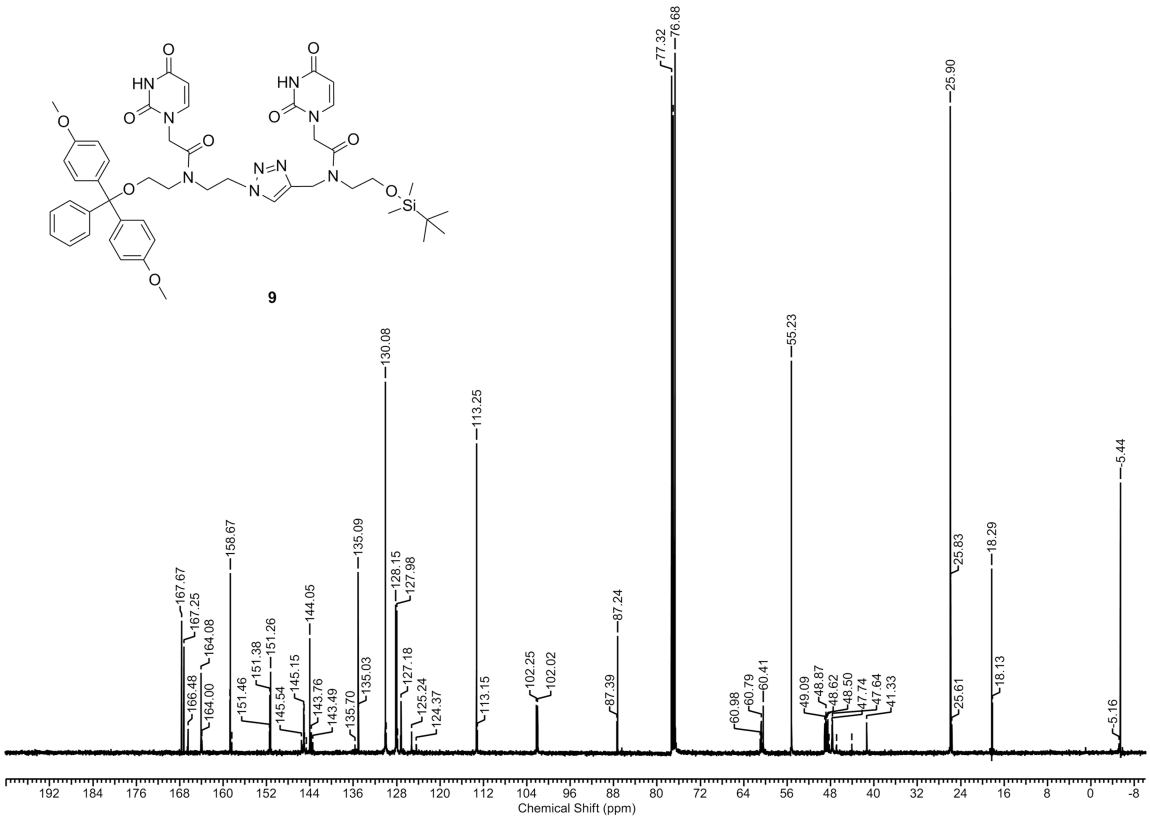

Figure A26. ^{13}C – NMR Spectrum of Compound **9** observed in $CDCl_3$ at 100 MHz.

5.2.15 Proton NMR Spectrum of Compound 10

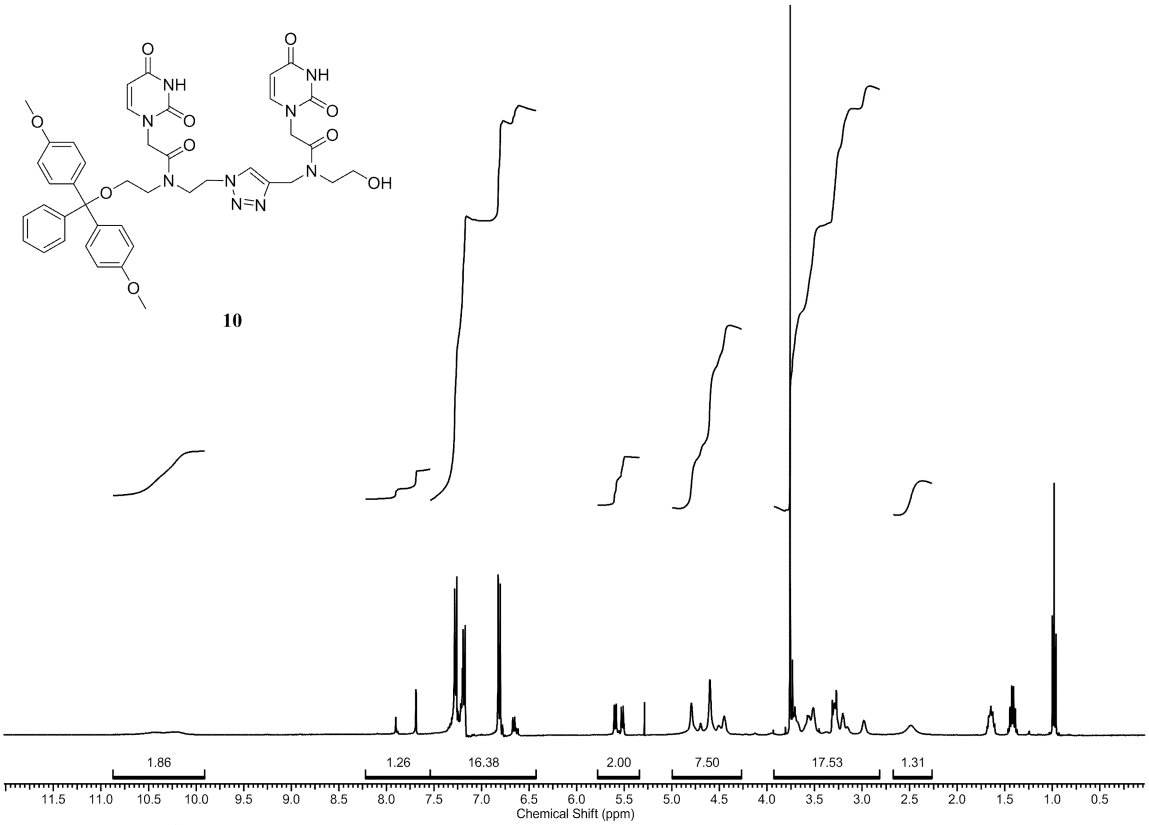

Figure A27. ^{1}H – NMR Spectrum of Compound **10** observed in $CDCl_3$ at 400 MHz.

5.2.16 Carbon NMR Spectrum of Compound 10

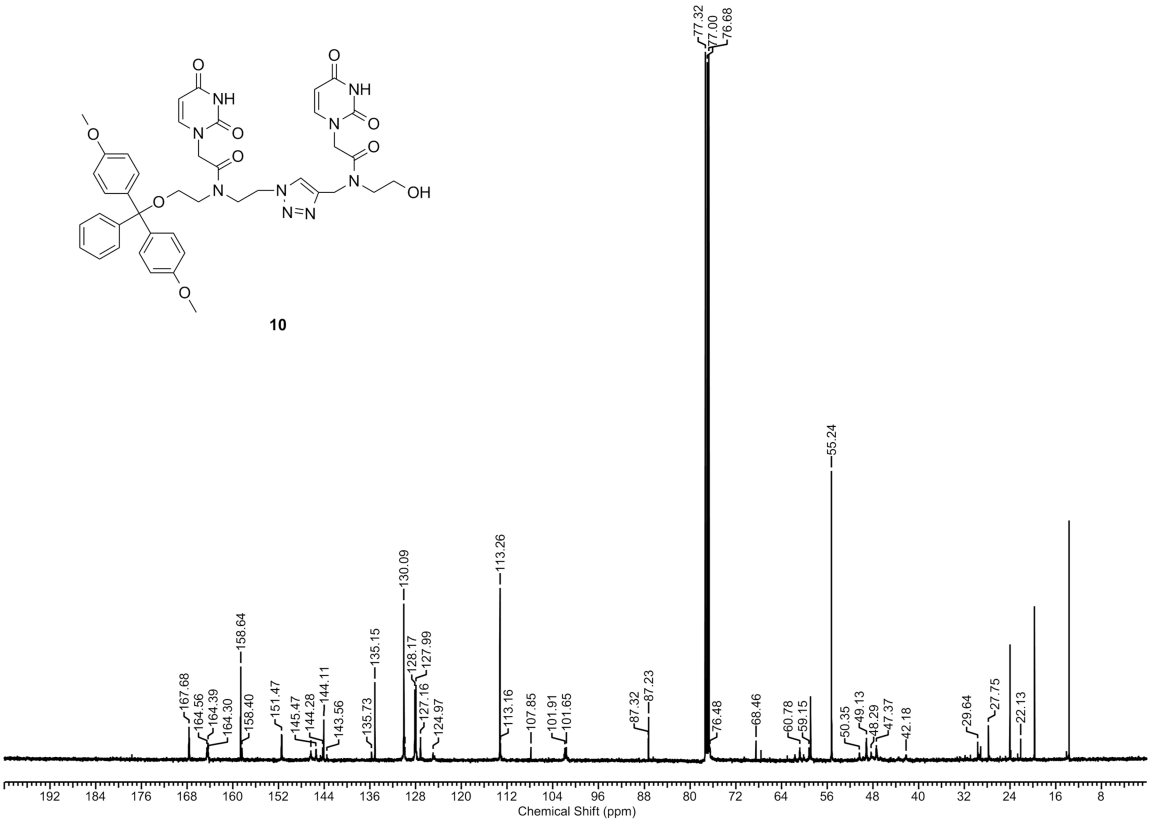

Figure A28. ^{13}C – NMR Spectrum of Compound **10** observed in $CDCl_3$ at 100 MHz.

5.2.17 Proton NMR Spectrum of Compound 11

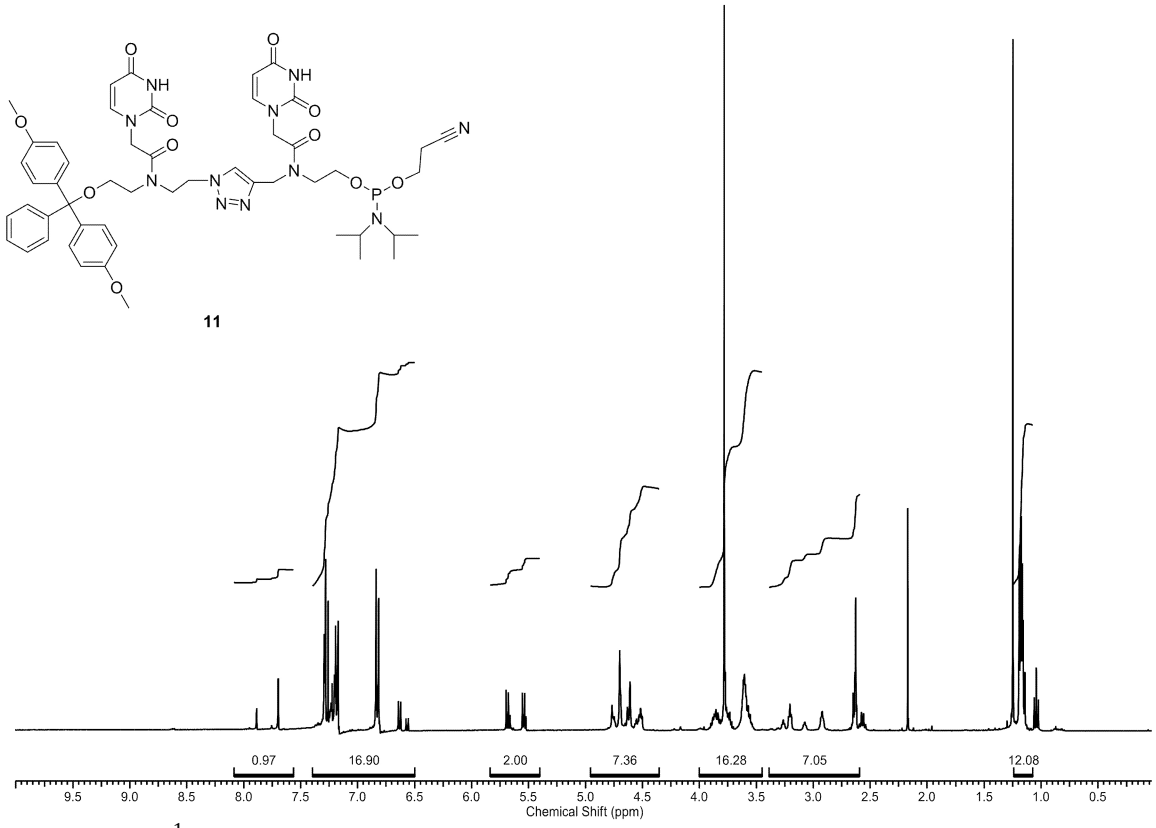

Figure A29. ^{1}H – NMR Spectrum of Compound **11** observed in $CDCl_3$ at 400 MHz.

5.2.18 Carbon NMR Spectrum of Compound 11

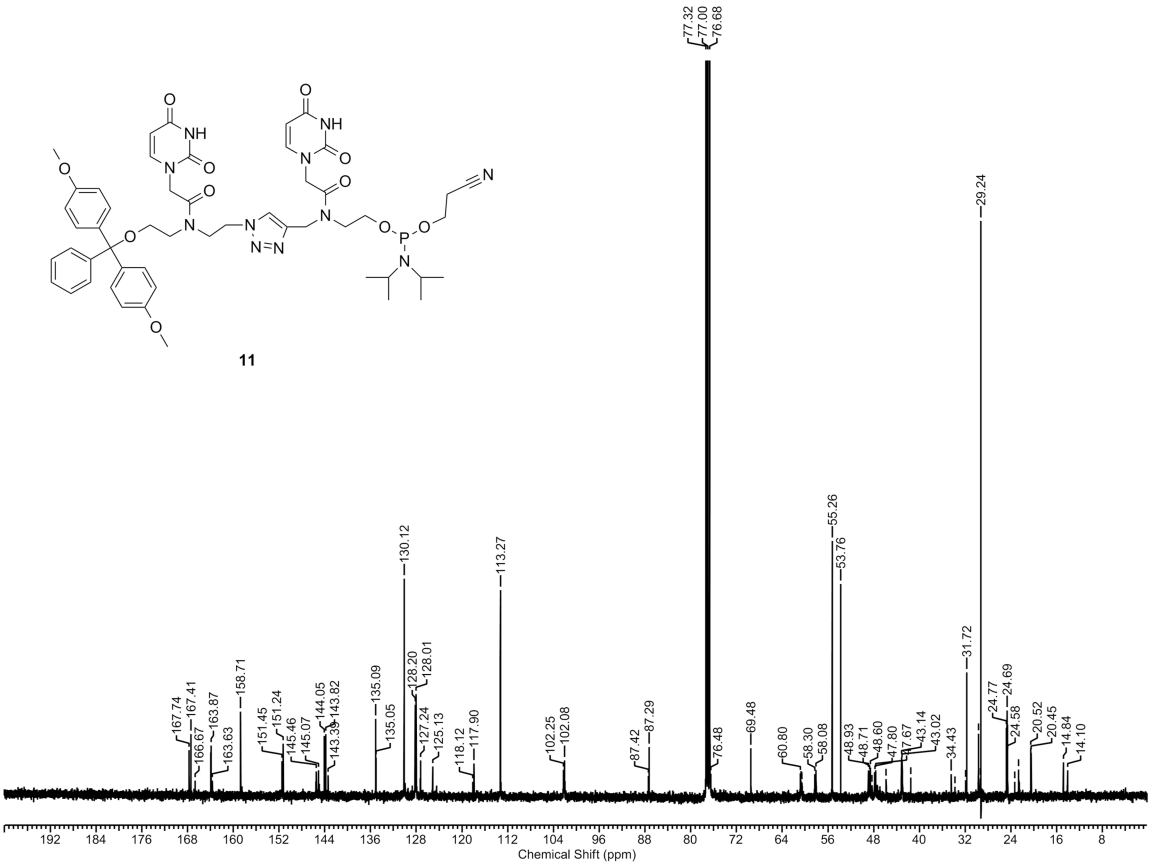

Figure A30. ^{13}C – NMR Spectrum of Compound **11** observed in $CDCl_3$ at 100 MHz.

Appendix II – Manuscript II

Bioorganic & Medicinal Chemistry Letters 22 (2012) 1722–1726

Contents lists available at SciVerse ScienceDirect

Bioorganic & Medicinal Chemistry Letters

journal homepage: www.elsevier.com/locate/bmcl

Efficient synthesis and cell-based silencing activity of siRNAS that contain triazole backbone linkages

Tim C. Efthymiou, Vanthi Huynh, Jaymie Oentoro, Brandon Peel, Jean-Paul Desaulniers *

Faculty of Science, University of Ontario Institute of Technology, 2000 Simcoe Street North, Oshawa, Ontario, Canada L1H 7K4

ARTICLE INFO

Article history:
Received 2 November 2011
Revised 16 December 2011
Accepted 20 December 2011
Available online 30 December 2011

Keywords:
Short interfering RNA
Modified nucleoside
Triazole linkage
Huisgen dipolar cycloaddition
Gene silencing

ABSTRACT

An efficient synthesis of siRNAs modified at the backbone with a triazole functionality is reported. Through the use of 4,4′-dimethoxytrityl (DMT) phosphoramidite chemistry, triazole backbone dimers were site-specifically incorporated throughout various siRNAs targeting both firefly luciferase and glyceraldehyde-3-phosphate dehydrogenase (GAPDH) gene transcripts as representatives of an exogenous and endogenous gene, respectively. Following the successful silencing of the *firefly* luciferase reporter gene, triazole-modified siRNAs were also found to be capable of silencing GAPDH in a dose-dependent manner. Backbone modifications approaching the 3′-end on the sense strand were tolerated without compromising siRNA potency. This study highlights the compatibility of triazole-modified siRNAs within the RNAi pathway, and the modification's potential to impart favorable properties to siRNAs designed to target other endogenous genes.

In 1998, Fire and Mello reported that short interfering RNAs (siRNAs) could be introduced into cells in *Caenorhabditis elegans* and block gene expression.[1] This process involves the incorporation of siRNAs into an RNA-induced silencing complex (RISC), which serves to select and deliver the guide strand to its target messenger RNA (mRNA) for selective gene silencing.[2] Since this discovery, there has been considerable interest in utilizing siRNAs as potential therapeutic agents in combating disease.[3] However, natural siRNAs are prone to degradation by nucleases and exhibit poor cell membrane permeability due to their polyanionic charge. There is wide interest in chemically modifying siRNAs in order to alleviate the aforementioned problems.

A vast number of studies have thoroughly explored the properties of chemically modified oligonucleotides that contain the unnatural architecture at the sugars[4] and bases.[5] However, relatively very little has been done with respect to modifying the internucleotide linkage of siRNAs with nonionic moieties. With respect to negatively charged backbone mimics, phosphorothioates (PS) have been shown to be accommodated within the RNAi pathway; however, ranges in potency are often observed and cytotoxicity is a concern.[6] Alternatively, functional data of siRNAs bearing boranophosphate linkages show RNAi compatibility and offer enhanced potency comparable to PS with reduced cytotoxicity.[7]

With respect to nonionic backbone modifications, two studies have shown that these can be accommodated within the 3′-overhangs of siRNAs. Iwase and co-workers have shown that an amide linkage enhances thermodynamic stability and resistance to nucleases.[8] Potenza and co-workers have also illustrated that an amide-bond at the 3′-end of siRNAs acts as a substrate for the RNAi pathway.[9]

The crystal structure of the RISC complex by Patel et al., complexed with a duplex oligonucleotide reveals that a number of key phosphodiester contacts are necessary for its interaction with the protein complex; however, many of these ionic contacts are not present on the sense strand of the oligonucleotide.[10] Therefore, we envisioned that by modifying the sense strand, we could synthesize novel siRNAs with uncharged backbones within the duplex that could thus serve as appropriate substrates for the RNAi pathway without compromising their potency.

Utilizing the well-known Cu(I)-assisted Huisgen 1,3-dipolar cycloaddition,[11] the triazole moiety can be introduced as an uncharged oligonucleotide backbone modification with relative ease. Although a variety of triazole-modified oligonucleotide mimics have been reported, most constructs are DNA-based.[12] Reports of click-ligated RNAs include one from El-Sagheer and Brown,[13] who were successful in synthesizing functional hairpin ribozymes containing both cross- and intra-strand triazole linkages. Other reports of triazoles within RNAs include work from Das and co-workers,[14a] and most recently from Rozners and co-workers[14b] who demonstrated site-specific incorporation of a triazole-linked nucleoside dimer within RNAs.

In previous work, we have synthesized a triazole-linked nucleoside dimer phosphoramidite based on a PNA-like structure, and this modification displayed compatibility when hybridized to its complement.[15] Despite the numerous examples of distinct nucleoside

* Corresponding author. Tel.: +1 905 721 8668x3621; fax: +1 905 721 3304.
E-mail address: jean-paul.desaulniers@uoit.ca (J.-P. Desaulniers).

0960-894X/$ - see front matter © 2011 Elsevier Ltd. All rights reserved.
doi:10.1016/j.bmcl.2011.12.104

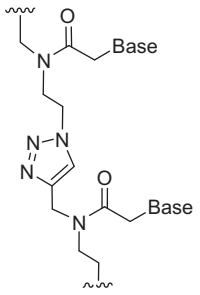

Figure 1. Triazole-linked nucleic acid.

backbone derivatives linked together through a triazole moiety, none of the derivatives have been reported as substrates within the RNAi pathway. Herein, we report the incorporation of triazole-linked nucleic acids based on a PNA-type scaffold (Fig. 1) within duplex siRNAs. The RNAs display effective gene silencing and thus exhibit a high degree of compatibility as RNAi substrates.

In this paper, we expanded the scope of siRNA sequences and modified them with a cytosine-triazole-uracil (C_tU) dimer in addition to the uracil-triazole-uracil (U_tU) dimer previously synthesized. Synthesis of the C_tU dimer phosphoramidite commenced through the generation of 2-azidoethanamine from bromoethylamine combined with sodium azide. This compound was alkylated with 2-bromoethoxy-*tert*-butyldimethylsilane[16] in 39% yield to afford azide linker **1**. Utilizing EDC as a coupling reagent, this compound was amide-bond coupled to N^4-benzoylcytosin-1-yl acetic acid[17] to generate monomer **2** in 62% yield. TBS-deprotection of **2** with 3HF-TEA afforded a monoalcohol, which was then protected with a 4,4′-dimethoxytrityl group (DMT) to produce compound **3** in 90% yield (Scheme 1).

In order to generate an appropriate alkyne monomer, alkyne linker **4** was synthesized in 71% yield by treating TBS-protected ethanolamine with limiting equivalents of propargyl bromide. This linker was amide-bond coupled to uracil-1-yl acetic acid[18] using EDC as the coupling reagent to produce monomer **5** in 52% yield (Scheme 2).

With both azide (**3**) and alkyne (**5**) monomers available, 1,4-triazole formation catalyzed with $CuSO_4$ and sodium ascorbate in a THF/H_2O solution afforded compound **6** in 98% yield. TBAF deprotection of the silyl protective group on compound **6** afforded compound **7** in 99% yield. Finally, compound **7** was treated with a phosphitylating reagent to afford the phosphoramidite **8** in 73% yield (Scheme 3). Both the C_tU and U_tU phosphoramidites were used to synthesize a variety of triazole-modified siRNAs.

Various siRNAs were synthesized, bearing one to three triazole backbone modifications through the use of an ABI DNA/RNA synthesizer. These siRNAs were designed to target *firefly* luciferase mRNA expressed within HeLa cells, in order to gauge their functionality within cells-based systems (Table 1).

To first examine the effects of our RNAs, we investigated the effect of circularly polarized light on our siRNA duplexes to determine whether our chemically modified duplexes were still able to retain A-type helical structure. Figure S1 (Supplementary data) illustrates that the siRNAs retain the characteristic A-form helix; however, a loss of helicity for double-stranded RNAs that contain the internal triazole backbone modification is observed.

In addition to the listing of luciferase-targeting siRNAs, Table 1 highlights melting temperature (T_m) data indicating that the modification can have either a destabilizing or stabilizing contribution on the dsRNA depending on its location.

In general, as the modification approaches the 5′-end of the sense strand, its contribution is less destabilizing. For example, RNAs **9**, **10** and **12** show very little destabilization relative to

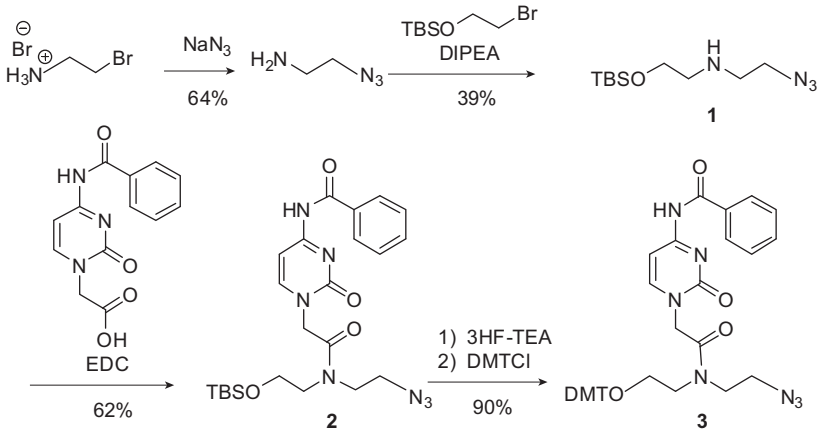

Scheme 1. Synthesis of azide intermediate.

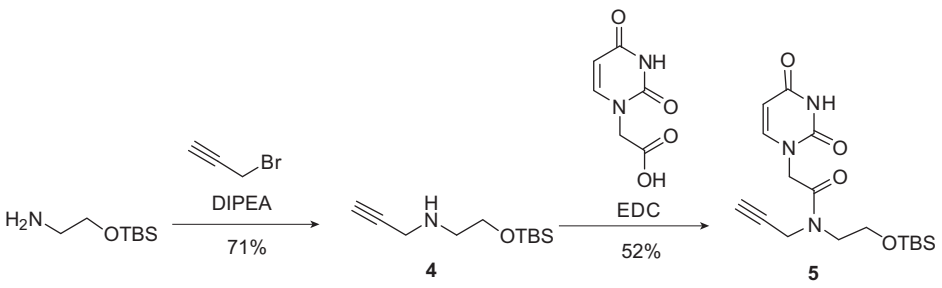

Scheme 2. Synthesis of alkyne intermediate.

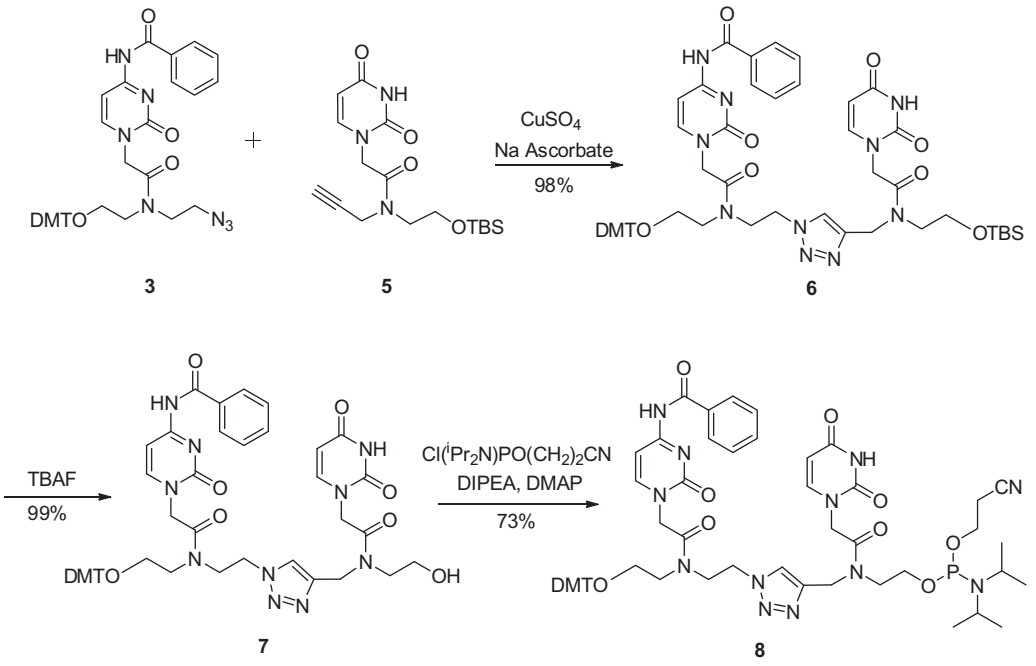

Scheme 3. Synthesis of C_tU phosphoramidite.

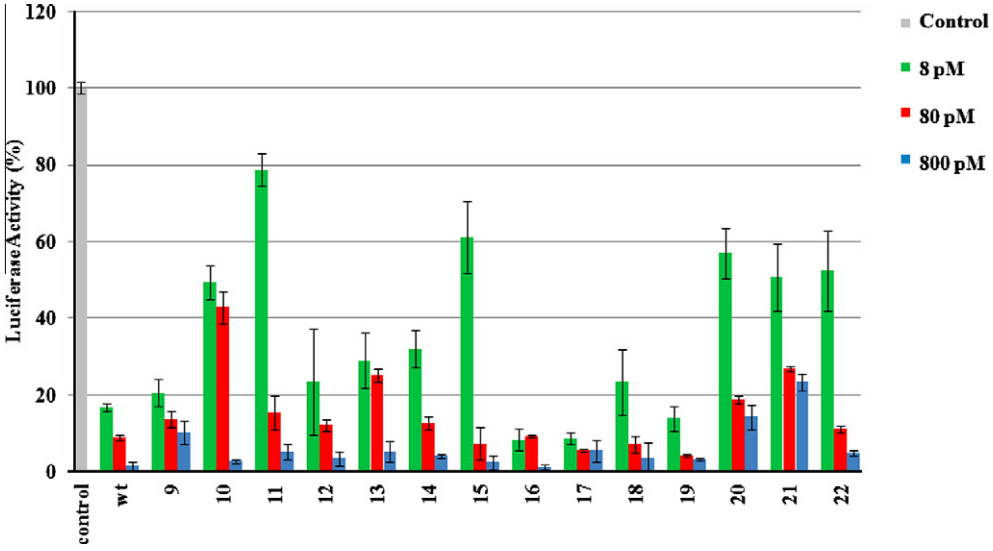

Figure 2. Reduction in *firefly* luciferase expression related to the potency of backbone-modified triazole-linked siRNAs using the Dual-luciferase reporter assay. The siRNAs were tested at 8, 80, and 800 pM, with *firefly* luciferase expression normalized to *Renilla* luciferase.

wild-type. However, the closer the modifications lie towards the center of the duplex, the greater the destabilizing contribution of that modification to the duplex. For instance, siRNAs **13**–**16** exhibit changes in T_m of ca. −7.5 to −13 °C. The effect of a U_tU modification on a 3′-overhang increases the T_m of siRNAs **15**, **17**, **18**, **20** and **22**, relative to the corresponding siRNA with dTdT overhangs, thus suggesting an element of stability. This stabilizing effect has been observed with other oligonucleotides that bear 3′-overhangs.[8,19] However, this trend is only observed when the modification is not in combination with any other triazole modifications within the same oligonucleotide strand (siRNAs **19** and **21** do not exhibit any increase in T_m). Finally, siRNA **21** contains three U_tU modifications within the sense strand. This siRNA bears a drop in T_m of −14.1 °C. SiRNA **11** contains two C_tU modifications, and exhibits a T_m drop of −20.3 °C relative to wild-type. Overall, our T_m data is consistent with other similar studies involving PNA–DNA chimeras[20] and triazole-linked RNAs.[14b]

To examine the effects of our backbone-modified siRNAs on the RNA interference pathway, we performed cell-based assays within HeLa cells. The cells were co-transfected with the siRNA duplexes identified in Table 1 at varying concentrations, along with plasmids expressing the target *firefly* luciferase and a non-target *Renilla* luciferase for use as an internal control. Following transfection with the desired siRNA construct, cells were lysed after 24 h, at which point luciferase activity was monitored (Fig. 2). The wild-type native siRNA inhibited luciferase expression in a dose-dependent manner, while the modified siRNAs triggered varying levels of silencing activity.

Table 1
Sequences of anti-luciferase siRNAs and T_m Data

RNA	siRNA duplex	T_m[a] (°C)	ΔT_m (°C)
wt	5'- CUUACGCUGAGUACUUCGAtt -3' 3'- ttGAAUGCGACUCAUGAAGCU -5'	71.4	--
9	5'- C$_t$UUACGCUGAGUACUUCGAtt -3' 3'- ttGAAUGCGACUCAUGAAGCU -5'	71.1	-0.3
10	5'- C$_t$UUACGCUGAGUACUUCGAtt -3' 3'- U$_t$UGAAUGCGACUCAUGAAGCU -5'	69.3	-2.1
11	5'- C$_t$UUACGCUGAGUAC$_t$UUCGAtt -3' 3'- ttGAAUGCGACUCAUGAAGCU -5'	51.1	-20.3
12	5'- CU$_t$UACGCUGAGUACUUCGAtt -3' 3'- ttGAAUGCGACUCAUGAAGCU -5'	67.9	-3.5
13	5'- CUUACGC$_t$UGAGUACUUCGAtt - 3' 3' - ttGAAUGCGACUCAUGAAGCU - 5'	58.4	-13.0
14	5'- CUUACGCUGAGUAC$_t$UUCGAtt - 3' 3' - ttGAAUGCGACUCAUGAAGCU - 5'	59.6	-11.4
15	5'- CUUACGCUGAGUAC$_t$UUCGAtt - 3' 3' - U$_t$UGAAUGCGACUCAUGAAGCU - 5'	63.9	-7.5
16	5'- CUUACGCUGAGUACU$_t$UCGAtt - 3' 3' - ttGAAUGCGACUCAUGAAGCU - 5'	62.9	-8.5
17	5'- CUUACGCUGAGUACUUCGAU$_t$U- 3' 3'- ttGAAUGCGACUCAUGAAGCU - 5'	72.1	+0.7
18	5'- CUUACGCUGAGUACUUCGAU$_t$U- 3' 3'-U$_t$UGAAUGCGACUCAUGAAGCU - 5'	72.5	+1.1
19	5'- CUUACGCUGAGUACU$_t$UCGAU$_t$U- 3' 3' - ttGAAUGCGACUCAUGAAGCU - 5'	61.7	-9.7
20	5'- CUUACGCUGAGUACU$_t$UCGAU$_t$U- 3' 3'- U$_t$UGAAUGCGACUCAUGAAGCU - 5'	62.2	-9.2
21	5'- CU$_t$UACGCUGAGUACU$_t$UCGAU$_t$U- 3' 3' - ttGAAUGCGACUCAUGAAGCU - 5'	57.3	-14.1
22	5'- CUUACGCUGAGUACUUCGAtt - 3' 3'-U$_t$UGAAUGCGACUCAUGAAGCU - 5'	73.1	+1.7

[a] T_ms were measured in triplicate in a sodium phosphate buffer (90 mM NaCl,10 mM Na_2HPO_4, 1 mM EDTA, pH 7) at 260 nm, from 10 to 95 °C. U$_t$U corresponds to the uracil-triazole-uracil modification; C$_t$U corresponds to the cytosine-triazole-uracil modification.

For siRNAs **9–12**, a reduction in potency relative to wild-type is generally observed, especially when using lower concentrations of siRNA (Fig. 2). These RNAs are chemically modified in the area of the 5′-sense region and in general, display a decrease in T_m relative to wild-type siRNA (Table 1). In accordance with other reports which have identified that siRNAs exhibit thermodynamic asymmetry,[21] our observations support that destabilizing this area may lead to decreased potency. SiRNAs **13** and **14** contain a single C$_t$U modification within an internal site of the sense strand, causing a large decrease in duplex thermal stability compared to wild-type (Table 1). There is also a noticeable decrease in potency observed with these two siRNAs relative to wild-type (Fig. 2).

RNAs **10**, **15**, **18**, **20** and **22** contain U$_t$U modifications at the 3′-overhang of the antisense strand. When the activity of these siRNAs is compared to their analogous RNAs lacking a 3′-U$_t$U modification in general, a reduction in activity is observed at lower concentrations. The effect of observing reduced activity of a large bulky 3′-modified overhang on the antisense has been previously observed.[22]

SiRNAs **16**, **17** and **19** contain U$_t$U modification at various positions near the 3'-end of the sense strand. Several of these siRNAs exhibit comparable or enhanced silencing when compared to wild-type siRNA. With respect to thermal stability, siRNAs **16** and **19** exhibit a drop in T_m. Destabilizing this area of the duplex along with the 3′-U$_t$U modification (siRNA **19**) may offer a favorable response by not only promoting favorable incorporation of the guide strand to form the active RISC-guide complex,[21a] but by increasing its resistance to nucleases. To determine whether a 3′-U$_t$U modified overhang provides enhanced stability to nucleases, we performed time-dependent stability assays in serum. The analysis involving siRNAs **17**, **18** and **22** illustrated that these 3′-U$_t$U modified duplex siRNAs have reduced susceptibility to degradation by nucleases relative to wild-type native siRNA (Fig. S2, Supplementary data).

Finally, siRNAs **11** and **21**, which contain multiple triazole modifications within their sense strands, exhibit low thermal stability and these siRNAs manage to effectively silence the target gene. This suggests that multiple triazoles within a duplex siRNA are

Table 2
Sequences of anti-GAPDH siRNAs

RNA	GAPDH siRNA duplex
23	5' – GGUCAUCCAUGACAACUUUtt – 3' 3' – ttCCAGUAGGUACUGUUGAAA – 5'
24	5' – GGUCAUCCAUGACAACU$_t$UUtt – 3' 3' – ttCCAGUAGGUACUGUUGAAA – 5'
25	5' – GGUCAUCCAUGACAACU$_t$U$_t$Utt – 3' 3' – ttCCAGUAGGUACUGUUGAAA – 5'
26	5' – GGUCAUCCAUGACAACUUU$_t$U – 3' 3' – ttCCAGUAGGUACUGUUGAAA – 5'

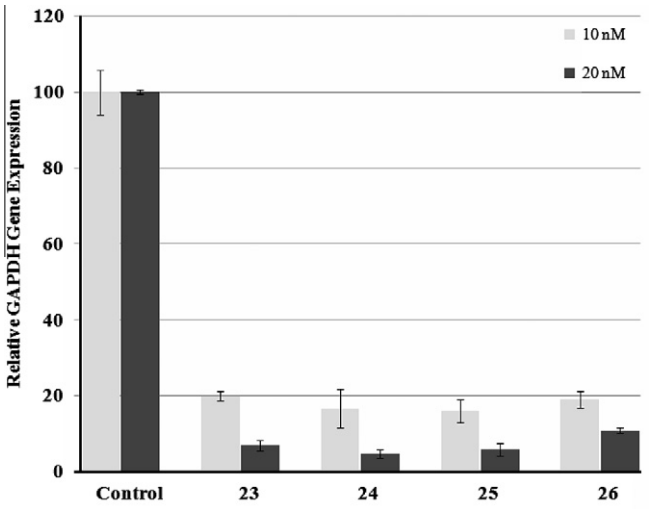

Figure 3. Analysis of GAPDH mRNA knockdown analyzed by real-time PCR following the treatment of HeLa cells with GAPDH siRNAs **23**–**26**. Levels of GAPDH expression were normalized to the internal reference gene 18S.

compatible within the RNAi pathway, albeit at reduced silencing efficiency compared to wild-type.

To determine whether this novel chemical modification would be amenable to endogenous targets, we synthesized and investigated the effect that our triazole backbone-modified siRNA would have on reducing the expression of glyceraldehyde-3-phosphate dehydrogenase (GAPDH). We synthesized three siRNAs bearing a U_tU triazole modification (siRNAs **24–26**). The siRNAs each contained a single U_tU modification placed either at positions 17–18, 18–19, or at the 3'-U_tU overhang of the sense strand (Table 2). The data from Figure 3 illustrates that our triazole-linked siRNAs show a dose-dependent downregulation of GAPDH at 10 and 20 nM comparable to wild-type (siRNA **23**). This result is significant because it highlights that our novel chemically modified siRNAs are capable of silencing relevant endogenous targets.

In conclusion, we are reporting the practical synthesis of siRNAs bearing triazoles interspersed throughout the backbone via DMT-phosphoramidite chemistry. Monomers **3** and **5** were readily synthesized through standard amide-bond coupling conditions. Via click chemistry, the final triazole-linked C_tU dimer phosphoramidite **8** was synthesized with an overall yield of 33% from monomers **3** and **5**. All RNA duplexes are substrates for the RNAi pathway. Therefore, a triazole in place of a phosphodiester backbone shows compatibility within siRNA duplexes and suggests that other novel backbone modifications may also act as proper substrates. To the best of our knowledge, there are no other reports of nonionic hydrophobic backbone mimics that silence gene expression when positioned within the internal Watson–Crick double-stranded region of siRNAs.

Acknowledgments

We acknowledge the National Sciences and Engineering Research Council and the Canada Foundation for Innovation for funding.

Supplementary data

Supplementary data associated with this article can be found, in the online version, at doi:10.1016/j.bmcl.2011.12.104.

References and notes

1. Fire, A.; Xu, S. Q.; Montgomery, M. K.; Kostas, S. A.; Driver, S. E.; Mello, C. C. *Nature* **1998**, *391*, 806.
2. (a) Hammond, S. M.; Bernstein, E.; Beach, D.; Hannon, G. J. *Nature* **2000**, *404*, 293; (b) Nykänen, A.; Haley, B.; Zamore, P. D. *Cell* **2001**, *107*, 309.
3. (a) Manoharan, M. *Biochim. Biophys. Acta* **1999**, *1489*, 117; (b) Corey, D. R. *J. Clin. Invest.* **2007**, *117*, 3615; (c) Watts, J. K.; Deleavey, G. F.; Damha, M. J. *Drug Discovery Today* **2008**, *13*, 842.
4. (a) Dowler, T.; Bergeron, D.; Tedeschi, A.-L.; Paquet, L.; Ferrari, N.; Damha, M. J. *Nucleic Acids Res.* **2006**, *34*, 1669; (b) Braasch, D. A.; Jensen, S.; Liu, Y.; Kaur, K.; Arar, K.; White, M. A.; Corey, D. R. *Biochemistry* **2003**, *42*, 7967; (c) Saneyoshi, H.; Seio, K.; Sekine, M. *J. Org. Chem.* **2005**, *70*, 10453; (d) Chiu, Y. L.; Rana, T. M. *RNA* **2003**, *9*, 1034; (e) Elmén, J.; Thornberg, H.; Ljungberg, K.; Frieden, M.; Westergaard, M.; Xu, Y.; Wahren, B.; Liang, Z.; Ørum, H.; Koch, T.; Wahlestedt, C. *Nucleic Acids Res.* **2005**, *33*, 439; (f) Ueno, Y.; Hirai, M.; Yoshikawa, K.; Kitamura, Y.; Hirata, Y.; Kiuchi, K.; Kitade, Y. *Tetrahedron* **2008**, *64*, 11328; (g) Manoharan, M.; Akinc, A.; Pandey, R. K.; Qin, J.; Hadwiger, P.; John, M.; Mills, K.; Charisse, K.; Maier, M. A.; Nechev, L.; Greene, E. M.; Pallan, P. S.; Rozners, E.; Rajeev, K. G.; Egli, M. *Angew. Chem. Int. Ed.* **2011**, *50*, 2284; (h) Zhang, N.; Tan, C.; Cai, P.; Zhang, P.; Zhao, Y.; Jiang, Y. *Bioorg. Med. Chem.* **2009**, *17*, 2441.
5. (a) Somoza, A.; Silverman, A. P.; Miller, R. M.; Chelliserrykattil, J.; Kool, E. T. *Chemistry* **2008**, *14*, 7978; (b) Xia, J.; Noronha, A.; Toudjarska, I.; Li, F.; Akinc, A.; Braich, R.; Frank-Kamenetsky, M.; Rajeev, K. G.; Egli, M.; Manoharan, M. *ACS Chem. Biol.* **2006**, *1*, 176.
6. Amarzguioui, M.; Holen, T.; Babaie, E.; Prydz, H. *Nucleic Acids Res.* **2003**, *31*, 589.
7. Hall, A. H. S.; Wan, J.; Shaughnessy, E. E.; Shaw, B. R.; Alexander, K. A. *Nucleic Acids Res.* **2004**, *32*, 5991.
8. Iwase, R.; Toyama, T.; Nishimori, K. *Nucleosides Nucleotides Nucleic Acids* **2007**, *26*, 1451.
9. Potenza, N.; Moggio, L.; Milano, G.; Salvatore, V.; Di Blasio, B.; Russo, A.; Messere, A. *Int. J. Mol. Sci.* **2008**, *9*, 299.
10. Wang, Y.; Juranek, S.; Li, H.; Sheng, G.; Tuschl, T.; Patel, D. J. *Nature* **2008**, *456*, 921.
11. Rostovtsev, V. V.; Green, L. G.; Fokin, V. V.; Sharpless, K. B. *Angew. Chem. Int. Ed.* **2002**, *41*, 2596.
12. (a) Isobe, H.; Fujino, T.; Yamazaki, N.; Guillot-Nieckowski, M.; Nakamura, E. *Org. Lett.* **2008**, *10*, 3729; (b) Lucas, R.; Neto, V.; Bouazza, A. H.; Zerrouki, R.; Granet, R.; Krausz, P.; Champavier, Y. *Tetrahedron Lett.* **2008**, *49*, 1004; (c) Fujino, T.; Yamazaki, N.; Isobe, H. *Tetrahedron Lett.* **2009**, *50*, 4101; (d) Chittepu, P.; Sirivolu, V. R.; Seela, F. *Bioorg. Med. Chem.* **2008**, *16*, 8427; (e) Chandrasekhar, S.; Srihari, P.; Nagesh, C.; Kiranmai, N.; Nagesh, N.; Idris, M. M. *Synthesis* **2010**, *21*, 3710; (f) El-Sagheer, A. H.; Brown, T. *J. Am. Chem. Soc.* **2009**, *131*, 3958; (g) Chouikhi, D.; Barluenga, S.; Winssinger, N. *Chem. Commun.* **2010**, *46*, 5476; (h) Varizhuk, A.; Chizhov, A.; Florentiev, V. *Bioorg. Chem.* **2011**, *39*, 127.
13. El-Sagheer, A. H.; Brown, T. *Proc. Natl. Acad. Sci. U.S.A.* **2010**, *107*, 15329.
14. (a) Parades, E.; Das, S. R. *Chembiochem* **2011**, *12*, 125; (b) Mutisya, D.; Selvam, C.; Kennedy, S. D.; Rozners, E. *Bioorg. Med. Chem. Lett.* **2011**, *21*, 3420.
15. Efthymiou, T. C.; Desaulniers, J.-P. *J. Heterocycl. Chem.* **2011**, *48*, 533.
16. Vader, J.; Sengers, H.; de Groot, A. *Tetrahedron* **1989**, *45*, 2131.
17. (a) Christensen, L.; Hansen, H. F.; Koch, T.; Nielsen, P. E. *Nucleic Acids Res.* **1998**, *26*, 2735; (b) Schwergold, C.; Depecker, G.; Di Giorgio, C.; Patino, N.; Jossinet, F.; Ehresmann, B.; Terreux, R.; Cabrol-Bass, D.; Condom, R. *Tetrahedron* **2002**, *58*, 5675.
18. Liu, X. J.; Chen, R. Y.; Weng, L. H.; Leng, X. B. *Heteroatom Chem.* **2000**, *11*, 422.
19. Petersheim, M.; Turner, D. H. *Biochemistry* **1983**, *22*, 256.
20. Bajor, Z.; Sági, G.; Tegyey, Z.; Kraicsovits, F. *Nucleosides Nucleotides Nucleic Acids* **2003**, *22*, 1963.
21. (a) Schwarz, D. S.; Hutvágner, G.; Du, T.; Xu, Z.; Aronin, N.; Zamore, P. D. *Cell* **2003**, *115*, 199; (b) Addepalli, H.; Meena; Peng, C. G.; Wang, G.; Fan, Y.; Charisse, K.; Jayaprakash, K. N.; Rajeev, K. G.; Pandey, R. K.; Lavine, G.; Zhang, L.; Jahn-Hofmann, K.; Hadwiger, P.; Manoharan, M.; Maier, M. A. *Nucleic Acids Res.* **2010**, *38*, 7320.
22. Somoza, A.; Terrazas, M.; Eritja, R. *Chem. Commun.* **2010**, *46*, 4270.

6.0 Supplementary Information – Chapter III – Manuscript II

6.1 NMR Spectra of Organic Compounds

6.1.1 Proton NMR Spectrum of Compound 1

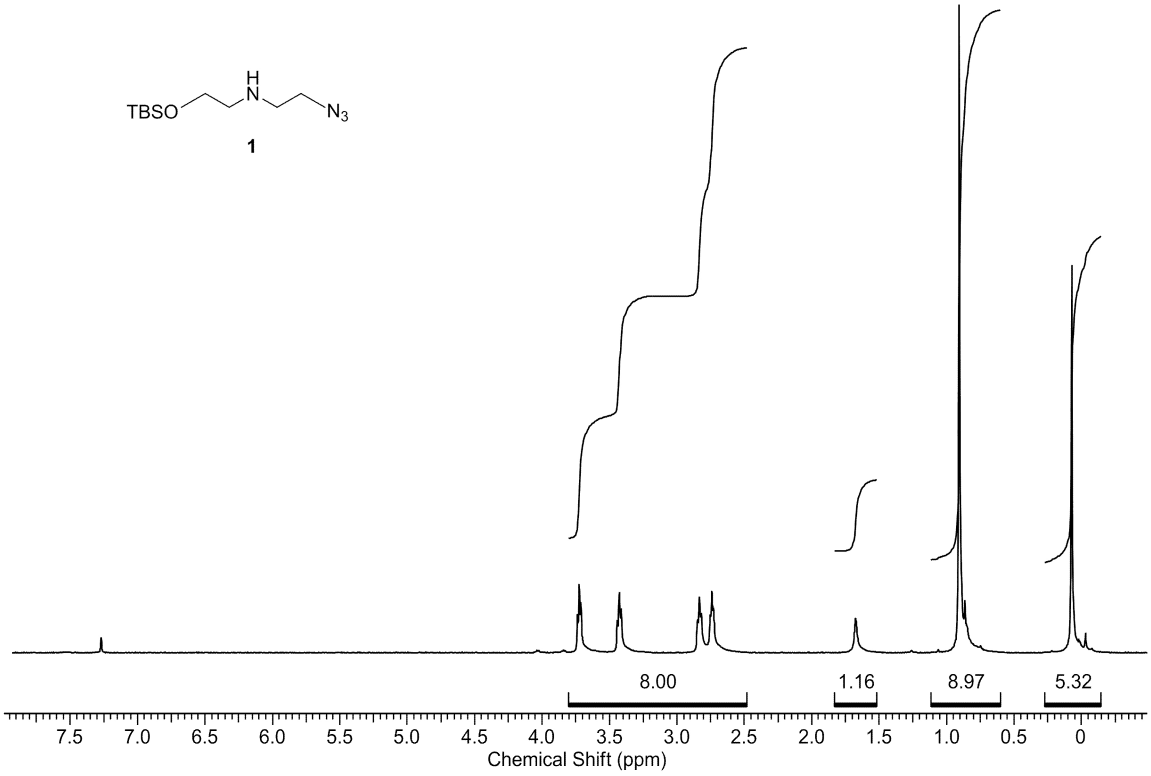

Figure A31. ^{1}H – NMR Spectrum of Compound **1** observed in $CDCl_3$ at 400 MHz.

6.1.2 Carbon NMR Spectrum of Compound 1

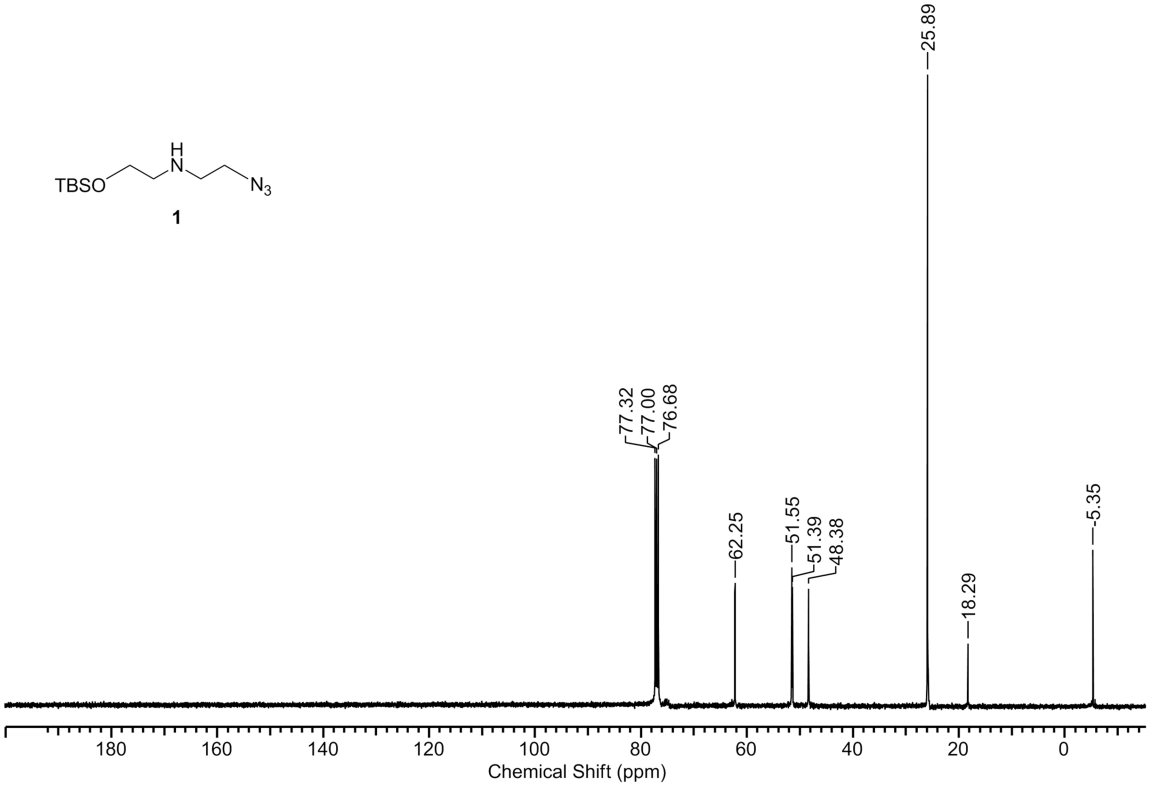

Figure A32. ^{13}C – NMR Spectrum of Compound **1** observed in $CDCl_3$ at 100 MHz.

6.1.3 Proton NMR Spectrum of Compound 2

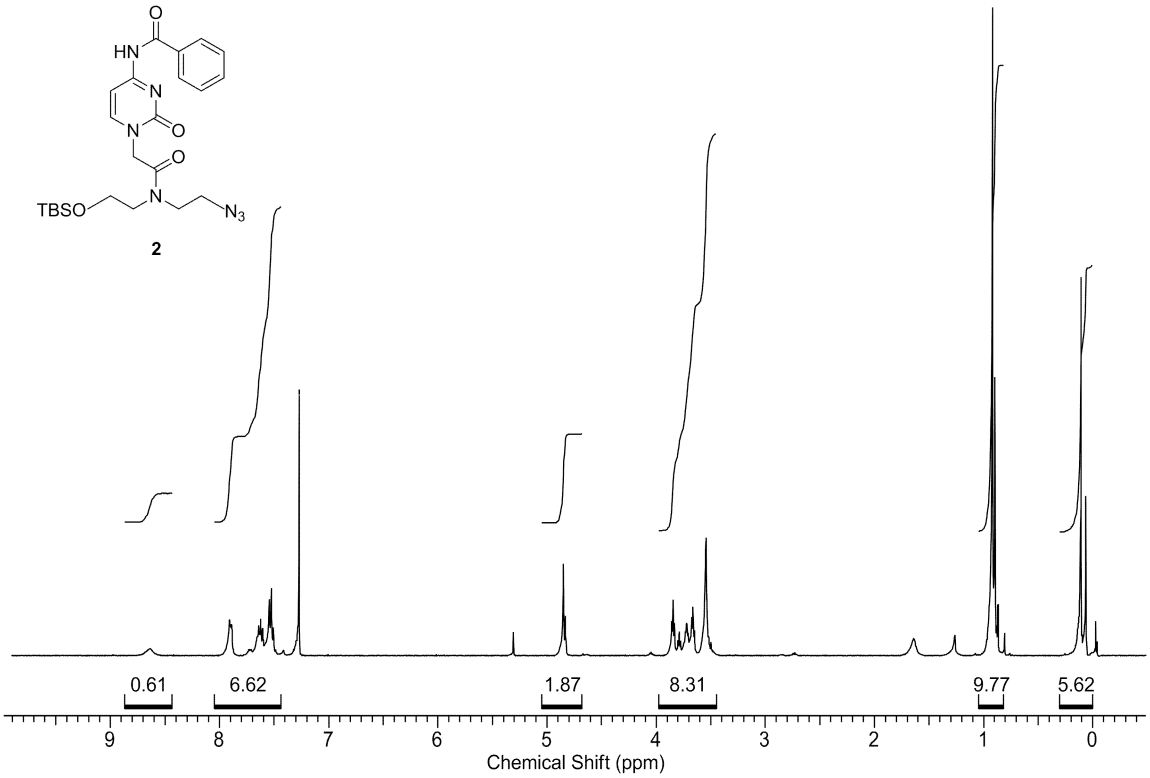

Figure A33. ^{1}H – NMR Spectrum of Compound **2** observed in $CDCl_3$ at 400 MHz.

6.1.4 Carbon NMR Spectrum of Compound 2

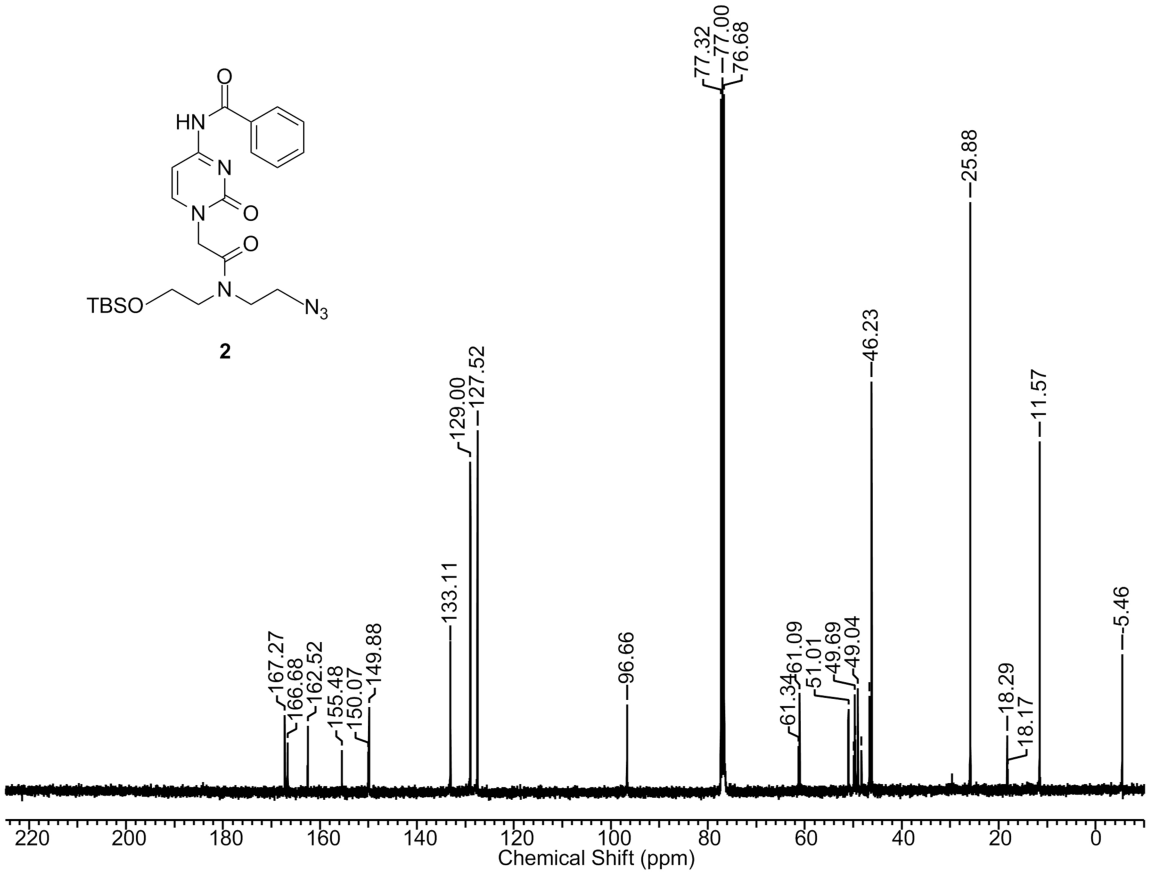

Figure A34. ^{13}C – NMR Spectrum of Compound **2** observed in $CDCl_3$ at 100 MHz.

6.1.5 Proton NMR Spectrum of Compound 3a

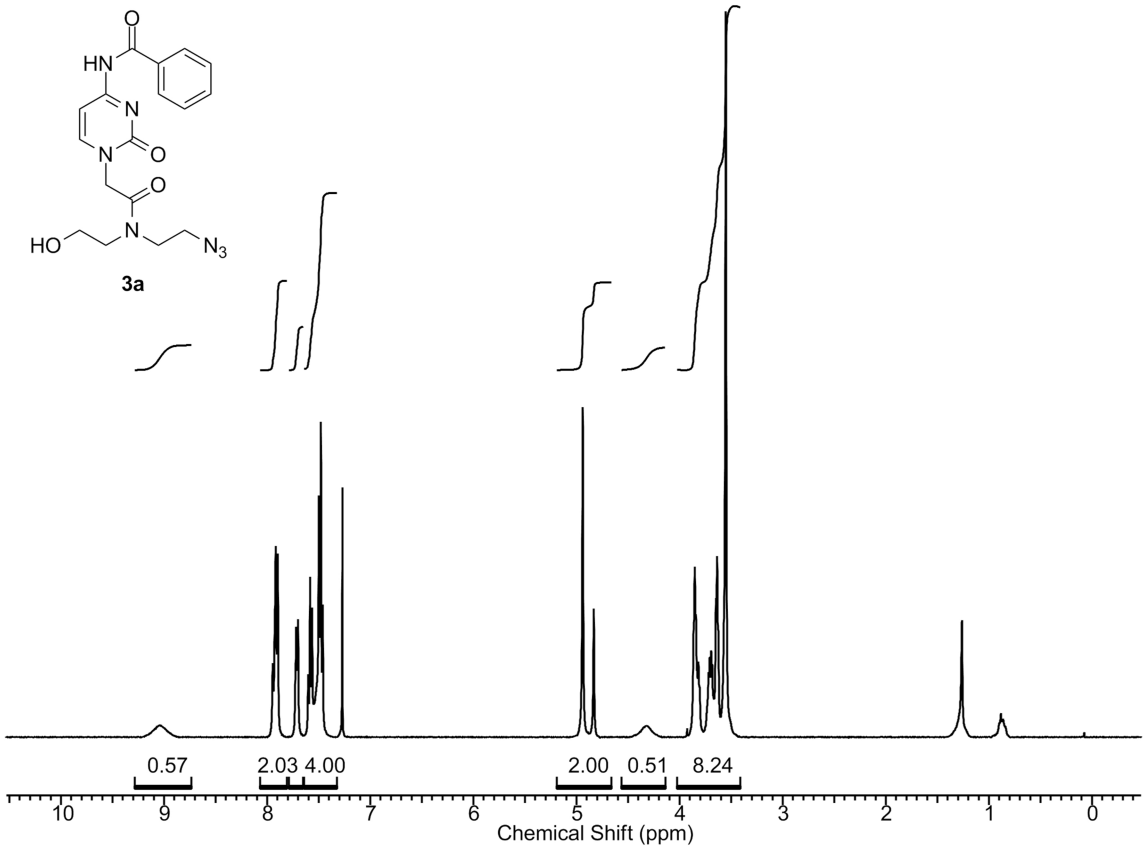

Figure A35. ^{1}H – NMR Spectrum of Compound **3a** observed in $CDCl_3$ at 400 MHz.

6.1.6 Carbon NMR Spectrum of Compound 3a

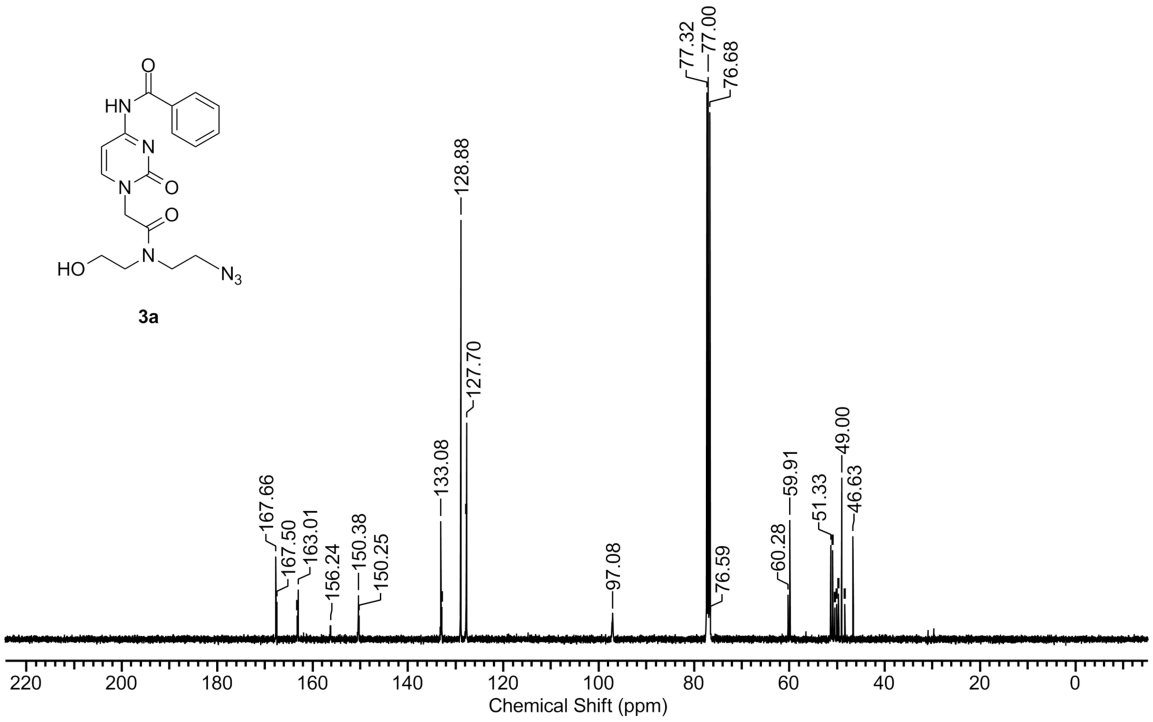

Figure A36. ^{13}C – NMR Spectrum of Compound **3a** observed in $CDCl_3$ at 100 MHz.

6.1.7 Proton NMR Spectrum of Compound 3

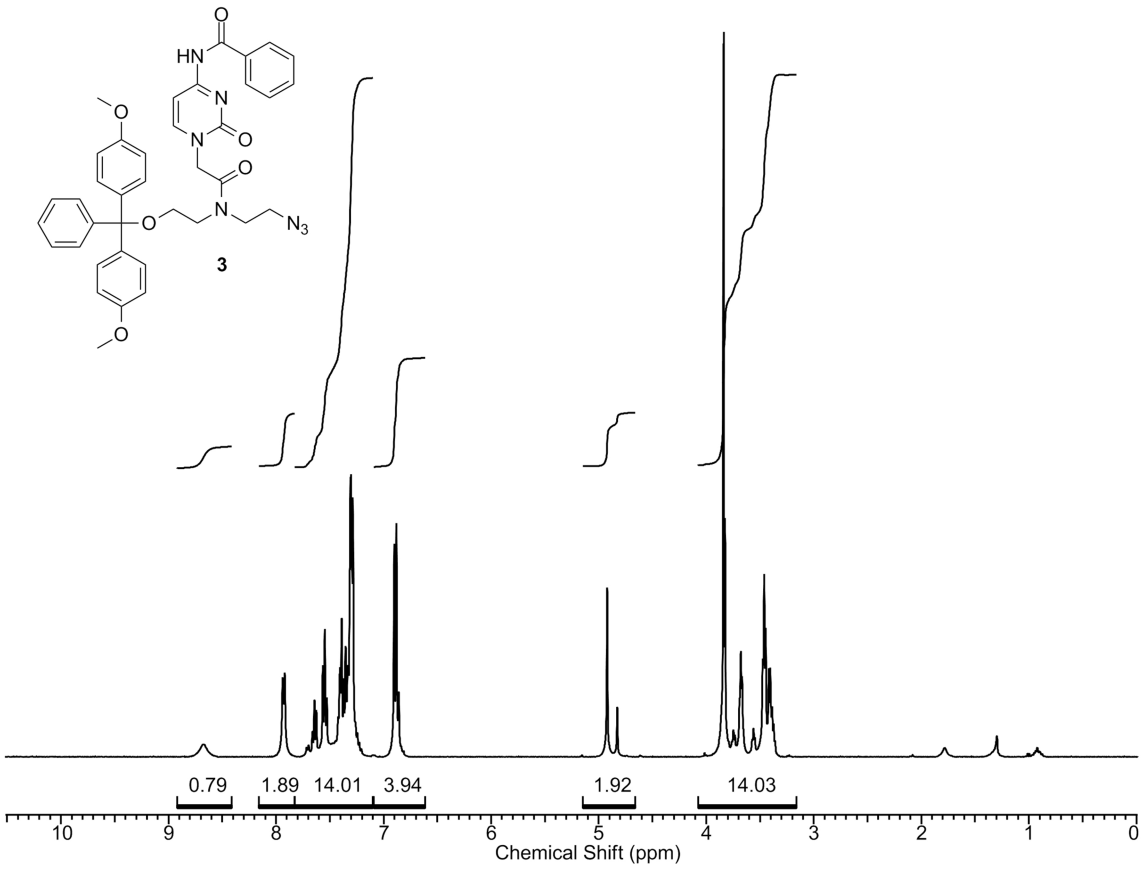

Figure A37. ^{1}H – NMR Spectrum of Compound **3** observed in $CDCl_3$ at 400 MHz.

6.1.8 Carbon NMR Spectrum of Compound 3

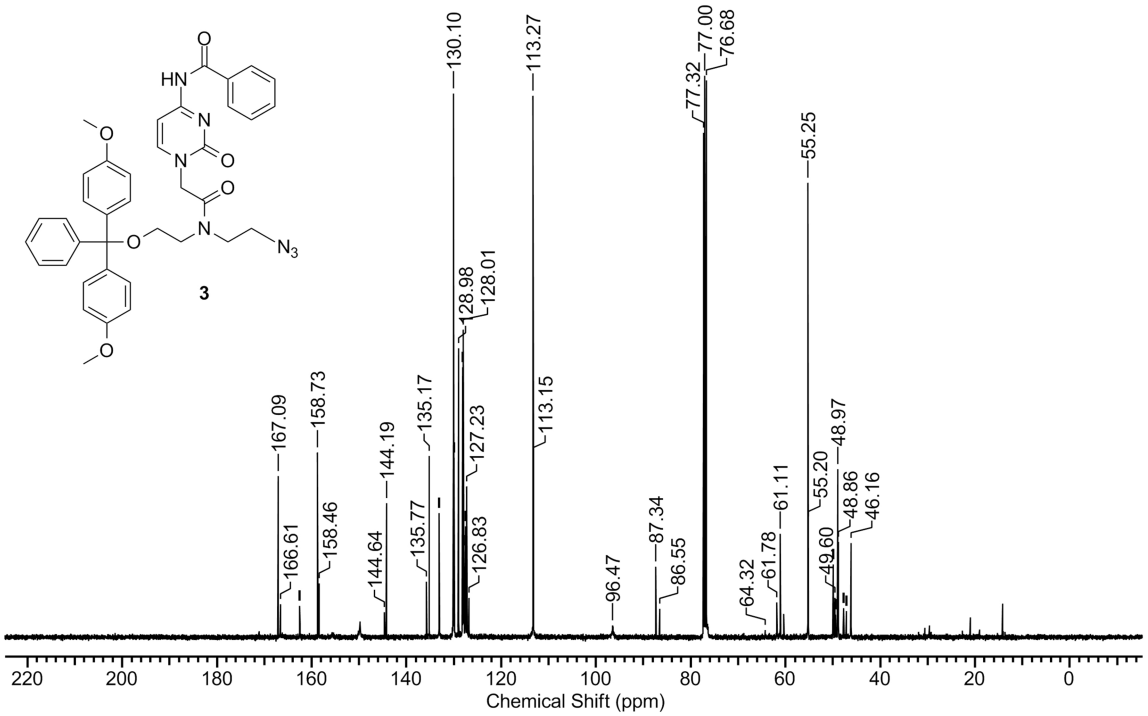

Figure A38. ^{13}C – NMR Spectrum of Compound **3** observed in $CDCl_3$ at 100 MHz.

6.1.9 Proton NMR Spectrum of Compound 4

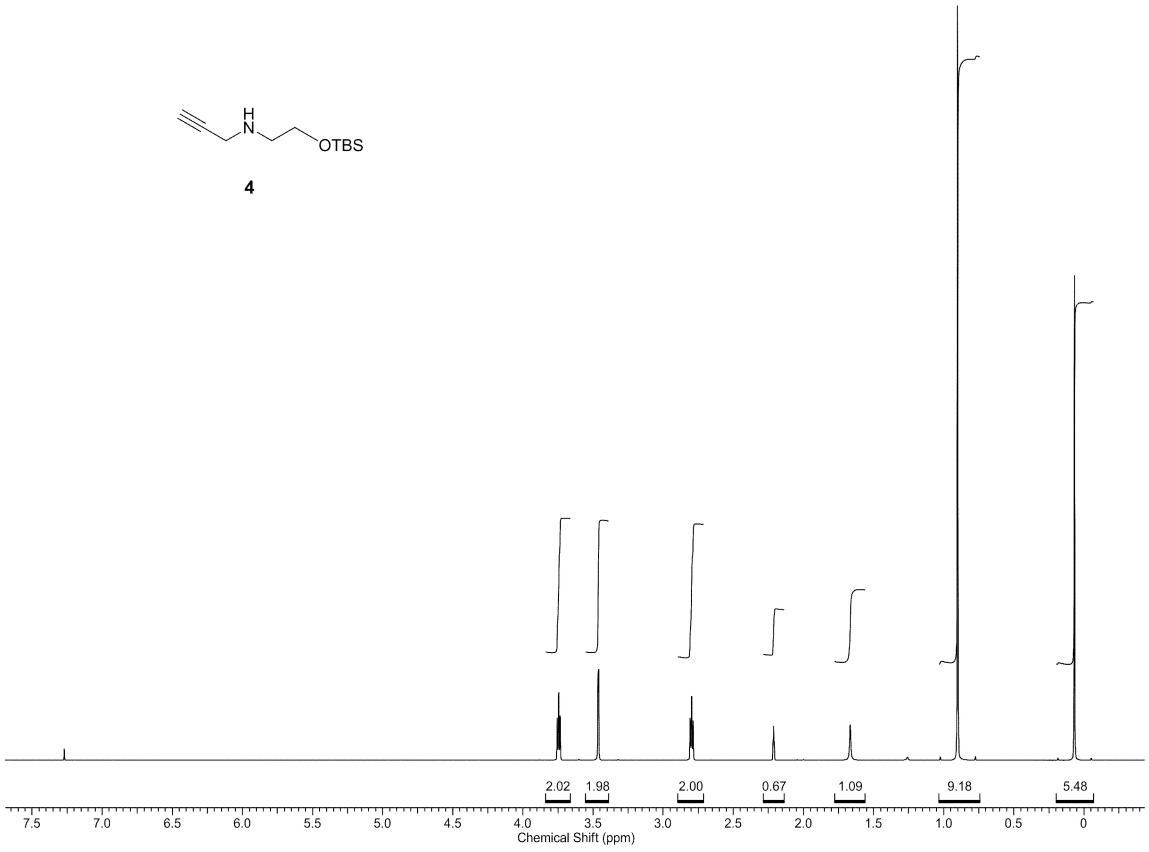

Figure A39. ^{1}H – NMR Spectrum of Compound **4** observed in $CDCl_3$ at 500 MHz.

6.1.10 Carbon NMR Spectrum of Compound 4

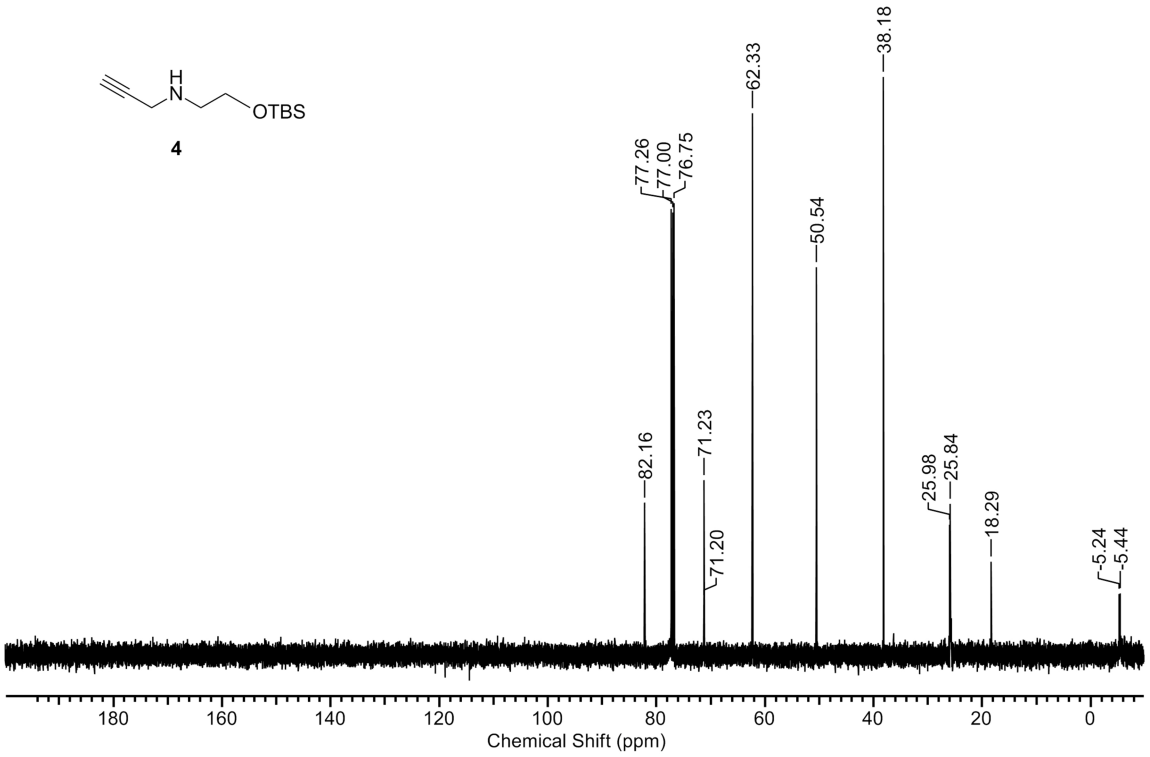

Figure A40. ^{13}C – NMR Spectrum of Compound **4** observed in $CDCl_3$ at 125 MHz.

6.1.11 Proton NMR Spectrum of Compound 5

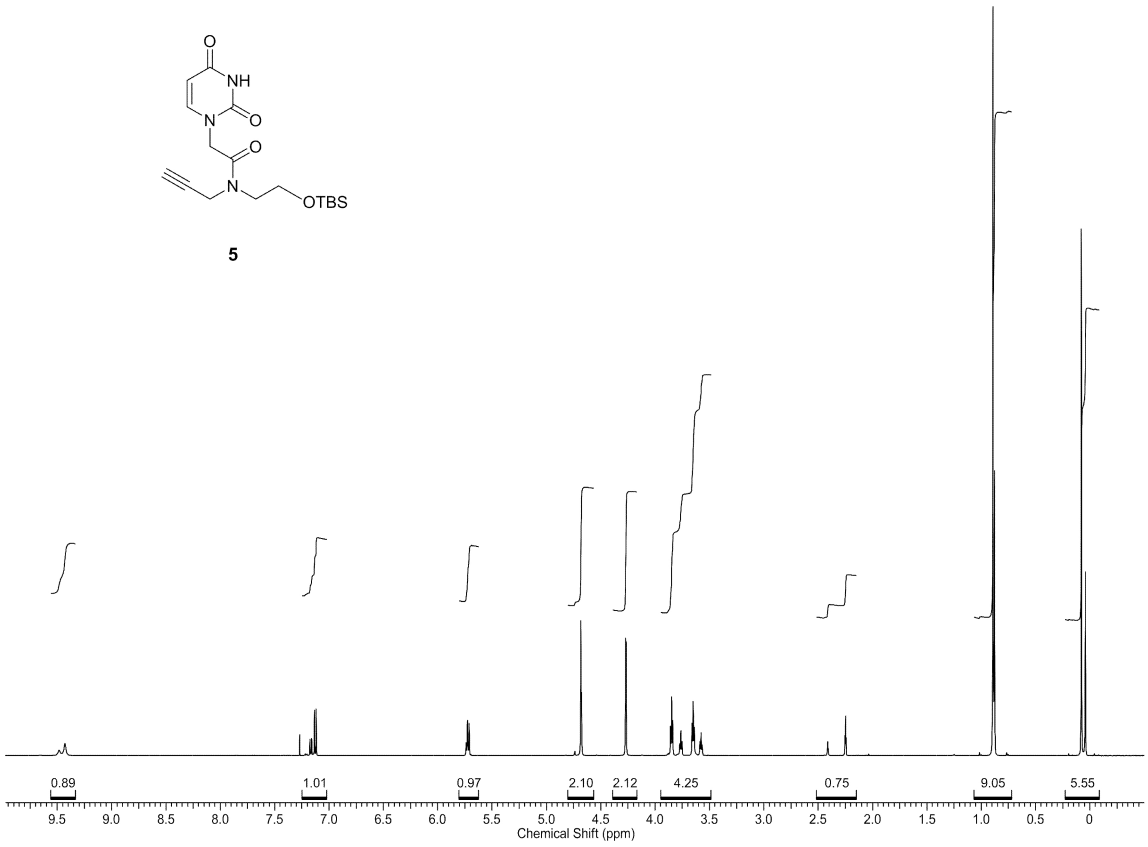

Figure A41. ^{1}H – NMR Spectrum of Compound **5** observed in $CDCl_3$ at 500 MHz.

6.1.12 Carbon NMR Spectrum of Compound 5

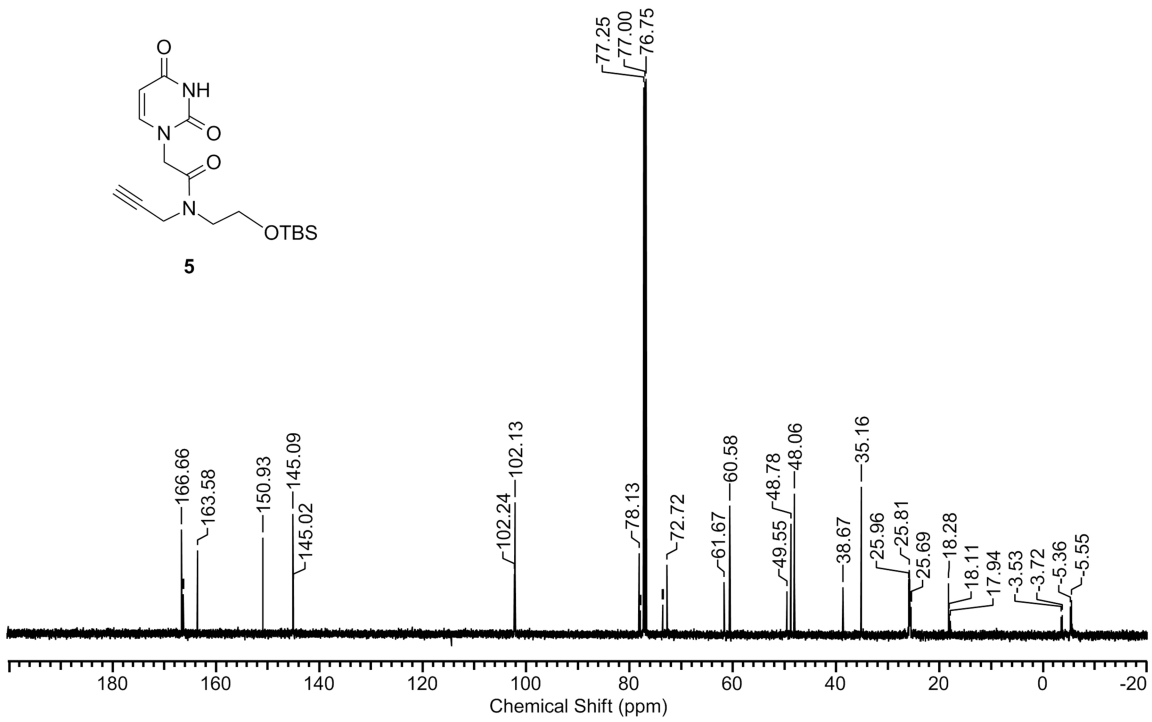

Figure A42. ^{13}C – NMR Spectrum of Compound **5** observed in $CDCl_3$ at 125 MHz.

6.1.13 Proton NMR Spectrum of Compound 6

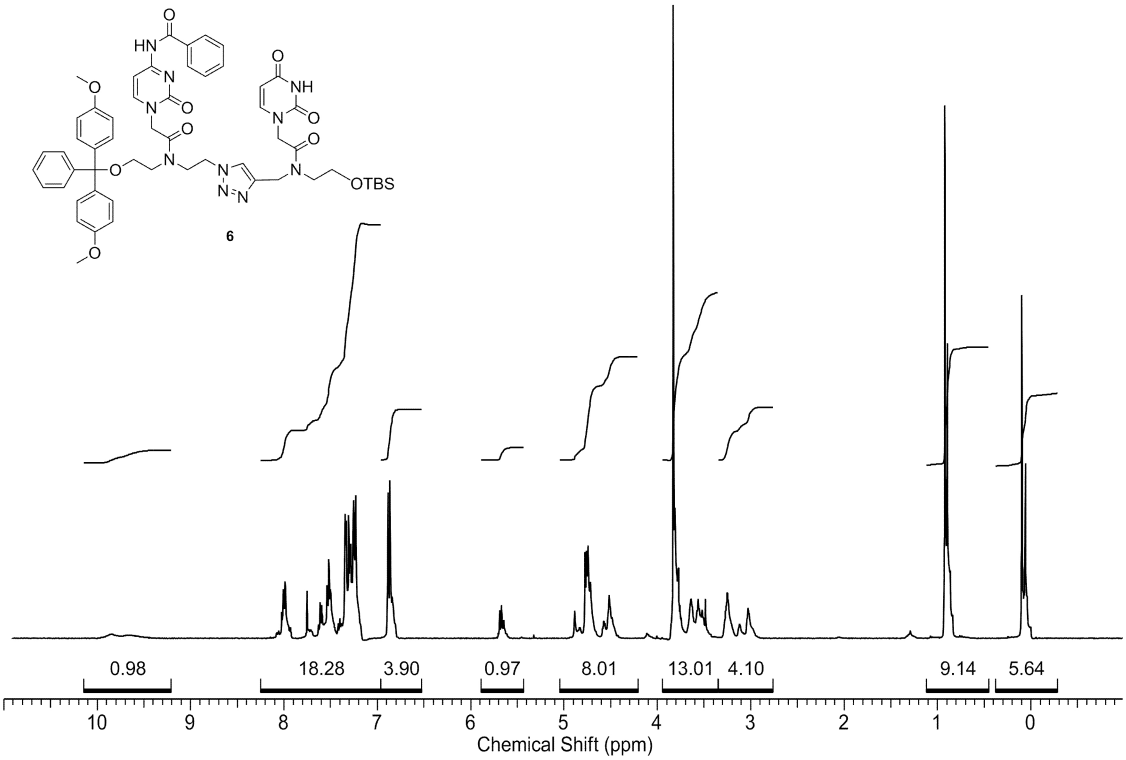

Figure A43. ^{1}H – NMR Spectrum of Compound **6** observed in $CDCl_3$ at 400 MHz.

6.1.14 Carbon NMR Spectrum of Compound 6

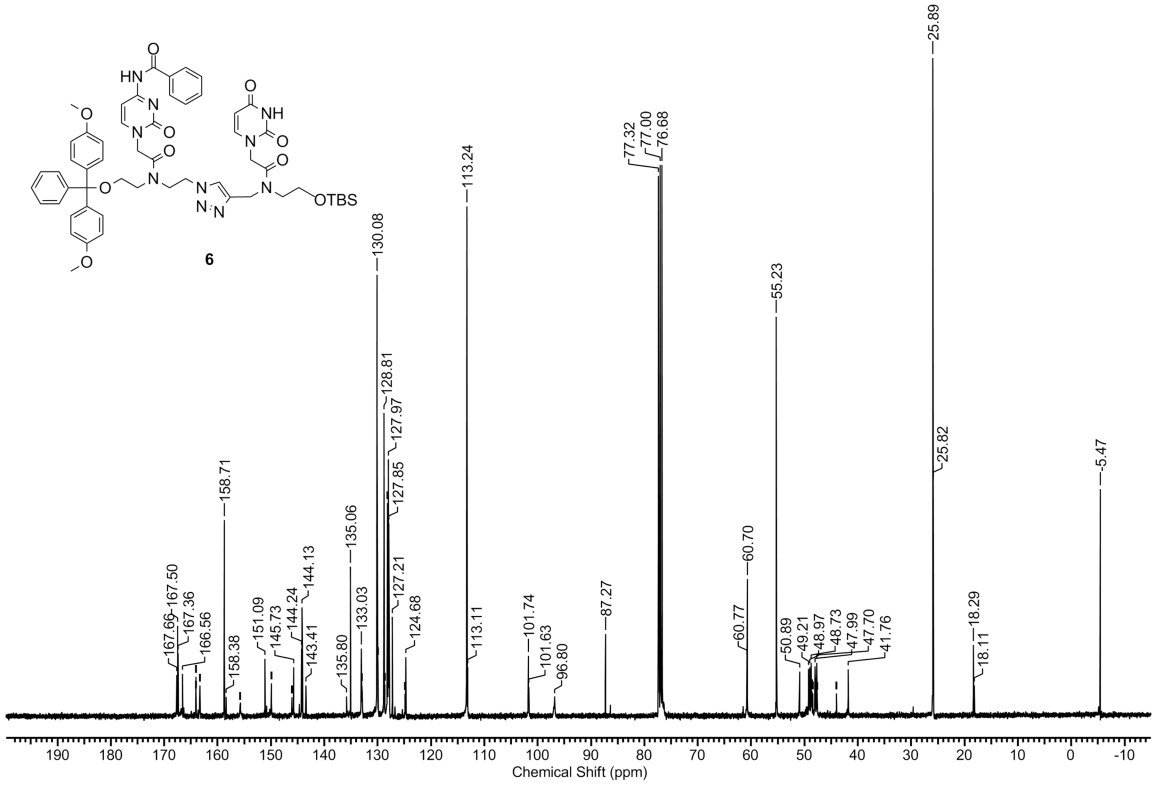

Figure A44. ^{13}C – NMR Spectrum of Compound **6** observed in $CDCl_3$ at 100 MHz.

6.1.15 Proton NMR Spectrum of Compound 7

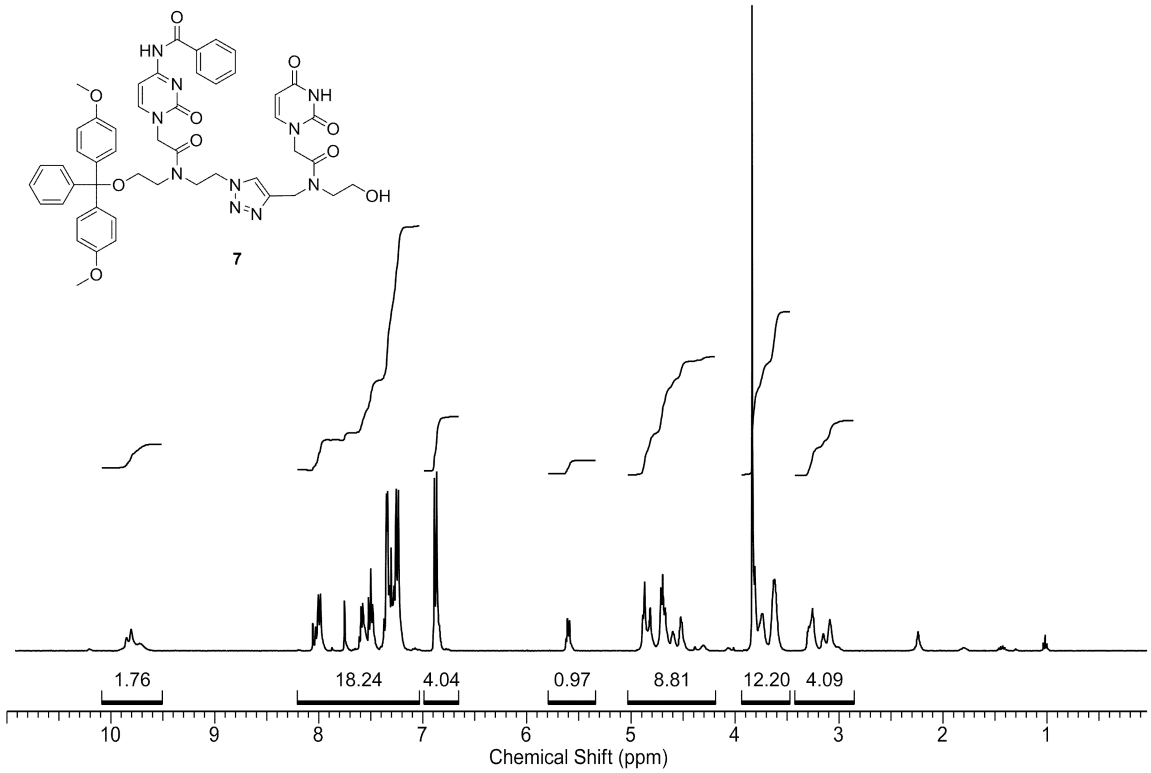

Figure A45. ^{1}H – NMR Spectrum of Compoud **7** observed in $CDCl_3$ at 400 MHz.

6.1.16 Carbon NMR Spectrum of Compound 7

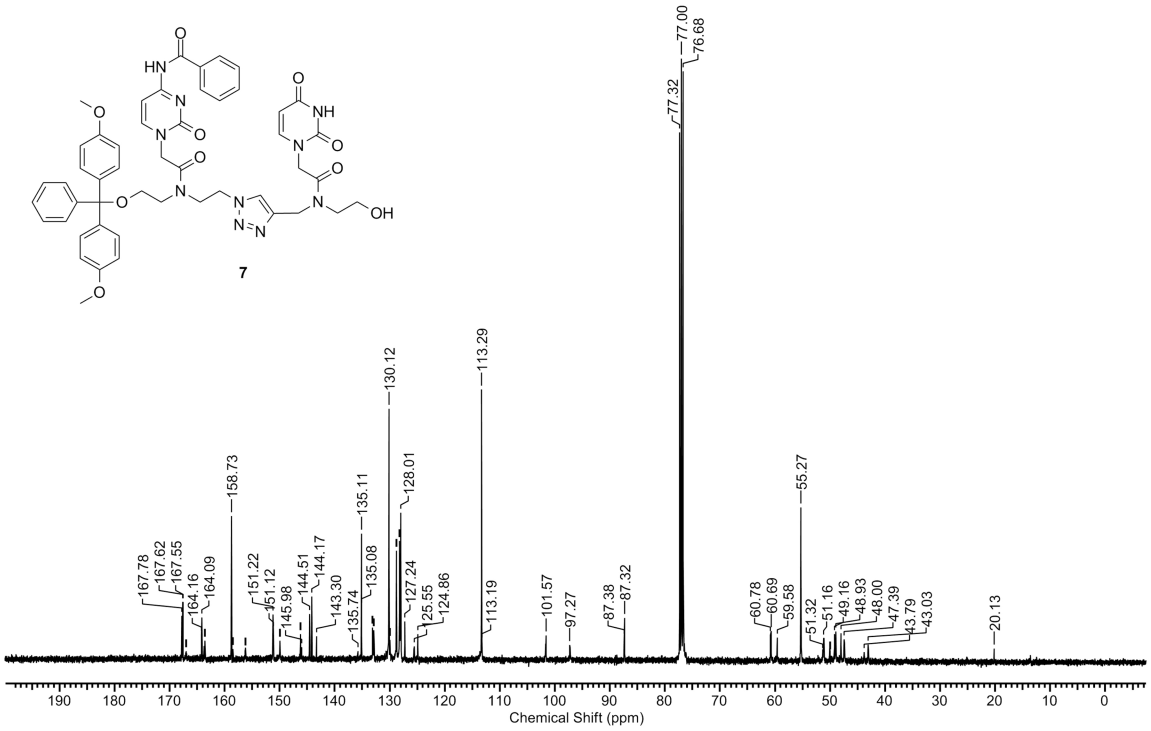

Figure A46. ^{13}C – NMR Spectrum of Compound **7** observed in $CDCl_3$ at 100 MHz.

6.1.17 Proton NMR Spectrum of Compound 8

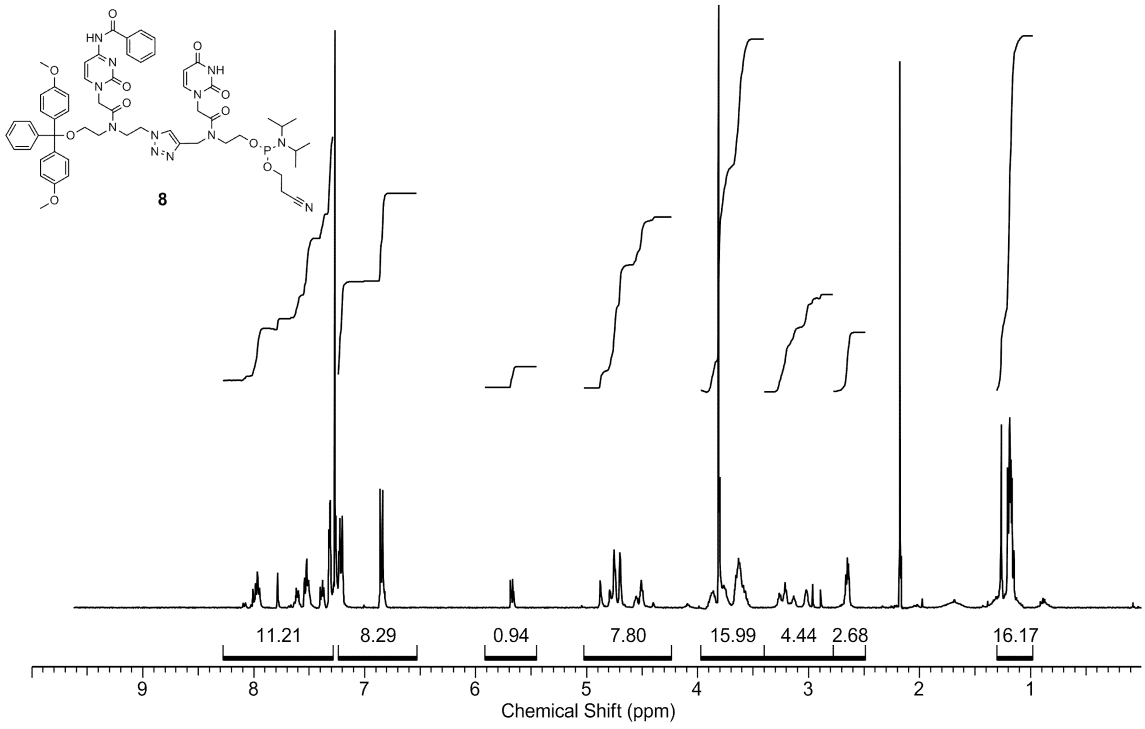

Figure A47. ^{1}H – NMR Spectrum of Compound **8** observed in $CDCl_3$ at 400 MHz.

6.1.18 Carbon NMR Spectrum of Compound 8

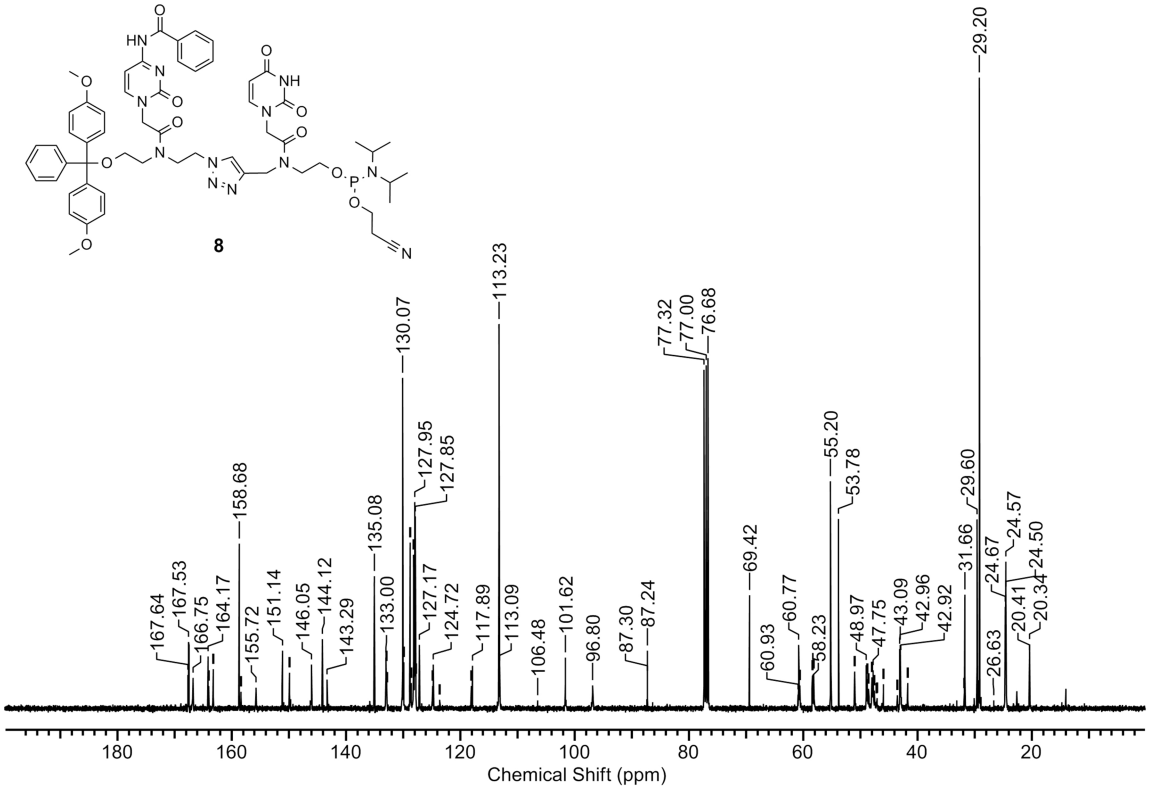

Figure A48. ^{13}C – NMR Spectrum of Compound **8** observed in $CDCl_3$ at 100 MHz.

6.1.19 Phosphorus NMR Spectrum of Compound 8

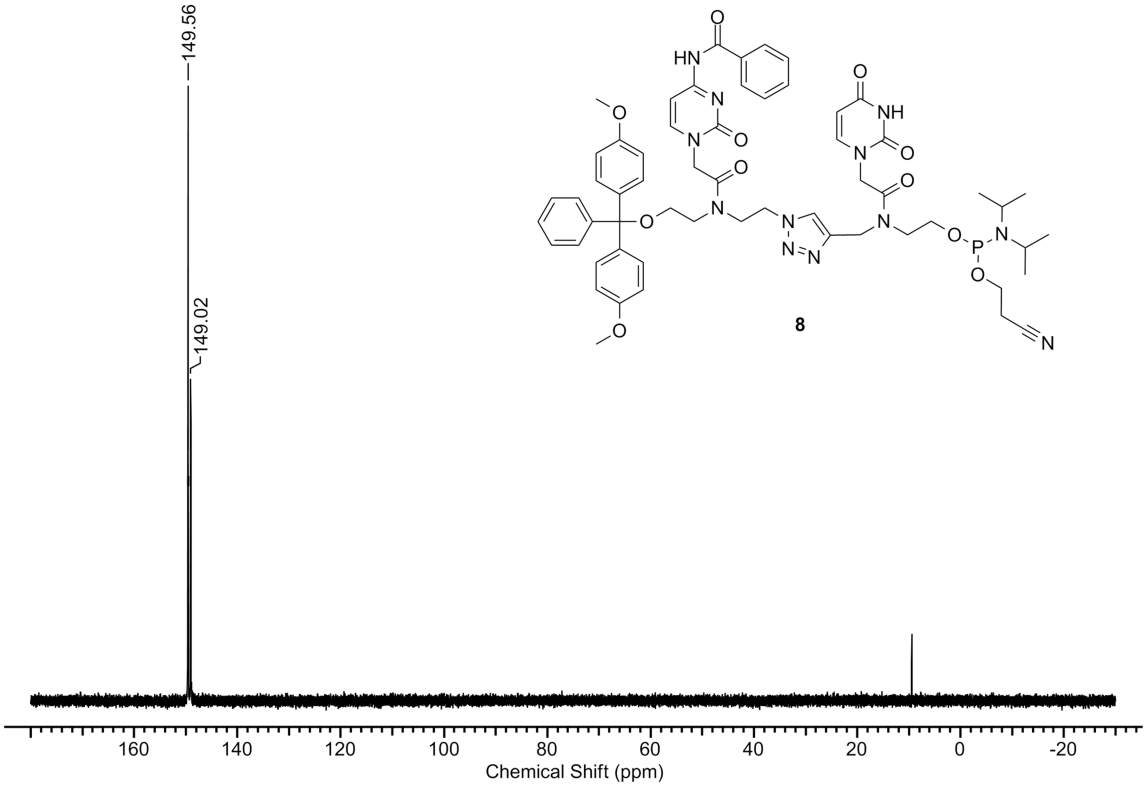

Figure A49. ^{31}P – NMR Spectrum of Compound **8** observed in $CDCl_3$ at 167 MHz.

6.2 Masses of Triazole-Modified RNA Molecules Recorded Using Quantitative Time-Of-Flight Spectrometry

Table A6. Predicted and recorded masses for U_tU and C_tU-modified sense and antisense RNAs

Sample No.	Sense and Antisense RNAs	Predicted Neutral Mass	Observed Neutral Mass
lucRNA 9	5′ - **C_tU**UACGCUGAGUACUUCGAtt - 3′	6587.0	6587.0
lucRNA 10	5′ - **C_tU**UACGCUGAGUA**C_tU**UCGAtt - 3′	6570.1	6570.1
lucRNA 11	5′ - C**U_tU**ACGCUGAGUACUUCGAtt - 3′	6587.0	6587.0
lucRNA 12	5′ - CUUACG**C_tU**GAGUACUUCGAtt - 3′	6587.0	6587.0
lucRNA 13	5′ - CUUACGCUGAGUA**C_tU**UCGAtt - 3′	6587.0	6587.0
lucRNA 14	5′ - CUUACGCUGAGUAC**U_tU**CGAtt - 3′	6587.0	6587.0
lucRNA 15	5′ - CUUACGCUGAGUACUUCGA**U_tU** - 3′	6591.0	6591.0
lucRNA 16	5′ - CUUACGCUGAGUAC**U_tU**CGA**U_tU** - 3′	6574.1	6574.1
lucRNA 17	5′ - C**U_tU**ACGCUGAGUAC**U_tU**CGA**U_tU** - 3′	6557.2	6557.2
lucRNA 18	5′-ph- UCGAAGUACUCAGCGUAAG**U_tU** -3′	6756.0	6757.0
gapdhRNA 19	5′ - GGUCAUCCAUGACAAC**U_tU**Utt - 3′	6570.9	6571.0
gapdhRNA 20	5′ - GGUCAUCCAUGACAACU**U_tU**tt - 3′	6570.9	6571.1
gapdhRNA 21	5′ - GGUCAUCCAUGACAACUUU**U_tU** - 3′	6574.9	6575.0

ESI Q-TOF recorded in negative electrospray mode after HPLC elution using two mobile phases; MeOH/H_2O (5:95) with 200 mM hexafluoroisopropyl alcohol and 8.1 mM triethylamine; and 70% MeOH.

6.3 Conformational Characteristics of Triazole-Modified siRNAs Observed Using Circular Dichroism Spectroscopy

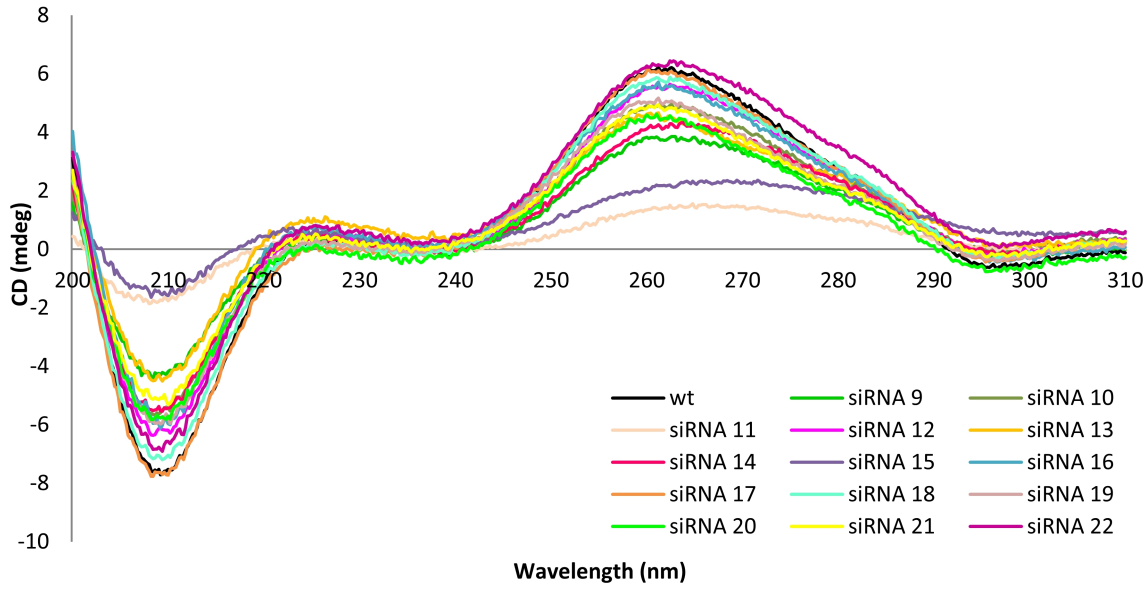

Figure A50. RNA duplex conformation of all anti-luciferase siRNAs displayed through circular dichroism spectroscopy. Wild-type and modified anti-luciferase siRNAs **9-22** (~2.4 nmol/duplex, except for siRNAs **11** & **15** at ~1.4 nmol/duplex) were suspended in 500 µL of a sodium phosphate buffer (90 mM NaCl, 10 mM Na_2HPO_4, 1 mM EDTA, pH 7) and the solution was scanned from 200–310 nm at 20 ^{0}C. All scans were performed in quadruplicate and averaged using version 2 of Jasco′s Spectra Manager software.

6.4 Nuclease Stability

6.4.1 Nuclease Stability of 3′ - U_tU Modified siRNAs

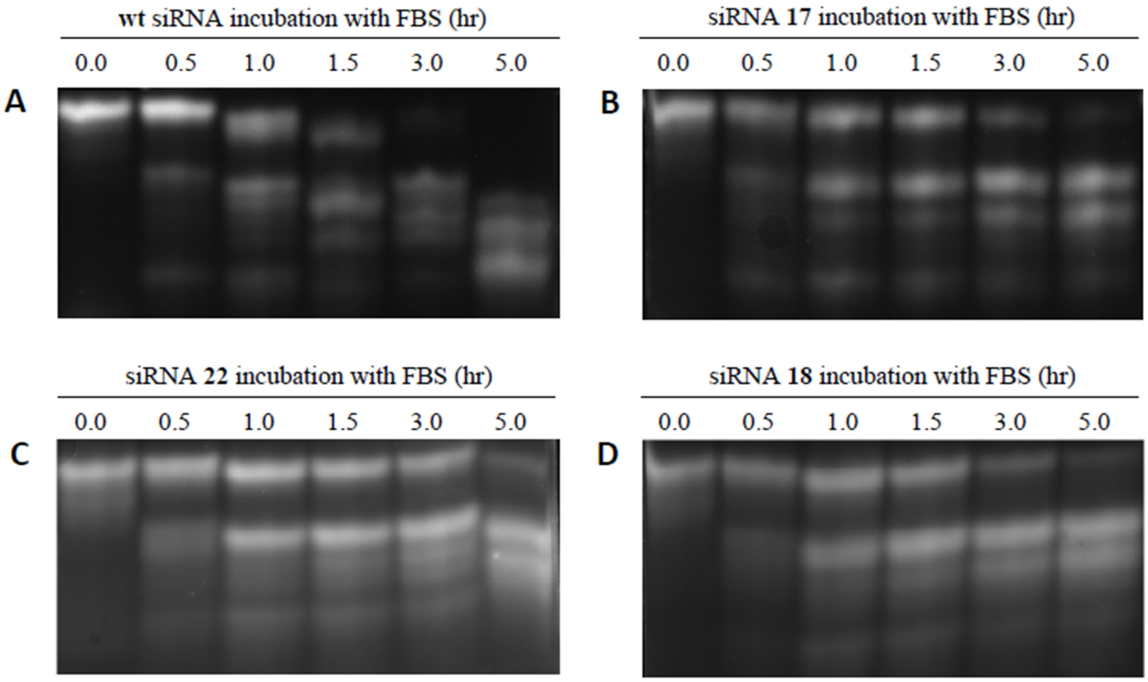

Figure A51. Native PAGE gel displaying degradation patterns of 3′-modified siRNAs in a time-dependent nuclease stability assay. (**A**) Degradation pattern of **wt** anti-luciferase siRNA. (**B**) Degradation pattern of siRNA **17**. (**C**) Degradation pattern of siRNA **22**. (**D**) Degradation pattern of siRNA **18**. Samples were incubated at 37 ^{0}C in 13.5% FBS before they were resolved in 20% PAGE at low voltage (80-90V) overnight at rt. Bands were stained with Gel Red (3X).

6.4.2 Silencing Activity of siRNAs Cleaved by Nucleases

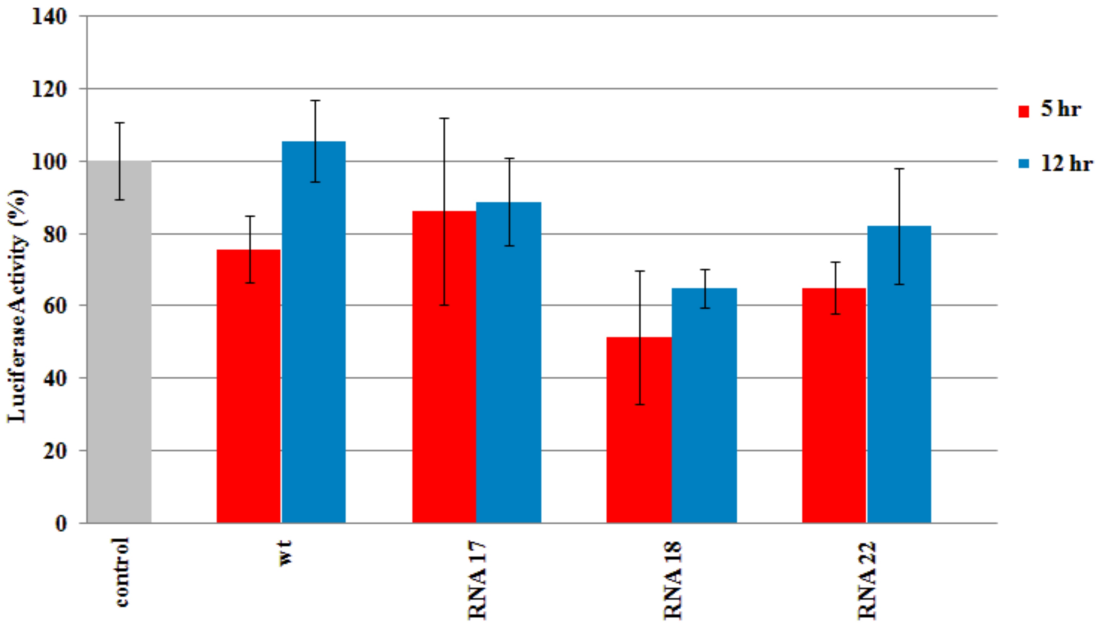

Figure A52. *Firefly* luciferase expression with siRNAs **wt**, **17**, **18** and **22** after incubation with 13.5% FBS using the Dual-luciferase reporter assay. Prior to transfection, the siRNAs were incubated with 13.5% FBS at 37 ^{0}C for 5 hours (red) or 12 hours (blue). The siRNAs were tested at 80 pM and their potency was measured using the Dual-luciferase reporter assay with *firefly* luciferase expression normalized to *Renilla* luciferase. Each value is the average of at least three independent experiments with the indicated error (SDOM). SiRNAs **wt** and **17** do not silence *firefly* luciferase to any significant degree at both 5 and 12 hours. Both siRNAs **wt** and **17** do not have an observable native 21-mer duplex band in the gel presented in Fig. S2 at the 5 hour point. The silencing data of siRNAs **18** and **22** suggests minimal silencing, likely due to the increased lifetime of these duplex siRNAs relative to siRNAs **wt** and **17** (see Fig. S2 for band pattern). As the incubation time increases to 12 hours, reduced silencing is observed. The data from this graph suggests that the cleaved siRNAs illustrated in Fig. S2 do not contribute to RNAi-knockdown.

Appendix III – Manuscript III

Bioorganic & Medicinal Chemistry Letters 22 (2012) 5590–5594

Contents lists available at SciVerse ScienceDirect

Bioorganic & Medicinal Chemistry Letters

journal homepage: www.elsevier.com/locate/bmcl

Evaluation of siRNAs that contain internal variable-length spacer linkages

Tim C. Efthymiou, Brandon Peel, Vanthi Huynh, Jean-Paul Desaulniers *

Faculty of Science, University of Ontario Institute of Technology, 2000 Simcoe Street North, Oshawa, Ontario, Canada L1H 7K4

ARTICLE INFO

Article history:
Received 15 June 2012
Accepted 2 July 2012
Available online 16 July 2012

Keywords:
Short interfering RNA
Alkyl linker
Gene silencing
RNA
Destabilization

ABSTRACT

The most widely accepted mechanism of RNAi-silencing involves the RNA-induced silencing complex (RISC) liberating the active antisense strand from the sense strand of an siRNA duplex to form an active RISC-antisense complex. This involves cleaving the sense strand between positions 9 and 10 from the 5′ end of the strand prior to dissociation. Destabilizing modifications near the center of the duplex in some cases can enhance the efficacy of the resultant construct and may trigger an alternative mechanism through which the sense strand is removed. By introducing alkyl spacers of varying lengths near or within the sense strand's cleavage site, this study illustrates that siRNAs, in most cases, retained potent RNAi-silencing activity. Our results highlight that by substituting the scissile phosphodiester linkage on the sense strand with non-cleavable alkyl chains provides a novel and alternative method to destabilize the central region of siRNAs.

RNA interference (RNAi) is an endogenous gene silencing pathway.[1] The process involves the cleavage of double-stranded RNA into short-interfering RNAs (siRNAs).[2] The siRNAs are comprised of two strands, a sense and an antisense (AS) strand. The antisense strand recognizes the target messenger RNA through Watson-Crick base-pair specificity following sense strand removal. For activation, siRNAs serve as substrates for the RNA-induced silencing complex (RISC) and this complex directs the antisense RNA strand to the template mRNA strand.[3,4]

There has been considerable interest in utilizing siRNAs as biomolecular scaffolds to target genes of interest that may be associated with disease.[5] However, their impact has been delayed due to problems associated with permeability, stability and off-target effects.[6,7] In order to overcome these limitations, there is attention directed at utilizing chemical modifications to overcome some of the inherent problems associated with the native structure of RNA.[8–11]

Over the last number of years, there have been numerous studies aimed at evaluating the mechanism of the RNAi pathway, and elucidating the method through which RISC removes the sense strand.[12–15] This process is important because ultimately the antisense strand must target the desired mRNA. Several studies have confirmed that the catalytic portion of Argonaute 2 (Ago2) cleaves the sense strand between positions 9 and 10, starting from the 5′-end of the strand.[14–16] This cleavage is thought to promote the dissociation of the sense strand from the antisense strand to help initiate an active RISC-antisense RNA complex.

However, there have been a number of studies that suggest that RISC-mediated cleavage of the sense strand is not an essential feature that governs activity.[13,14,17] For example, Zamore and coworkers demonstrated that the substitution of the scissile phosphodiester on the sense strand with a phosphorothioate linkage significantly reduced cleavage by Ago2, yet RNAi activity was retained.[13] This study suggested that an alternative mechanism for sense strand dissociation was possible for RNAi activity. Other studies have illustrated that a pre-cleaved (nicked siRNA) at the sense strand's Ago2 cleavage site resulted in efficient RNAi activity, which indicates that an actual cleavage event per se is not an essential requirement to illicit a potent RNAi response.[14,18,19] Furthermore, Manoharan and coworkers demonstrated that a 2′-*O*-methyl or phosphorothioate modification at the Ago2 cleavage site of the sense strand with destabilizing chemical modifications were well tolerated within functional siRNAs.[17] Among those already mentioned, there are many other examples of chemical modifications performed on, or near the sense strand's cleavage site that are well tolerated by RISC.[20–24]

One of the features that is believed to help promote a bypass mechanism involves destabilization of the central region of a siRNA. Many of the methods to achieve destabilization include the incorporation of chemically modified bases, mismatches and/or abasic sites.[14,24–26] Many of the reported modifications require multiple steps to synthesize and expertise in nucleoside phosphoramidite chemistry. The goal of this study is to retain siRNA efficacy through duplex destabilization using various alkyl linkers as simple alternatives to mismatches or other chemically modified derivatives. Alkyl linker phosphoramidites such as those used in this study are commercially available and thus their preparation does not rely on in-house multi-step phosphoramidite syntheses.

* Corresponding author. Tel.: +1 905 721 8668 x3621; fax: +1 905 721 3304.
E-mail address: jean-paul.desaulniers@uoit.ca (J.-P. Desaulniers).

0960-894X/$ - see front matter Crown Copyright © 2012 Published by Elsevier Ltd. All rights reserved.
http://dx.doi.org/10.1016/j.bmcl.2012.07.006

Based on the aforementioned reports and the well-established principle of thermodynamic asymmetry exhibited within siRNAs,[27–29] a variety of different length alkyl spacer chains was chosen for this study to replace typical destabilizing modifications.

The C3 spacer places three carbons between the oxygens of the phosphodiester linkages, which is exactly the same number of carbons between native RNA. The C4 and C5 spacer naturally have one or two additional carbons, respectively. These were chosen as it had been shown previously that alkyl bulges with increased carbon length can be used for siRNA constructs.[30] Each introduction of these alkyl spacer modifications was designed to replace the distance of a single nucleoside.

The E8 and C9 spacers contain eight or nine atoms between phosphodiester functionalities, respectively. The intention of these spacer derivatives is to span across two nucleotides with each introduction in RNA. Native RNA contains nine atoms between alternating phosphodiesters. Finally, the E17 spacer contains 17 atoms and is a mimic designed to span across three bases. Figure 1 illustrates the structural differences amongst the different alkyl spacer linkers used.

Various siRNAs were synthesized or purchased commercially that contained a combination of the linkers identified in Figure 1. The siRNAs generated target *firefly* luciferase mRNA transcribed from the plasmid pGL3 and expressed within mammalian cells (Table 1). The siRNAs were tested in a dose-dependent manner and their silencing data is illustrated in Figure 2.

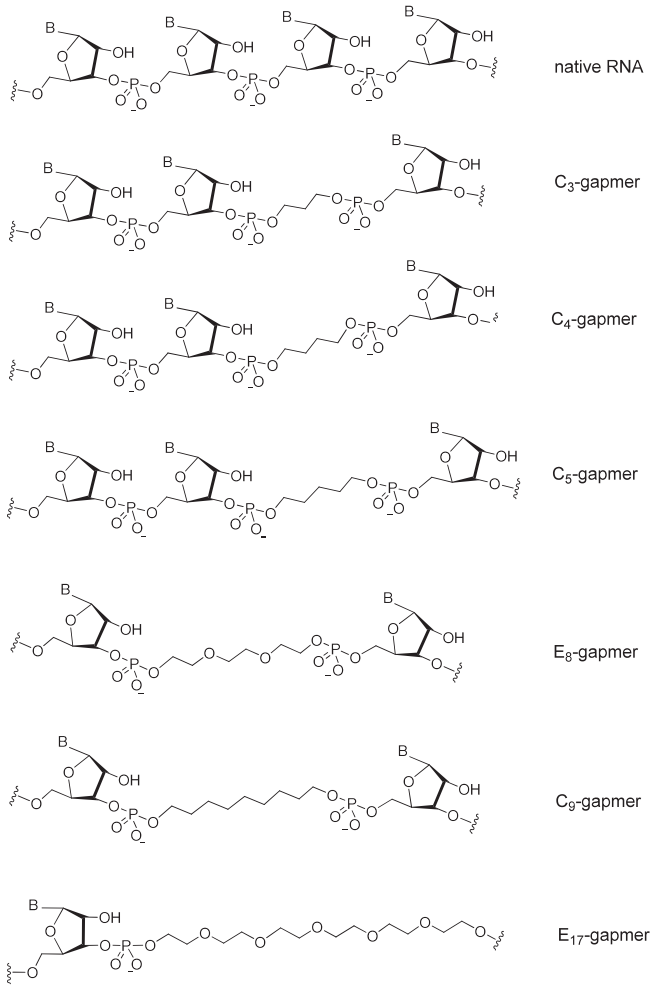

Figure 1. Structure of various alkyl spacer linkers used within siRNAs.

Table 1
Sequences of anti-luciferase siRNAs and T_m data[31]

RNA	siRNA duplex	T_m (°C)	ΔT_m (°C)
wt	5'- CUUACGCUGAGUACUUCGAtt -3' 3'- ttGAAUGCGACUCAUGAAGCU -5'	71.4	--
1	5'- CUUC_3CGCUGAGUACUUCGAtt -3' 3'- ttGAAUGCGACUCAUGAAGCU -5'	--	--
2	5'- CUUACGC_4UGAGUACUUCGAtt -3' 3'- ttGAAUGCGACUCAUGAAGCU -5'	55.0	-16.4
3	5'- CUUC_4CGC_4UGAGUACUUCGAtt -3' 3'- ttGAAUGCGACUCAUGAAGCU -5'	55.3	-16.1
4	5'- CUUACGCUGAGUC_4CUUCGAtt -3' 3'- ttGAAUGCGACUCAUGAAGCU -5'	56.8	-14.6
5	5'- CUUACGCUGAGUACUC_4CGAtt -3' 3'- ttGAAUGCGACUCAUGAAGCU -5'	--	--
6	5'- CUUACGCUGAGUC_3CUC_3CGAtt -3' 3'- ttGAAUGCGACUCAUGAAGCU -5'	53.5	-17.9
7	5'- CUUACGCUGAGUC_4CUC_4CGAtt -3' 3'- ttGAAUGCGACUCAUGAAGCU -5'	56.7	-14.7
8	5'- CUUACGCUGAGUC_5CUC_5CGAtt -3' 3'- ttGAAUGCGACUCAUGAAGCU -5'	50.9	-20.5
9	5'- CUUACGCUC_3AGUACUUCGAtt -3' 3'- ttGAAUGCGACUCAUGAAGCU -5'	52.3	-19.1
10	5'- CUUACGCUC_4AGUACUUCGAtt -3' 3'- ttGAAUGCGACUCAUGAAGCU -5'	50.8	-20.6
11	5'- CUUACGCUC_5AGUACUUCGAtt -3' 3'- ttGAAUGCGACUCAUGAAGCU -5'	50.6	-20.8
12	5'- CUUACGCUGC_3GUACUUCGAtt -3' 3'- ttGAAUGCGACUCAUGAAGCU -5'	55.3	-16.1
13	5'- CUUACGCUGC_4GUACUUCGAtt -3' 3'- ttGAAUGCGACUCAUGAAGCU -5'	52.4	-19.0
14	5'- CUUACGCUGC_5GUACUUCGAtt -3' 3'- ttGAAUGCGACUCAUGAAGCU -5'	52.9	-18.5
15	5'- CUUACGCUC_3C_3GUACUUCGAtt -3' 3'- ttGAAUGCGACUCAUGAAGCU -5'	49.7	-21.7
16	5'- CUUACGCUC_4C_4GUACUUCGAtt -3' 3'- ttGAAUGCGACUCAUGAAGCU -5'	51.0	-20.4
17	5'- CUUACGCUC_5C_5GUACUUCGAtt -3' 3'- ttGAAUGCGACUCAUGAAGCU -5'	50.5	-20.9
18	5'- CUUACGCUGAC_4UACUUCGAtt -3' 3'- ttGAAUGCGACUCAUGAAGCU -5'	51.6	-19.8
19	5'- CUUACGCUC_4AC_4UACUUCGAtt -3' 3'- ttGAAUGCGACUCAUGAAGCU -5'	48.8	-22.6
20	5'- CUUACGCUGC_4C_4UACUUCGAtt -3' 3'- ttGAAUGCGACUCAUGAAGCU -5'	50.9	-20.5
21	5'- CUUACGC-E_8-AGUACUUCGAtt -3' 3'- ttGAAUGCGACUCAUGAAGCU -5'	54.7	-16.7
22	5'- CUUACGCU-E_8-GUACUUCGAtt -3' 3'- ttGAAUGCGACUCAUGAAGCU -5'	52.2	-19.2
23	5'- CUUACGCUG-E_8-UACUUCGAtt -3' 3'- ttGAAUGCGACUCAUGAAGCU -5'	50.0	-21.4
24	5'- CUUACGC-C_9-AGUACUUCGAtt -3' 3'- ttGAAUGCGACUCAUGAAGCU -5'	50.4	-21.0
25	5'- CUUACGCU-C_9-GUACUUCGAtt -3' 3'- ttGAAUGCGACUCAUGAAGCU -5'	51.3	-20.1
26	5'- CUUACGCUG-C_9-UACUUCGAtt -3' 3'- ttGAAUGCGACUCAUGAAGCU -5'	49.3	-22.1
27	5'- CUUACGC-E_{17}-GUACUUCGAtt -3' 3'- ttGAAUGCGACUCAUGAAGCU -5'	54.4	-17.0
28	5'- CUUACGCU-E_{17}-UACUUCGAtt -3' 3'- ttGAAUGCGACUCAUGAAGCU -5'	50.9	-20.5

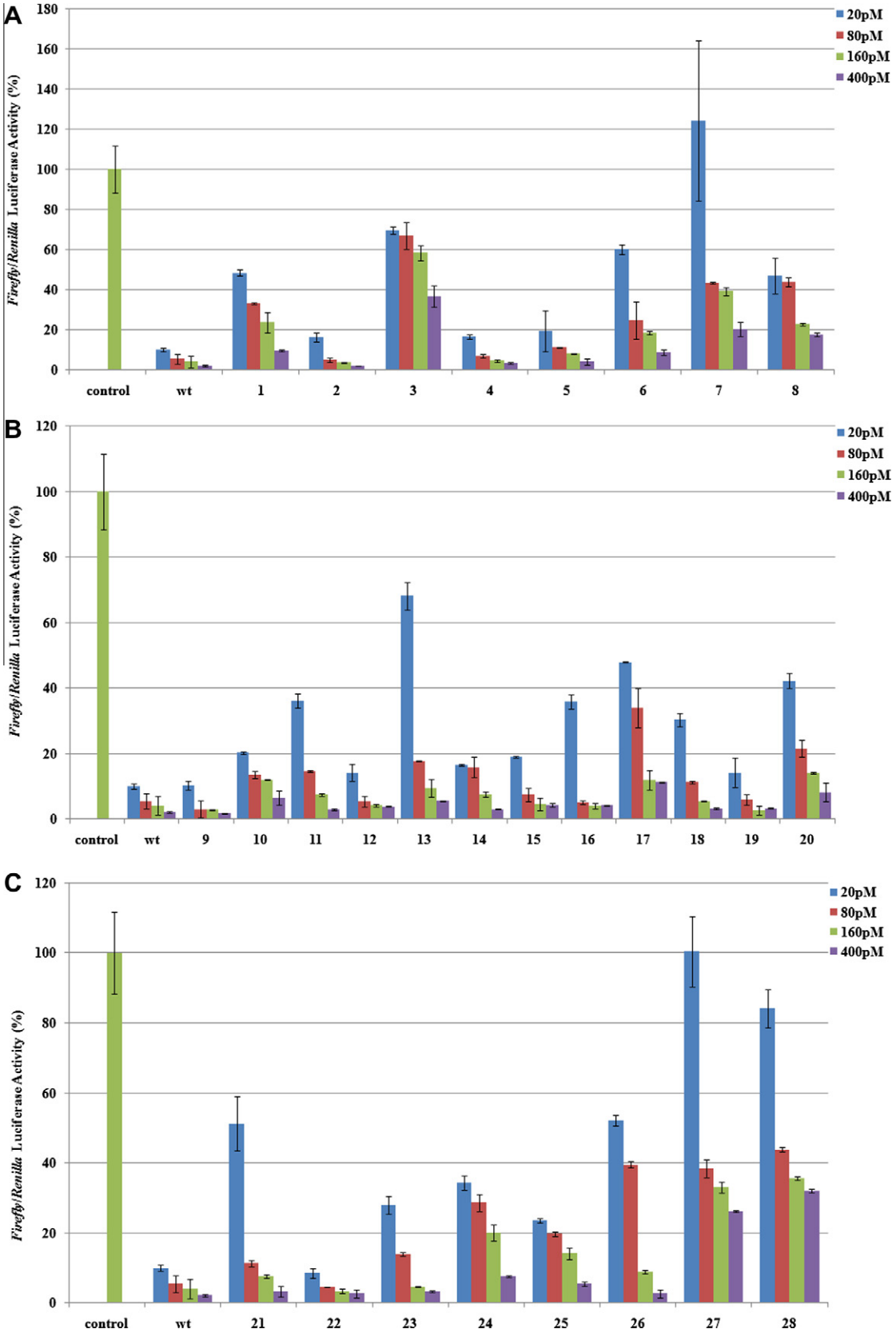

Figure 2. Reduction of luciferase activity as a function of siRNA activity using the Dual-luciferase reporter assay. Alkyl chain-modified siRNAs were tested in HeLa cells at 20, 80, 160 and 400 pM, with *firefly* luciferase expression normalized to *Renilla* luciferase. (A) SiRNAs with alkyl spacers near the terminal ends of the sense strand. (B) Centrally-modified siRNAs, each containing one or two single (C3, C4 or C5) spacers. (C) Centrally-modified siRNAs, each containing a double (E8 or C9) or a triple (E17) spacer.

Table 1 also highlights the melting temperature (T_m) for the various siRNAs. Not surprisingly, all linkers display a degree of destabilization. With respect to destabilization close to the 5′-end of the sense strand (siRNA **1**), a loss of activity relative to wild-type is observed. Activity is comparable to the parent siRNA as the duplex is destabilized closer to its center (siRNA **2**). In contrast, single modifications close to the 3′-end of the sense strand exhibit potency comparable to wild-type siRNA (siRNAs **4** and **5**). This observation is consistent with trends observed with the asymmetry rule of siRNAs.[28] However, if two alkyl chain linkages are placed at both position 4 and 7 (siRNA **3**) or at 13 and 16 (siRNAs **6**–**8**) of the sense strand, this results in siRNAs exhibiting reduced gene silencing properties, likely due to the large destabilization occurring at those positions (Fig. 2A).

We next examined the effect of placing C3, C4 and C5 spacer linkers within the central region of the siRNA, with a focus on positions 9, 10 and 11 which constitute and/or surround the Ago2 cleavage site (Fig. 2B). Placing a C3 spacer in place of a nucleobase at position 9 (siRNA **9**), displays silencing efficiency very comparable to wild-type. Although the T_m of siRNA **9** is almost 20 degrees below the T_m of the wild-type siRNA, no change in potency is observed. As we increase the number of atoms from C3 to C4 and C5 (siRNAs **10** and **11**) a small drop in potency is observed. For position 10, all single spacer siRNAs (siRNAs **12–14**) exhibit potent gene silencing ability, particularly at concentrations greater than 20 pM. A single C4 spacer was introduced at position 11 (siRNA **18**) producing a siRNA which also displayed efficient gene silencing. Even though substantial drops in T_m were observed with all single spacer siRNAs, the data suggests that they are compatible within the RNAi machinery.

We next turned our attention to multiple spacer modifications within the internal region of the siRNA, while continuing to focus on the Ago2 cleavage site (Fig. 2B). With respect to spanning two spacers across the 9–10 region of the sense strand of the siRNA, the C3-double spacer (siRNA **15**) was quite effective at all concentrations tested. In addition, as the number of atoms increased, a slight reduction in potency was observed, especially with a two-atom increase in linker length (siRNA **17**) and at lower concentrations. Nevertheless, the gene-silencing capabilities of siRNAs bearing two spacers at these positions were relatively unhindered at higher concentrations. We investigated the effect of a double spacer linkage spanning positions 10–11 of the sense strand (siRNA **20**), and we observed that it was also quite effective at silencing, albeit at reduced efficacy to wild-type siRNA. With the addition of yet another spacer siRNA containing two C4 linkages across positions 9 and 11 of the sense strand (siRNA **19**), the collective data suggests that siRNAs containing multiple and destabilizing spacer units within the central region act as suitable substrates for the RNAi machinery.

Following these results, we focused our attention on non-cleavable linkers spanning across two (E8 and C9) to three (E17) nucleosides within the sense strand (Fig. 2C). We were surprised to find that even though these large linkers were presumably bypassing the sense strand cleavage mechanism, siRNA efficacy was not severely compromised as expected. It is noteworthy to observe that the duplex containing the E8 spacer across positions 9 and 10 (siRNA **22**) was capable of silencing luciferase with efficiency comparable to wild-type siRNA, despite containing the non-cleavable linkage. The siRNA with the C9 spacer spanning positions 9 and 10 (siRNA **25**) also demonstrated an active silencing profile, although not as potent as its E8 counterpart. It was generally found that E8 linker-modified siRNAs (siRNAs **21**–**23**) were slightly more effective at silencing than C9-modified siRNAs (siRNAs **24**–**26**). SiRNAs modified with non-cleavable E17 linkages (siRNAs **27** and **28**), spanning positions 8–10 or 9–11 did not silence as efficiently as the other spacers. This indicates that function was severely compromised by the extended linkage (covering the distance of three nucleobases).

We are presenting a novel method to destabilize the central region through the use of simple alkyl linkers that are able to span within the central region of siRNAs. Many of the linkers used within siRNAs are capable of gene silencing as efficiently as wild-type siRNA. Our data suggests that non-cleavable long linkers, up to nine atoms in length that span the equivalent of two nucleobases at and near the Ago2 cleavage site are effective substrates for the RNAi machinery. As this linker is increased to seventeen atoms, thus replacing three nucleobases, we observe a drop in efficacy. To confirm that the alkyl linker is essential for activity, we tested some 'true space' (TS) siRNAs containing segmented sense strands annealed to unmodified antisense strands (Table S1). The segments varied in length in order that they reveal spaces in the sense strand with missing residues near and across the Ago2 cleavage site. These TS siRNAs were not capable of effective gene silencing signifying the importance of an actual linkage between residues that are separated by at least one space on the same strand. See Fig S1 and Table S1 for details (Supporting data).

In conclusion, this study presents a simple means to destabilize the central region of siRNAs through the use of alkyl linkers. Alkyl linkers are attractive substituents due to their commercial availability and their robust compatibility with standard DMT-phosphoramidite chemistry and related protocols.[32,31] In addition, the longer neutrally-charged linkers such as E8, C9 and E17 assist in reducing the overall polyanionic charge of the siRNA. The ability to use a non-cleavable alkyl linker within the central region of an siRNA opens the future possibility of further chemically modifying it with desired functionality that can assist with some of the problems associated with siRNAs such as delivery, stability, and off-targeting. For example, designing a linker with positively-charged nitrogens at physiological pH may assist with cell membrane permeability. Future studies include delineating new structure–function relationships of novel functionalized spacer moieties within siRNAs.

Acknowledgments

We acknowledge the National Sciences and Engineering Research Council and the Canada Foundation for Innovation for funding.

Supplementary data

Supplementary data associated with this article can be found, in the online version, at http://dx.doi.org/10.1016/j.bmcl.2012.07.006. These data include MOL files and InChiKeys of the most important compounds described in this article.

References and notes

1. Fire, A.; Xu, S. Q.; Montgomery, M. K.; Kostas, S. A.; Driver, S. E.; Mello, C. C. *Nature* **1998**, *391*, 806.
2. Knight, S. W.; Bass, B. L. *Science* **2001**, *293*, 2269.
3. Elbashir, S. M.; Harborth, J.; Lendeckel, W.; Yalcin, A.; Weber, K.; Tuschl, T. *Nature* **2001**, *411*, 494.
4. Bumcrot, D.; Manoharan, M.; Koteliansky, V.; Sah, D. W. Y. *Nat. Chem. Biol.* **2006**, *2*, 711.
5. Tuschl, T. *Nature Biotechnol.* **2002**, *20*, 446.
6. Watts, J. K.; Deleavey, G. F.; Damha, M. J. *Drug Discov. Today* **2008**, *13*, 842.
7. Snove, O.; Rossi, J. J. *ACS Chem. Biol.* **2006**, *1*, 274.
8. Peacock, H.; Kannan, A.; Beal, P. A.; Burrows, C. J. *J. Org. Chem.* **2011**, *76*, 7295.
9. Phelps, K.; Morris, A.; Beal, P. A. *ACS Chem. Biol.* **2012**, *7*, 100.
10. Chernolovskaya, E. L.; Zenkova, M. A. *Curr. Opin. Mol. Ther.* **2010**, *12*, 158.
11. Efthymiou, T. C.; Huynh, V.; Oentoro, J.; Peel, B.; Desaulniers, J.-P. *Bioorg. Med. Chem. Lett.* **2012**, *3*, 1722.
12. Elbashir, S. M.; Martinez, J.; Patkaniowska, A.; Lendeckel, W.; Tuschl, T. *EMBO J.* **2001**, *20*, 6877.
13. Matranga, C.; Tomari, Y.; Shin, C.; Bartel, D. P.; Zamore, P. D. *Cell* **2005**, *123*, 607.

14. Leuschner, P. J. F.; Ameres, S. L.; Kueng, S.; Martinez, J. *EMBO Rep.* **2006**, *7*, 314.
15. Rand, T. A.; Petersen, S.; Du, F. H.; Wang, X. D. *Cell* **2005**, *123*, 621.
16. Wang, Y. L.; Juranek, S.; Li, H. T.; Sheng, G.; Wardle, G. S.; Tuschl, T.; Patel, D. J. *Nature* **2009**, *461*, 754.
17. Addepalli, H.; Meena; Peng, C. G.; Wang, G.; Fan, Y. P.; Charisse, K.; Jayaprakash, K. N.; Rajeev, K. G.; Pandey, R. K.; Lavine, G.; Zhang, L. G.; Jahn-Hofmann, K.; Hadwiger, P.; Manoharan, M.; Maier, M. A. *Nucleic Acids Res.* **2010**, *38*, 7320.
18. Bramsen, J. B.; Laursen, M. B.; Damgaard, C. K.; Lena, S. W.; Babu, B. R.; Wengel, J.; Kjems, J. *Nucleic Acids Res.* **2007**, *35*, 5886.
19. Lu, X. Z.; Yang, G. D.; Zhang, J.; Fu, H. Y.; Jin, L. A.; Wei, M. Y.; Wang, L.; Lu, Z. F. *Appl. Microbiol. Biotechnol.* **2011**, *90*, 583.
20. Braasch, D. A.; Jensen, S.; Liu, Y. H.; Kaur, K.; Arar, K.; White, M. A.; Corey, D. R. *Biochemistry* **2003**, *42*, 7967.
21. Kraynack, B. A.; Baker, B. F. *RNA* **2006**, *12*, 163.
22. Deleavey, G. F.; Watts, J. K.; Alain, T.; Robert, F.; Kalota, A.; Aishwarya, V.; Pelletier, J.; Gewirtz, A. M.; Sonenberg, N.; Damha, M. J. *Nucleic Acids Res.* **2010**, *38*, 4547.
23. Fauster, K.; Hartl, M.; Santner, T.; Aigner, M.; Kreutz, C.; Bister, K.; Ennifar, E.; Micura, R. *ACS Chem. Biol.* **2012**, *7*, 581.
24. Petrova, N. S.; Meschaninova, M. I.; Venyaminova, A. G.; Zenkova, M. A.; Vlassov, V. V.; Chernolovskaya, E. L. *FEBS Lett.* **2011**, *585*, 2352.
25. Somoza, A. S. A. P.; Miller, R. M.; Chelliserrykattil, J.; Kool, E. T. *Chemistry* **2008**, *14*, 7978.
26. Hernandez, A. R.; Peterson, L. W.; Kool, E. T. *ACS Chem. Biol.* **2012**.
27. Aronin, N. *Gene Ther.* **2006**, *13*, 509.
28. Schwarz, D. S.; Hutvagner, G.; Du, T.; Xu, Z. S.; Aronin, N.; Zamore, P. D. *Cell* **2003**, *115*, 199.
29. Khvorova, A.; Reynolds, A.; Jayasena, S. D. *Cell* **2003**, *115*, 209.
30. Ueno, Y.; Yoshikawa, K.; Kitamura, Y.; Kitade, Y. *Bioorg. Med. Chem. Lett.* **2009**, *19*, 875.
31. T_m s were measured in triplicate in a sodium phosphate buffer (90 mM NaCl, 10 mM Na_2HPO_4, 1 mM EDTA, pH 7) at 260 nm, at a rate of 0.5 °C/min from 10 °C to 95 °C.
32. Caruthers, M. H. *Science* **1985**, *230*, 281.

7.0 Supplementary Information – Chapter IV – Manuscript III

7.1 Tables

Table A7. Sequences of Mismatched (MM) and True-Space (TS) anti-luciferase siRNAs.

Sample No.	Sense and Antisense RNAs	T_m (^{0}C)	[a]ΔT_m (^{0}C)
MM1	5′- CUUACGCU**C**AGUACUUCGAtt -3′ 3′- ttGAAUGCGACUCAUGAAGCU -5′	61.8	-9.6
MM2	5′ - CUUACGCU**CU**GUACUUCGAtt - 3′ 3′- ttGAAUGCGACUCAUGAAGCU -5′	60.5	-10.9
MM3	5′- CUUACGCU**CUC**UACUUCGAtt -3′ 3′- ttGAAUGCGACUCAUGAAGCU -5′	52.9	-18.5
TS1	5′- CUUACGCU AGUACUUCGAtt -3′ 3′- ttGAAUGCGACUCAUGAAGCU -5′	47.5	-23.9
TS2	5′- CUUACGCU GUACUUCGAtt -3′ 3′- ttGAAUGCGACUCAUGAAGCU -5′	46.4	-25.0
TS3	5′- CUUACGCU UACUUCGAtt -3′ 3′- ttGAAUGCGACUCAUGAAGCU -5′	39.9	-31.5

[a] T_m's are compared to that obtained for the wild-type duplex (71.4 ^{0}C).

7.2 Figures

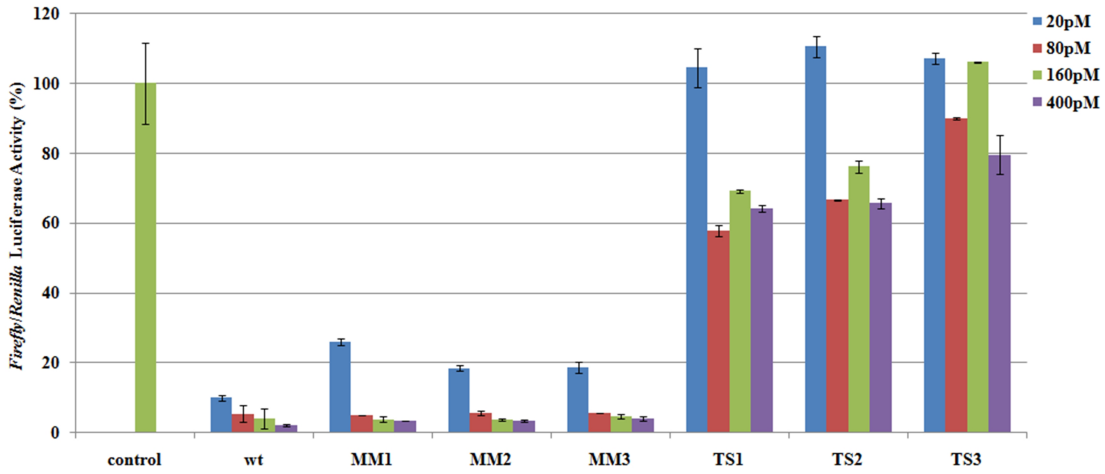

Figure A53. Reduction of *firefly* luciferase expression using four concentrations (20, 80, 160 and 400 pM) of siRNAs containing destabilizing mismatches (MM) or missing residues (TS) in the central region of the duplex (Table A7). *Firefly* luciferase expression is normalized to *Renilla* luciferase.

Appendix IV – Detailed Experimental Procedures

8.0 Experimental Protocols

8.1 Mammalian Cell Culturing & Assays

8.1.1 Thawing HeLa Cells

A 50 mL fulcan tube containing 10 mL of growth medium (Dulbecco′s modified eagle′s medium (DMEM) (Sigma) with 10% Fetal bovine serum (FBS) (Perbio) and 1% Penicillin-Streptomycin (Sigma)) is warmed at 37 ^{o}C in preparation for the frozen cells. A cryovial stored in the vapor phase of liquid N_2 containing 950k frozen cells, is placed into a portable cooler at -80 ^{o}C for transport. After removing the vial from the cooler, 500 µL of warm growth medium is immediately added to the tube and gently mixed with the cells as they thaw. The 500 µL mixture of medium and thawed cells is removed from the vial and added into the fulcan tube containing the growth medium. Another 500 µL of medium is added to the frozen cell vial, mixed, removed. This process is repeated until the all cells have thawed and are contained within the fulcan tube. The cells are then centrifuged at 1200 rpm for 5 min, after which the medium is discarded. The pellet is resuspended in 1 mL of new 37 ^{o}C growth medium and the entire amount is then added to a small culture flask containing 10 mL of growth medium. The cells are incubated for 24 hr at 37 ^{o}C with 5% CO_2, after which they are passaged (section **8.2**) and all cells are added to a large culture flask containing 25 mL of growth medium. These cells are then incubated at 37 ^{o}C with 5% CO_2 until they reach 70 – 80% confluency (3 – 4 days), at which point they are sub-cultured (section **8.2**) once again.

8.1.2 Sub-Culturing HeLa Cells

Either 24 hr post-cell thawing or at 70 – 80% confluency, the growth medium is removed from the culture flask and the cells are washed twice with 10 mL of cool phosphate buffer saline solution (0.01 M phosphate buffered saline (NaCl 138 mM; KCl 2.7 mM; pH 7.4) (Sigma). Being surface-adhering cells, the HeLa cells are dispersed by adding 1 – 2 mL of 37 ^{o}C 0.25% trypsin (SAFC Bioscience) to a small or large culture flask, respectively. The cells are then incubated with the trypsin for approximately 2 min at 37 ^{o}C with 5% CO_2, after which they are re-suspended in 10 mL of 37 ^{o}C growth medium and placed in a 50 mL fulcan tube. The cells are centrifuged at 1200 rpm for 5 min and the supernatant

is discarded. The pellet is re-suspended in 5 mL of 37 ºC growth medium and the cell concentration is determined using a hemacytometer (mix 50 µL of cells with 150 µL of Trypan blue (Sigma)). After determining the concentration of cells in the growth medium, they are diluted to a concentration of $1x10^6$/mL with 37 ºC growth medium. To a culture flask containing 24 mL of 37 ºC growth medium, 1 mL of cells is added and they are incubated at 37 ºC with 5% CO_2 until they reach 70 – 80% confluency.

8.1.3 Protocol for Freezing HeLa Cells

After sub-culturing the cells and diluting them to a concentration of $1x10^6$ cells/mL with 37 ºC growth medium (section **8.2**), 50 µL of dimethylsulfoxide (DMSO) (Fisher) is added to a sterile cryovial. We then add 950 µL of suspended cells (950k cells) to the DMSO, and mix this solution only once. The cells are stored at -80 ºC for 24 hr and then transferred the vapor phase of liquid N_2 for long-term storage.

8.1.4 Dual-Luciferase Reporter Assay

8.1.4.1 Transfection of HeLa Cells with siRNAs

After passaging and achieving a $1x10^6$ cell concentration (Section **8.2**) using growth medium without antibiotics (DMEM containing 10% FBS), HeLa cells were seeded on 12-well plates (Greiner Bio-One) by adding 100 µL of cells (100k cells) to each well, with each well containing 1 mL of identical growth medium devoid of antibiotics. The plates were incubated at 37 ºC with 5% CO_2. After 24 hr and in preparation for the transfection of HeLa cells, 100 ng of each luciferase-expressing plasmid (pGL3 (Promega) and pRLSV40 (York University) was added to a microfuge tube on ice. To the same tube, amounts ranging from 0.01 – 1 pmol of a particular siRNA was added in order to achieve a final siRNA concentration of 8 pM to 800 pM. To this tube was then added 100 µL of Gibco′s Opti-Mem Reduced Serum Medium 1X (Invitrogen). In a separate microfuge tube kept at room temperature, 1 µg of Lipofectamine 2000 (Invitrogen) followed by 100 µL of Opti-Mem was added, thoroughly mixed, and left at room temperature. After 5 min, this solution was added to the plasmid/siRNA tube, thoroughly mixed, and left to stand at room temperature for an additional 20 min. Several pairs of tubes were setup at the same time for each assay utilizing this protocol, with each pair of

tubes used for a separate siRNA, or siRNA concentration being tested. After 20 mins, the siRNA/plasmid/Opti-Mem/lipofectamine mixtures were added to the seeded wells of the 12-well plate. Each siRNA or siRNA concentration being tested was added to its own well. The plates were re-incubated at 37 ºC with 5% CO_2 in order for the transfection to take place.

8.1.4.2 Measuring siRNA Efficacy Using the Dual-Reporter Luciferase Assay

After 24 hr, the cell growth medium was discarded from each well, followed by washing each well twice with 1x PBS buffer. To each well was then added 250 µL of 1X passive lysis buffer (5X stock) supplied from the Dual-luciferase Reporter Assay System (Promega) and warmed to room temperature. The plates were gently agitated for 20 min at room temperature in order to ensure that all cells are lysed. 10 µL of each cell lysate was loaded in triplicate onto a white and opaque 96-well plate (Costar). Using a multichannel pipette, 50 µL of luciferase assay substrate was quickly added and mixed with each set of triplicates. Substrate was added to a maximum of four sets of triplicates for each luminescence reading, due to the time-sensitive nature of the substrate-enzyme reaction. Using the KC4 program on a Synergy HT (Bio-Tek) plate luminometer, luminescence was recorded for each well containing substrate. After this reading, 50 µL of Stop & Go *Renilla* luciferase substrate was added and mixed to the exact same triplicate wells in order to fully inhibit the *firefly* luciferase reaction and start the *Renilla* luciferase reaction. Luminescence was once again for the same wells. This process was repeated for each new set of triplicates until all samples were analyzed. The ratio of *firefly*/*renilla* luminescence expressed as a percentage relates the reduction in *firefly* expression to siRNA efficacy when compared to untreated controls. Each value is the average of at least three independent experiments with the indicated error (SDOM).

8.1.5 Quantitative Real-Time PCR

8.1.5.1 HeLa Cell Post-Transfection Preparation

After the addition of siRNAs to 12-well plates seeded with HeLa cells for final siRNA concentrations of 10 – 20 nM per well, and the 24 hr transfection period (section **8.1.4.1**), the growth medium was discarded and each well was washed twice with 4 ºC 1X PBS

buffer. Cells were dispersed after adding 100 µL of 0.25% trypsin to each well and incubating the plate at 37 °C with 5% CO_2 for 2 min. The detached cells from each well were then added to separate microfuge tubes containing 1 mL of 37 °C growth medium without antibiotics. The cells were centrifuged at 1200 rpm for 5 min at 37 °C, after which the supernatant was discarded and the cells were re-suspended in 500 µL of the same growth medium without antibiotics. After counting the cells and ensuring equal cell concentrations for each sample for a maximum of 250k cells/sample, the cells were re-pelleted at 1200 rpm for 5 min at 4 °C, the supernatant was discarded, and the pellets were placed on ice. After re-suspending the pellets in 500 µL of ice-cold 1X PBS buffer (Ambion), the cells were re-pelleted at 1200 rpm for 5 min at 4 °C, followed by discarding the supernatant and placing the pellets back on ice.

8.1.5.2 Cell Lysis & Reverse Transcription (RT)

The following protocols involve the use of reagents found in the Cells-to-cDNA kit by Ambion. To the pellets was added ice-cold 100 uL of cell lysis buffer II and these solutions were then vortexed. Until lysis buffer was added to each sample, all other samples remained on ice. After all samples contained lysis buffer and were vortexed, the samples were immediately incubated at 75 °C for 10 min. After placing the samples back on ice, to each tube was added 2 uL of DNase 1 and these mixtures were gently vortexed, and briefly centrifuged to concentrate the solutions. These mixtures were then incubated at 37 °C for 15 min in order to activate the DNase enzyme. The samples were then heated to 75 °C for 5 min to deactivate DNase 1.

To new and sterile microfuge tubes on ice, 5 µL of cell lysate (template RNA) from each sample is added, along with 4 µL of dNTP mix, 2 µL of random decamers, and 9 µL of nuclease-free H_2O. In order to denature both the template RNA and the primers, the samples are heated at 70 °C for 3 min, placed on ice for 1 min, briefly centrifuged and then replaced on ice. To these tubes is added 2 µL of 10X RT buffer, 1 µL of M-MLV RT (reverse transcriptase) or 1 µL of H_2O for No-RT (NRT) control, and 1 µL of RNase Inhibitor. The solutions are then incubated at 42 °C for 45 min for the reverse transcription of RNA, which yields template cDNA for PCR. To inactivate the RT,

samples were incubated at 95 °C for 10 min. At this stage, the samples could be stored at -20 °C until needed, or they could be immediately used for amplification.

8.1.5.3 Quantitative Real-Time PCR

To each reaction tube within the 96-well PCR plate (BIO-RAD) was added the following: 2 µL of template cDNA (or 2 µL of H_2O for No-template control (NTC)), 10 µL of SsoFast EvaGreen Supermix (BIO-RAD) as the source of SYBR green dye and *Taq* Polymerase, 800 nM of forward/reverse GAPDH and 20 nM of forward/reverse 18S primers (as concentrated in nuclease-free H_2O as possible so as not to exceed reaction volume), each topped up to a 20 µL reaction volume with nuclease-free H_2O. Master Mixes for each set of primers were made up in order to simplify the addition of reagents to each reaction tube, therefore only requiring the addition of 2 µL of template cDNA or H_2O (NTC) to each reaction tube before adding 18 µL of Master Mix. NRT controls were performed for each new siRNA and/or siRNA concentration for each set of primers (# of siRNAs and/or # of [siRNA] x 2 primer sets = # of NRTs), in addition to NTC controls performed for each set of primers (2 primer sets = 2 NTCs).

The GAPDH forward and reverse primers were 5′- AGG GCT GCT TTT AAC TCT GG -3′ and 5′- TTG ATT TTG GAG GGA TCT CG - 3′, respectively, yielding a 200-bp amplicon. The 18S forward and reverse primers were 5′- CGG CTA CCA CAT CCA AGG AAG -3′ and 5′- CGC TCC CAA GAT CCA ACT AC -3′, respectively, yielding a 247-bp amplicon. Utilizing a CFX96 Real-Time reactor (BIO-RAD), the protocol to amplify both GAPDH and 18S transcripts consisted of the following events: pre-heat to 95 °C for 60 sec; 40 cycles of denaturing at 95 °C for 5 sec and annealing/elongating at 47 °C for 20 sec. The protocol concluded with thermal denaturation analysis of the PCR products by raising the temperature from 65 to 95 °C at 0.5 °C /min and measuring the absorbance at 260 nm. GAPDH gene expression was normalized to 18S using the Comparative *Ct* method ($2^{(\Delta Ct_{18S}-\Delta Ct_{GAPDH})}$), while error was calculated as the overall coefficient of variance ($CV = \sqrt{CV_{18S}^2 + CV_{GAPDH}^2}$).

8.2 Oligonucleotide Quantification, Purification and Characterization

8.2.1 Oligonucleotide Quantification

Following the full deprotection of synthesized single-strands of DNA and RNA oligonucleotides, each sample was dried down using a SC210A Speed-Vac (Thermo) and re-dissolved in 200 µL of nuclease-free H_2O. Using 1 mL UV-compatible disposable plastic cuvettes, 1 µL of the re-dissolved sample was added to 999 µL of nuclease-free H_2O, and this solution was thoroughly mixed. After measuring the absorbance of this solution at 260 nm using a Genesys 10S Vis Spectrophotometer (Thermo), the value obtained was then multiplied by the total volume of the stock oligonucleotide sample (200 µL). This optical density (OD) value **A** is then plugged into the Beer-Lambert equation: $\mathbf{A=\varepsilon bc}$; where $\boldsymbol{\varepsilon}$ is the extinction coefficient particular to the oligonucleotide sequence; **b** is the sample′s path length of 10 mm; and **c** is the oligonucleotide′s molar concentration in 1 mL of solution. The $\boldsymbol{\varepsilon}$ value is determined for each individual DNA or RNA oligonucleotide using the following link to a web tool provided by Integrated DNA Technologies (IDT): http://www.idtdna.com/analyzer/Applications/OligoAnalyzer/. After determining the concentration **c** in mol/L per mL, we then calculate the new oligonucleotide concentration in 200 µL (stock volume). This new concentration is considered the crude oligonucleotide concentration, since the molecules hasn′t undergone purification at this point. This method of determining the concentrations of oligonucleotide samples is used to form the relationship between ODs of oligonucleotides and their molar concentrations.

8.2.2 PAGE Gel Electrophoresis

To visualize the purity of our fully deprotected single-stranded DNA and RNA oligonucleotides with adequate resolution not offered by agarose-based gels, we required the use of concentrated polyacrylamide gel electrophoresis (PAGE). The recipes required to make the polyacrylamide solution are as follows: For the 10X stock Tris/Borate/EDTA (TBE) buffer, we dissolved 108 g of Tris Base (Fisher), 55 g of Boric Acid (Fisher), and 40 mL of 0.5 M EDTA (pH 8.3) (Fisher) in nuclease-free H_2O for a total volume of 1 L;

for the 40% stock acrylamide solution, we dissolved 380 g of acrylamide (Sigma) and 20 g of bis-acrylamide (Sigma) in nuclease-free H_2O for a total volume of 1 L; for the bromophenol blue loading buffer, we dissolved 74 mg of *EDTA (Fisher), 4.8 g of *Urea (Acros), 50 µL of 1M *Tris-base (pH 5.0) (Fisher) (1.21 g/10 mL of H_2O for 1 M solution; adjust to pH 7.5 with conc. HCl), 1.5 mL of glycerol (Fisher), and 25 mg of bromophenol blue (Fisher) in nuclease-free H_2O, for a total volume of 10 mL. *These reagents were only added to the denaturing loading buffer.

The recipe for a 20% polyacrylamide gel is as follows: 30 mL of 40% acrylamide, 6 mL of 10X TBE, 25.23g of Urea (7 M), 80 µL of 25% ammonium persulfate (APS) (Fisher) (375 mg of APS for 1.5 mL of 25% solution; lasts 1 month at 4 ^{o}C), and 80 uL tetramethylethylenediamine (TEMED) topped up to 60 mL with nuclease-free H_2O. After mixing all of the ingredients together and making sure to add the last two ingredients after everything else is dissolved, the gel solidifies in the PAGE apparatus where it is kept moist by the 0.5X TBE running buffer (25 mL of 10X TBE in 475 mL of H_2O), which is also in contact with both the anode and cathode. For visualizing oligonucleotide purity, 0.05 to 0.5 ODs of oligonucleotide can be combined with denaturing loading dye for a total volume of 20 µL and added to each well. For purification, a maximum of 2 ODs of oligonucleotide can be added to each well, combined with denaturing loading dye for a total volume of 20 µL. PAGE is then performed at 300V for 5 hr, or until the bromophenol blue band has travelled 75% of the gel′s length. The gels can be visualized by staining them for 30 min in a solution of dilute solution of ethidium bromide in 0.5X TBE running buffer, or by UV-shadowing, where the gel is placed on a fluorescent silica background and bands of interest will appear dark against this background due to the sample′s absorbance of UV light.

8.2.3 Post-Synthetic Oligonucleotide Purification

8.2.3.1 Crush & Soak Oligonucleotide Purification

After fully deprotecting, quantifying, and visualizing synthesized oligonucleotides on a gel, further purification was required if more than one band was present. This process began with the Crush & Soak Method, where 2 ODs of quantified crude oligonucleotide

was added to each well of a 20% PAGE gel which was run for 5 hr and visualized using the UV-shadowing technique (section **8.2.2**). At least 20 to 24 ODs of each oligonucleotide was run on a single PAGE gel in order to maximize the final yield of purified sample. After identifying the bands of interest, they were physically excised from the gel and placed in microfuge tubes. After freezing the gel pieces in a dry ice/EtOH bath for 5 min, the pieces were chopped up as much as possible using a skinny scoopula. The chopped up pieces were re-frozen in the dry ice/EtOH bath and then suspended in 500 µL of gel eluting buffer (1 mL (0.3 M) of 3 M NaOAc (pH 5.2) (Fisher), 2.9 mg (1 mM) EDTA in 10 mL buffer solution), where they were quickly chopped even further as they began to defrost in the buffer. This slurry was re-frozen in the dry ice/EtOH bath for another 15 min and then left to thaw at room temperature for 15 min. After incubating the slurry overnight at 37 ^{o}C, the slurry was filtered through a 0.4 micron syringe filter and the filtrate was collected in a sterile microfuge tube, and dried down in the speed-vac.

8.2.3.2 EtOH Precipitation and Desalting of Gel-Purified Oligonucleotides

Following the crush & soak method, the oligonucleotides were then in cold ethanol. After drying down the oligonucleotide samples on a speed-vac, the pellets were re-suspended in 600 µL of EtOH, chilled in dry ice. To these mixtures, 25 µL of 3 M NaOAc (pH 5.2) (2.46 g of NaOAc in 10 mL of H_2O; adjust to pH 5.2) was added and the solutions were vortexed and placed in dry ice for 1 hr. After centrifuging the samples at 12k rpm for 30 min at 4 ^{o}C, as much supernatant as possible was discarded from each sample. The pellets were re-suspended in 600 µL of cold EtOH and the process was repeated 2 to 3X without adding any additional NaOAc. After the final removal of supernatant, the samples were dried down using the speed-vac.

The dried samples were dissolved in 500 µL of nuclease-free H_2O and desalted using 3000 MW cellulose centrifugal filters (Millipore). The samples were loaded into the filters which were then spun at 12k rpm for approximately 10 min at 25 ^{o}C, or until there was roughly 50 µL of oligonucleotide solution left. Added to this remaining amount was 400 – 500 µL of H_2O and the sample was re-spun. This process was repeated for a total of 3 to 4X, after which the remaining 50 µL of sample was collected in a microfuge tube

and dried down. The purified sample was then re-suspended in 100 µL of nuclease-free H_2O and quantified (section **8.2.1**).

8.2.4 Circular Dichroism and UV-Monitored Thermal Denaturation

In a microfuge tube, equimolar amounts of each purified DNA or RNA oligonucleotide (0.5 ODs) (section **8.2.1**) were added to their compliment in 500 µL of a sodium phosphate buffer (90 mM NaCl (Sigma), 10 mM Na_2HPO_4 (Fisher), 1 mM EDTA, pH 7). The strands were denatured at 90 °C for 2 min and then slowly cooled to rt, thus annealing the complimentary strands. The 500 µL samples of newly-formed duplexes were added to quartz cuvettes with 1 mm path lengths, sealed with Teflon caps in preparation for CD and T_m measurements using a Jasco J-815 spectropolarimeter. The CDs of each RNA duplex were recorded in quadruplicate, scanning from 200 to 310 nm at 20 °C in the sodium phosphate buffer, with a scanning rate of 10 nm/min and a 0.2 nm data pitch. The average of four accumulations was calculated using Jasco′s Spectra Manager version 2 software and adjusted against the baseline measurement of the buffer.

Melting temperatures (T_m) were measured at 260 nm following CD measurements for each sample and using the same solution. Sample temperatures were slowly increased from 10 to 95 °C, at a rate of 0.5 °C /min. The absorbance was measured at the end of each 0.5 °C increment, which was every minute. Absorbance readings were automatically adjusted against the baseline absorbance of the sodium phosphate buffer. After averaging the range of absorbance values obtained from three independent experiments for each siRNA, T_m′s were calculated using Meltwin software version 3.5 assuming the Van′t Hoff two-state model.

8.3 Transformation of *E. Coli* and Mini-Preparation of pGL3/SV40 Plasmids

Using competent DH5α cells, several copies of both pGL3 and SV40 plasmids could be prepared. After thawing 50 µL of competent DH5α *E. coli* cells on ice, 100 ng of either plasmid (pGL3 or SV40) were gently mixed with the cells. The cells were first incubated on ice for 15 min, then heat-shocked at 42 °C for exactly 1 min, and then replaced on ice for 2 min. To the cells was then added 950 µL of room temperature LB broth, and this mixture was incubated at 37 °C for 1 hr at 250 rpm. The cells were then pelleted at 14k

rpm for 30 sec, the supernatant was discarded, then the pellet was re-suspended in 100 µL of LB broth. The cells were then plated onto ampicillin-containing agar plates and then grown overnight to select for ampicillin resistance given to cells which were successfully transformed. After identifying ampicillin-resistant bacterial colonies, culture tubes filled with 5 mL of LB and 100 µg/mL of ampicillin were inoculated with single ampicillin-resistant colonies, and these cultures were then incubated at 37 °C for exactly 16 hr.

The process of harvesting the bacterial cells began by centrifuging the culture tubes at 8000 rpm for 3 min at room temperature. Each additional step of the plasmid preparation involved the use of reagents from the QIAprep Spin Miniprep kit (Qiagen). After discarding the supernatant, the pellet was re-suspended and thoroughly mixed with 250 µL of pre-lysis re-suspension buffer (buffer P1) containing 100 µg/mL RNase inhibitor (RNase A), and transferred to a microfuge tube. To this suspension was added 250 µL of lysis buffer (buffer P2), and the tube was gently inverted to mix the contents. At this point, the solution turns blue as an indication of cell lysis. To neutralize the suspension, 350 µL of a neutralizing solution (buffer N3) was added and the contents of the tube wer thoroughly mixed by inverting the tube 4 to 6 times. This solution was mixed until it was no longer blue, but white and cloudy throughout. The tubes were then centrifuged for 10 min at 13k rpm and a white precipitate was formed. The supernatants were transferred to individual QIAprep spin columns by decanting them. The columns were flash-centrifuged for 60 sec in order to discard the flow-through. The columns were then washed by adding 750 µL of wash buffer (buffer PE; contains EtOH) and flash-centrifuging for another 60 sec. After discarding the flow-through from the collection microfuge tube, the column was spun again for an additional 60 sec in order to remove any remaining EtOH. The column was then removed from the collection tube and placed into a clean and sterile microfuge tube. The DNA was collected from the column by adding either 50 µL of column eluting buffer (buffer EB; 10 mM Tris-HCl, pH 8.5) or nuclease-free H_2O directly in the center of the column. After letting the buffer or H_2O stand for 5 min, the column was flash-centrifuged for one last minute in order to elute the plasmid trapped inside. The purified plasmids were quantified (section **8.2.1**) and their ability to express the enzyme they code for and produce an appropriate level of luminescence was tested using the dual-reporter luciferase assay (section **8.1.4.2**).

8.4 $^{1}H/^{13}C$ – NMR of Small Molecules

For each small molecule synthesized, approximately 10 to 15 mg of compound was dissolved in 1 mL of deuterated solvent ($CDCl_3$ or d_6-DMSO (Sigma)). All solubilized compounds were filtered through Pasteur pipettes equipped with glass wool filters into clean NMR tubes. NMRs were either performed on our own Varian 400 MHz or a Varian 500 MHz, located at Trent University. With lock values hovering around 40 to 50, ^{1}H-NMRs were performed for either 16 or 32 transients and ^{13}C-NMRs were typically performed overnight for 20k to 50k transients. All acquired spectra were processed and integrated using ACD Labs software build 9.06. Peaks for experiments performed in $CDCl_3$ were referenced to 7.27 ppm, while peaks for experiments performed in d_6-DMSO were referenced to 2.50 ppm.